



## Control of microbial soil communities by *Pseudomonas*-produced secondary metabolites

Hansen, Morten Lindqvist

*Publication date:*  
2021

*Document Version*  
Publisher's PDF, also known as Version of record

[Link back to DTU Orbit](#)

*Citation (APA):*  
Hansen, M. L. (2021). *Control of microbial soil communities by Pseudomonas-produced secondary metabolites*. DTU Bioengineering.

---

### General rights

Copyright and moral rights for the publications made accessible in the public portal are retained by the authors and/or other copyright owners and it is a condition of accessing publications that users recognise and abide by the legal requirements associated with these rights.

- Users may download and print one copy of any publication from the public portal for the purpose of private study or research.
- You may not further distribute the material or use it for any profit-making activity or commercial gain
- You may freely distribute the URL identifying the publication in the public portal

If you believe that this document breaches copyright please contact us providing details, and we will remove access to the work immediately and investigate your claim.

# Control of microbial soil communities by *Pseudomonas*-produced secondary metabolites

Morten Lindqvist Hansen

PhD thesis

November 2021

Technical University of Denmark  
Department of Biotechnology and Biomedicine  
Section for Microbial and Chemical Ecology  
Center for Microbial Secondary Metabolites  
Infection Microbiology Group





---

## Preface

This Ph.D. thesis was submitted as partial fulfilment of the requirements to obtain a Ph.D. degree from the Technical University of Denmark (DTU). The work has been carried out from September 2018 to November 2021 in the Infection Microbiology Group at the Department of Biotechnology and Biomedicine, DTU. The Ph.D. project also included a one-month external stay supervised by Michael Kühn at the Marine Biological Section, Copenhagen University, Denmark.

The Ph.D. project was supervised by Professor MSO, Lars Jelsbak, and co-supervised by Associate Professor, Ling Ding.

The project was carried out as part of the Center for Microbial Secondary Metabolites (CeMiSt) and funded by the Danish National Research Foundation (DNRF137).

Morten Lindqvist Hansen



---

## Abstract

Bacteria and other microbes produce a variety of secondary metabolites, which are highly specialized natural products predominantly known for their antimicrobial properties. However, natural concentrations of secondary metabolites in the nutrient-limited environments of soil are thought to rarely exceed the levels required for their antimicrobial functions demonstrated *in vitro*. Additionally, an increasing amount of research has shown that subinhibitory concentrations of toxic secondary metabolites can elicit responses in neighboring microorganisms. Thus, the role of these chemicals in natural environments might expand much beyond microbial antagonism.

The focus of this thesis has been on soil-dwelling *Pseudomonas* spp. of the *P. fluorescens* group, as they hold an immense potential for secondary metabolite production and are known as key determinants of plant protection towards phytopathogenic microorganisms associated with certain soils. Specifically, we have focused on the metabolites DAPG, pyoluteorin, and orfamide A produced by strains of the biocontrol species, *P. protegens*. The work presented here describes their role in microbial interactions and *vice versa* the effects of interactions on their biosynthesis and fate.

We developed two methodologies for accurate and high-throughput differentiation of *Pseudomonas* spp. in environmental samples. The former, a *Pseudomonas*-specific amplicon sequencing method, allows for taxonomic identification and relative quantification of *Pseudomonas* spp., while clearly outperforming the 16S rRNA-based gold standard. Secondly, we engineered a whole-cell biosensor, which enables rapid and effortless screening of isolates for producers of DAPG, compared to PCR-based techniques and analytical chemical methods. These methods allow for detailed investigations of *Pseudomonas* population dynamics across ecosystems (*e.g.* different soils and crops).

Additionally, we employed both dual- and multispecies communities in combination with analytical chemistry to investigate the role of *Pseudomonas*-produced secondary metabolites in microbial interactions. The first study led to the discovery of a dynamic, genus-specific interaction sequentially affecting the production of antimicrobial secondary metabolites (DAPG and pyoluteorin) in *P. protegens*. This study sheds light on the underlying mechanisms of *Pseudomonas*-specific interactions affecting the biosynthesis of metabolites relevant for biological control of phytopathogenic microorganisms. In the second study, we utilized a four-species synthetic microbial community as a reproducible framework to investigate compositional perturbations caused by secondary metabolites

---

produced by the invading *P. protegens*. The results from this study revealed a community-level interaction affecting the fate of orfamide A, as the metabolite was enzymatically inactivated and subsequently degraded by separate community members. The outcome of these two studies demonstrates the significance of combining *in vitro* lab-scale systems and analytical chemistry to reveal and characterize the types of metabolite interactions occurring within dual- and multispecies communities.

The work presented in this thesis provide novel insight into the potential roles of *Pseudomonas*-produced secondary metabolites, as well as tools for detailed investigations of *Pseudomonas*-ecology. From a biotechnological perspective, the results from this thesis may assist in discovery and isolation of *Pseudomonas* strains with agricultural application (*e.g.* biocontrol), while also contributing to a deeper understanding of metabolite signaling to potentiate the design and assembly of efficient biocontrol consortia with desirable functionality.

---

## Resumé

Bakterier og andre mikrober producerer et bredt udvalg af såkaldte sekundære metabolitter, hvilket er molekyler bedst kendt for deres antimikrobielle aktivitet. Koncentrationerne af disse metabolitter i nærings-begrænsede miljøer, såsom jord, er dog sjældent vist at nå de niveauer, der kræves for deres antimikrobielle funktion påvist *in vitro*. Det er ydermere blevet dokumenteret, at subinhibitoriske koncentrationer af ellers toksiske metabolitter kan fremkalde et respons i omkringliggende mikroorganismer. Derfor forventes det, at rollen af disse kemiske stoffer formegentlig ekspanderer til langt mere end blot antimikrobiel aktivitet i deres naturlige miljøer.

Fokus for denne PhD har været på jord-Pseudomonader, især arter fra *Pseudomonas fluorescens*-gruppen, eftersom de har et enormt potentiale med hensyn til produktion af diverse sekundære metabolitter, samt at visse arter i denne gruppe er knyttet til beskyttelse af planter mod patogene mikroorganismer, grundet deres produktion af netop sekundære metabolitter. Vi har specifikt fokuseret på tre metabolitter (DAPG, pyoluteorin og orfamid A), der alle produceres af stammer inden for arten, *P. protegens*, kendt for dens biokontrol-kapacitet. Det arbejde, vi præsenterer her, beskriver rollen af disse metabolitter i forbindelse med mikrobielle interaktioner, samt effekterne af netop interaktioner på biosyntesen og skæbnen af metabolitterne.

Vi har udviklet to metoder til at kunne skelne præcist og effektivt mellem *Pseudomonas* arter i jordprøver. Den første er en *Pseudomonas*-specifik amplikon sekventerings metode, som kan benyttes til taksonomisk identificering og relativ kvantificering af *Pseudomonas* arter. Vores metode udkonkurrerer klart den ellers velkendte og vidt benyttede 16S rRNA-baserede metode til differentiering mellem nært beslægtede *Pseudomonas* arter. Derudover, har vi genetisk konstrueret en levende biosensor, hvilket er en bakterie-celle udviklet til at respondere på tilstedeværelsen af DAPG. Det åbner muligheden for at screene jord-isolater for producenter af DAPG på en effektiv og økonomisk måde, hvilket er en klar fordel sammenlignet med ellers arbejdskrævende PCR-baserede teknikker og dyre analytisk kemiske metoder. Disse to værktøjer (*Pseudomonas*-specifik amplikon sekventering og DAPG-biosensor) muliggør detaljerede undersøgelser af populations-dynamikker blandt *Pseudomonas* arter på tværs af økosystemer (f.eks. forskellige afgrøder eller jordtyper).

Vi har ydermere studeret rollen af *Pseudomonas*-producerede sekundære metabolitter i forbindelse med mikrobielle interaktioner ved brug af en kombination af analytisk kemi og enten to- eller flerarts

---

mikrobielle systemer. I det første af disse studier opdagede vi en dynamisk interaktion mellem to *Pseudomonas* arter, der sekventielt påvirkede produktionen af de antimikrobielle metabolitter, DAPG og pyoluteorin, i *P. protegens*. I dette studie demonstrerede vi den underliggende mekanisme bag en *Pseudomonas*-specifik interaktion, der påvirker biosyntesen af metabolitter med relevans for biokontrol af plantepatogene mikroorganismer. I det sidste studie benyttede vi et syntetisk, reproducerbart mikrobielt system bestående af fire forskellige bakterier til at undersøge, hvorvidt sekundære metabolitter produceret af den invaderende *P. protegens* havde udtalte effekter på systemets bakterie-mæssige sammensætning. Resultater fra dette studie påviste en interaktion involverende forskellige bakterie-arter, der påvirkede skæbnen af den *Pseudomonas*-producerede metabolit, orfamid A. Vi opdagede at metabolitten først blev enzymatisk inaktiveret af én bakterie, hvorefter en eller flere andre bakterier var i stand til at nedbryde den. Totalt set, har vi demonstreret vigtigheden af at kombinere både to- og flerarts systemer *in vitro* på laboratorie-skala og analytisk kemi for at undersøge og karakterisere de forskellige typer af interaktioner, der påvirker eller forårsages af sekundære metabolitter.

Arbejdet præsenteret i denne afhandling tilføjer ny viden omkring de potentielle roller af *Pseudomonas*-producerede sekundære metabolitter, samt værktøjer til detaljerede undersøgelser af *Pseudomonas*-baseret økologi. Set fra et bioteknologisk perspektiv, kan vores resultater bidrage til opdagelse og isolering af nye *Pseudomonas*-arter til brug inden for landbrug i form af biokontrol. Derudover bidrager resultaterne også til en dybere forståelse af metabolit-baseret signalering mellem bakterier, hvilket i sidste ende kan hjælpe til at designe og sammensætte konsortier af mikroorganismer med ønsket funktionalitet til mere effektiv biokontrol.

---

## Acknowledgements

I would like to express my gratitude to my supervisors, Lars Jelsbak and Ling Ding, and the Center for Microbial Secondary Metabolites (CeMiSt) for giving me the opportunity to do this PhD. I am especially thankful for my supervisor, Lars. You always had time for questions and discussions, even during holidays. I have truly learned a lot from your guidance over the course of the three years.

Special thanks go to the co-authors of all the papers, both students and faculty members. Particularly, the people in the natural products group (Mario Wibowo, Scott A. Jarmusch, and Aaron J.C. Andersen), who have contributed not only with amazing collaborations, but certainly also with their incredible patience while advising a molecular microbiologist on analytical chemistry. Secondly, thanks go to Mikael Lenz Strube for organizing two excellent CeMiSt-sponsored workshops on bioinformatics enabling the buildup of a pipeline for genome assembly and for continuous guidance on statistical analyses. Lastly, thanks to all the members of CeMiSt for a truly inspiring environment with great discussions (especially Lone Gram and Thomas Ostenfeld Larsen for their scientific input throughout the years).

Thanks also go to the talented students that I was fortunate enough to supervise throughout the years and for their amazing contributions to the work of this PhD. So, thank you Zhiming He, Jonas Greve Lauritsen and Zsófia Dènes. The project would never have turned out the way it has, without you.

I would also like to express my appreciation for the past and present people in and around the Infection Microbiology Group, who all contributed to making the three years a truly enjoyable time. First, my office-buddy, Mikkel Anbo, for daily banter and scientific discussions. Next, Amalie Møller Hillman for her positive attitude, yet occasionally (too) talkative persona. Thanks also go to Grith Maigaard Hermansen for amazing supervision during my time as Master student and inspiring me to pursue a PhD position. And lastly, our laboratory technician, Susanne “Søs” Koefoed, who contributed to make life around the lab less complicated – something that I truly came to appreciate, as she retired (too early!).

Then came corona... First of all, I would like to thank the developers of Zoom (although they might never read this) for potentiating continuous group meetings, supervisor discussions, and even conferences, despite a global pandemic. Secondly, thanks go to Mikael Kühl for taking his time to

---

supervise my “exotic” external stay at the Marine Biological Section in Elsinore and showing me around their beautiful harbor area.

I am truly grateful for the people taking their time to read through and comment on this thesis: Povilas “Paul” Sazinas, Sabrina M. Pittroff, Amalie, and Grith.

Last, but not least, my deepest gratitude goes to my family for their continuous love and support. You never stopped believing in me and this work is partly your achievement as well.

---

# Contents

PREFACE	I
ABSTRACT	II
RESUMÉ	IV
CONTENTS	VIII
LIST OF PUBLICATIONS	X
ABBREVIATIONS	XI
LIST OF FIGURES	XII
<b>CHAPTER 1   INTRODUCTION</b> .....	<b>1</b>
AIM OF THE PROJECT	2
OUTLINE OF THIS THESIS	3
<b>CHAPTER 2   THE <i>PSEUDOMONAS FLUORESCENS</i> GROUP AND THEIR ASTONISHING DIVERSITY</b> .....	<b>4</b>
THE DIVERSITY OF THE <i>PSEUDOMONAS</i> GENUS	5
THE GENETIC POTENTIAL OF THE <i>P. FLUORESCENS</i> GROUP	7
DETECTING <i>PSEUDOMONAS</i> -DIVERSITY IN NATURAL ENVIRONMENTS	9
<b>CHAPTER 3   <i>PSEUDOMONAS</i>-PRODUCED SECONDARY METABOLITES</b> .....	<b>10</b>
2,4-DIACETYLPHLOROGLUCINOL (DAPG)	12
PYOLUTEORIN	13
ORFAMIDE A	17
DETECTING SECONDARY METABOLITES AND THEIR PRODUCERS	19
<b>CHAPTER 4   MICROBIAL INTERACTIONS AND THE ROLE OF <i>PSEUDOMONAS</i>-PRODUCED SECONDARY METABOLITES</b> .....	<b>23</b>
MICROBIAL INTERACTIONS AND THEIR ECOLOGICAL EFFECTS	25
BIOTRANSFORMATION OF SECONDARY METABOLITES	28
THE SYNCOM APPROACH	29
<b>CHAPTER 5   PRESENT INVESTIGATIONS – RESULTS AND DISCUSSION</b> .....	<b>32</b>
PAPER 1   IDENTIFICATION AND DIFFERENTIATION OF <i>PSEUDOMONAS</i> SPECIES IN FIELD SAMPLES USING AN <i>rpoD</i> AMPLICON SEQUENCING METHODOLOGY	33
PAPER 2   A WHOLE-CELL BIOSENSOR FOR DETECTION OF 2,4-DIACETYLPHLOROGLUCINOL (DAPG)-PRODUCING BACTERIA FROM GRASSLAND SOIL	36
PAPER 3   COMMUNICATION IS KEY: SEQUENTIAL INTERSPECIES INTERACTIONS AFFECT PRODUCTION OF ANTIMICROBIAL SECONDARY METABOLITES IN <i>PSEUDOMONAS PROTEGENS</i> DTU9.1	39

---

PAPER 4   COUNTER-ACTING <i>PSEUDOMONAS</i> INVASION: COMMUNITY-LEVEL RESISTANCE TOWARDS <i>PSEUDOMONAS</i> -PRODUCED SECONDARY METABOLITES	42
CHAPTER 6   <b>CONCLUSIONS AND PERSPECTIVES</b>	45
<b>BIBLIOGRAPHY</b>	48
CHAPTER 7   <b>RESEARCH PAPERS</b>	59

---

## List of Publications

J. G. Lauritsen, **M. L. Hansen**, P. K. Bech, L. Jelsbak, L. Gram, and M. L. Strube, Identification and Differentiation of *Pseudomonas* Species in Field Samples Using an rpoD Amplicon Sequencing Methodology. *mSystems* **6**, e00704-21 (2021).

**M. L. Hansen**, Z. He, M. Wibowo, and L. Jelsbak, A Whole-Cell Biosensor for Detection of 2,4-Diacetylphloroglucinol (DAPG)-Producing Bacteria from Grassland Soil. *Appl. Environ. Microbiol.* **87**, e01400-20 (2021)

**M. L. Hansen**, M. Wibowo, S. A. Jarmusch, T. O. Larsen, and L. Jelsbak, Communication is key: Sequential interspecies interactions affect production of antimicrobial secondary metabolites in *Pseudomonas protegens* DTU9.1. *Submitted* (2021)

**M. L. Hansen**, Z. Dènes, M. Wibowo, S. A. Jarmusch, A. J. C. Andersen, M. L. Strube, and L. Jelsbak, Counter-acting *Pseudomonas* invasion: Community-level resistance towards *Pseudomonas*-produced secondary metabolites. *In preparation* (2021)

## Not included in this thesis

G. M. M. Hermansen, **M. L. Hansen**, S. M. H. Khademi, and L. Jelsbak, Intergenic evolution during host adaptation increases expression of the metallophore pseudopaline in *Pseudomonas aeruginosa*. *Microbiology* **164**, 1038–1047 (2018)

P. Sazinas, **M. L. Hansen**, M. I. Aune, M. H. Fischer, and L. Jelsbak, A Rare Thioquinolobactin Siderophore Present in a Bioactive *Pseudomonas* sp. DTU12.1. *Genome Biol. Evol.* **11**, 3529–3533 (2019)

---

## Abbreviations

SM	Secondary metabolite
DNA	Deoxyribonucleic acid
RNA	Ribonucleic acid
MLSA	Multilocus sequence alignment
ANI	Average Nucleotide Identity
PCR	Polymerase chain reaction
BGC	Biosynthetic gene cluster
PG	Phloroglucinol
MAPG	Monoacetylphloroglucinol
DAPG	2,4-Diacetylphloroglucinol
PKS	Polyketide synthase
NRPS	Non-ribosomal peptide synthase
CLP	Cyclic lipopeptide
HPLC	High-pressure liquid chromatography
MS	Mass-spectrometry
MSI	Mass-spectrometry imaging
SynCom	Synthetic community
HR-LCMS	High-resolution liquid chromatography-mass spectrometry

---

## List of figures

Figure 1 | Maximum likelihood phylogeny of *Pseudomonas* spp. based on protein sequences of 100 single-copy orthologous genes

Figure 2 | Comparing total genome, core, and pangenome size of the 166 *Pseudomonas* type strains

Figure 3 | The functions of *Pseudomonas*-produced SMs

Figure 4 | DAPG biosynthesis

Figure 5 | Pyoluteorin biosynthesis

Figure 6 | Biosynthesis of DAPG and pyoluteorin is interlinked

Figure 7 | Biosynthesis of orfamide A

Figure 8 | The concept of whole-cell biosensors

Figure 9 | *Pseudomonas* spp. richness stimulates antifungal response *in vivo*

Figure 10 | The helper bacteria, *Mycetocola* spp., halt and disarm mushroom pathogen by enzymatic inactivation of cyclic lipopeptides

Figure 11 | Comparing the *rpoD*-based and the standard 16S *rRNA* amplicon sequencing approach

Figure 12 | Utilizing an engineered whole-cell DAPG biosensor for detection of DAPG-producing bacteria

Figure 13 | Sequential interspecies interaction affect SM-production in *P. protegens* DTU9.1

Figure 14 | Microbial interaction between *R. globerulus* and *P. protegens* resulting in enzymatic inactivation of orfamide A

# Chapter 1

## Introduction

**M**icrobial secondary metabolites (SMs) have historically been acknowledged for their antibiotic properties, and have thus been exploited by mankind for the treatment of infectious diseases in both humans and plants. However, despite their high impact in medicinal fields, the scope of these chemicals in natural environments is extremely vast, having functions and roles that expand much beyond microbial antagonism. Research has already demonstrated additional traits of SMs, including their involvement in microbial signaling (1, 2), bacterial motility (3), acquisition of trace metals (4), and even serving as food source for other microbes (5). Technological advances within the field of DNA sequencing and genome mining have greatly improved our ability to elucidate microbial community structures and their SM potential. Yet, our knowledge of microbial interactions mediated by SMs remains limited.

Soil and rhizosphere environments have been predicted to encompass the highest diversity of microorganisms (6). Particularly, the genus of *Pseudomonas* and more specifically the group of *Pseudomonas fluorescens* have received a great deal of attention due to their omnipresence in natural soil environments (7), as well as their vast repertoire of SMs with relevance to plant growth promotion and biological control of pathogenic microorganisms (8, 9). While previous research has surveyed the secondary metabolome of *Pseudomonas* spp., the functions, role, and fate of these *Pseudomonas*-produced SMs has yet to be elucidated in the context of microbial interactions.

## Aim of the project

The PhD project was carried out in collaboration with the Center for Microbial Secondary Metabolites, which represents an interdisciplinary research center with a joint goal of unravelling the natural role of SMs. Thus, the purpose of this project has been:

Purpose | Provide novel insight into the natural role(s) of *Pseudomonas*-produced SMs

The experimental investigations of this project focused primarily on SMs produced by known *Pseudomonas* biocontrol agents. The overall aims of the research presented in this thesis were as follows:

Aim | Investigate the ecological dynamics of soil *Pseudomonas* and their SM-production

To this end, we developed a *Pseudomonas*-specific amplicon sequencing approach for characterization of natural environments with respect to taxonomic differentiation and relative bacterial enumeration (Paper 1). Secondly, we engineered a whole-cell biosensor for detection of an industrially important *Pseudomonas*-produced SM (Paper 2).

Aim | Characterize the role of *Pseudomonas*-produced SMs in microbial interactions

To address this aim, we investigated the interspecies interactions between two *Pseudomonas* strains and their effects on SM-production (Paper 3). Secondly, we applied a synthetic community approach to address the contribution of *Pseudomonas*-produced SMs on the ability of *P. protegens* to invade a microbial community, which further revealed the effect of a microbial resistance mechanism on the fate of a *Pseudomonas*-produced SM (Paper 4).

## Outline of this thesis

The thesis is structured in 7 chapters, where the opening Chapter 1 introduced the background for the PhD thesis along with the overall research aims. Chapter 2 introduces the *Pseudomonas* diversity and the complex *Pseudomonas fluorescens* group. Chapter 3 provides an overview of the relevant *Pseudomonas*-produced SMs examined in the present investigations. Chapter 4 presents current knowledge of the role of *Pseudomonas*-produced SMs in microbial interactions and a promising, alternative approach to investigate the effects of SM-mediated interactions. Background information for the individual research papers is presented in Chapter 5 along with a representation and discussion of the main findings, while conclusions and perspectives of the research papers and the project as a whole are provided in Chapter 6. The final Chapter 7 includes the four full-length research papers.

## Chapter 2

### The *Pseudomonas fluorescens* group and their astonishing diversity

*Pseudomonas* is a genus comprised of Gram-negative, rod-shaped,  $\gamma$ -Proteobacteria known for their metabolic versatility and natural presence in various niches. These bacteria have been studied extensively and have proven to be excellent model organisms. *Pseudomonas* are associated with different environments and properties. For instance, *P. aeruginosa* is a well-characterized opportunistic pathogen playing a detrimental role in chronic infections of cystic fibrosis patients (10). The species *P. putida* has been exploited in biodegradation of natural products and transformation of industrially relevant chemicals (11). Some species of *Pseudomonas* (*P. tolaasii* and *P. syringae*) are known for their plant pathogenicity (12, 13), while other species within the Pseudomonadaceae family have been associated with the suppression of plant diseases caused by phytopathogens (7). Particularly the latter case has received a great deal of attention over the past two decades, as the utilization of plant-beneficial bacteria offers a much-needed alternative to the use of hazardous chemical pesticides in the control of phytopathogenic microorganisms. A tremendous amount of research has been conducted to demonstrate the capabilities of various *Pseudomonas* spp. in relation to plant growth-promotion and biocontrol mediated by SMs (8, 14). However, due to the challenge of studying multispecies interactions, knowledge of the natural ecological role of *Pseudomonas*-produced SMs has remained relatively sparse.

## The diversity of the *Pseudomonas* genus

Bacterial diversity represents one of the central topics of microbial ecology. Understanding the microbial diversity is a key factor in the study of natural environments and their microbial inhabitants. Taxonomy, which encompasses the characterization and nomenclature of microbial species, is perhaps the most fundamental scientific discipline within the field of microbial ecology and is essential for accurate identification and differentiation of strains, as well as communication and collaboration across research groups. The *Pseudomonas* genus is among one of the most diverse bacterial genera currently comprising 270 validly published species (15). The advent of gene sequencing technologies enabled the comparison of divergent microorganisms by assessing similarities in universally distributed genes, such as the 16S rRNA gene encoding the small subunit ribosomal RNA in bacteria (16, 17). While this approach has provided extensive insight into the taxonomic characterization of the bacterial kingdom, it has proven inadequate for distinguishing closely related entities at the species and strain level (18). In the case of *Pseudomonas* spp., it has been shown that the nucleotide similarity of the 16S rRNA gene across distantly related species in many cases exceeds 99% (19), which underlines the inadequacy of this universal marker for proper taxonomic description of the *Pseudomonas* genus.

Since sequencing of the 16S rRNA gene has been the gold standard for taxonomic identification for several decades, it has led to multiple cases of misclassification within the *Pseudomonas* genus (20). Thus, researchers alluded to housekeeping genes as alternative phylogenetic markers, including *rpoD* (encoding the sigma 70 subunit of RNA polymerase), *gyrB* (encoding the beta-subunit of gyrase), and *rpoB* (encoding the beta-subunit of RNA polymerase) (19, 21–23). These genes display a much greater nucleotide dissimilarity – even among closely related species (21). Mulet et al. demonstrated that considering several phylogenetic markers simultaneously with the Multilocus Sequence Analysis (MLSA) method, the taxonomic identification of novel *Pseudomonas* isolates could be reliably inferred (21). This approach greatly enhanced our understanding of the *Pseudomonas* taxonomy and led to the identification of groups and subgroups within the genus (21, 23).

The technological advances within the field of genome sequencing and phylogenomics have enabled more sophisticated analyses of bacterial taxonomy. The housekeeping genes utilized in MLSA are part of the core genome, whereas certain phylogenomic approaches, such as the Average Nucleotide

Identity (ANI), estimate similarities across entire genomes (24). This has the potential to reveal significant differences between closely related species, which may have phenotypical characteristics represented outside the core genome. As the number of available genome sequences has increased rapidly over the past decade, efforts have been made to fully capture the diversity of the *Pseudomonas* genus by analyzing a large set of known type strains. This would in turn create a robust framework for identification of novel species isolates. Hesse et al. compared the phylogeny of 166 type strains of *Pseudomonas* spp. by constructing a maximum likelihood tree based on the protein sequence of 100 single-copy orthologous genes (25). This analysis confirmed the remarkable diversity of the *Pseudomonas* genus as shown previously using smaller datasets and less advanced methods (21, 23). Furthermore, the 165 type strains (excluding the unusual species, *P. caeni*) have been utilized for taxonomic characterization throughout this PhD project.

Secondly, Hesse et al. sought to evaluate how well the 166 type strains represented the genomic diversity of the *Pseudomonas* genus among the publicly available genomes (25). This approach revealed 350 clusters, where 189 of them lacked the presence of a type strain, thus potentially representing novel species of *Pseudomonas* (Figure 1). The *P. fluorescens* group has long been recognized for its vast diversity (21, 22), which has led to the classification of several subgroups. However, as shown in Figure 1, the analysis of publicly available *Pseudomonas* genomes further identified 105 clusters within the *P. fluorescens* group without association to a known type strain (depicted in Figure 1 as branches without a black box in the outer ring) (25). Most novel clusters fell within existing subgroups, except for four located between the *P. protegens* and *P. corrugata* subgroups, suggesting the potential for a new *P. fluorescens* subgroup. This does however indicate that the 166 type strains analyzed by Hesse et al. (25) represent an adequate framework for taxonomic identification of novel *Pseudomonas* entities, but continuous efforts are required to uncover the complete genomic diversity of the genus.

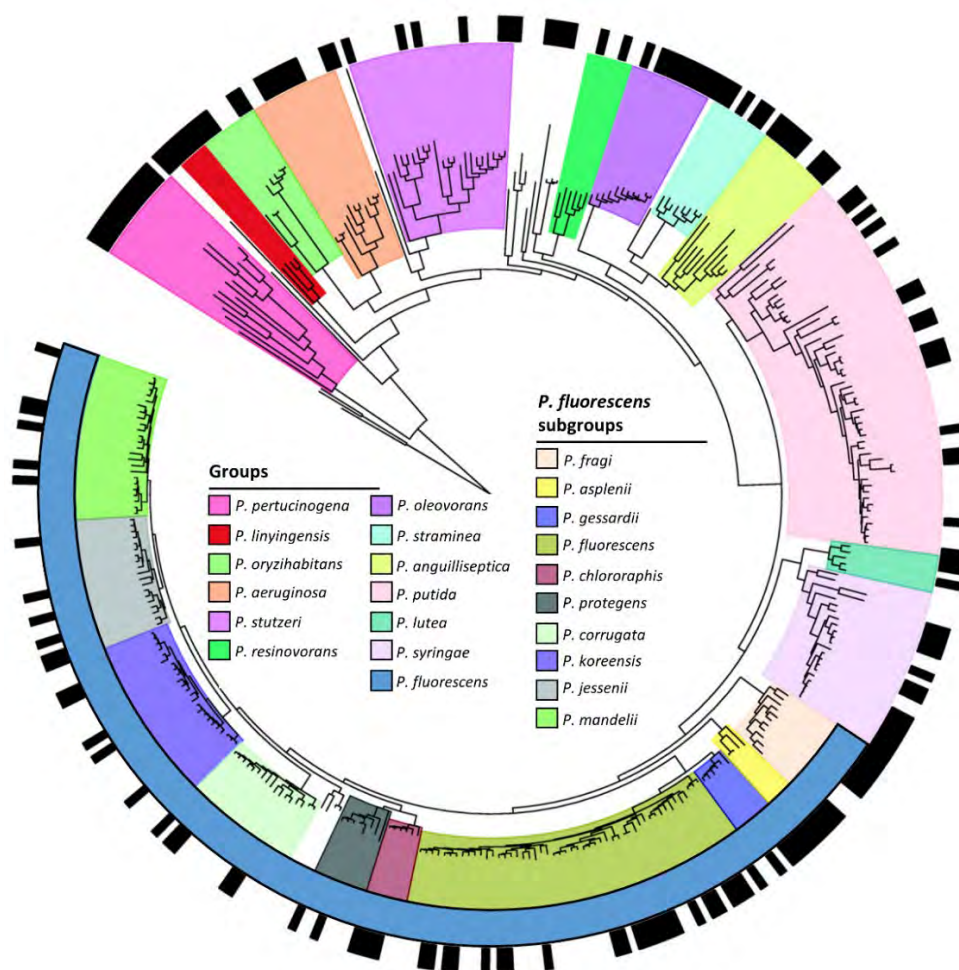


Figure 1 | Maximum likelihood phylogeny of *Pseudomonas* spp. based on protein sequences of 100 single-copy orthologous genes. The phylogenetic tree includes 355 strains of *Pseudomonas* spp., where 166 of them represent known type strains. Phylogenetically distant groups are highlighted in separate colors. The diverse group of *P. fluorescens* is further divided into ten subgroups. Type strains are highlighted by a black box in the outer ring. Three genomes of *Cellvibrio* spp. were included as outgroup. The figure has been adapted and modified from Hesse et al. (25).

## The genetic potential of the *P. fluorescens* group

Several species of the *P. fluorescens* group have previously been associated with plant growth-promoting properties and production of SMs relevant for biocontrol (14, 26). Previously, efforts have been made to further characterize the heterogeneity within the *P. fluorescens* group utilizing phylogenomic approaches (22, 27). Hesse et al. showed that species belonging to the *P. fluorescens* group have some of the largest genomes within the *Pseudomonas* genus (Figure 2A) (25). The vast genomic diversity of *Pseudomonas* spp. is reflected by the relatively small size of the core genome shared among the various species (8, 25). The core genome comprises genes essential for bacterial

proliferation, such as housekeeping genes and those encoding RNAs. The accessory pangenome comprises group-, subgroup-, and species-specific genes, including biosynthetic gene clusters (BGCs) encoding enzymes required to produce SMs.

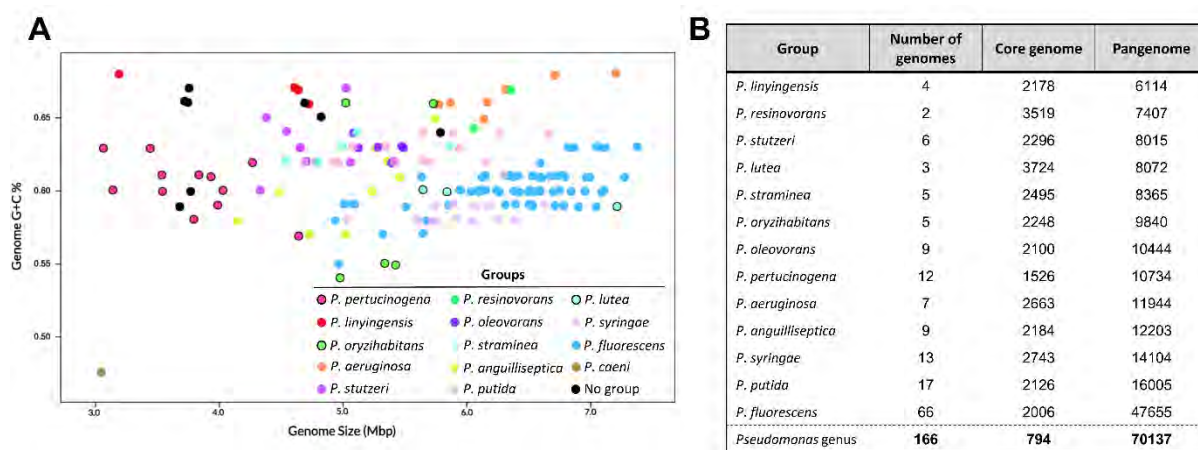


Figure 2 | Comparing total genome, core, and pangenome size of the 166 *Pseudomonas* type strains. **A**) Relationship between genomic G+C content and genome size. Each phylogenetic group is highlighted by color, as depicted in the figure. **B**) Identification and enumeration of orthologous proteins constituting the core and pangenome across the 13 phylogenetic groups comprising the *Pseudomonas* genus. The figure has been adapted and modified from Hesse et al. (25).

It was demonstrated that the pangenome size of the *P. fluorescens* group greatly exceeded that of the remaining groups (25). Although biased by the number of genomes analyzed per group, this suggests an immense and diverse genetic potential of this particular phylogenetic group (Figure 2B). It was demonstrated that specific traits, such as production of biocontrol-relevant SMs, siderophores, toxins, and SMs related to plant-microbe interactions, were phylogenetically distributed and in many cases specific to individual subgroups (22, 27). Surprisingly, Garrido-Sanz et al. further identified striking correlations between the topology derived from MLSA and phylogenomic analyses of the diverse *P. fluorescens* group (22). Additionally, the phylogeny based on genetic loci for two SMs involved in biological control was shown to be reminiscent of that based on housekeeping genes (28). Taken together, these findings suggest that ecological characteristics represented by the accessory pangenome evolved alongside the core genome of *Pseudomonas* (22, 28). This further underlines that accurate taxonomic identification is a good proxy for prediction of species-associated, ecological traits within the *Pseudomonas* genus. More recently, Stefanato et al. genetically and phenotypically analyzed a large population of isolates belonging to the *P. fluorescens* group, identifying strong

correlations between phylogeny, production of SMS, and antagonism towards specific phytopathogenic microorganisms (9). Collectively, these studies underline the importance of systematically considering bacterial taxonomy to accurately describe the *Pseudomonas* diversity in natural environments and elucidate their ecological role.

## **Detecting *Pseudomonas*-diversity in natural environments**

An important aspect of microbial ecology is the investigation of microbial community composition and species abundance. With the advent of next-generation sequencing technologies, exploiting the universal presence and high nucleotide variability of the 16S rRNA gene has been the gold standard for detection and identification of bacteria (17, 29). Amplicon sequencing, which is the combination of environmental DNA extraction, amplification via polymerase chain reaction (PCR), next-generation Illumina sequencing, and alignment to an ever-expanding public database of 16S rRNA genes (30), has significantly improved our understanding of natural environments. Aside from gaining insight into the relative abundance of microbes *in situ*, this technique has pushed the boundaries of microbial detection by allowing for the identification of yet unculturable microorganisms (17). However, as alluded to above, the 16S rRNA gene has proven insufficient for accurate taxonomic characterization at the species level of *Pseudomonas*.

Mulet et al. suggested the single housekeeping gene, *rpoD*, as an excellent phylogenetic marker for the identification of *Pseudomonas* species in environmental samples (31). Additionally, by comparing the phylogenetic distances across 107 *Pseudomonas* type strains, the *rpoD* gene displayed the highest discriminatory power compared to the other housekeeping genes (*gyrB* and *rpoB*), as well as 16S rRNA (21). These early studies led to the development of an *rpoD*-based amplicon sequencing approach for the 454/Roche GS-FLX platform, which allowed for *Pseudomonas*-specific, culture-independent characterization of environmental samples (32). However, this sequencing platform was later discontinued. Thus, with the increasing appreciation for group-, subgroup-, and even species-specific traits associated with *Pseudomonas* spp. (9, 22), there is a need for developing a culture-independent, amplicon-based methodology. We developed such an approach utilizing the modern Illumina sequencing platform for detection and differentiation of *Pseudomonas* species in natural environments (Chapter 7 | Paper 1).

## Chapter 3

### ***Pseudomonas*-produced secondary metabolites**

The flexibility of the *Pseudomonas* spp. pangenome (Figure 2B) indicates that individual strains have evolved to specific life-styles (8). This suggests that accessory functions, such as SM production, could play essential roles in the ability of *Pseudomonas* species to adapt to specific environments. The secondary metabolism of the *P. fluorescens* group has been studied extensively, due to the associations between members of this diverse group of bacteria, plant growth-promotion and biological control of phytopathogens mediated by SMs (14, 26). These SMs include diffusible metabolites and volatiles. The first group of diffusible SMs are the siderophores, such as the pyoverdines and pyochelin, which are capable of scavenging metal ions from the limited pool of trace metals available in soil (4, 14). Members of the *P. fluorescens* group have furthermore been shown to produce a plethora of small, diffusible, and antimicrobial SMs, including 2,4-diacetylphloroglucinol (DAPG), pyoluteorin, pyrrolnitrin, and phenazines (14, 26). Another group of metabolites often found in *Pseudomonas* species are the cyclic lipopeptides with surfactant and antimicrobial properties (3, 33). Lastly, certain *Pseudomonas* spp., including members of the *P. fluorescens* group, produce the volatile compound, hydrogen cyanide, which is a potent inhibitor of the cytochrome *c* oxidase, as well as other metalloproteins, and is therefore poisonous to most organisms (8, 14, 28).

Over the past three decades, a particular focus has been devoted to characterizing strains of the species *P. protegens*, as these bacteria have been directly correlated with natural suppressiveness to disease caused by phytopathogens in various crops. This protective capacity has been attributed to their diverse secondary metabolome (26, 34, 35). Most of these SMs were detected and analyzed chemically. However, the increased accessibility of whole-genome sequences, as well as software for prediction of SM production via conserved domains of biosynthetic genes, such as antiSMASH (36), has revolutionized the field of genome mining for characterization of species isolates and identification of novel SMs. The strain *P. fluorescens* Pf-5 (later *P. protegens* Pf-5) was the first member

of the *P. fluorescens* group to have its genome fully sequenced (37). This led to the identification of three hitherto uncharacterized BGCs, where the SM production of two of them has been deciphered, including the biosynthesis of rhizoxin (38) and the cyclic lipopeptide, orfamide A (39). In the following subsections, the biosynthesis, regulation, and function of DAPG, pyoluteorin, and orfamide A (Figure 3) will be highlighted, as these three SMs have been the focus of our investigations.

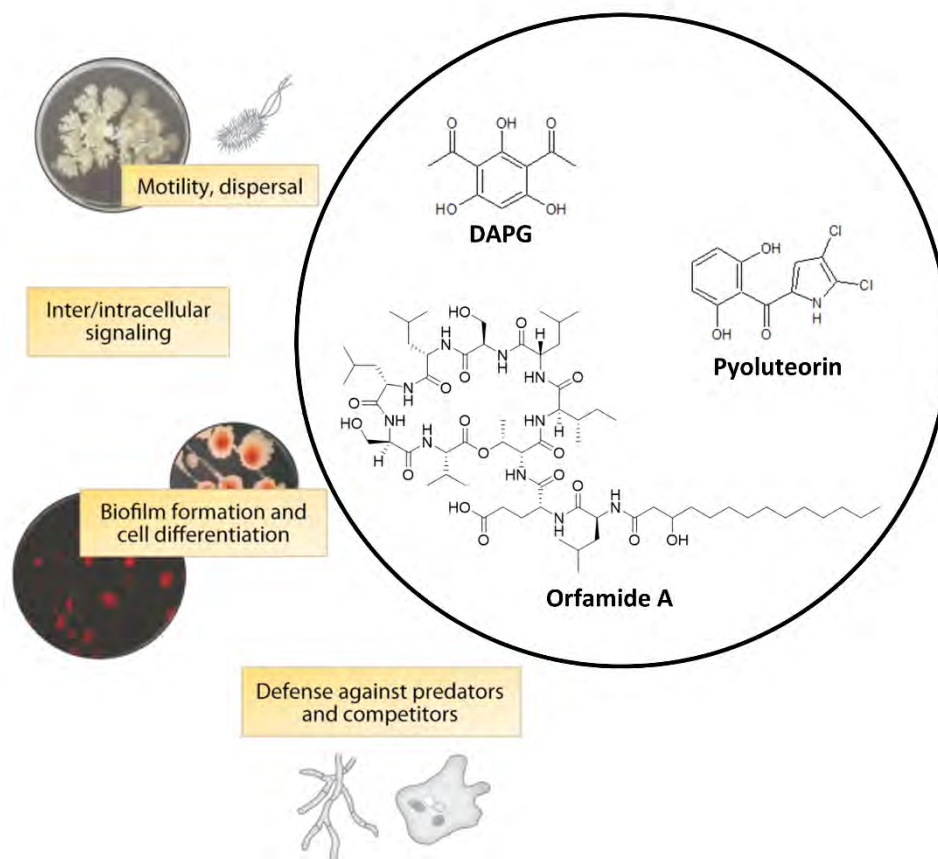


Figure 3 | **The functions of *Pseudomonas*-produced SMs.** The SMs (DAPG, pyoluteorin, and orfamide A) are involved in defense against competitors, intra- and intercellular signaling, motility, and biofilm formation. The image was adapted and modified from Raaijmakers and Mazzola (40).

## 2,4-diacetylphloroglucinol (DAPG)

The antimicrobial SM, DAPG, is primarily produced by a subset of species within the *P. fluorescens* group, which includes many, but not all members of the *P. corrugata* and *P. protegens* subgroups (41). Though, its BGC has also been identified in distantly related *Pseudomonas* species and even outside the  $\gamma$ -proteobacteria class (41). DAPG has been recognized for its antifungal and antibacterial properties (42, 43). Moreover, this metabolite was shown to be a key determinant in natural biocontrol associated with disease-suppressive soils (34, 44). Furthermore, Phillips et al. demonstrated that DAPG triggered a significantly increased exudation of amino acids from certain plant roots, thus providing the DAPG-producing, root-colonizing *Pseudomonas* with additional growth substrates (45).

DAPG is a polyketide antibiotic, whose biosynthesis, regulation, and transport is governed by proteins encoded by a conserved BGC consisting of eight genes (*phIHGFACBDE* – Figure 4). The biosynthesis of DAPG is initiated by the type III polyketide synthase (PKS), PhID, which catalyzes the condensation of three molecules of malonyl-CoA into the phenolic precursor, phloroglucinol (PG) (46). PG is then acetylated by the enzyme complex, PhIACB, first into monoacetylphloroglucinol (MAPG) and subsequently DAPG (Figure 4) (47). Bottiglieri et al. characterized the hydrolase, PhIG, which specifically degrades DAPG to MAPG, suggesting a mechanism for fine-tuning the concentration of DAPG (48).

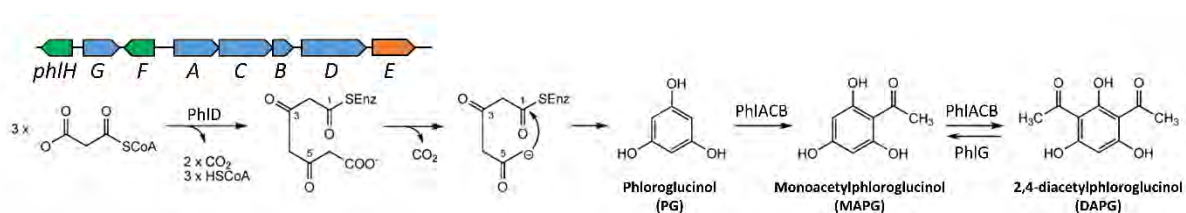


Figure 4 | **DAPG biosynthesis.** (Top part) Schematic overview of the DAPG biosynthetic gene cluster. Genes are depicted as colored arrows (Biosynthetic genes, blue; Regulation, green; Efflux, orange). The bottom part of the figure shows the biosynthesis of DAPG. The figure has been adapted and modified from Gross and Loper (8).

The gene, *phIE*, encodes a putative transmembrane permease that provides resistance towards the antimicrobial metabolite in the producing cell (49). The DAPG gene cluster of *Pseudomonas* also possesses two genes encoding TetR family regulators, *phIF* and *phIH*. PhIF has been shown to repress transcription of the *phIACBDE* operon by binding to an operator site located upstream of *phIA*, thus

negatively controlling the production of DAPG (50). However, DAPG biosynthesis is auto-inductive as it can bind to the PhIF repressor, thereby relieving transcriptional repression (51). PhIH, on the other hand, negatively controls the transcription of *phIG*, and the repression is similarly relieved in the presence of DAPG (52). Thus, DAPG-producing *Pseudomonas* possess intricate and complex ways of fine-tuning the levels of this metabolite. Additionally, studies with the strain *P. protegens* Pf-5 have revealed cross-talk between the DAPG and pyoluteorin biosynthetic pathways further regulating the production of DAPG (53, 54), which will be elaborated below.

## Pyoluteorin

Pyoluteorin is an antimicrobial SM produced by species of *P. protegens* and certain strains of soil-dwelling *P. aeruginosa*. It was historically identified as an anti-oomycete compound against the plant pathogen, *Pythium ultimum* (55, 56). However, it has also been recognized for its antibacterial properties (54). This metabolite differs from conventional polyketide SMs in that it is biosynthesized as a hybrid molecule consisting of a modified amino acid moiety and a polyketide group (8). The biosynthetic gene cluster associated with the production of pyoluteorin is comprised of 17 genes (Figure 5), where the operon consisting of *pltABCDEFGHI* encodes enzymes responsible for biosynthesis. The genes, *pltM*, *pltR*, and *pltZ*, are involved in transcriptional regulation (54, 57), while the operon, *pltHIJKNO*, encodes a putative ABC transport system controlling the efflux of pyoluteorin (58). As shown in Figure 5, the biosynthesis of pyoluteorin initiates with the activation of L-proline by PltF at the expense of adenosine triphosphate (ATP), and subsequent attachment to the peptide-carrier protein (PCP), PltL (59). The flavoprotein, PltE, then desaturates the prolyl moiety, yielding the intermediate, pyrrolyl-S-PltL (60).

Dorrestein et al. further confirmed the subsequent dichlorination by the PltA halogenase, resulting in the final modified amino acid moiety, dichloropyrrolyl-S-PltL (60). Gross and Loper suggested that the dichloropyrrolyl residue is then transferred to the type I PKS, PltB and PltC, where three molecules of malonyl-CoA are added (8). As opposed to the type III PKS, many type I PKS's are categorized as modular enzymes containing sequences of separate elongation modules, each with a number of domains (61). In the case of PltB and PltC, the dichloropyrrolyl residue is transferred to the ketosynthase domain (KS) of module 1 (Figure 5).

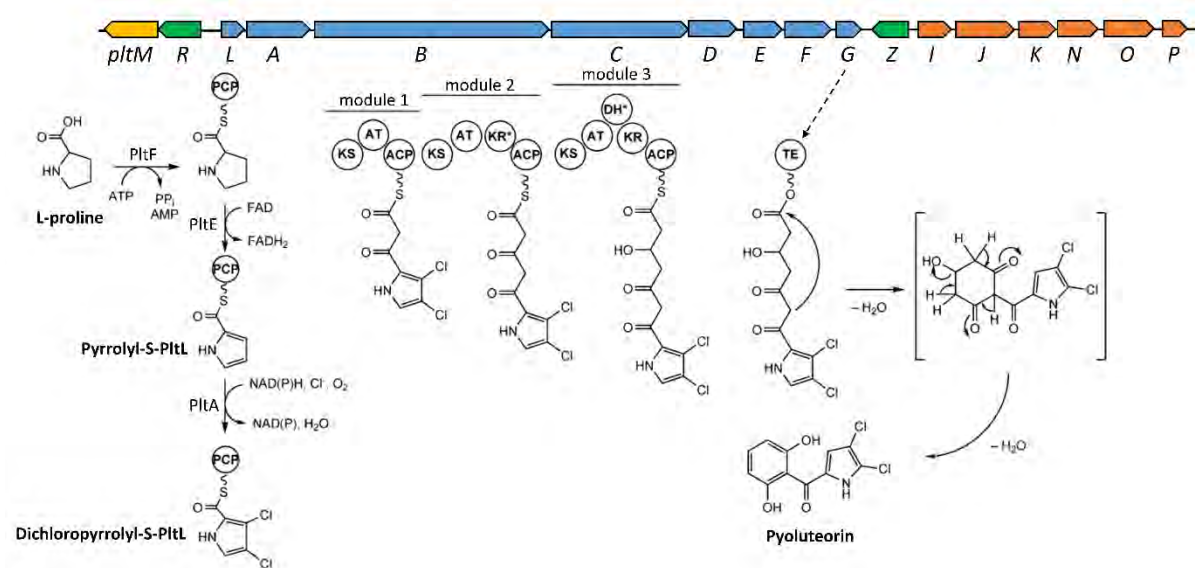


Figure 5 | **Pyoluteorin biosynthesis.** (Top part) Schematic overview of the pyoluteorin biosynthetic gene cluster. Genes are depicted as colored arrows (Biosynthetic genes, blue; Regulation, green; Efflux, orange; PItM halogenase, yellow). The bottom part of the figure shows the proposed biosynthesis of pyoluteorin. Asterisks denote predicted inactive domains in PItB and PItC from *P. protegens* Pf-5. The figure has been adapted and modified from Gross and Loper (8).

Next, a molecule of malonyl-CoA is loaded onto the acyl-carrier protein (ACP), catalyzed by the acyltransferase domain (AT). The dichloropyrrolyl residue located at the KS domain reacts with the malonyl-group in a Claisen condensation reaction, resulting in an elongated polyketide chain. Then, the elongated chain is moved to the next ketosynthase domain (KS) of module 2, where a similar reaction occurs. Module 3, on the other hand, contains an active ketoreductase (KR) domain, catalyzing the reduction of a keto group into a hydroxy group. Finally, the polyketide chain is released and circularized to form a resorcinol ring by the thioesterase, PItG (8), yielding the final product, pyoluteorin. However, as alluded to by Gross and Loper (8) and shown by an asterisk at the respective domain in Figure 5, analysis of the gene sequences in *P. protegens* Pf-5 revealed that PItB contains an inactive KR domain. Likewise, PItC has an inactive dehydratase (DH) domain – a domain, which is capable of catalyzing the dehydration of a hydroxyl-group to form a double bond in the polyketide chain (61). This could suggest that the polyketide originally had a different molecular structure, and mutations occurring through evolution and adaptation have resulted in specific domain inactivation yielding the resorcinol ring and in turn giving rise to the biosynthesis of pyoluteorin. Alternatively, the proposed biosynthetic pathway is incorrect and the domains perceived as inactive are in fact active and catalyzing yet uncharacterized reactions.

Similar to the biosynthesis of DAPG, expression of the pyoluteorin BGC is tightly controlled by the two transcriptional regulators, PltR and PltZ. PltR acts as a LysR family transcriptional activator by binding to the *Pp/ltL* promoter and recruiting the RNA polymerase (54). PltZ, on the other hand, is another transcriptional repressor of the TetR family, which controls the transcription of both the biosynthetic operon (*pltLABCDEFG*, (62)) and the efflux-associated operon (*pltIJKNOP*, (57)). Similar to the DAPG biosynthetic pathway, pyoluteorin acts as an auto-inducer of its own expression by binding to the PltZ repressor (62). However, Yan et al. (54) identified a novel mechanism catalyzed by the halogenase, PltM, mediating cross-talk between the DAPG and pyoluteorin biosynthetic pathways (Figure 6).

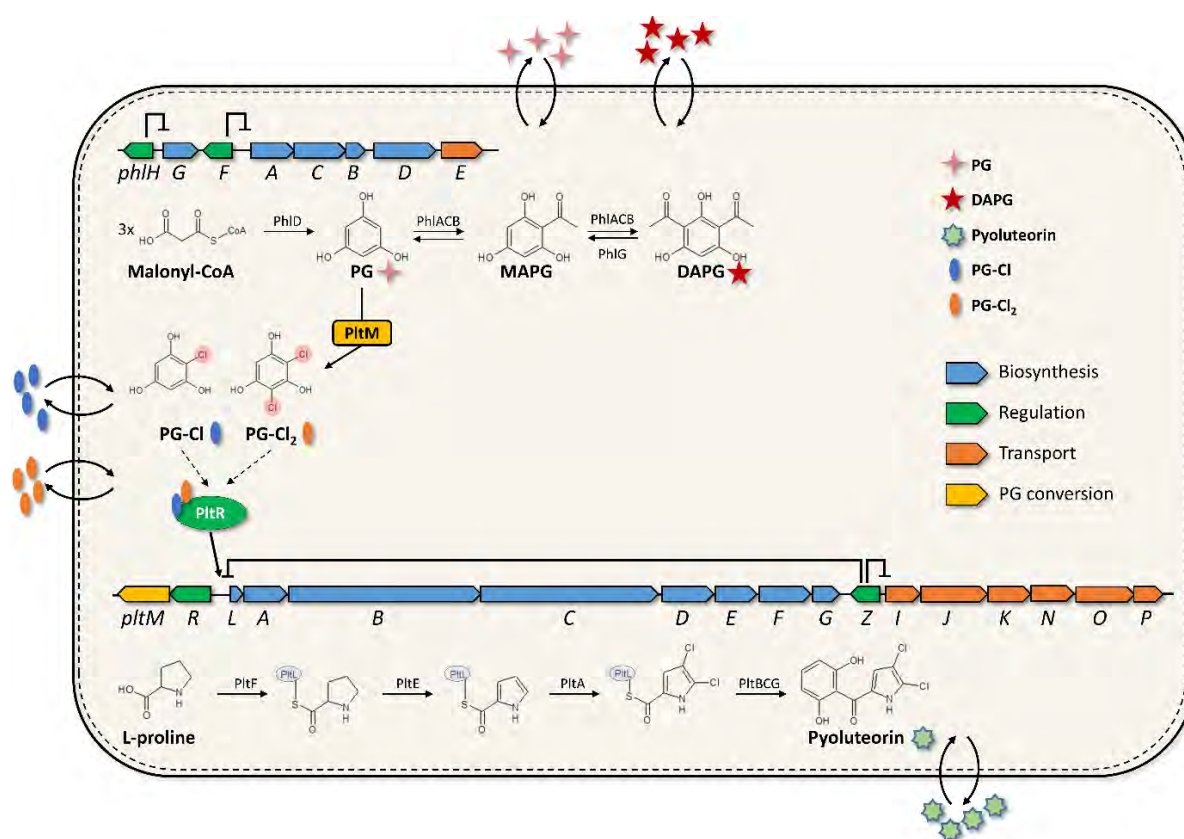


Figure 6 | **Biosynthesis of DAPG and pyoluteorin is interlinked.** PG from the DAPG pathway is converted to PG-Cl and/or PG-Cl<sub>2</sub> by PltM, which in turn activates transcription of the pyoluteorin BGC. PG, DAPG, pyoluteorin, PG-Cl and PG-Cl<sub>2</sub> can be released and function in cell-cell communication. Thick black lines from regulatory genes indicate their transcriptional control (arrow = activation, T-line = repression). The figure has been adapted and modified from Yan et al. (54).

Initially, Kidarsa et al. observed that a  $\Delta phlD$  knockout mutant in *P. protegens* Pf-5 unable to produce PG was incapable of producing DAPG and pyoluteorin (53). This suggested that PG could be involved in the biosynthesis of both metabolites. To rule out the possibility of PG being a substrate in the biosynthesis of pyoluteorin (as it resembles the polyketide group), Kidarsa et al. added purified

resorcinol to cultures of a  $\Delta phlD$  knockout mutant. However, no pyoluteorin production was observed (53). Subsequently, Yan et al. found that PG is converted by PltM to either PG-Cl and/or PG-Cl<sub>2</sub>, which in turn binds to the PltR activator, presumably altering its confirmation and allowing for transcriptional activation of the *plt* biosynthetic operon, as shown in Figure 6 (54).

As indicated in Figure 6, both DAPG and pyoluteorin in *P. protegens* Pf-5 function in intercellular communication, acting as signaling molecules inducing their own biosynthesis (51, 63). Additionally, through clever construction of knockout mutants and cocultivation experiments, it was shown that PG, PG-Cl, and PG-Cl<sub>2</sub> function in cell-cell communication (54, 64), thus acting as intra- and intercellular signaling molecules further governing the fine-tuned expression of DAPG and pyoluteorin. On the other hand, Raaijmakers et al. reported that DAPG-production in the biocontrol agent, *P. fluorescens* Q2-87 (member of the *P. corrugata* subgroup) depended on population-density in the rhizosphere of wheat roots rather than intercellular induction (65). This could indicate an evolutionary distinction between the *P. protegens* and *P. corrugata* subgroups in their ability to modulate SM-production. Taken together, these findings suggest that certain SMs have multiple functions, and increased knowledge of those functions may improve our understanding of their roles in natural environments.

## Orfamide A

Another class of SMs produced by many species of *Pseudomonas* and *Bacillus*, as well as other bacteria are the cyclic lipopeptides (CLPs). This class of metabolites consists of a varied-length oligopeptide chain (8-25 amino acids) and a fatty acid tail, thus representing amphiphilic molecules with a hydrophobic and a hydrophilic moiety (3, 66). As opposed to conventional proteins and enzymes, these metabolites are synthesized by non-ribosomal peptide synthases (NRPSs), which comprise a group of megaenzymes with modular structures similar to the modular type I PKSs reminiscent of an assembly line (67).

Each module normally consists of three domains: A peptide-carrier protein domain (PCP), which holds the activated substrate to be elongated. An adenylation domain (A) responsible for selection of the amino acid utilized for elongation. And lastly, a condensation domain (C), which catalyzes the formation of the peptide bond between the substrate and the amino acid selected by the A domain (67). The amino acid specificity of each adenylation domain is linked to a conserved stretch of residues within the protein domain (68), which has enabled the bioinformatic deduction of CLP structure based on DNA sequence with software such as antiSMASH (36). The lipid moiety of the CLP molecule is believed to be introduced via *N*-acylation to the first amino acid comprising the oligopeptide chain catalyzed by the first condensation domain (3, 66). As the elongated lipopeptide reaches the end of the assembly line at the PCP domain of the final module, it is released and cyclized by one or in some cases a tandem of thioesterase (TE) domains (66). The TE domain catalyzes the cyclization of the oligopeptide chain resulting in the formation of a macrocyclic ring. Raaijmakers et al. ascribed the diversity in peptide ring size associated with CLPs from various *Pseudomonas* spp. to the high degree of specificity of the TE domain, as it selectively catalyzes cyclization between specific amino acid residues (69).

In the case of *P. protegens*, a new class of *Pseudomonas*-produced CLPs, the orfamides, were isolated and characterized by Gross et al. utilizing a genomisotopic approach with <sup>15</sup>N-labeled leucine (39), following the identification of a BGC in *P. protegens* Pf-5 predicted to synthesize the novel lipopeptide (37). The BGC is comprised of three genes, *ofaABC*, encoding an NRPS assembly line with ten modules, each containing the classic C-A-PCP domain structure (Figure 7). *In silico* analysis of the adenylation domains allowed for prediction of the amino acid sequence of orfamide A (37), which was

subsequently confirmed by nuclear magnetic resonance (NMR) analysis of the isolated CLP (39). The macrocyclic peptide ring of orfamide A was shown to form via an esterification between the hydroxyl-group of threonine and the carboxylic group of the C-terminal valine (Figure 7). Additionally, the biosynthetic genes involved in orfamide production are flanked by LuxR-type regulators, controlling the expression of the BGC (70), as well as genes encoding efflux proteins (71). These features have been omitted from the BGC displayed in Figure 7.

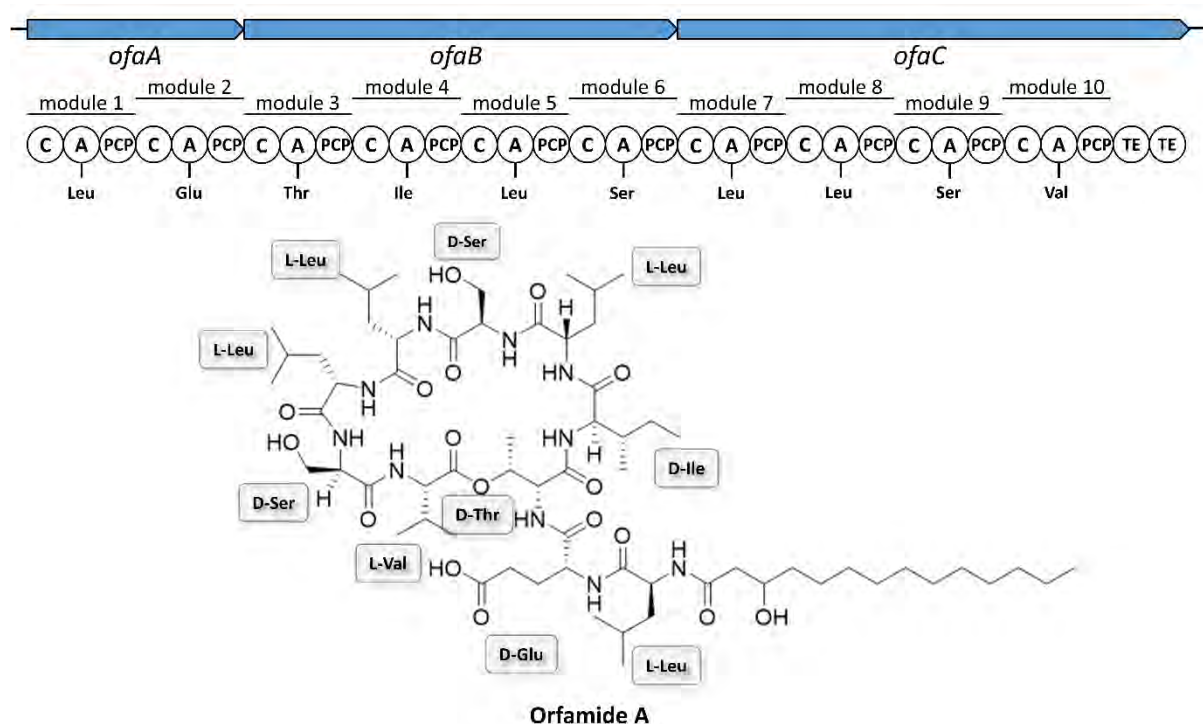


Figure 7 | **Biosynthesis of orfamide A.** (Top part) Schematic overview of the orfamide A biosynthetic gene cluster. Biosynthetic genes are depicted as blue arrows. Each gene encodes an NRPS with several modules, each containing the C-A-PCP architecture. *In silico* analysis has allowed the prediction of selected amino acids by the A domains. (Bottom part) The molecular structure of orfamide A along with the stereoisomeric designation of each amino acid. The figure design was inspired by Gross and Loper (8) and Ma et al. (71).

The *Pseudomonas*-produced CLPs have been shown to be involved in several biological functions. Most notably, CLPs reduce the surface tension of water, thus acting as biosurfactants (3, 33, 66). This, in turn, plays an essential role in bacterial swarming motility, as the lipopeptides reduce the tension between bacterial cells and the surface, which allows for the spread of *Pseudomonas* spp. when combined with their flagella-based motility (3, 66). Moreover, the CLPs affect the formation of microbial biofilms, which are dense aggregates of bacterial cells stabilized by secreted polymers and

polysaccharides. However, depending on the type of CLP, the outcome of biofilm formation may differ (3). The CLP, viscosin, was shown to be crucial in the ability of *P. fluorescens* SBW25 to form biofilm on a polypropylene surface (72). On the other hand, Kruijt et al. demonstrated that wildtype *P. putida* 267 was unable to form biofilm, whereas a knockout mutant incapable of producing the CLP, putisolvin, gained the ability to form a substantial biofilm (73). Interestingly, addition of purified viscosin significantly reduced biofilm formation of the non-viscosin producer, *P. aeruginosa* PAO1, in the early stages of microcolony formation (3), suggesting that *Pseudomonas*-produced CLPs may adversely affect biofilm formation in foreign species.

Lastly, the *Pseudomonas*-produced CLPs (including orfamide A) have antimicrobial properties towards many Gram-positive bacteria and a few Gram-negative ones (33), as well as certain fungi and oomycetes (33, 39). CLPs are thought to incorporate into the cellular plasma membrane, due to their amphiphilic nature, causing perturbations that eventually lead to cell lysis (66). The *Pseudomonas*-produced CLPs, including orfamide A, thus represent intriguing SMs with several biologically relevant functions that could prove essential for the producing bacterium.

## **Detecting secondary metabolites and their producers**

An essential aspect of investigating the ecological dynamics of SM-producers in natural environments is the detection of the metabolite in question or the associated biosynthetic genes. This process can occur either in the laboratory, while testing isolated species, or directly *in situ*. While phylogenetic approaches, as described in Chapter 2, can aid in the prediction of SM-production, they are limited to groupings of species and phenotypic traits based on known type strains and their well-characterized secondary metabolome. Thus, in order to surpass this limitation, researchers have relied on PCR-based or DNA-hybridization techniques for confirming the presence of biosynthetic genes and on analytical-chemical methods for detection of the desired SM. Raaijmakers et al. employed a DNA-hybridization method to enumerate DAPG-producing fluorescent *Pseudomonas* in different soils, showing a clear correlation between the presence of DAPG producers and disease-suppressiveness (74). However, the primers designed in this study did not discriminate between genotypes of *Pseudomonas*. To circumvent that issue, Mavrodi et al. developed a quantitative, culture-independent PCR-based identification technique using multiple genotype-specific primer pairs (75). This allowed for the

detection of two genotypic populations of indigenous DAPG-producing *Pseudomonas* in the rhizosphere of wheat grown in disease-suppressive soil (75). Nevertheless, DNA-based identification techniques are biased towards a collection of known sequences to facilitate appropriate primer design, which could in turn lead to false negative results.

As opposed to DNA-based methods described above, there are also methodologies involving direct detection of a specific metabolite. Certain SMs have unique biochemical properties, such as the high affinity for  $\text{Fe}^{3+}$  ions of siderophores or the presence of a reactive cyanide ion in hydrogen cyanide. These properties have been exploited in the development of chemical detection assays, including the Chrome Azurol S (CAS)-agar plate (76) and the Feigl-Anger paper (77) for detection of siderophore and hydrogen cyanide production, respectively. The presence of the specific metabolite results in a chemical reaction, leading to a visible color change, thus allowing for rapid, cost-efficient, and high-throughput screening of bacterial isolates. However, such biochemical properties are usually rare. Another approach for direct detection of specific SMs involves the exploitation of the regulatory systems associated with transcriptional control of biosynthetic genes in a concept known as *whole-cell biosensors* (78, 79). In general, the simplest biosensor consists of two elements heterologously expressed in a suitable host (79, 80): a constitutively expressed regulatory gene cloned from the SM-producing organism and a reporter gene (such as *gfp* or *lacZ*) cloned downstream of the respective promoter ( $P_{\text{BGC}}$ ) controlled by the regulatory protein (Figure 8).

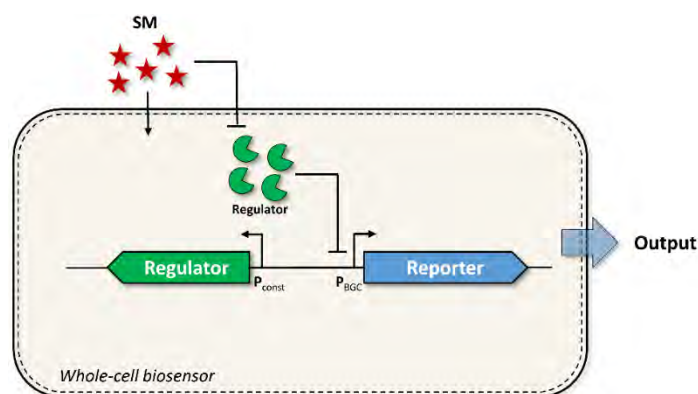


Figure 8 | **The concept of whole-cell biosensors.** Schematic design of a whole-cell biosensor. The biosensor responds to the presence of an SM by relieving the regulator-mediated repression on  $P_{\text{BGC}}$ , which in turn leads to reporter expression and a detectable output.

The regulatory protein is commonly a transcriptional repressor blocking expression of the reporter gene in the absence of the specific SM. On the other hand, if the whole-cell biosensor experiences

sufficient levels of the SM, the repression is relieved, leading to expression of the reporter gene and a visible, quantifiable output (*e.g.* fluorescent or colorimetric). Lautenschläger et al. recently engineered a *Bacillus* whole-cell biosensor for the detection of  $\beta$ -lactam antibiotics and successfully demonstrated the production of  $\beta$ -lactams by a collection of *Streptomyces* soil isolates (81). Sun et al. proposed a more general use of the biosensor concept combined with genome mining for detection of novel SMs (82). Whole-cell biosensors thus represent a promising, genetically engineered, and highly adaptable alternative to chemical assays that enable high-throughput screenings of large collections of species isolates for producers of specific SMs. In the case of *Pseudomonas*-produced SMs, both DAPG (51) and pyoluteorin (63) act as autoinducing metabolites as they interact with the PhIF (50) and PltZ (62) repressor proteins, thus positively regulating the transcription of their respective BGCs. Currently, no efficient screening methods exist for detection of either DAPG or pyoluteorin production. Thus, we engineered a PhIF-based whole-cell biosensor for detection of DAPG to efficiently screen *Pseudomonas* isolates and gain insight into the ecological dynamics of DAPG-producers in natural environments (Chapter 7 | Paper 2).

The last set of methods for directly detecting SMs rely on analytical chemistry. These are powerful techniques allowing for identification and quantification of metabolites. The most common method for analysis of SMs is high-pressure liquid chromatography (HPLC). Metabolites are initially extracted from a biological sample (*e.g.* bacterial culture or soil) and subsequently run through a column containing an adsorbent. The metabolites interact differently with the adsorbent due to physicochemical properties (*e.g.* size or polarity) and are thus separated as the extract is processed through the column. This technique can further be combined with mass-spectrometry (MS) for simultaneous separation and structural identification of metabolites.

HPLC-MS was utilized to detect production of DAPG by indigenous bacteria *in situ* in the rhizosphere of wheat grown in a disease-suppressive soil and could further show a correlation between population density and quantity of DAPG (65). Likewise, pyoluteorin production was observed in the rhizosphere of wheat roots grown in gnotobiotic artificial soil inoculated with *P. protegens* CHA0 (83). Furthermore, by utilizing a combination of PCR-based and HPLC-MS detection, it was shown that DAPG-producing *Pseudomonas* species accumulated to similar population levels in the rhizospheres of different plant species, whereas the production of DAPG was significantly affected by plant species (84). Combined, these studies provided evidence for *in situ* production of DAPG and pyoluteorin in the

rhizosphere of different crops with concentrations ranging from 20-250 ng/g fresh root (65, 83, 84). Detection and quantification of SMs *in situ* is a key feature for investigating the role of SMs in natural environments.

While HPLC-MS indeed is a powerful technique, it has several drawbacks. It utilizes expensive and extremely sensitive equipment, and thus also requires trained personnel to operate. Secondly, the outcome of using HPLC-MS is restricted by a limit of detection controlled by technical advances within the field. Bonsall et al. reported that DAPG was undetectable in non-rhizosphere environments (85), therefore questioning if the metabolite is even produced under these scarce conditions. Thus, the approach of using engineered whole-cell biosensors for the detection and quantification of SMs offers an alternative solution to analytical chemistry. Since biosensors rely on genetic circuits, they are readily optimized through genetic engineering via the introduction of additional modules to reduce transcriptional leakiness, increase sensitivity, and amplify the output signal (79). This in turn has the potential to surpass the existing detection limits of analytical chemistry.

Finally, development of the technique called matrix-assisted laser desorption/ionization-time-of-flight (MALDI-TOF) MS imaging (referred to as MSI) has allowed the analysis of spatial distribution of SMs (86, 87). Initially, a sample (*e.g.* bacterial colony or tissue section) is covered by a crystalline matrix, which allows for molecular ionization and desorption (87). Subsequently, a laser operating within a predefined 2D-grid irradiates the matrix-covered sample. For each spot hit by the laser, a mass-spectrum is recorded along with its respective x and y coordinates. This provides a 2D image of a given sample with recordings of each detected molecule, including SMs (87). Thus, MSI represents an exciting technique for addressing fundamental questions regarding metabolite production, spatial distribution, and importantly, chemical communication and interaction between organisms. Geier et al. recently demonstrated a culture-independent combination of MSI with fluorescence *in situ* hybridization to visualize spatial bacterial and metabolite distribution (88). As will be described below, bacteria live surrounded by a multitude of other organisms in natural environments with whom they continuously interact. Therefore, another significant advantage of MSI is the ability to chemically and visually analyze microbial interactions mediated by SMs (89).

## Chapter 4

### **Microbial interactions and the role of *Pseudomonas*-produced secondary metabolites**

**D**etecting the production of SMs, as well as unraveling the bacterial diversity and community composition in natural environments, is only part of understanding the microbial ecology. Bacteria are not solitary organisms, in fact, they exist in complex and diverse microbial communities, where soil and rhizosphere environments have been shown to exhibit the largest bacterial diversity (6). This gives rise to a myriad of interspecies interactions affecting microbial composition and behavior. As microbes exist in these complex and diverse, yet stable and functional communities, two ecological questions have been and still are the subject of immense research:

- i) What types of interactions occur between microbes?
- ii) What are the effects of such microbial interactions?

It was previously shown that competition between culturable bacteria was more commonly observed than cooperation, measured as the ratio of bacterial productivity (CO<sub>2</sub> emission) between monocultures and bacterial mixtures (90). Contrarily, by utilizing a novel high-throughput kChip approach (91), it was recently demonstrated that positive interactions occurred frequently among distantly related, culturable soil bacteria grown on 40 different carbon sources across 180,408 pairwise interactions (92). These contradicting findings thus indicate that we still lack knowledge of the types of interactions occurring between microbes, and hence also of the mediators of microbial interactions.

Bioactive SMs are thought to play an essential role in microbial interactions, as they have historically been viewed as weapons employed by microbes to combat competitors and proliferate in complex microbial habitats, such as the soil and rhizosphere (93). However, the actual concentration of SMs in

the nutrient-limited, natural environments is thought to rarely exceed the levels required for their antimicrobial functions demonstrated *in vitro*. It has been shown that subinhibitory concentrations of antibiotics stimulate alterations to the transcriptome of the target organism (94). Thus, it was postulated that the concept of hormesis applies to these bioactive SMs – that is, at subinhibitory concentrations they stimulate a stress response in the target organism, whereas at elevated, inhibitory concentrations they function antagonistically (95). This has in turn spurred the conceptualization of bacterial competition sensing, in which bacteria are hypothesized to have evolved mechanisms of sensing and responding to the presence of toxic SMs (1, 96, 97).

Thus, microbial interactions may be mediated by antimicrobial SMs, but more importantly, the interactions may also affect the production of SMs (89, 98–101). Lozano et al. identified a two-component antibiotic-induced response (Air) system in *Chromobacterium violaceum* capable of detecting hygromycin A produced by *Streptomyces* spp. and antibiotics with similar function, resulting in increased biosynthesis of violacein (102). A recent study by Bujis et al. similarly indicated a stimulatory function of the SMs andrimid and holomycin produced by *Vibrio coralliilyticus* and *Photobacterium galathea*, respectively (103). Cocultivation of the two marine bacteria resulted in a significantly induced production of both metabolites, suggesting a potential arms-race induced by ecological competition mediated by SM-secretion (103). Pairwise cocultures are thus an excellent approach to investigate the effects of microbial interactions. Along those lines, Tyc et al. investigated the effects of pairwise cocultures of 146 soil bacteria on the antimicrobial activity, which is correlated with SM-production (104). Approximately 28% of the pairwise interactions led to an altered antibacterial activity compared to monocultures. Interestingly, in almost half of the interactions, the coculture exhibited antimicrobial activity against at least one target pathogen, while the monocultures did not (104). This suggests that investigations of microbial interactions are key to unraveling their effects and thereby elucidating the potential roles of SMs in natural microbial habitats, whether that be as signals acting in a complex microbial language or as antibiotics representing microbial weapons.

## Microbial interactions and their ecological effects

One of the most well-studied examples of naturally occurring biocontrol is the phenomenon of disease-suppressive soils. Disease-suppression has been identified in multiple soils across the world (105–107). An important characteristic of suppressive soils is the fact that pasteurization leads to loss of disease-suppressiveness (14), indicating that the suppressiveness is of microbial origin. Thus, to identify key microorganisms associated with disease-suppression, Mendes et al. compared the diversity and bacterial composition between suppressive and conducive soils (7). No significant differences in the taxonomic diversity were observed, but a clear distinction in abundance of the different bacterial taxa was found (7), which is in agreement with a previous study analyzing the microbial composition of rhizosphere soil suppressive to black-root rot (108). This suggests that disease-suppressiveness is correlated to population-density of specific bacteria, such as *Pseudomonas* spp. (44, 74, 109).

Accordingly, Mendes et al. found that *Pseudomonas* spp. isolated from disease-suppressive soil were predominantly antagonistic towards the fungal pathogen *Rhizoctonia solani* (7). These isolates represented 10 phylogenetically distinct haplotypes (7), which aligns with previous findings showing the presence of several *Pseudomonas* genotypes in disease-suppressive soil, suggesting a potential link between increased species richness and ecosystem functioning with respect to disease suppression (110, 111). While the species richness of the disease-suppressive soil analyzed by Mendes et al. displayed exclusively haplotypes of *Pseudomonas* spp. related to DAPG-producers of the *P. corrugata* subgroup, examining the species abundance revealed a dominating presence of only three haplotypes (7). Closer investigation of representatives from each of these three haplotypes led to the identification of *Pseudomonas* sp. SH-C52 – a non-DAPG-producing species, capable of producing six non-ribosomal peptides, one of which, Thanamycin, was shown to attribute the antifungal activity (7, 112, 113). This suggests that DAPG produced by some of the dominating haplotypes might play an essential role in the rhizosphere of plants growing in disease-suppressive soil, but it is not necessarily the sole contributor to pathogen-antagonism.

It has previously been shown that high species richness positively affects the community productivity measured as bacterial respiration (114). More recent studies have examined whether increasing *Pseudomonas* biodiversity affects functionality in terms of SM-production and antimicrobial activity

(115–118). One research group investigated the effect of genotypic richness on functionality by establishing communities with up to 8 genotypes of DAPG-producing *Pseudomonas* spp. (115–117). Utilizing *in vitro* agar-based experiments, a positive correlation between increasing genotypic richness and DAPG-production was observed (115). Secondly, as shown in Figure 9, Hu et al. demonstrated that an increasing biodiversity of DAPG-producing *Pseudomonas* significantly reduced the disease incidence in tomato plants, likely due to the antagonistic effects on the fungal pathogen, *Ralstonia solanacearum* (117). Additionally, the increased genotypic richness led to an elevated presence of the DAPG-producing *Pseudomonas* species (117), which correlates with increased DAPG-production, since DAPG the biosynthesis is population-dependent (65).

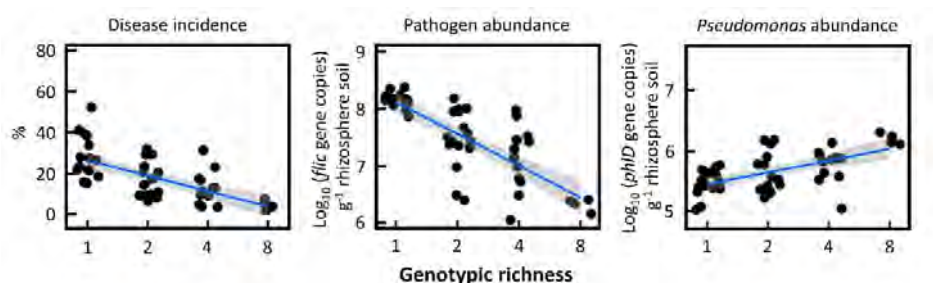


Figure 9 | *Pseudomonas* spp. richness stimulates antifungal response *in vivo*. Increasing the *Pseudomonas* genotypic richness reduced the incidence of tomato wilt disease caused by the phytopathogenic bacterium, *Ralstonia solanacearum*, and lead to a greater growth inhibition of the pathogen 35 days post inoculation. Simultaneously, genotypic richness positively affected the *Pseudomonas* population density. Adapted and modified from Hu et al. (117).

However, the opposite effect was observed in the rhizosphere of Alfalfa roots when testing the same set of 8 DAPG-producing *Pseudomonas*, resulting in antagonistic interspecies interactions and reduced plant protection against phytopathogenic invasion (116). This could suggest that plant species have a major impact on the functionality of their respective root microbiomes, which is in accordance with the results obtained previously, demonstrating that certain plants (wheat, sugar beet, and potato) accumulated significantly higher densities of DAPG-producing *Pseudomonas* (84). Another research group investigated the effects of species richness in communities with up to 8 phylogenetically distant species, where only a single species exhibited antifungal activity *in vitro* due to production of DAPG (118). It was demonstrated that increased *Pseudomonas* spp. richness reduced the suppression of take-all disease of wheat, because of bacterial antagonism among the different *Pseudomonas* species (118). While Kehe et al. reported a high frequency of positive interactions among culturable soil

bacteria, they also identified predominantly negative interactions (competition or amensalism) occurring among closely related species, such as *Pseudomonas-Pseudomonas* interactions (92). Thus, there is a confounding discrepancy in the types of interspecies interactions occurring between *Pseudomonas* spp. affecting their functionality in terms of SM-production and plant protection. However, only limited efforts have been devoted to address the underlying molecular mechanisms. We investigated the interspecies interactions between two distantly related soil *Pseudomonas* (species from the *P. putida* group and the *P. protegens* subgroup) and discovered a remarkable sequential interaction involving bacterial competition sensing, antagonistic interactions, and modified SM-production (Chapter 7 | Paper 3).

## Biotransformation of secondary metabolites

Extending beyond *Pseudomonas*-specific interactions, a high-throughput analysis of microbial interactions showed that 22% of pairwise interactions among soil bacteria suppressed antimicrobial activity, despite isolates displaying such activity in monoculture (104). As mentioned above, one type of microbial interaction involves the alteration of SM-production. However, bacteria have evolved intricate resistance mechanisms to circumvent the toxic properties of certain SMs – one of which includes enzymatic inactivation, thereby changing the molecular structure and thus the fate of the metabolite (119, 120). Notably, it was reported that the CLP, daptomycin, was exceptionally susceptible to inactivation by several soil isolates of Actinobacteria (119), and the most common inactivation mechanism was hydrolysis of the thermodynamically sensitive ester bond connecting the macrocyclic peptide ring (120). The suppression of antibiotic production and degradation is thought to be a crucial aspect of microbial community stability, as the suppressors/degraders protect not only themselves, but also neighboring species (121). For example, Hermenau et al. identified that the presence of the Actinobacteria, *Mycetocola* spp., protected the mushroom, *Agaricus bisporus*, from infection by *Pseudomonas tolaasii* (Figure 10) (122). Specifically, it was shown that *Mycetocola* spp. secreted esterases capable of cleaving the ester bond of two CLPs (pseudodesmin A and tolaasin I) produced by *P. tolaasii*, rendering them inactive and unable to carry out their function as swarming agent and toxin, respectively (122).

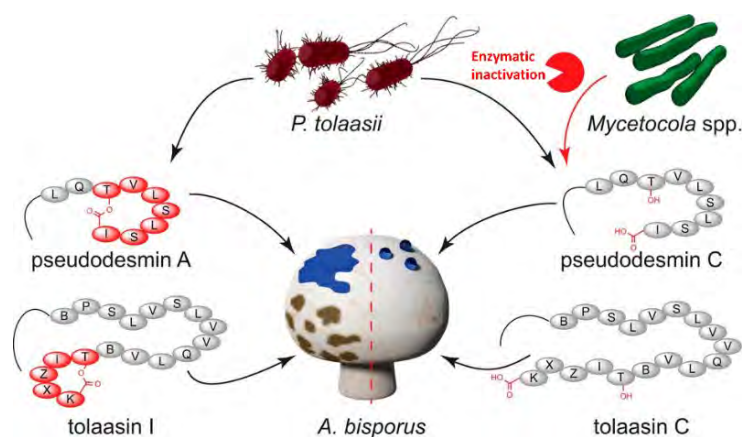


Figure 10 | The helper bacteria, *Mycetocola* spp., halt and disarm mushroom pathogen by enzymatic inactivation of cyclic lipopeptides. The mushroom pathogen, *P. tolaasii*, produces the CLPs pseudodesmin A as swarming agent and tolaasin I as toxins against the mushroom, *A. bisporus*. The presence of *Mycetocola* spp. leads to enzymatic inactivation of both CLPs via hydrolysis of the ester bond connecting the macrocyclic peptide ring (displayed as red nodes). Amino acid sequence of the CLPs is depicted in one-letter code. Adapted from Hermenau et al. (122).

Contrarily, Zhang et al. identified a cooperative defensive interaction between two soil bacteria (*Pseudomonas* and *Paenibacillus*) involving the *Pseudomonas*-produced CLP, syringafactin (123). Syringafactin induced the expression of peptidases in *Paenibacillus*, resulting in enzyme-release and subsequent enzymatic alteration of the syringafactin structure (123). This in turn yielded an amoebicidal byproduct, thus representing a cooperative defensive strategy to avoid protozoan predation resulting from a bacterial interaction (123). Taken together, these studies demonstrate the vast diversity of microbial interactions and their effects, thus clearly underlining the importance of studying the underlying molecular mechanisms.

## The SynCom approach

Studies of multispecies ecosystems are inherently challenging due to the increasing complexity resulting from microbial interactions. Thus, the majority of research within the field of microbial ecology has focused on one of two contrasting approaches. The reductionists sacrifice ecological context by designing simple and predictable ecosystems of one or few species to allow for detailed investigations of biotic interactions (92, 104, 124, 125). The holistic approach, on the other hand, attempts to preserve the ecological complexity of natural environments using technologies for direct *in situ* detection and characterization (7, 126, 127). Over the past decade, significant effort has been devoted to bridge the gap between these two approaches. Microbial synthetic communities (SynComs) represent a promising intermediate to investigate the effects of multispecies interactions and improve our understanding of community-level properties emerging as a consequence of microbial interactions (124, 125, 128, 129). The rational engineering principle behind construction of SynComs can be described as either a bottom-up or a top-down approach (129).

The bottom-up approach resembles the concept of synthetic biology, as it relies solely on predetermined properties of individual species to achieve a microbial assembly with a desired functionality, similar to the construction of genetic circuits based on individual and well-characterized genetic parts (129, 130). As mentioned above, Jousset and co-workers employed a bottom-up approach to define SynComs of DAPG-producing *Pseudomonas* spp. in order to explore the ecological effects (*e.g.* antimicrobial activity and plant protection) of increasing genotypic richness (115–117).

Contrarily, the engineering of SynComs based on the top-down approach relies on ecological context, as members are selected from a defined set of microbes present in a given environment (e.g. rhizosphere), in order to achieve a synthetic microbial assembly representative of the ecological diversity (90, 114, 129, 131, 132). The top-down approach has been a common choice for designing simplified, yet representative communities of environmentally associated bacteria in order to investigate community-level properties (131–134). Construction and analysis of a seven-membered SynCom with representative, culturable bacteria from the maize rhizosphere revealed a keystone species responsible for maintaining microbial community composition (131). Lozano et al. similarly used a top-down approach to demonstrate bacterial co-dependence in a simple, three-membered SynCom, as *Bacillus cereus* inhibited the production of a toxic *Pseudomonas*-produced SM, allowing the co-existence of *Flavobacterium johnsoniae* (81). While these studies utilized SynComs to investigate microbial interactions among its members, SynComs can be further employed to examine compositional perturbations caused by introduced external factors (e.g. plants or SM-producing bacterial invaders). It was shown that plant genotype and exudation of plant-derived SMs significantly affect the root-associated microbiota of *Arabidopsis thaliana* (132, 133). Collectively, this indicates that SynComs, despite their genotypic simplicity compared to natural environments (6), are a useful tool for investigating complex multispecies assemblages and achieving a deeper understanding of community-level interactions. Similar to Voges et al. (132) and Bodenhausen et al. (133), we utilized a SynCom consisting of naturally co-occurring and morphologically distinguishable soil bacteria (135) as a reproducible microcosm to investigate the impact of *Pseudomonas*-SMs on microbial community composition. This led to the discovery of a community-level inactivation and subsequent degradation of the *Pseudomonas*-produced CLP, orfamide A (Chapter 7 | Paper 4).

In addition to the vast microbial diversity of rhizosphere and soil environments and the plethora of interactions occurring between microbes, an obvious factor affecting the majority of these microbes is spatial organization. While traditional liquid culture experiments provide a good basis for classical microbiology, they neglect the possibility of spatial distribution. As demonstrated empirically by Kerr et al., local dispersal promoted biodiversity in a non-transitive system of three competing species, whereas continuous mixing destabilized the community composition (136). Technological advances have led to the development of artificial soils, such as the hydrogel-based system (137), providing a laboratory-scale approach to establish microbial communities, while allowing for spatial distribution.

The hydrogel-based system was recently utilized to introduce spatial structure for the validation of observed microbial interactions in an artificial soil environment (123). Considering the diffusional gradient of antimicrobial SMs (1, 96, 97) and their hypothesized hormetic properties (*e.g.* stimulatory or inhibitory, (95)), the combined use of an artificial soil system and a defined microbial SynCom could represent a suitable approach to investigate the role of SMs in microbial interactions, while permitting ecologically relevant spatial organization.

## Chapter 5

### Present investigations – results and discussion

The research presented in this PhD thesis addresses the two overall aims presented in Chapter 1 as an investigation of the ecological dynamics of soil *Pseudomonas* and their SM-production, followed by studying the role of *Pseudomonas*-produced SMs in specific microbial interactions. The present investigations follow the chronological order of the PhD project, as the initial endeavor into the vast diversity of soil *Pseudomonas* naturally revealed the necessity for developing methods to differentiate the closely related species more accurately (Paper 1) and detect producers of specific metabolites in a cost-efficient and high-throughput fashion (Paper 2). As described in Chapter 4, previous research has clearly demonstrated the ecological effects of microbial interactions. The second part of the thesis encompassed a more focused approach to unravel the underlying molecular mechanisms of such microbial interactions involving and affecting *Pseudomonas*-produced SMs – both *Pseudomonas*-specific (Paper 3) and across higher taxonomic levels (Paper 4). Thus, the outcome of the present investigations provides novel insight into the potential roles of specific *Pseudomonas*-produced SMs.

## Paper 1 | Identification and Differentiation of *Pseudomonas* Species in Field Samples Using an *rpoD* Amplicon Sequencing Methodology

Amplicon sequencing is a powerful, culture-independent approach to characterize the diversity and relative microbial abundance in natural environments. While the standard 16S rRNA approach has yielded invaluable insight into the relative abundance of bacteria *in situ* (17), it has proven insufficient for accurate taxonomic characterization at the species level of *Pseudomonas*. There is a clear advantage of enabling accurate differentiation of *Pseudomonas* spp., due to the appreciation for group-, subgroup-, and even species-specific traits associated with the various species (9, 22). The single housekeeping gene, *rpoD*, is an excellent phylogenetic marker for the differentiation of *Pseudomonas* species (31) and thus represents a prime candidate as target gene for a *Pseudomonas*-specific amplicon sequencing approach.

Aim | Develop an *rpoD*-based amplicon sequencing approach to accurately differentiate *Pseudomonas* spp. in environmental samples

In this study we developed an *rpoD*-based amplicon sequencing approach for the Illumina MiSeq 300PE platform using the *Pseudomonas*-specific primers described previously (31). The primers target a 760-nucleotide region of the *rpoD* gene, thus leaving a 160-nucleotide gap using the 300PE platform. This issue was circumvented by incorporating a new bioinformatic pipeline involving bowtie2 inspired from annotation of transcriptome sequencing data. We tested the ability of our novel approach to distinguish between genomic DNA from 16 different *Pseudomonas* species by comparing the performance to that of the standard amplicon sequencing targeting the V3-V4 of the 16S rRNA gene (Figure 11). The *rpoD*-based approach enabled the identification of all 16 strains, albeit with relative abundances differing slightly from theoretical values. However, our approach clearly outperformed the standard 16S rRNA sequencing method, as the sample composition was classified incorrectly throughout the five replicates.

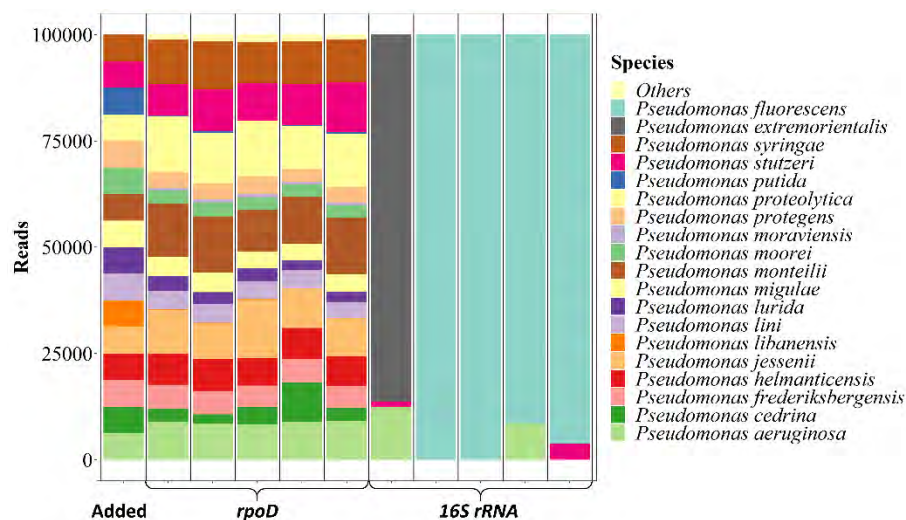


Figure 11 | Comparing the *rpoD*-based and the standard 16S *rRNA* amplicon sequencing approach. A predefined mixture of DNA from 16 *Pseudomonas* spp. was analyzed with the standard 16S *rRNA* and the novel *rpoD*-based amplicon sequencing approach. The left column indicates theoretical abundance of DNA from each species. The *rpoD*-based approach clearly distinguishes between both closely and distantly related species.

We demonstrated the applicability of our method by classifying the *Pseudomonas* diversity in 13 different environmental soil samples. Firstly, we determined the total bacterial diversity in each sample by 16S *rRNA* amplicon sequencing, revealing a low abundance of *Pseudomonas* (0.008% to 0.73%). Regardless of the low relative abundance, the *rpoD*-based method enabled taxonomic differentiation of *Pseudomonas* at the species level. However, the number of reads mapping to *rpoD* varied from 133.4 to 4,022.2 per sample, despite starting with a total of 10,446,888 reads before filtration. This indicates a large number of false positive reads, potentially arising as a result of using a *Pseudomonas*-specific amplification method on a large pool of DNA, where *Pseudomonas* only constitutes a minor fraction. Rarefaction curves additionally confirmed an uneven saturation in samples with fewer reads. Further optimization of primers against a larger set of negative controls could potentially decrease the amount of randomly amplified DNA, while increasing the *Pseudomonas*-specificity.

Lastly, we compared the use of our culture-independent *rpoD*-based method to a cultivation-based characterization of the 13 environmental samples. We isolated colonies from *Pseudomonas*-selective ¼ King's B agar plates supplemented with ampicillin, chloramphenicol and cycloheximide (138). Cultivation-based methods are commonly used to describe the diversity and abundance of *Pseudomonas* spp. in environmental samples (7, 108). Additionally, Mehrabi et al. utilized a

*Pseudomonas*-selective isolation to rationally design mixed species communities covering the diversity of the most abundant species in the endo- and rhizosphere of wheat roots (118). While *Pseudomonas* spp. are readily cultured *in vitro*, the choice of isolation media has been shown to affect the observed diversity (139). The *rpoD*-based approach developed in this study allowed for the identification of several species not observed from cultivation, including members of the *P. lutea* group, as well as species of the *P. mandelii* and *P. gessardii* subgroups of *P. fluorescens*. This indicates that our method increases the chances of capturing “rare” or uncultivable species and may thus represent a valuable tool for more accurate determination of *Pseudomonas*-specific ecology.

As mentioned in Chapter 4, there is conflicting evidence for the ecological effects of increased *Pseudomonas* diversity (117, 118). However, neither of these studies address the community composition. As shown by Niu et al., community surveillance is a powerful tool to monitor population dynamics and enable the identification of potential species responsible for maintaining or destabilizing community structure (131), thus affecting the ecosystem functionality. Aside from improved *in situ* differentiation of *Pseudomonas* spp., the *rpoD*-based method could provide significant impact to SynCom-studies by enabling accurate community surveillance of closely related *Pseudomonas*.

## Paper 2 | A Whole-Cell Biosensor for Detection of 2,4-Diacetylphloroglucinol (DAPG)-Producing Bacteria from Grassland Soil

DAPG is a metabolite of particular interest, known for its antifungal and antibacterial properties (42, 43), and recognized as a key determinant of natural biocontrol associated with disease-suppressive soils (34, 44). However, detection of DAPG and its producers relies on either laborious, potentially error-prone DNA-based techniques or expensive, low-throughput analytical chemical methods. Whole-cell biosensors are genetically engineered alternatives relying on natural regulatory systems that enable cost-efficient, high-throughput screenings for specific SMs.

Aim | Engineer and demonstrate the use of a whole-cell biosensor for detection of DAPG and its producers

In this paper, we engineered a whole-cell biosensor for detection of DAPG and DAPG-producing microorganisms. The design utilized genetic parts characterized previously (140, 141) assembled in two modules; a response module and an output module, separated by a strong transcriptional terminator (Figure 12A). In the presence of DAPG, PhIF-mediated repression of the respective  $P_{phlA}$  promoter is relieved, leading to expression of *lacZ*, which encodes a  $\beta$ -galactosidase capable of producing a colorimetric output on plates supplemented with X-gal. The sensitivity of the biosensor was assayed with purified DAPG, yielding a measurable response at nanomolar concentrations, which correlate with the observed levels of DAPG in the rhizosphere of wheat roots (65, 85).

We sampled 30 *Pseudomonas* spp. from a grassland soil site annually for two consecutive years and utilized the biosensor to screening for DAPG-producing species (Figure 12B). The biosensor accurately identified three DAPG-producing isolates observed as *Pseudomonas* colonies surrounded by a blue halo, which was confirmed by LC-MS.

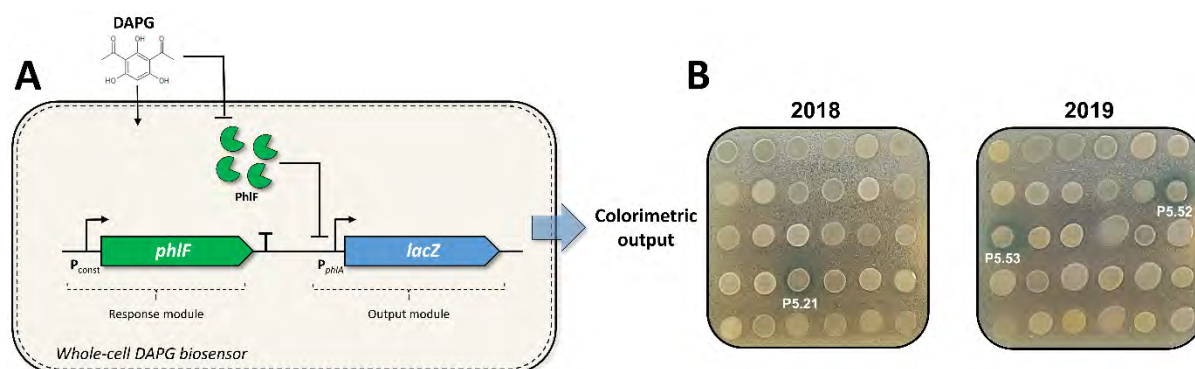


Figure 12 | **Utilizing an engineered whole-cell DAPG biosensor for detection of DAPG-producing bacteria. A)** The biosensor consisting of two modules responds to the presence of DAPG by relieving the PhIF-mediated repression on the  $P_{phIA}$  promoter controlling *lacZ* expression. **B)** The whole-cell biosensor was employed to identify DAPG-producing *Pseudomonas* spp. in grassland soil samples.

In the final part of the study, we demonstrated the applicability of the whole-cell biosensor for high-throughput screening of environmental samples to explore the ecological dynamics of DAPG-producing *Pseudomonas* spp. in bulk soil. We observed frequencies of DAPG-producers ranging from 0.35% - 17% of the isolated *Pseudomonas* (equivalent of  $10^1$ - $10^3$  CFU/g soil), which is consistent with previously estimated values for non-rhizosphere soil (85). However, as the production of DAPG is population-dependent (65), it raises the question if the metabolite is even produced in non-rhizosphere environments. Whole-cell biosensors are highly tunable genetic devices. The addition of extra modules for signal amplification (142) or noise propagation (143) can increase sensitivity and output dynamics, thus lowering the limit of detection. Even simple nucleotide substitutions, such as tuning the translational efficiency of the PhIF repressor by changing ribosome binding site (141), have been shown to improve the signal-to-noise ratio without compromising output levels (144). Thus, further genetic optimization of biosensors could have the potential to surpass the detection limit of analytical chemistry and potentially even allow for *in situ* detection in areas of low population densities of DAPG-producers.

In our study we opted for a coculture-based approach to facilitate biosensor-guided detection of DAPG-producers. However, whole-cell biosensors are biological devices and are thus prone to microbial interactions, which could affect either the viability of the biosensor or the SM-production by the target species. Though, potential interactions between the *Pseudomonas*-isolates and the *E. coli* biosensor did not appear to affect the detection of DAPG-producers. In future assays, this concern

could be circumvented entirely by incorporating an overlay technique, in which the cultivation of SM-producing *Pseudomonas* spp. and the biosensor is separated (81, 104). A second caveat to whole-cell biosensors and genetic circuits in general is the specificity towards the input molecule (*i.e.* the specificity of the repressor protein controlling output expression). Here, we demonstrated the specificity towards DAPG by comparing the dose-response relationship to the structurally similar precursors of DAPG (PG and MAPG). The biosensor exhibited excellent specificity towards DAPG with only a minor response at high concentrations of MAPG. Although in hindsight, we could have tested additional natural products of diverse origin related to DAPG, similar to Yan et al. (52). Thus, we successfully engineered a whole-cell biosensor for detection of DAPG-producing microorganisms, providing a cost-efficient, high-throughput approach for screening of environmental samples.

Finally, high-throughput screening of the three soil environments revealed nine *Pseudomonas* isolates unable to produce DAPG, yet able to elicit a biosensor response. As the PhIF repressor, incorporated in our biosensor, naturally controls expression of the DAPG biosynthetic genes, we hypothesized that these nine isolates could modulate DAPG production in *Pseudomonas* species known to produce DAPG (such as *P. protegens*) through microbial interactions. This hypothesis was further investigated in Paper 3.

### Paper 3 | Communication is key: Sequential interspecies interactions affect production of antimicrobial secondary metabolites in *Pseudomonas protegens* DTU9.1

Previous studies have shown contradicting results related to correlations between *Pseudomonas* species richness and antagonistic activity towards plant pathogens (7, 115–118). Improving our knowledge of the processes that affect this antagonism is crucial for understanding microbe-based disease-suppressiveness and potentially designing functional biocontrol consortia. Due to the confounding discrepancy in the types of interspecies interactions occurring between *Pseudomonas* spp. and their effects on SM-production and plant protection, there is a need to investigate the underlying molecular mechanisms.

Aim | Investigate the effect(s) of genus-specific interactions between two distantly related *Pseudomonas* spp. on SM-production in *P. protegens* DTU9.1

In this study, we describe a sequential interspecies interaction affecting the SM-production in *P. protegens* DTU9.1 (referred to as DTU9.1). We pursued the hypothesis arising from **Paper 2**, stating that the nine isolates capable of eliciting a response in our DAPG-responsive biosensor, yet unable to produce DAPG themselves, could affect the production of DAPG in DTU9.1 and potentially other DAPG-producers via unknown cell-cell interactions. We narrowed down the number of isolates to one, *P. capeferrum* F8 (referred to as F8), as cocultures between F8 and DTU9.1 resulted in inhibited DAPG-production and induced pyoluteorin biosynthesis.

We demonstrated that those opposing effects on SM-production in DTU9.1 were caused by separate mechanisms. A distance assay revealed that pyoluteorin biosynthesis was increased in a distance-dependent manner, whereas DAPG production was unaffected. Antibiotic production is costly (145), thus bacteria have evolved mechanisms of strictly regulating the expression of BGCs and often require elicitors to induce their expression, such as toxic SMs or other cues from competing strains. This suggests that induced production of pyoluteorin could be a response in DTU9.1 to bacterial competition sensing (1, 96, 146). We further demonstrate that distance-dependent induction of pyoluteorin biosynthesis is a commonly observed response in DTU9.1 to distantly related species of *Pseudomonas*. Secondly, we found that DAPG production was inhibited by the release of an intracellular molecule upon lysis of F8. Intracellular molecules released upon lysis have previously

been shown to affect SM-production in another species of *Pseudomonas* (146). In our study we discovered that lysis of F8 occurred as a result of induced pyoluteorin in DTU9.1, which in turn led to the release of an intracellular molecule from F8 capable of inhibiting DAPG production in DTU9.1 (Figure 13). Lastly, we showed that cocultivation of F8 and DTU9.1 resulted in a greatly increased antibacterial activity towards the phytopathogenic bacteria, *Pectobacterium carotovorum* and *Dickeya solani*, resulting from induced pyoluteorin production. A similar phenomenon was observed previously, resulting from interspecies interactions between *P. protegens* CHA0 and three environmental isolates of *Pseudomonas* spp., increasing the antibacterial activity towards *B. subtilis* (147).

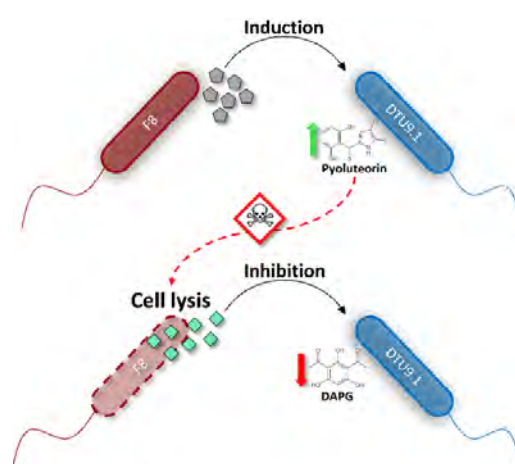


Figure 13 | **Sequential interspecies interaction affect SM-production in *P. protegens* DTU9.1.** *P. protegens* DTU9.1 responds to a secreted cue (grey pentagons) from *P. capeferrum* F8 by inducing biosynthesis of pyoluteorin. The increased concentration of pyoluteorin exceeds tolerable levels for F8, leading to cell lysis and release of an intracellular metabolite (cyan diamonds), which in turn inhibits production of DAPG in DTU9.1.

While the research presented in this study supports the model proposed in Figure 13, we did, however, not manage to identify the secreted molecules from F8 either inducing pyoluteorin biosynthesis or inhibiting DAPG production, despite extensive hypothesis-testing (not mentioned in the paper). To identify the molecule inducing biosynthesis of pyoluteorin we constructed knockout mutants in F8 of the most prominent BGCs responsible for producing SMs that could act as danger signals due to their inherent antimicrobial nature. These included the CLP, putisolvin, and an unknown polyketide. Additionally, we knocked out the ppul-rsaL-ppuR quorum-sensing system, as quorum-sensing has been shown to potentially mediate cross-talk between different bacterial species (148). We also surveyed the acidity surrounding the F8 colony using two-dimensional pH microsensor measurements (149), as certain species of *Pseudomonas* have been shown to acidify their

surroundings by secretion of gluconic acid, thus affecting the SM-production in neighboring bacteria (150). However, neither of these attempts affected the distance-dependent induction of pyoluteorin biosynthesis in DTU9.1.

Thus, future experiments could involve transposon mutagenesis in F8, followed by high-throughput screenings for potential candidates incapable of inducing transcription of the pyoluteorin BGC. Furthermore, we limited our scope to the investigation of DAPG and pyoluteorin, as their biosynthesis is interlinked (54). Though, as shown by Dubuis et al., interspecies interactions among distantly related *Pseudomonas* spp. may affect the Gac/Rsm global regulatory pathway (147, 151), which is known to control the expression of other BGCs, including orfamide A (70). Thus, construction of either a *gacA* mutant or  $P_{rsmY}/P_{rsmZ}$  reporter fusions could provide valuable information to whether the distance-dependent induction of pyoluteorin biosynthesis is related to the Gac/Rsm regulatory pathway. Lastly, future efforts could include analytical chemistry for fractionation and bioassay-guided detection of the molecules from F8 capable of either inhibiting DAPG production or inducing pyoluteorin biosynthesis.

In conclusion, this paper has provided further insight into the molecular mechanisms underlying *Pseudomonas*-specific interactions. Knowledge of the mechanisms underlying microbial interactions can prove valuable in understanding the ecology associated with disease-suppressive and conducive soils, as well as aiding in designing optimized consortia for improved biocontrol.

## Paper 4 | Counter-acting *Pseudomonas* invasion: Community-level resistance towards *Pseudomonas*-produced secondary metabolites

Antagonistic SMs are well-described for their influence on suppression of soil-borne phytopathogens. However, limited research has been devoted to investigate their impact on indigenous soil bacteria and the contribution of these SMs to the ability of biocontrol agents to invade natural soil and rhizosphere microbiomes. Here, we use a SynCom approach, as demonstrated previously (132, 133), cultivated in an artificial soil to determine the role and effects of SM-production in *P. protegens* DTU9.1 in relation to community invasion in an environment allowing for spatial distribution.

**Aim | Investigate the contribution of *Pseudomonas*-produced SMs to the ability of *P. protegens* DTU9.1 to invade a microbial community**

In this paper, we employed a recently developed, four-species SynCom consisting of naturally co-occurring soil bacteria (135) for investigating microbial interactions mediated by and affecting *Pseudomonas*-produced SMs in a multispecies community. We initially constructed knockout mutants in DTU9.1 incapable of producing DAPG ( $\Delta\text{phlACB}$ ), pyoluteorin ( $\Delta\text{pltA}$ ), or orfamide A ( $\Delta\text{ofaA}$ ) to investigate the contribution of these SMs on the ability of DTU9.1 to invade the microbial community. We observed that each variant of DTU9.1 (WT or mutants) caused similar perturbations to the microbial composition and that the sampling time was the main driver of community composition, suggesting that bacterial growth rates could be a key predictor of population dynamics in our system. However, pyoluteorin and orfamide A affected the bacterial composition to a lesser, but significant degree during the early stages of community assembly (Day 1 and Day 4), as evidenced by a PERMANOVA.

This finding prompted us to investigate the tolerance of the SynCom members towards these two SMs. This revealed a minimal inhibitory concentration (MIC) of pyoluteorin at 8  $\mu\text{g/ml}$  of three SynCom members, which was lower than the mean concentration of pyoluteorin in the artificial soil system quantified by High-resolution liquid chromatography-mass spectrometry (HR-LCMS) after 7 days of cultivation. This could suggest that the naturally co-occurring SynCom members have evolved mechanisms of cooperative defense, *e.g.* multispecies biofilm formation, which has been shown to decrease antibiotic susceptibility (152, 153). Alternatively, it could indicate that prolonged incubation (> 7 days) would allow for increased pyoluteorin production and reveal a more pronounced

antagonistic effect. Additionally, we observed an increased production of pyoluteorin when DTU9.1 was cultivated with the SynCom compared to axenic cultivation. This could suggest that the danger response leading to induced pyoluteorin biosynthesis (Paper 3) extends beyond a genus-specific interaction, thus representing a more general response in *P. protegens* to bacterial competition.

Secondly, we found that the Actinobacterium, *Rhodococcus globerulus* D757 (referred to as D757), exhibited susceptibility towards orfamide A with an MIC of 8 µg/ml. During axenic cultivation of DTU9.1 in the artificial soil, orfamide A reached a mean concentration of 25.58 µg/ml. However, metabolite-quantification by HR-LCMS showed a mean concentration of 3.87 µg/ml after 7 days of cocultivation with the SynCom. Subsequent chemical analysis, including molecular network analysis (154), tandem MS, and MSI (Figure 14), revealed a dire fate of orfamide A resulting from multiple microbial interactions. In this paper, we found that D757 was able to inactivate orfamide A by hydrolyzing the ester bond connecting the macrocyclic ring (Figure 14). This phenomenon has been commonly observed among Actinobacteria as a resistance mechanism against toxic *Pseudomonas*-CLPs (120, 122).

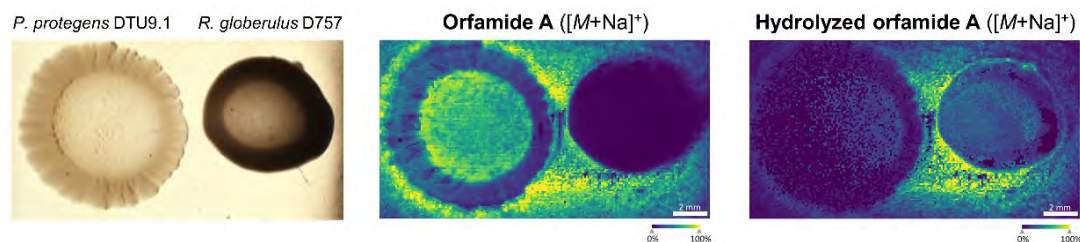


Figure 14 | **Microbial interaction between *R. globerulus* and *P. protegens* resulting in enzymatic inactivation of orfamide A.** MS imaging of colonies of DTU9.1 (left) and D757 (right) revealed the effect of a microbial interaction. D757 secretes an enzyme capable of hydrolyzing the ester bond of orfamide A, resulting in the accumulation of linearized and inactive orfamide A at the interface between the two bacteria.

Aside from being a resistance mechanism, we found that hydrolysis of orfamide A also inhibited the swarming motility of DTU9.1. This suggests that D757 confers a spatial restriction to the invasive spread of DTU9.1, which is consistent with the model stating that antibiotic degradation stabilizes microbial communities (121). Thus, a future experiment should include an artificial soil system inoculated with DTU9.1 and all SynCom members except D757 to investigate the effect of unaffected orfamide A on community composition. However, this neglects any positive interactions associated with the presence of D757. Therefore, another option is to first identify the gene encoding the

secreted hydrolase/esterase in D757 capable of catalyzing the hydrolytic inactivation of orfamide A, and secondly construct a knockout mutant in D757. Including this knockout mutant would represent the ideal SynCom to study the effect of orfamide A on community composition, although it would include a significant amount of protein chemistry (120, 122).

Furthermore, inactivation of orfamide A could have an indirect benefit to the entire SynCom. It was previously demonstrated that certain *Pseudomonas*-produced CLPs negatively affects biofilm formation (3, 73). One could hypothesize that orfamide A can negatively affect the formation of a protective, multispecies biofilm, thereby exposing the pyoluteorin-sensitive SynCom members. Thus, in the absence of D757, the collective efforts of orfamide A and pyoluteorin leads to invasive spread of DTU9.1, community destabilization, and antibiosis, resulting in *Pseudomonas*-dominance. The enzymatic inactivation of orfamide A by D757 may therefore serve not only as a resistance mechanism, but also as a community-level protective mechanism.

Lastly, the molecular network analysis of metabolites extracted from the artificial soil systems further showed degradation products of orfamide A during cocultivation with the SynCom. However, pairwise cocultivation experiments between DTU9.1 and each SynCom member only resulted in hydrolysis in the culture with D757 and absence of degradation products. This could indicate that linearization caused by D757 is a prerequisite for subsequent degradation by one or several of the remaining SynCom members. Preliminary results with chemically linearized orfamide A indicate that *Stenotrophomonas indicatrix* D763 can degrade the metabolite post-hydrolysis. Microbial catabolism of antibiotics has been demonstrated previously among a diverse collection of soil bacteria (5, 155). Crofts et al. further identified a conserved sequential strategy among three distantly related genera for degradation of penicillin: first the  $\beta$ -lactam ring is hydrolyzed, then the inactivated antibiotic is degraded, allowing the bacteria to grow on penicillin as sole carbon source (5). In this study, we discovered a potential community-level microbial interaction, resulting in microbial inactivation and catabolism of a *Pseudomonas*-produced SM. Thus, the presence of D757 and enzymatic inactivation of orfamide A might serve as a protective mechanism and provide a growth benefit to the SynCom, as the linearized version becomes digestible.

## Chapter 6

### Conclusions and perspectives

Secondary metabolites have predominantly been viewed as antibiotics and thus served as therapeutics for treating infectious diseases in humans and plants. However, these SMs are natural products of microbial origin and the concentrations required to achieve their therapeutic effects often greatly exceed those reported in their natural settings. This has in turn raised questions regarding the natural role of microbial SMs (*e.g.* if they are in fact weapons in microbial warfare). Due to the antimicrobial properties of most SMs, research has suggested that they might serve as signals in microbial communication. The diffusional gradient of SMs in the soil thus represents a way of sensing immediate danger, as microbes experience tolerable, subinhibitory levels of antimicrobial SMs, resulting in a response of their own. Soil and rhizosphere environments are home to a magnificent diversity of microorganisms, including bacteria of the genus *Pseudomonas*. Particularly, the group *P. fluorescens* has been the topic of intensive research, as its members are inherently known for their vast repertoire of SMs functioning in microbial competition, motility, and trace metal acquisition – all of which have been shown to positively affect the inhibition of phytopathogens. However, the role and fate of these *Pseudomonas*-produced SMs in the context of microbial interactions is less well-characterized.

First, the work presented in this thesis provides novel insight into the ecological dynamics of soil-dwelling *Pseudomonas* species. We developed two methodologies for accurate, cost-efficient, and high-throughput differentiation of *Pseudomonas* spp. and detection of producers of the important SM, DAPG. The *rpoD*-based amplicon sequencing method led to the discovery of *Pseudomonas* spp. in different soil environments not detected by standard *Pseudomonas*-selective isolation. While the method may need further improvement to circumvent the accumulation of random reads, likely owing to the limited pool of *Pseudomonas* DNA template in soil, it clearly outshines the existing 16S rRNA amplicon methodology for differentiation of species in the *Pseudomonas* genus. The results from this

study additionally open up for detailed investigations of *Pseudomonas* population dynamics across different ecosystems (e.g. lab-scale systems or different crops).

Secondly, we developed a whole-cell biosensor for detection of DAPG and DAPG-producing microorganisms. This biological device allows for rapid and effortless screening of isolates, compared to laborious PCR-based techniques or expensive and cumbersome analytical chemical methods. Furthermore, whole-cell biosensors hold the potential for genetic optimization to surpass the current limits of detection associated with analytical chemistry to enable *in situ* detection of SMs – even in non-rhizosphere environments. Additionally, the work presented here provides a framework for construction of novel biosensors for detection of other SMs. Recently, Yan et al. characterized the transcriptional regulation of the pyoluteorin BGC controlled by the pyoluteorin-responsive PltZ repressor (62). Thus, a PltZ-based whole-cell biosensor for detection of pyoluteorin would be an obvious addition.

Previous research has demonstrated contradicting effects arising as a result of *Pseudomonas*-diversity, which supports the potential for genus-specific interactions affecting SM-production and thus antimicrobial activity of *Pseudomonas* species. We discovered a sequential interspecies interaction involving bacterial competition sensing, resulting in an induced antibacterial response in *P. protegens* and subsequent lysis of *P. capeferrum*, which in turn released an intracellular molecule inhibiting DAPG production in *P. protegens*. Our work sheds light on the underlying mechanisms of *Pseudomonas*-specific interactions affecting the biosynthesis of SMs relevant for biological control of phytopathogenic microorganisms. Alongside similar studies of dual-species interactions (101–104), this investigation clearly demonstrates the complexity and dynamics of microbial interactions. This underlines the importance of considering the molecular mechanisms of microbial interactions to improve our understanding of *Pseudomonas*-ecology and aid in the design of optimized biocontrol consortia to achieve desirable functions. Overall, the results from this study point towards an unexplored area of dynamic microbial interactions among *Pseudomonas* spp., which should now be systematically investigated.

Lastly, we have demonstrated the significance of considering multispecies communities to unravel the complex, community-level interactions mediated by and affecting *Pseudomonas*-produced SMs. We opted for a laboratory-scale artificial soil as cultivation system, allowing for spatial distribution of

microbes. Additionally, we utilized a SynCom consisting of morphologically distinguishable, naturally co-occurring soil bacteria to enable temporal community surveillance. This approach allowed us to track perturbations in community composition caused by *Pseudomonas*-produced SMs, as well as fluctuations in SM-levels quantified by analytical chemistry. This in turn revealed a community-level interaction affecting the fate of orfamide A. Taken together, our work has demonstrated the powerful use of SynComs to increase genotypic and environmental complexity to gain insight into ecologically relevant microbial interactions.

Taken together, the outcome of this project clearly demonstrates that the combination of analytical chemistry and *in vitro* lab-scale systems are instrumental for unraveling the types of metabolite interactions occurring within dual- and multispecies communities. Our results show that this approach is undoubtedly beneficial to achieve a deeper understanding of the chemical interactions among microbes. While the interactions and their effects presented in this thesis has primarily focused on *in vitro* systems, we still lack evidence of their effects or occurrence *in situ*. In relation to metabolite production and metabolite-mediated interactions, the results from this thesis show that *in vitro* dual- and multispecies communities can serve to build testable hypotheses for potential *in situ* investigations. In addition, a combination of molecular tools (such as tools developed in this thesis and other studies) and recent advances in *in situ* analytical chemistry (88), will likely advance our understanding of SMs and their role(s) in natural settings. From a biotechnological perspective, the results from this thesis may assist in discovery and isolation of *Pseudomonas* strains with agricultural application (*e.g.* biocontrol) and potentially also new approaches based on metabolite signalling and elicitation to design and assemble efficient biocontrol consortia.

## Bibliography

1. D. M. Cornforth, K. R. Foster, Competition sensing: the social side of bacterial stress responses. *Nat. Rev. Microbiol.* **11**, 285–293 (2013).
2. D. Romero, M. F. Traxler, D. López, R. Kolter, Antibiotics as Signal Molecules. *Chem. Rev.* **111**, 5492–5505 (2011).
3. J. M. Raaijmakers, I. De Bruijn, O. Nybroe, M. Ongena, Natural functions of lipopeptides from *Bacillus* and *Pseudomonas*: more than surfactants and antibiotics. *FEMS Microbiol. Rev.* **34**, 1037–1062 (2010).
4. J. Kramer, Ö. Özkaya, R. Kümmerli, Bacterial siderophores in community and host interactions. *Nat. Rev. Microbiol.* **18**, 152–163 (2019).
5. T. S. Crofts, *et al.*, Shared strategies for  $\beta$ -lactam catabolism in the soil microbiome. *Nat. Chem. Biol.* **14**, 556–564 (2018).
6. L. R. Thompson, *et al.*, A communal catalogue reveals Earth’s multiscale microbial diversity. *Nature* **551**, 457–463 (2017).
7. R. Mendes, *et al.*, Deciphering the rhizosphere microbiome for disease-suppressive bacteria. *Science* **332**, 1097–1100 (2011).
8. H. Gross, J. E. Loper, Genomics of secondary metabolite production by *Pseudomonas* spp. *Nat. Prod. Rep.* **26**, 1408–46 (2009).
9. F. L. Stefanato, *et al.*, Pan-genome analysis identifies intersecting roles for *Pseudomonas* specialized metabolites in potato pathogen inhibition. *bioRxiv*, 1–35 (2019).
10. A. Folkesson, *et al.*, Adaptation of *Pseudomonas aeruginosa* to the cystic fibrosis airway: an evolutionary perspective. *Nat. Rev. Microbiol.* **10**, 841–851 (2012).
11. L. P. Wackett, *Pseudomonas putida*—a versatile biocatalyst. *Nat. Biotechnol.* **21**, 136–138 (2003).
12. K. Scherlach, *et al.*, Biosynthesis and Mass Spectrometric Imaging of Tolaasin, the Virulence Factor of Brown Blotch Mushroom Disease. *ChemBioChem* **14**, 2439–2443 (2013).
13. M. S. Hwang, R. L. Morgan, S. F. Sakar, P. W. Wang, D. S. Guttman, Phylogenetic characterization of virulence and resistance phenotypes of *Pseudomonas syringae*. *Appl. Environ. Microbiol.* **71**, 5182–5191 (2005).
14. D. Haas, G. Défago, Biological control of soil-borne pathogens by fluorescent pseudomonads. *Nat. Rev. Microbiol.* **3**, 307–319 (2005).
15. A. C. Parte, LPSN—list of prokaryotic names with standing in nomenclature. *Nucleic Acids Res.* **42**, D613–D616 (2014).
16. C. R. Woese, G. E. Fox, Phylogenetic structure of the prokaryotic domain: The primary kingdoms. *Proc. Natl. Acad. Sci.* **74**, 5088–5090 (1977).

17. P. Yarza, *et al.*, Uniting the classification of cultured and uncultured bacteria and archaea using 16S rRNA gene sequences. *Nat. Rev. Microbiol.* **12**, 635–645 (2014).
18. J. S. Johnson, *et al.*, Evaluation of 16S rRNA gene sequencing for species and strain-level microbiome analysis. *Nat. Commun.* **10**, 1–11 (2019).
19. M. Mulet, M. Gomila, B. Lemaitre, J. Lalucat, E. García-Valdés, Taxonomic characterisation of *Pseudomonas* strain L48 and formal proposal of *Pseudomonas entomophila* sp. nov. *Syst. Appl. Microbiol.* **35**, 145–149 (2012).
20. P. N. Tran, M. A. Savka, H. M. Gan, In-silico Taxonomic Classification of 373 Genomes Reveals Species Misidentification and New Genospecies within the Genus *Pseudomonas*. *Front. Microbiol.* **8**, 1–7 (2017).
21. M. Mulet, J. Lalucat, E. García-Valdés, DNA sequence-based analysis of the *Pseudomonas* species. *Environ. Microbiol.* **12**, 1513–1530 (2010).
22. D. Garrido-Sanz, *et al.*, Genomic and Genetic Diversity within the *Pseudomonas fluorescens* Complex. *PLoS One* **11**, e0150183 (2016).
23. M. Gomila, A. Peña, M. Mulet, J. Lalucat, E. García-Valdés, Phylogenomics and systematics in *Pseudomonas*. *Front. Microbiol.* **6**, 1–13 (2015).
24. M. Richter, R. Rosselló-Móra, Shifting the genomic gold standard for the prokaryotic species definition. *Proc. Natl. Acad. Sci.* **106**, 19126–19131 (2009).
25. C. Hesse, *et al.*, Genome-based evolutionary history of *Pseudomonas* spp. *Environ. Microbiol.* **20**, 2142–2159 (2018).
26. J. M. Raaijmakers, M. Vlami, J. T. de Souza, Antibiotic production by bacterial biocontrol agents. *Antonie Van Leeuwenhoek* **81**, 537–547 (2002).
27. J. E. Loper, *et al.*, Comparative Genomics of Plant-Associated *Pseudomonas* spp.: Insights into Diversity and Inheritance of Traits Involved in Multitrophic Interactions. *PLoS Genet.* **8**, e1002784 (2012).
28. M. Frapolli, J. F. Pothier, G. Défago, Y. Moëgne-Loccoz, Evolutionary history of synthesis pathway genes for phloroglucinol and cyanide antimicrobials in plant-associated fluorescent pseudomonads. *Mol. Phylogenet. Evol.* **63**, 877–890 (2012).
29. C. Quast, *et al.*, The SILVA ribosomal RNA gene database project: improved data processing and web-based tools. *Nucleic Acids Res.* **41**, 590–596 (2013).
30. P. Yarza, *et al.*, The All-Species Living Tree project: A 16S rRNA-based phylogenetic tree of all sequenced type strains. *Syst. Appl. Microbiol.* **31**, 241–250 (2008).
31. M. Mulet, A. Bennisar, J. Lalucat, E. García-Valdés, An *rpoD*-based PCR procedure for the identification of *Pseudomonas* species and for their detection in environmental samples. *Mol. Cell. Probes* **23**, 140–147 (2009).
32. D. Sánchez, *et al.*, *rpoD* Gene Pyrosequencing for the Assessment of *Pseudomonas* Diversity in a Water Sample from the Woluwe River. *Appl. Environ. Microbiol.* **80**, 4738–4744 (2014).

33. N. Geudens, J. C. Martins, Cyclic Lipodepsipeptides From *Pseudomonas* spp. – Biological Swiss-Army Knives. *Front. Microbiol.* **9**, 1–18 (2018).
34. J. M. Whipps, Microbial interactions and biocontrol in the rhizosphere. *J. Exp. Bot.* **52**, 487–511 (2001).
35. C. Voisard, *et al.*, “Biocontrol of Root Diseases by *Pseudomonas fluorescens* CHA0: Current Concepts and Experimental Approaches” in *Molecular Ecology of Rhizosphere Microorganisms: Biotechnology and the Release of GMOs*, (John Wiley & Sons, Ltd, 2007), pp. 67–89.
36. M. H. Medema, *et al.*, antiSMASH: rapid identification, annotation and analysis of secondary metabolite biosynthesis gene clusters in bacterial and fungal genome sequences. *Nucleic Acids Res.* **39**, W339–W346 (2011).
37. I. T. Paulsen, *et al.*, Complete genome sequence of the plant commensal *Pseudomonas fluorescens* Pf-5. *Nat. Biotechnol.* **23**, 873–878 (2005).
38. J. E. Loper, M. D. Henkels, B. T. Shaffer, F. A. Valeriote, H. Gross, Isolation and identification of rhizoxin analogs from *Pseudomonas fluorescens* Pf-5 by using a genomic mining strategy. *Appl. Environ. Microbiol.* **74**, 3085–3093 (2008).
39. H. Gross, *et al.*, The Genom isotopic Approach: A Systematic Method to Isolate Products of Orphan Biosynthetic Gene Clusters. *Chem. Biol.* **14**, 53–63 (2007).
40. J. M. Raaijmakers, M. Mazzola, Diversity and Natural Functions of Antibiotics Produced by Beneficial and Plant Pathogenic Bacteria. *Annu. Rev. Phytopathol.* **50**, 403–424 (2011).
41. J. Almario, *et al.*, Distribution of 2,4-Diacetylphloroglucinol Biosynthetic Genes among the *Pseudomonas* spp. Reveals Unexpected Polyphyletism. *Front. Microbiol.* **8**, 1218 (2017).
42. C. Keel, *et al.*, Suppression of Root Diseases by *Pseudomonas fluorescens* CHA0: Importance of the Bacterial Secondary Metabolite 2,4-Diacetylphloroglucinol. *Mol. Plant-Microbe Interact.* **5**, 4–13 (1992).
43. D. Cronin, *et al.*, Ecological interaction of a biocontrol *Pseudomonas fluorescens* strain producing 2,4-diacetylphloroglucinol with the soft rot potato pathogen *Erwinia carotovora* subsp. *atroseptica*. *FEMS Microbiol. Ecol.* **23**, 95–106 (2006).
44. J. M. Raaijmakers, D. M. Weller, Natural Plant Protection by 2,4-Diacetylphloroglucinol-Producing *Pseudomonas* spp. in Take-All Decline Soils. *Mol. Plant-Microbe Interact.* **11**, 144–152 (1998).
45. D. A. Phillips, T. C. Fox, M. D. King, T. V. Bhuvaneshwari, L. R. Teuber, Microbial Products Trigger Amino Acid Exudation from Plant Roots. *Plant Physiol.* **136**, 2887–2894 (2004).
46. J. Achkar, M. Xian, H. Zhao, J. W. Frost, Biosynthesis of Phloroglucinol. *J. Am. Chem. Soc.* **127**, 5332–5333 (2005).
47. M. G. Bangera, L. S. Thomashow, Identification and Characterization of a Gene Cluster for Synthesis of the Polyketide Antibiotic 2,4-Diacetylphloroglucinol from *Pseudomonas fluorescens* Q2-87. *J. Bacteriol.* **181**, 3155–3163 (1999).

48. M. Bottiglieri, C. Keel, Characterization of PhIG, a hydrolase that specifically degrades the antifungal compound 2,4-diacetylphloroglucinol in the biocontrol agent *Pseudomonas fluorescens* CHA0. *Appl. Environ. Microbiol.* **72**, 418–27 (2006).
49. A. Abbas, *et al.*, The putative permease PhIE of *Pseudomonas fluorescens* F113 has a role in 2,4-diacetylphloroglucinol resistance and in general stress tolerance. *Microbiology* **150**, 2443–2450 (2004).
50. A. Abbas, *et al.*, Characterization of interactions between the transcriptional repressor PhIF and its binding site at the phIA promoter in *Pseudomonas fluorescens* F113. *J. Bacteriol.* **184**, 3008–3016 (2002).
51. U. Schnider-Keel, *et al.*, Autoinduction of 2,4-diacetylphloroglucinol biosynthesis in the biocontrol agent *Pseudomonas fluorescens* CHA0 and repression by the bacterial metabolites salicylate and pyoluteorin. *J. Bacteriol.* **182**, 1215–1225 (2000).
52. X. Yan, *et al.*, Transcriptional Regulator PhIH Modulates 2,4-Diacetylphloroglucinol Biosynthesis in Response to the Biosynthetic Intermediate and End Product. *Appl. Environ. Microbiol.* **83**, e01419-17 (2017).
53. T. A. Kidarsa, N. C. Goebel, T. M. Zabriskie, J. E. Loper, Phloroglucinol mediates cross-talk between the pyoluteorin and 2,4-diacetylphloroglucinol biosynthetic pathways in *Pseudomonas fluorescens* Pf-5. *Mol. Microbiol.* **81**, 395–414 (2011).
54. Q. Yan, B. Philmus, J. H. Chang, J. E. Loper, Novel mechanism of metabolic co-regulation coordinates the biosynthesis of secondary metabolites in *Pseudomonas protegens*. *Elife* **6**, e22835 (2017).
55. C. R. Howell, R. D. Stipanovic, Suppression of *Pythium ultimum* -Induced Damping-Off of Cotton Seedlings by *Pseudomonas fluorescens* and its Antibiotic, Pyoluteorin. *Phytopathology* **70**, 712–715 (1980).
56. M. Maurhofer, C. Keel, D. Haas, G. Défago, Pyoluteorin production by *Pseudomonas fluorescens* strain CHA0 is involved in the suppression of *Pythium* damping-off of cress but not of cucumber. *Eur. J. Plant Pathol.* **100**, 221–232 (1994).
57. X. Huang, *et al.*, Identification and characterization of pltZ, a gene involved in the repression of pyoluteorin biosynthesis in *Pseudomonas* sp. M18. *FEMS Microbiol. Lett.* **232**, 197–202 (2004).
58. X. Huang, A. Yan, X. Zhang, Y. Xu, Identification and characterization of a putative ABC transporter PltHIJKN required for pyoluteorin production in *Pseudomonas* sp. M18. *Gene* **376**, 68–78 (2006).
59. M. G. Thomas, M. D. Burkart, C. T. Walsh, Conversion of L-Proline to Pyrrolyl-2-Carboxyl-S-PCP during Undecylprodigiosin and Pyoluteorin Biosynthesis. *Chem. Biol.* **9**, 171–184 (2002).
60. P. C. Dorrestein, E. Yeh, S. Garneau-Tsodikova, N. L. Kelleher, C. T. Walsh, Dichlorination of a pyrrolyl-S-carrier protein by FADH<sub>2</sub>- dependent halogenase PltA during pyoluteorin biosynthesis. *Proc. Natl. Acad. Sci.* **102**, 13843–13848 (2005).

61. C. L. Bender, V. Rangaswamy, J. Loper, Polyketide Production by Plant-Associated Pseudomonads. *Annu. Rev. Phytopathol.* **37**, 175–196 (2003).
62. Q. Yan, M. Liu, T. Kidarsa, C. P. Johnson, J. E. Loper, Two Pathway-Specific Transcriptional Regulators, PltR and PltZ, Coordinate Autoinduction of Pyoluteorin in *Pseudomonas protegens* Pf-5. *Microorganisms* **9**, 1–14 (2021).
63. M. Brodhagen, M. D. Henkels, J. E. Loper, Positive Autoregulation and Signaling Properties of Pyoluteorin, an Antibiotic Produced by the Biological Control Organism *Pseudomonas fluorescens* Pf-5. *Appl. Environ. Microbiol.* **70**, 1758–1766 (2004).
64. J. C. Clifford, *et al.*, Phloroglucinol functions as an intracellular and intercellular chemical messenger influencing gene expression in *Pseudomonas protegens*. *Environ. Microbiol.* **18**, 3296–3308 (2016).
65. J. M. Raaijmakers, R. F. Bonsall, D. M. Weller, Effect of Population Density of *Pseudomonas fluorescens* on Production of 2,4-Diacetylphloroglucinol in the Rhizosphere of Wheat. *Phytopathology* **89**, 470–475 (1999).
66. S. Götze, P. Stallforth, Structure, properties, and biological functions of nonribosomal lipopeptides from pseudomonads. *Nat. Prod. Rep.* **37**, 29–54 (2020).
67. R. Finking, M. A. Marahiel, Biosynthesis of Nonribosomal Peptides. *Annu. Rev. Microbiol.* **58**, 453–488 (2004).
68. T. Stachelhaus, H. D. Mootz, M. A. Marahiel, The specificity-conferring code of adenylation domains in nonribosomal peptide synthetases. *Chem. Biol.* **6**, 493–505 (1999).
69. J. M. Raaijmakers, I. De Bruijn, M. J. D. De Kock, Cyclic Lipopeptide Production by Plant-Associated *Pseudomonas* spp.: Diversity, Activity, Biosynthesis, and Regulation. *Mol. Plant-Microbe Interact.* **19**, 699–710 (2007).
70. P. M. Sobrero, A. Muzlera, J. Frescura, E. Jofré, C. Valverde, A matter of hierarchy: activation of orfamide production by the post-transcriptional Gac-Rsm cascade of *Pseudomonas protegens* CHA0 through expression upregulation of the two dedicated transcriptional regulators. *Environ. Microbiol. Rep.* **9**, 599–611 (2017).
71. Z. Ma, *et al.*, Biosynthesis, chemical structure, and structure-activity relationship of orfamide lipopeptides produced by *Pseudomonas protegens* and related species. *Front. Microbiol.* **7**, 1–16 (2016).
72. I. De Bruijn, *et al.*, Genome-based discovery, structure prediction and functional analysis of cyclic lipopeptide antibiotics in *Pseudomonas* species. *Mol. Microbiol.* **63**, 417–428 (2007).
73. M. Kruijt, H. Tran, J. M. Raaijmakers, Functional, genetic and chemical characterization of biosurfactants produced by plant growth-promoting *Pseudomonas putida* 267. *J. Appl. Microbiol.* **107**, 546–556 (2009).
74. J. M. Raaijmakers, D. M. Weller, L. S. Thomashow, Frequency of Antibiotic-Producing *Pseudomonas* spp. in Natural Environments. *Appl. Environ. Microbiol.* **63**, 881–7 (1997).

75. O. V Mavrodi, D. V Mavrodi, L. S. Thomashow, D. M. Weller, Quantification of 2,4-diacetylphloroglucinol-producing *Pseudomonas fluorescens* strains in the plant rhizosphere by real-time PCR. *Appl. Environ. Microbiol.* **73**, 5531–8 (2007).
76. B. Schwyn, J. B. Neilands, Universal chemical assay for the detection and determination of siderophores. *Anal. Biochem.* **160**, 47–56 (1987).
77. F. Feigl, V. Anger, Replacement of benzidine by copper ethylacetoacetate and tetra base as spot-test reagent for hydrogen cyanide and cyanogen. *Analyst* **91**, 282–284 (1966).
78. A. S. Khalil, J. J. Collins, Synthetic biology: applications come of age. *Nat. Rev. Genet.* **11**, 367–379 (2010).
79. X. Wan, T. Y. H. Ho, B. Wang, “Engineering Prokaryote Synthetic Biology Biosensors” in *Handbook of Cell Biosensors*, (Springer International Publishing, 2019), pp. 1–37.
80. K. Y. Wen, J. W. Rutter, C. P. Barnes, L. Dekker, “Fundamental Building Blocks of Whole-Cell Biosensor Design” in *Handbook of Cell Biosensors*, (Springer, Cham, 2020), pp. 1–23.
81. N. Lautenschläger, P. F. Popp, T. Mascher, Development of a novel heterologous  $\beta$ -lactam-specific whole-cell biosensor in *Bacillus subtilis*. *J. Biol. Eng.* **14**, 1–14 (2020).
82. Y. Q. Sun, *et al.*, Development of a Biosensor Concept to Detect the Production of Cluster-Specific Secondary Metabolites. *ACS Synth. Biol.* **6**, 1026–1033 (2017).
83. M. Maurhofer, C. Keel, D. Haas, G. Défago, Influence of plant species on disease suppression by *Pseudomonas fluorescens* strain CHAO with enhanced antibiotic production. *Plant Pathol.* **44**, 40–50 (1995).
84. M. Bergsma-Vlami, M. E. Prins, J. M. Raaijmakers, Influence of plant species on population dynamics, genotypic diversity and antibiotic production in the rhizosphere by indigenous *Pseudomonas* spp. *FEMS Microbiol. Ecol.* **52**, 59–69 (2005).
85. R. F. Bonsall, D. M. Weller, L. S. Thomashow, Quantification of 2,4-Diacetylphloroglucinol Produced by Fluorescent *Pseudomonas* spp. In Vitro and in the Rhizosphere of Wheat. *Appl. Environ. Microbiol.* **63**, 951–955 (1997).
86. A. Bauermeister, H. Mannocho-Russo, L. V. Costa-Lotufo, A. K. Jarmusch, P. C. Dorrestein, Mass spectrometry-based metabolomics in microbiome investigations. *Nat. Rev. Microbiol.*, 1–18 (2021).
87. A. Bouslimani, L. M. Sanchez, N. Garg, P. C. Dorrestein, Mass spectrometry of natural products: current, emerging and future technologies. *Nat. Prod. Rep.* **31**, 718–729 (2014).
88. B. Geier, *et al.*, Spatial metabolomics of in situ host–microbe interactions at the micrometre scale. *Nat. Microbiol.* **5**, 498–510 (2020).
89. M. F. Traxler, J. D. Watrous, T. Alexandrov, P. C. Dorrestein, R. Kolter, Interspecies interactions stimulate diversification of the *Streptomyces coelicolor* secreted metabolome. *MBio* **4**, e00459-13 (2013).

90. K. R. Foster, T. Bell, Competition, Not Cooperation, Dominates Interactions among Culturable Microbial Species. *Curr. Biol.* **22**, 1845–1850 (2012).
91. J. Kehe, *et al.*, Massively parallel screening of synthetic microbial communities. *Proc. Natl. Acad. Sci.* **116**, 12804–12809 (2019).
92. J. Kehe, *et al.*, Positive interactions are common among culturable bacteria. *Sci. Adv.* **7**, 1–10 (2021).
93. J. Davies, What are antibiotics? Archaic functions for modern activities. *Mol. Microbiol.* **4**, 1227–1232 (1990).
94. E. B. Goh, *et al.*, Transcriptional modulation of bacterial gene expression by subinhibitory concentrations of antibiotics. *Proc. Natl. Acad. Sci.* **99**, 17025–17030 (2002).
95. J. Davies, G. B. Spiegelman, G. Yim, The world of subinhibitory antibiotic concentrations. *Curr. Opin. Microbiol.* **9**, 445–453 (2006).
96. S. Westhoff, G. P. van Wezel, D. E. Rozen, Distance-dependent danger responses in bacteria. *Curr. Opin. Microbiol.* **36**, 95–101 (2017).
97. M. LeRoux, S. B. Peterson, J. D. Mougous, Bacterial danger sensing. *J. Mol. Biol.* **427**, 3744–3753 (2015).
98. S. Westhoff, A. M. Kloosterman, S. F. A. van Hoesel, G. P. van Wezel, D. E. Rozen, Competition sensing changes antibiotic production in streptomyces. *MBio* **12**, e02729-20 (2021).
99. M. I. Abrudan, *et al.*, Socially mediated induction and suppression of antibiosis during bacterial coexistence. *Proc. Natl. Acad. Sci.* **112**, 11054–11059 (2015).
100. P. Garbeva, M. W. Silby, J. M. Raaijmakers, S. B. Levy, W. De Boer, Transcriptional and antagonistic responses of *Pseudomonas fluorescens* Pf0-1 to phylogenetically different bacterial competitors. *ISME J.* **5**, 973–985 (2011).
101. N. Lee, *et al.*, Iron competition triggers antibiotic biosynthesis in *Streptomyces coelicolor* during coculture with *Myxococcus xanthus*. *ISME J.* **14**, 1111–1124 (2020).
102. G. L. Lozano, *et al.*, A chemical counterpunch: *Chromobacterium violaceum* ATCC 31532 produces violacein in response to translation-inhibiting antibiotics. *MBio* **11**, e00948-20 (2020).
103. Y. Buijs, *et al.*, Enhancement of antibiotic production by co-cultivation of two antibiotic producing marine Vibrionaceae strains. *FEMS Microbiol. Ecol.* **97**, fiab41 (2021).
104. O. Tyc, *et al.*, Impact of interspecific interactions on antimicrobial activity among soil bacteria. *Front. Microbiol.* **5**, 1–10 (2014).
105. D. M. Weller, J. M. Raaijmakers, B. B. M. Gardener, L. S. Thomashow, Microbial populations responsible for specific soil suppressiveness to plant pathogens. *Annu. Rev. Phytopathol.* **40**, 309–48 (2002).
106. J. Almario, D. Muller, G. Défago, Y. Moënne-Loccoz, Rhizosphere ecology and phytoprotection in soils naturally suppressive to *Thielaviopsis* black root rot of tobacco. *Environ. Microbiol.* **16**, 1949–1960 (2014).

107. B. B. Landa, *et al.*, Differential ability of genotypes of 2,4-diacetylphloroglucinol-producing *Pseudomonas fluorescens* strains to colonize the roots of pea plants. *Appl. Environ. Microbiol.* **68**, 3226–3237 (2002).
108. M. Kyselková, *et al.*, Comparison of rhizobacterial community composition in soil suppressive or conducive to tobacco black root rot disease. *ISME J.* **3**, 1127–1138 (2009).
109. J. T. De Souza, D. M. Weller, J. M. Raaijmakers, Frequency, Diversity, and Activity of 2,4-Diacetylphloroglucinol-Producing Fluorescent *Pseudomonas* spp. in Dutch Take-all Decline Soils. *Phytopathology* **93**, 54–63 (2003).
110. M. Frapolli, G. Défago, Y. Moëgne-Loccoz, Multilocus sequence analysis of biocontrol fluorescent *Pseudomonas* spp. producing the antifungal compound 2,4-diacetylphloroglucinol. *Environ. Microbiol.* **9**, 1939–1955 (2007).
111. B. B. M. Gardener, *et al.*, Genotypic and Phenotypic Diversity of phlD-Containing *Pseudomonas* Strains Isolated from the Rhizosphere of Wheat. *Appl. Environ. Microbiol.* **66**, 1939–1946 (2000).
112. J. Watrous, *et al.*, Mass spectral molecular networking of living microbial colonies. *Proc. Natl. Acad. Sci.* **109**, E1743–E1752 (2012).
113. M. Van Der Voort, *et al.*, Genome mining and metabolic profiling of the rhizosphere bacterium *Pseudomonas* sp. SH-C52 for antimicrobial compounds. *Front. Microbiol.* **6**, 1–14 (2015).
114. T. Bell, J. A. Newman, B. W. Silverman, S. L. Turner, A. K. Lilley, The contribution of species richness and composition to bacterial services. *Nature* **436**, 1157–1160 (2005).
115. A. Jousset, *et al.*, Biodiversity and species identity shape the antifungal activity of bacterial communities. *Ecology* **95**, 1184–1190 (2014).
116. J. Becker, N. Eisenhauer, S. Scheu, A. Jousset, Increasing antagonistic interactions cause bacterial communities to collapse at high diversity. *Ecol. Lett.* **15**, 468–474 (2012).
117. J. Hu, *et al.*, Probiotic diversity enhances rhizosphere microbiome function and plant disease suppression. *MBio* **7**, e01790-16 (2016).
118. Z. Mehrabi, *et al.*, *Pseudomonas* spp. diversity is negatively associated with suppression of the wheat take-all pathogen. *Sci. Rep.* **6**, 1–10 (2016).
119. V. M. D’Costa, K. M. McGrann, D. W. Hughes, G. D. Wright, Sampling the Antibiotic Resistome. *Science* **311**, 374–377 (2006).
120. V. M. D’Costa, *et al.*, Inactivation of the lipopeptide antibiotic daptomycin by hydrolytic mechanisms. *Antimicrob. Agents Chemother.* **56**, 757–764 (2012).
121. E. D. Kelsic, J. Zhao, K. Vetsigian, R. Kishony, Counteraction of antibiotic production and degradation stabilizes microbial communities. *Nature* **521**, 516–519 (2015).
122. R. Hermenau, S. Kugel, A. J. Komor, C. Hertweck, Helper bacteria halt and disarm mushroom pathogens by linearizing structurally diverse cyclolipopeptides. *Proc. Natl. Acad. Sci.* **117**, 23802–23806 (2020).

123. S. Zhang, R. Mukherji, S. Chowdhury, L. Reimer, P. Stallforth, Lipopeptide-mediated bacterial interaction enables cooperative predator defense. *Proc. Natl. Acad. Sci.* **118**, e2013759118 (2021).
124. O. Marín, B. González, M. J. Poupin, From Microbial Dynamics to Functionality in the Rhizosphere: A Systematic Review of the Opportunities With Synthetic Microbial Communities. *Front. Plant Sci.* **12**, 1–12 (2021).
125. R. Tecon, *et al.*, Bridging the Holistic-Reductionist Divide in Microbial Ecology. *mSystems* **4**, e00265-18 (2019).
126. J. A. Huber, *et al.*, Microbial population structures in the deep marine biosphere. *Science* **318**, 97–100 (2007).
127. J. Raes, I. Letunic, T. Yamada, L. J. Jensen, P. Bork, Toward molecular trait-based ecology through integration of biogeochemical, geographical and metagenomic data. *Mol. Syst. Biol.* **7**, 1–9 (2011).
128. T. Grosskopf, O. S. Soyer, Synthetic microbial communities. *Curr. Opin. Microbiol.* **18**, 72–77 (2014).
129. J. Dolinšek, F. Goldschmidt, D. R. Johnson, Synthetic microbial ecology and the dynamic interplay between microbial genotypes. *FEMS Microbiol. Rev.* **40**, 961–979 (2016).
130. C. D. Smolke, P. A. Silver, Informing Biological Design by Integration of Systems and Synthetic Biology. *Cell* **144**, 855–859 (2011).
131. B. Niu, J. N. Paulson, X. Zheng, R. Kolter, Simplified and representative bacterial community of maize roots. *Proc. Natl. Acad. Sci.* **114**, E2450–E2459 (2017).
132. M. J. E. E. Voges, Y. Bai, P. Schulze-Lefert, E. S. Sattely, Plant-derived coumarins shape the composition of an Arabidopsis synthetic root microbiome. *Proc. Natl. Acad. Sci.* **116**, 12558–12565 (2019).
133. N. Bodenhausen, M. Bortfeld-Miller, M. Ackermann, J. A. Vorholt, A Synthetic Community Approach Reveals Plant Genotypes Affecting the Phyllosphere Microbiota. *PLoS Genet.* **10**, e1004283 (2014).
134. L. Zhuang, *et al.*, Synthetic community with six *Pseudomonas* strains screened from garlic rhizosphere microbiome promotes plant growth. *Microb. Biotechnol.* **14**, 488–502 (2021).
135. C. N. Lozano-Andrade, M. Wibowo, M. L. Strube, Á. T. Kovács, Synthetic community invasion depends on secondary metabolite production in *Bacillus subtilis*. *Manuscr. prep.* (2021).
136. B. Kerr, M. A. Riley, M. W. Feldman, B. J. M. Bohannan, Local dispersal promotes biodiversity in a real-life game of rock–paper–scissors. *Nature* **418**, 171–174 (2002).
137. L. Ma, *et al.*, Hydrogel-based transparent soils for root phenotyping in vivo. *Proc. Natl. Acad. Sci.* **166**, 11063–11068 (2019).

138. B. B. Landa, H. A. E. De Werd, B. B. McSpadden Gardener, D. M. Weller, Comparison of three methods for monitoring populations of different genotypes of 2,4-diacetylphloroglucinol-producing *Pseudomonas fluorescens* in the rhizosphere. *Phytopathology* **92**, 129–137 (2002).
139. N. Aagot, O. Nybroe, P. Nielsen, K. Johnsen, An Altered *Pseudomonas* Diversity Is Recovered from Soil by Using Nutrient-Poor *Pseudomonas*-Selective Soil Extract Media. *Appl. Environ. Microbiol.* **67**, 5233–5239 (2001).
140. A. J. Meyer, T. H. Segall-Shapiro, E. Glassey, J. Zhang, C. A. Voigt, *Escherichia coli* “Marionette” strains with 12 highly optimized small-molecule sensors. *Nat. Chem. Biol.* **15**, 196–204 (2019).
141. B. Canton, A. Labno, D. Endy, Refinement and standardization of synthetic biological parts and devices. *Nat. Biotechnol.* **26**, 787–793 (2008).
142. X. Wan, *et al.*, Cascaded amplifying circuits enable ultrasensitive cellular sensors for toxic metals. *Nat. Chem. Biol.* **15**, 540–548 (2019).
143. S. Hooshangi, S. Thiberge, R. Weiss, Ultrasensitivity and noise propagation in a synthetic transcriptional cascade. *Proc. Natl. Acad. Sci.* **102**, 3581–3586 (2005).
144. M. Mimee, *et al.*, An ingestible bacterial-electronic system to monitor gastrointestinal health. *Science* **360**, 915–918 (2018).
145. Q. Yan, *et al.*, Secondary metabolism and interspecific competition affect accumulation of spontaneous mutants in the GacS-GacA regulatory system in *Pseudomonas protegens*. *MBio* **9**, e01845-17 (2018).
146. M. Le Roux, *et al.*, Kin cell lysis is a danger signal that activates antibacterial pathways of *pseudomonas aeruginosa*. *Elife* **2015**, 1–65 (2015).
147. C. Dubuis, D. Haas, Cross-species GacA-controlled induction of antibiosis in pseudomonads. *Appl. Environ. Microbiol.* **73**, 650–654 (2007).
148. S. Wellington, E. Peter Greenberg, Quorum sensing signal selectivity and the potential for interspecies cross talk. *MBio* **10**, e00146-19 (2019).
149. M. Lichtenberg, R. D. Nørregaard, M. Kühn, Diffusion or advection? Mass transfer and complex boundary layer landscapes of the brown alga *Fucus vesiculosus*. *J. R. Soc. Interface* **14**, 1–10 (2017).
150. J. Galet, *et al.*, Gluconic acid-producing *Pseudomonas* sp. prevent  $\gamma$ -actinorhodin biosynthesis by *Streptomyces coelicolor* A3(2). *Arch. Microbiol.* **196**, 619–627 (2014).
151. K. Lapouge, M. Schubert, F. H. T. Allain, D. Haas, Gac/Rsm signal transduction pathway of  $\gamma$ -proteobacteria: from RNA recognition to regulation of social behaviour. *Mol. Microbiol.* **67**, 241–253 (2008).
152. K. T. Elvers, K. Leeming, H. M. Lappin-Scott, Binary and mixed population biofilms: time-lapse image analysis and disinfection with biocides. *J. Ind. Microbiol. Biotechnol.* **29**, 331–338 (2002).

153. M. Burmølle, *et al.*, Enhanced biofilm formation and increased resistance to antimicrobial agents and bacterial invasion are caused by synergistic interactions in multispecies biofilms. *Appl. Environ. Microbiol.* **72**, 3916–3923 (2006).
154. M. Wang, *et al.*, Sharing and community curation of mass spectrometry data with Global Natural Products Social Molecular Networking. *Nat. Biotechnol.* **34**, 828–837 (2016).
155. G. Dantas, M. O. A. Sommer, R. D. Oluwasegun, G. M. Church, Bacteria subsisting on antibiotics. *Science* **320**, 100–103 (2008).

## Chapter 7

### Research papers

**T**he remaining part of this thesis consists of full-length research papers prepared during this PhD project. The papers are enclosed as follows:

#### Paper 1

J. G. Lauritsen, **M. L. Hansen**, P. K. Bech, L. Jelsbak, L. Gram, and M. L. Strube, Identification and Differentiation of *Pseudomonas* Species in Field Samples Using an rpoD Amplicon Sequencing Methodology. *mSystems* **6**, e00704-21 (2021).

#### Paper 2

**M. L. Hansen**, Z. He, M. Wibowo, and L. Jelsbak, A Whole-Cell Biosensor for Detection of 2,4-Diacetylphloroglucinol (DAPG)-Producing Bacteria from Grassland Soil. *Appl. Environ. Microbiol.* **87**, e01400-20 (2021)

#### Paper 3

**M. L. Hansen**, M. Wibowo, S. A. Jarmusch, T. O. Larsen, and L. Jelsbak, Communication is key: Sequential interspecies interactions affect production of antimicrobial secondary metabolites in *Pseudomonas protegens* DTU9.1. *Submitted* (2021)

#### Paper 4

**M. L. Hansen**, Z. Dènes, M. Wibowo, S. A. Jarmusch, A. J. C. Andersen, M. L. Strube, and L. Jelsbak, Counter-acting *Pseudomonas* invasion: Community-level resistance towards *Pseudomonas*-produced secondary metabolites. *In preparation* (2021)

# Paper 1

---

## Identification and Differentiation of *Pseudomonas* Species in Field Samples Using an *rpoD* Amplicon Sequencing Methodology

Lauritsen J.G., Hansen M.L., Bech P.K., Jelsbak L., Gram L., and Strube M.L.

*mSystems*, 2021, 6(4), e00704-21



# Identification and Differentiation of *Pseudomonas* Species in Field Samples Using an *rpoD* Amplicon Sequencing Methodology

 Jonas Greve Lauritsen,<sup>a</sup>
 Morten Lindqvist Hansen,<sup>a</sup>
 Pernille Kjersgaard Bech,<sup>a</sup>
 Lars Jelsbak,<sup>a</sup>
 Lone Gram,<sup>a</sup>
 Mikael Lenz Strube<sup>a</sup>

<sup>a</sup>Department of Biotechnology and Biomedicine, Technical University of Denmark, Kongens Lyngby, Denmark

**ABSTRACT** Species of the genus *Pseudomonas* are used for several biotechnological purposes, including plant biocontrol and bioremediation. To exploit the *Pseudomonas* genus in environmental, agricultural, or industrial settings, the organisms must be profiled at the species level as their bioactivity potential differs markedly between species. Standard 16S rRNA gene amplicon profiling does not allow for accurate species differentiation. Thus, the purpose of this study was to develop an amplicon-based high-resolution method targeting a 760-nucleotide (nt) region of the *rpoD* gene enabling taxonomic differentiation of *Pseudomonas* species in soil samples. The method was benchmarked on a 16-member *Pseudomonas* species mock community. All 16 species were correctly and semiquantitatively identified using *rpoD* gene amplicons, whereas 16S rRNA V3-V4 amplicon sequencing only correctly identified one species. We analyzed the *Pseudomonas* profiles in 13 soil samples in northern Zealand, Denmark, where samples were collected from grassland (3 samples) and agriculture soil (10 samples). *Pseudomonas* species represented up to 0.7% of the 16S rRNA gene abundance, of which each sampling site contained a unique *Pseudomonas* composition. Thirty culturable *Pseudomonas* strains were isolated from each grassland site and 10 from each agriculture site and identified by Sanger sequencing of the *rpoD* gene. In all cases, the *rpoD* amplicon approach identified more species than were found by cultivation, including hard-to-culture nonfluorescent pseudomonads, as well as more than were found by 16S rRNA V3-V4 amplicon sequencing. Thus, *rpoD* profiling can be used for species profiling of *Pseudomonas*, and large-scale prospecting of bioactive *Pseudomonas* may be guided by initial screening using this method.

**IMPORTANCE** A high-throughput sequencing-based method for profiling of *Pseudomonas* species in soil microbiomes was developed and identified more species than 16S rRNA gene sequencing or cultivation. *Pseudomonas* species are used as biocontrol organisms and plant growth-promoting agents, and the method will allow tracing of specific species of *Pseudomonas* as well as enable screening of environmental samples for further isolation and exploitation.

**KEYWORDS** microbiome analyses, *Pseudomonas*, diversity, *rpoD*, 16S rRNA, amplicon sequencing

*Pseudomonas* species are ubiquitous and can be isolated from a range of environments, including plant rhizospheres, marine habitats, and animal tissues (1–4). While the genus contains species that are pathogenic to plants and animals, several species express traits that enable their use in bioremediation, plant growth promotion, or plant disease suppression (5–8). The underlying beneficial mechanisms are often linked to specific species or even strains, including the production of pathogen-suppressing secondary metabolites, such as the antibiotic 2,4-diacetylphloroglucinol

**Citation** Lauritsen JG, Hansen ML, Bech PK, Jelsbak L, Gram L, Strube ML. 2021. Identification and differentiation of *Pseudomonas* species in field samples using an *rpoD* amplicon sequencing methodology. *mSystems* 6:e00704-21. <https://doi.org/10.1128/mSystems.00704-21>.

**Editor** Ryan McClure, Pacific Northwest National Laboratory

**Copyright** © 2021 Lauritsen et al. This is an open-access article distributed under the terms of the [Creative Commons Attribution 4.0 International license](https://creativecommons.org/licenses/by/4.0/).

Address correspondence to Mikael Lenz Strube, [milst@dtu.dk](mailto:milst@dtu.dk).

**Received** 8 June 2021

**Accepted** 14 July 2021

**Published** 3 August 2021

(DAPG) and pyoverdine siderophores (5, 9–11). Also, some strains promote growth of plants by solubilizing inorganic nutrients, such as phosphate and iron, or by producing plant hormones (11–14). Members of the *Pseudomonas fluorescens* group, in particular, are a major source of bioactivity since they have markedly larger genomes than other pseudomonads (15) and a high number of biosynthetic gene clusters, as determined by genomic analysis (16). In addition to strains expressing these and other beneficial traits, it is also becoming clear that the structure and diversity of the *Pseudomonas* community in bulk and rhizosphere soils *per se* can be associated with suppression of crop fungal pathogens (17, 18). Studies on the distribution, abundance, and diversity of *Pseudomonas* spp. in soil and rhizosphere often rely on cultivation-dependent analyses. However, Aagot et al. and others have demonstrated that cultivation of individual species of *Pseudomonas* is dependent on the specific conditions used (e.g., level of nutrients), and the decision to use a specific cultivation medium is thus a source of bias (19). Given these biases, linking specific *Pseudomonas* species and/or community structures to certain ecosystem performance metrics (including suppression of crop fungal pathogens) remains a challenge.

Amplicon sequencing of the 16S rRNA gene has become the standard for culture-independent, taxonomic profiling of environmental microbial communities. However, the 16S rRNA genes are very similar across closely related *Pseudomonas* species, with less than 1% nucleotide dissimilarity between many of the species (20). For example, in the subgroup of *P. putida*, the dissimilarities are between 0.16 and 2.31% (20). Therefore, 16S rRNA gene profiling only provides taxonomic resolution at the genus level, and studies of *Pseudomonas* community structures and dynamics at the species level require sequencing and analyses of other housekeeping genes. The *rpoD* gene, which encodes the sigma 70 factor of RNA polymerase, is an excellent target gene for phylogenetic and taxonomic analyses of *Pseudomonas* species (21). Using a highly selective pair of *Pseudomonas rpoD* primers, PsEG30F and PsEG790R (21), an *rpoD* amplicon sequencing method was used to analyze environmental DNA obtained from a single water sample (22). The method was developed for the 454/Roche GS-FLX platform and used an in-house *rpoD* database for sequence analysis. Given the discontinuation of the 454/Roche GS-FLX platform and the understanding of *Pseudomonas* phylogeny, there is a need for development of an amplicon-based method for reliable identification and differentiation of *Pseudomonas* species from environmental samples.

The purpose of the present study was to develop an amplicon sequencing protocol compatible with the Illumina MiSeq 300PE platform and to establish a new and improved bioinformatic pipeline with an updated database built upon the *Pseudomonas* type strain collection and taxonomic framework from Hesse et al. (15). The *rpoD* amplicon method allowed *Pseudomonas* species differentiation in environmental soil samples and can guide future bioprospecting endeavors.

## RESULTS

***In silico* target gene evaluation.** We evaluated nine genes and their accompanying primer sets (14 in total) for their phylogenetic discriminatory power using *in silico* PCR against two sets of genomes. The first was a library of the 166 type strain genomes of Hesse et al. (15) acting as a well-curated collection of all known *Pseudomonas* species and their phylogeny, although with most genomes being in contig form. The second was a library of 465 genomes of *Pseudomonas* species available from NCBI, all of which are complete but with high redundancy and incomplete taxonomy (Table 1). The *rpoD* primer pair PsEG30F and PsEG790R (21) resulted in the best phylogenetic resolution along with the highest total number of individual *Pseudomonas* genomes amplified and the lowest total non-*Pseudomonas* amplifications. This pair amplified 160/166 (96.39%) of type strains and 460/465 (98.92%) of the complete genomes (see Table S3 in the supplemental material), with no amplification of the negative controls. The *gyrB* gene primers UP-1E and APrU showed 100% amplification of the type strains, but unfortunately also amplified 25% of the negative controls and had multiple instances of amplicons much longer than

**TABLE 1** Overview of genes and primers selected as primary targets for evaluation of 465 *Pseudomonas* strains with the *in\_silico*\_PCR algorithm

Target gene	Primer name	Sequence (5'→3')	Length (nt)	Reference
16S rRNA	16S-341F	CCTACGGGNGGCWGCAG	464	42
	16S-805R	GACTACHVGGGTATCTAATCC		42
	16sF-LYP-3	GCGTAGAGTTTGATCCTGGCTCAG	1,253	26
	16sR-LYP-3	GACGGCGGTGTGTRCA		26
	16S-rRNA-F	AGCGGCGGACGGGTGAGTAATG	1,300	27
	16S-rRNA-R	AAGGAGGGGATCCAGCCGCA		27
<i>atpD</i>	atpD-F	CTGGCCGSATCATGGACG	900	27
	atpD-F	GTCCATGCCAGGATSGCG		27
<i>carA</i>	carA-F	TTCAACACCGCCATGACCGG	700	27
	carA-R	TGATGRCCSAGGCAGATRCC		27
<i>gapA</i>	gapA-Fps	CGCCATYCGCAACCCG	690	28
	gapA-Rps	CCCAYTCGTTGTCGTACCA		28
<i>gltA</i>	gltA-F	GGTGACAATGGCATTCTGC	294	26
	gltA-R	GTGCTGCGRRTATTGATGT		26
<i>gyrB</i>	gyrBBAUP2	GCGGAAGCGGCCNGSNATGTA		29
	APrU	GCNNGRTCYTTYTCYTRCA		30
	UP-1E	AYGSNGGNGGNARTTYRA	888–891	30
	APrU	GCNNGRTCYTTYTCYTRCA		30
<i>recA</i>	recA-F	TCSGGYARACCACSCTGAC	600	27
	recA-R	RTACCAGGCRCCGACTTCT		27
<i>rpoB</i>	LAPS	TGGCCGAGAACCAGTTCCGCGT	1,247	31
	LAPS27	CGGCTTCGTCCAGCTTGTTCCAG		31
<i>rpoD</i>	PsEG30F	ATYGAAATCGCCAARCG	437	21
	PsJL490R	AGYTTGATYGGGATGAA		This study
	PsEG30F	ATYGAAATCGCCAARCG	575	21
	PsJL628R	GGGAACWKGCAGGAARTC		This study
	PsEG30F <sup>a</sup>	ATYGAAATCGCCAARCG	736	21
	PsEG790R <sup>a</sup>	CGGTTGATKTCCTTGA		21

<sup>a</sup>Primers used for this study.

the expected length. To further evaluate the phylogenetic resolution of the primers, a multiple-sequence alignment of the amplicons and the resulting phylogeny was compared to the study by Hesse et al. (15), in which the 166 distinct *Pseudomonas* type strains were phylogenetically resolved based on multiple-locus sequencing typing of 100 genes. Here, the *rpoD* primers PsEG30F and PsEG790R from Mulet et al. (21) produced amplicons with the closest similarity to the phylogenetic map of Hesse et al. (15) and separated all species in the phylogenetic tree. The primers generated an ~760-nucleotide (nt)-long amplicon of the *rpoD* gene, which unfortunately led to a sequencing gap of 160 nt using the 300PE platform. Therefore, two new reverse primers were designed, PsJL490R and PsJL628R: however, both had lower amplification of the type strain genomes, at 89.16 and 83.73%, respectively. Moreover, the PsJL490R primer had poor *in vitro* amplification for the species of the synthetic community, while the PsJL628R primer showed unspecific amplification of the negative controls *Stenotrophomonas maltophilia*, *Achromobacter xylosoxidans*, and *Azospirillum brasilense* (see Fig. S1 in the supplemental material). Phylogenetic trees generated from these amplicons had comparable resolving power to the PsEG30F and PsEG790R pair, albeit with fewer nodes overall. As a consequence, we chose the PsEG30F and PsEG790R primer pair for *Pseudomonas* profiling. The universal 16S rRNA V3-V4 primers amplified 100% of the whole genomes and 87.95% of the type strains (owing to 16S genes often being the breakpoint in contigs). As noted previously (20), many of the amplicons are identical across *Pseudomonas* species and hence cannot be used for species resolution (see Fig. S2 in the supplemental material).

**Synthetic community primer testing.** To benchmark the amplicon protocol, a mixture of DNAs from 16 *Pseudomonas* strains was used to test the performance of the candidate *rpoD* primers in comparison with the standard V3-V4 16S rRNA gene amplicon sequencing approach. The 16 strains were selected to challenge the method across the genus by including five groups of *Pseudomonas* species (*P. aeruginosa*, *P.*

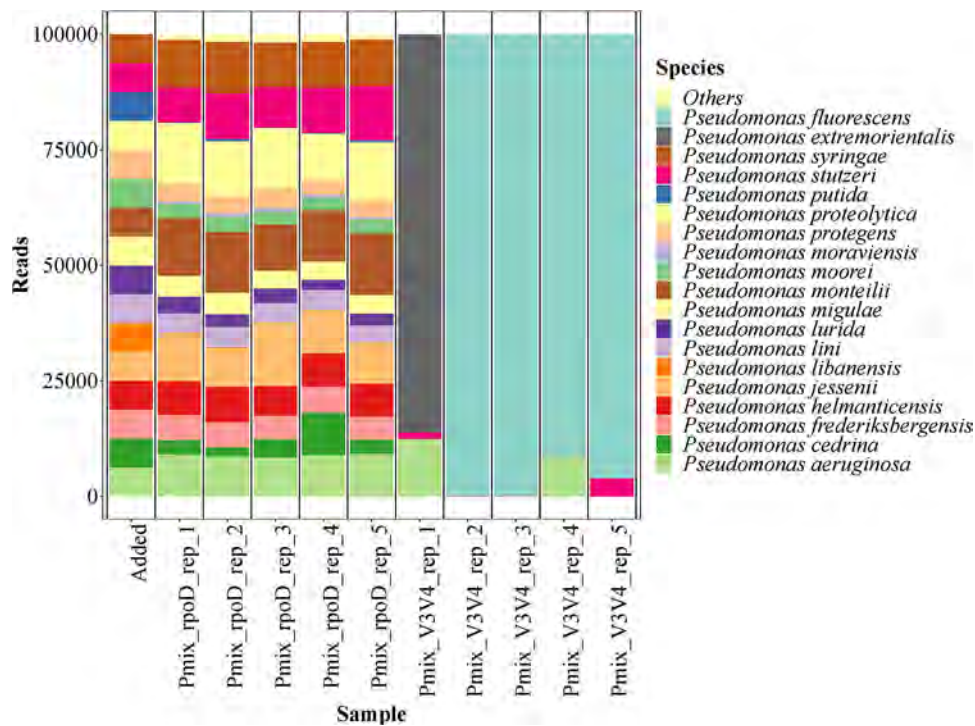


**FIG 1** Composition of a defined mixture of DNAs from 16 *Pseudomonas* species as analyzed by *rpoD* gene amplicon sequencing and V3-V4 16S rRNA gene sequencing in comparison to the theoretical composition. The leftmost bar shows the assumed theoretical abundances in the defined *Pseudomonas* DNA mixture. Each sample has been normalized to 100,000 reads.

*fluorescens*, *P. putida*, *P. stutzeri*, and *P. syringae*) and on fine resolution by selecting closely related species especially within subgroups (*P. fluorescens*, *P. mandelii*, and *P. jessenii*). In contrast to the V3-V4 amplicons, PE300 Illumina reads of the *rpoD* amplicons do not overlap and hence cannot be analyzed by standard operational taxonomic unit (OTU)-based methods. To overcome this challenge, each read pair was instead aligned to a custom database of *rpoD* genes using bowtie2 (23).

The *rpoD* amplicon method was able to identify all 16 strains, with abundances close to expected values (Fig. 1) and with a very low level of variation across the five technical replicates (Table 2). Of note, two species were underestimated: *P. putida* somewhat (~4% of expected value) and *P. libanensis* severely so (~1% of expected value). In contrast, the V3-V4 method erroneously classified the sample composition as being mainly *P. fluorescens* or *P. extremorientalis*, where the latter was not a part of the mixture. Also, small numbers of *P. stutzeri* and *P. aeruginosa* were detected by the V3-V4 approach. The beta dispersions—a measure of multivariate variation within groups—of the V3-V4 replicates were 4 times higher than those of the *rpoD* replicates, although this difference was not significant. The negative controls for both primer sets had low numbers of reads, later revealed to be common contaminants and adaptors.

**The microbial and *Pseudomonas* species composition in soil.** Soil was sampled from different sites, ranging from grassland to agricultural field soil. A total of 13 soil samples with 5 replicates each (65 samples in total) were analyzed, and after demultiplexing according to barcodes and primers, a total of 10,446,888 reads were available. Following this, 100,814 *rpoD* read pairs (201,628 reads) were annotated at the species level for the genus of *Pseudomonas* with sufficiently high confidence (minimum bit score of 10). According to the general purpose metagenomics classification tool Centrifuge (24), the non-*Pseudomonas* reads were approximately 50% PCR/adaptor artifacts (“Synthetic constructs”), along with the commonly found contaminant *Bradyrhizobium*, which was also found in the negative control. The overall mean and median values observed for the

**TABLE 2** List of *Pseudomonas* species used in the artificial DNA mixture for positive control

<i>Pseudomonas</i> species	Strain	Group <sup>a</sup>	Type strain	<i>rpoD</i> relative ratio (%) <sup>b</sup>
<i>P. aeruginosa</i>	PAO1	<i>P. aeruginosa</i>	Yes	140.38 ± 5.59
<i>P. cedrina</i>	May11.4	<i>P. fluorescens</i>	No	69.38 ± 45.31
<i>P. frederiksbergensis</i>	Nina6.10	<i>P. mandelii</i>	No	85.08 ± 4.04
<i>P. helmanticensis</i>	Nina1.7	<i>P. koreensis</i>	No	114.60 ± 7.36
<i>P. jessenii</i>	May3.1	<i>P. jessenii</i>	No	161.69 ± 34.83
<i>P. libanensis</i>	Nina5.10	<i>P. fluorescens</i>	No	1.82 ± 1.00
<i>P. lini</i>	Nina1.6	<i>P. mandelii</i>	No	66.73 ± 4.50
<i>P. lurida</i>	Nina3.4	<i>P. fluorescens</i>	No	45.56 ± 8.51
<i>P. migulae</i>	DSM 17966	<i>P. mandelii</i>	Yes	67.20 ± 5.35
<i>P. monteil</i>	DSM 14164	<i>P. putida</i>	Yes	192.34 ± 23.44
<i>P. moorei</i>	DSM 12647	<i>P. jessenii</i>	Yes	47.53 ± 3.51
<i>P. protegens</i>	DTU9.1	<i>P. protegens</i>	No	58.01 ± 6.16
<i>P. proteolytica</i>	May3.3	<i>P. gessardii</i>	No	194.56 ± 20.10
<i>P. putida</i>	KT2440	<i>P. putida</i>	Yes	4.12 ± 2.71
<i>P. stutzeri</i>	DSM 5190	<i>P. stutzeri</i>	Yes	151.88 ± 24.48
<i>P. syringae</i>	DSM 10604	<i>P. syringae</i>	Yes	164.45 ± 9.25

<sup>a</sup>The groups and subgroups of *Pseudomonas* according to Hesse et al. (15).

<sup>b</sup>Observed values for *rpoD* relative abundance versus theoretical abundance are given as mean ± standard deviation, where 100% is the expected value.

annotated *rpoD* reads across all samples were 1,558 and 598, respectively. The average number of *Pseudomonas rpoD* reads per sampling site varied between 133.4 (P8) and 4,022.2 (S7). Rarefaction curves revealed uneven saturation in some samples with low read depth (see Fig. S3 in the supplemental material). Moreover, we observed that quite a few read pairs were concordantly mapped, at 5.52%, likely owing to the high level of PCR artifact nonpseudomonal reads. In addition, less than 0.01% were discordantly mapped.

Using the relative abundances (Fig. 2), the performance of the method on the natural samples was investigated across biological replicates. The most abundant species

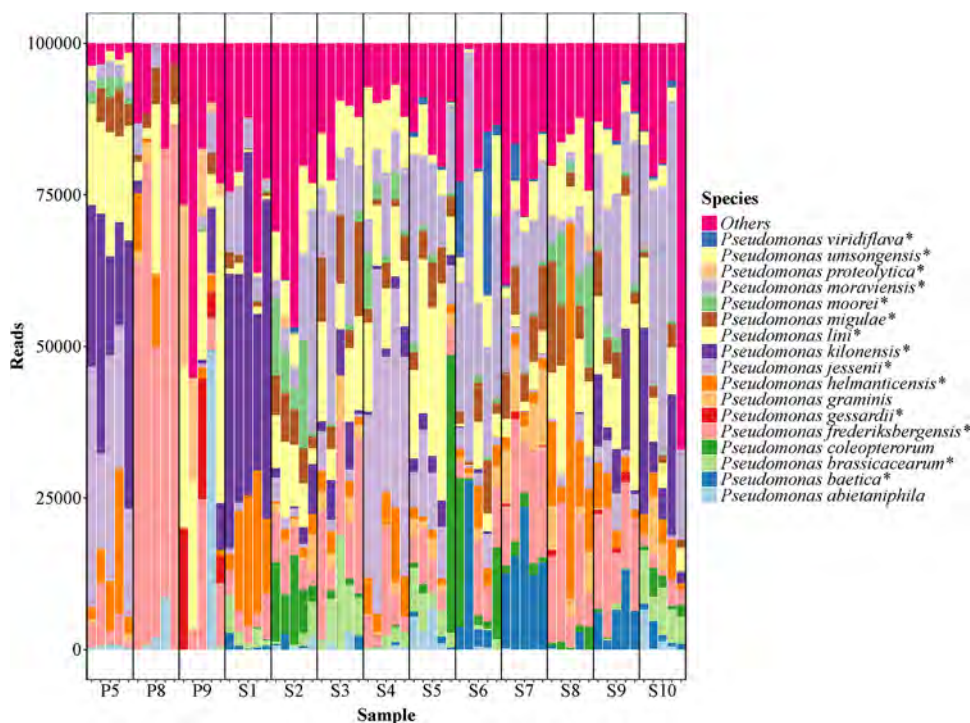


**FIG 2** Relative abundances of the 20 most abundant *Pseudomonas* species in 13 soil samples as analyzed by *rpoD* amplicon sequencing. Each sample has been normalized to 100,000 reads. Fluorescent species are marked by \*. S1, corn; S2, fallow (grass); S3, S7, and S9, wheat; S4, rye; S5, barley; S6, rapeseed; S8, grass seed; S10, Lucerne; P5 and P9, pristine short grass; P8, pristine long grass.

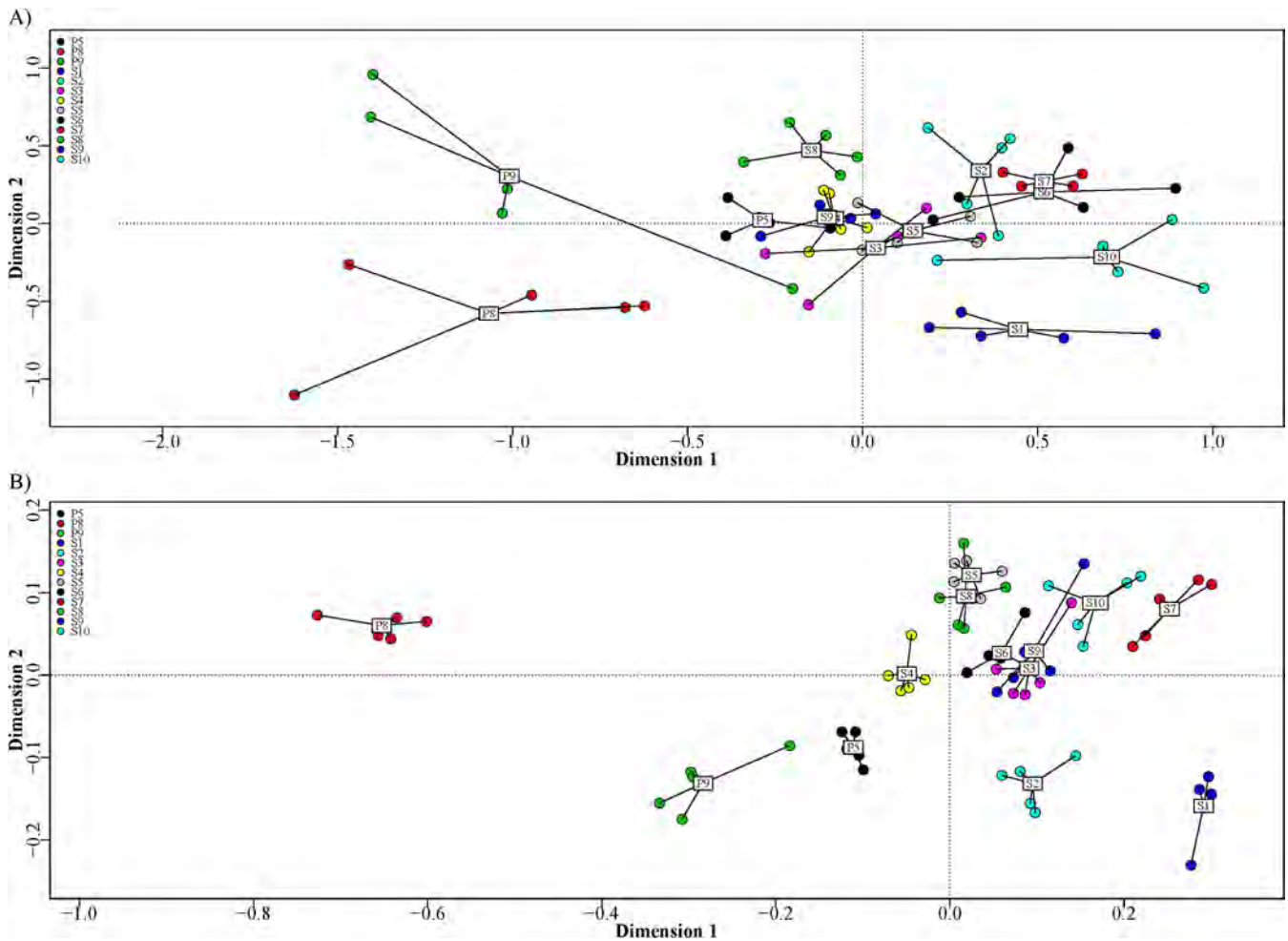


**FIG 3** Multivariate analysis by NMDS using Bray-Curtis distances of 13 soil sample sites using amplicon sequencing of (A) the *rpoD* gene (stress 0.1883) and (B) the V3-V4 region of the rRNA gene (stress 0.1039). S1, corn; S2, fallow (grass); S3, S7, and S9, wheat; S4, rye; S5, barley; S6, rapeseed; S8, grass seed; S10, Lucerne; P5 and P9, pristine short grass; P8, pristine long grass.

represented the four groups *P. syringae*, *P. lutea* (*P. graminis*), *P. putida* (*P. coleopterorum*), and *P. fluorescens* (marked by stars in Fig. 2). Within the group *P. fluorescens*, the five subgroups *P. jessenii* (*P. jessenii*, *P. moorei*, and *P. umsongensis*), *P. gessardii* (*P. gessardii* and *P. proteolytica*), *P. korensis* (*P. baetica*, *P. helmanticensis*, and *P. moraviensis*), *P. mandelii* (*P. frederiksbergensis*, *P. lini*, and *P. migulae*), and *P. corrugata* (*P. brassicacearum*, and *P. kilonensis*) were identified. Overall, similar abundances were found in replicate samples. This was confirmed by non-metric multidimensional scaling (NMDS) analysis (Fig. 3), in which biological replicates clustered together, although with different degrees of variation. The beta dispersions of the sites were negatively correlated ( $r = -0.455$ ) to estimated *Pseudomonas* load through quantitative PCR (qPCR), suggesting that the variation increased as *Pseudomonas* abundance decreased. The two sample sites P8 and P9 had the highest internal variation, likely owing to the low read count in these samples.

The individual sites in the *rpoD* amplicon analysis differed in species composition, despite being sampled from similar ecological environments (Fig. 2). For instance, the wheat soil samples S3, S7, and S9 had different *Pseudomonas* composition. *P. moraviensis*, *P. lini*, *P. helmanticensis*, and *P. frederiksbergensis* were common in most or all sampled soils; however, their relative abundances varied between sites.

The standard V3-V4 amplicon methodology resulted in a total of 6,947,525 mapped reads with an average of 106,885 per sample. A total of 378 families were identified, with the dominant families being *Xanthomonadaceae*, *Sphingomonadaceae*, *Planctomycetaceae*,

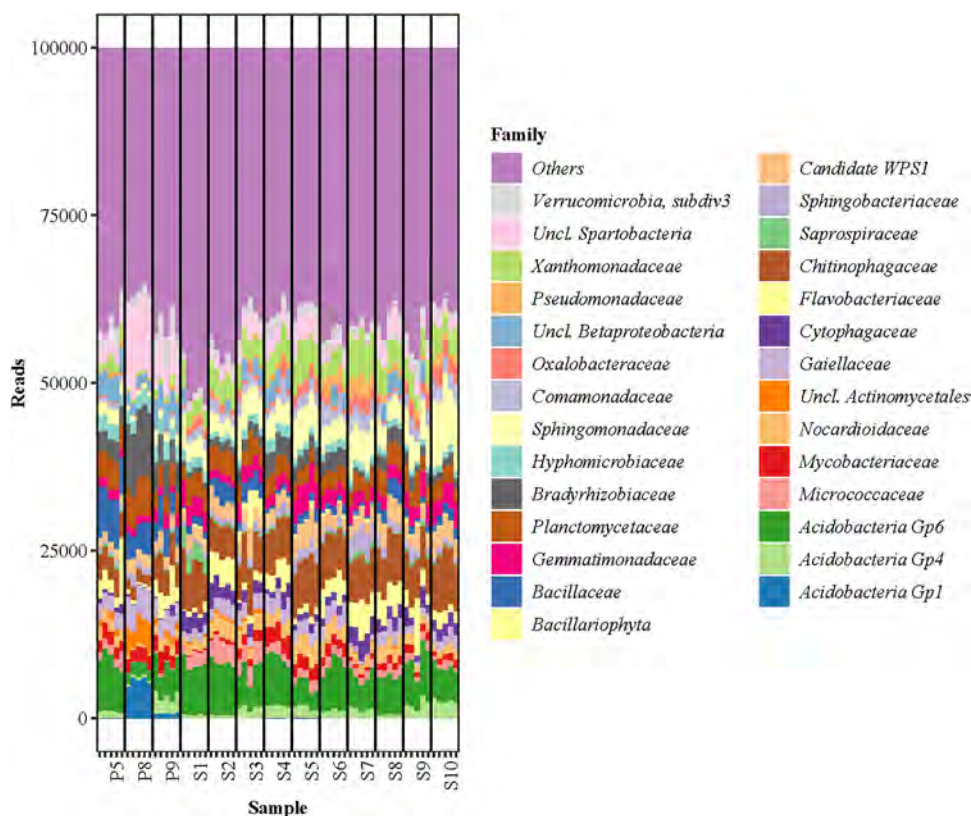


**FIG 4** Relative abundances of the 20 most abundant bacterial families in 13 soil samples as analyzed by amplicon sequencing of the V3-V4 region of the rRNA gene. Each sample has been normalized to 100,000 reads. S1, corn; S2, fallow (grass); S3, S7, and S9, wheat; S4, rye; S5, barley; S6, rapeseed; S8, grass seed; S10, Lucerne; P5 and P9, pristine short grass; P8, pristine long grass.

*Chitinophagaceae*, and *Acidobacteria* (group 6) (Fig. 4). At the family level, only smaller variations within sample sites were observed, as visually evident in the NMDS (Fig. 3), such as the unique presence of *Acidobacteria* (group 1) in the P8 and P9 sites. The average relative abundances of *Pseudomonas* varied from 0.008% (P8) to 0.73% (S8) in the different communities (Table 3). At the species level, V3-V4 typically only identified one or two species in higher relative abundances, and similar to the synthetic communities, these species were assigned to be *P. fluorescens* and *P. aeruginosa*. Each site had, on average, a 70% ( $P = 0.00004$ ) larger beta dispersion when profiled for *Pseudomonas* with the V3-V4 method compared to the *rpoD* method, and all had at least one sample with a species not found in the other replicates.

A standard curve comparing threshold cycle ( $C_T$ ) values from qPCR and cell numbers was generated using pure cultures of *P. moorei* and *Bacillus subtilis* and used to estimate total rather than relative abundance. The average total CFU/g soil per sample site (Table 3) ranged from  $2.1 \times 10^7$  (S7) to  $1.1 \times 10^8$  (S1 and P5). The average number of *Pseudomonas* CFU/g soil was calculated by multiplication by the relative abundance of *Pseudomonas* found in the V3-V4 amplicons (Table 3) and ranged from  $6.5 \times 10^3$  (P8) to  $4.2 \times 10^5$  (P5) CFU/g soil.

**Isolation and identification of presumptive *Pseudomonas*.** The *rpoD* amplicon culture-independent method for *Pseudomonas* species profiling was compared to cultivation-based profiling. Colonies were isolated from each of the sites on King's agar B<sup>+++</sup>, which is commonly used for *Pseudomonas* isolation (25): 10 from each of the S1 to S10 sites and 30 for the grassland samples P5, P8, and P9. The isolates were taxonomically classified by Sanger sequencing of part of the *rpoD* gene amplified with primers PsEG30F and PsEG790R and alignment to the *rpoD* database used for the amplicon analysis. In the grassland samples, 88 of the 90 isolates were classified at the species

**TABLE 3** Average total CFU per site estimated by qPCR and estimated relative and absolute abundance of *Pseudomonas* species based on V3-V4 amplicon sequencing

Site	Total bacteria (CFU/g soil)	Relative level of <i>Pseudomonas</i> (%)	Total <i>Pseudomonas</i> (CFU/g soil)
P5	$1.10 \times 10^8$	0.381	$4.19 \times 10^5$
P8	$8.13 \times 10^7$	0.008	$6.50 \times 10^3$
P9	$5.30 \times 10^7$	0.027	$1.43 \times 10^4$
S1	$1.10 \times 10^8$	0.288	$3.17 \times 10^5$
S2	$3.37 \times 10^7$	0.053	$1.79 \times 10^4$
S3	$3.56 \times 10^7$	0.021	$7.48 \times 10^3$
S4	$4.81 \times 10^7$	0.290	$1.39 \times 10^5$
S5	$2.21 \times 10^7$	0.065	$1.44 \times 10^4$
S6	$2.78 \times 10^7$	0.649	$1.80 \times 10^5$
S7	$2.13 \times 10^7$	0.209	$4.45 \times 10^4$
S8	$4.29 \times 10^7$	0.731	$3.14 \times 10^5$
S9	$4.27 \times 10^7$	0.126	$5.38 \times 10^4$
S10	$2.73 \times 10^7$	0.276	$7.53 \times 10^4$

level. Of particular interest were the species belonging to the *P. fluorescens* group, which encompassed 94% (83/88) of the isolates. This agrees with culture-independent profiling of P5 and P8, in which 97% (P5) and 93% (P8) of the *rpoD* reads were assigned to species in the *P. fluorescens* group. In P9, the fraction of species in the *P. fluorescens* group was lower (52%), which was predominantly due to a high fraction of *P. abietaniphila* species (39.5%), which was not observed by cultivation (Fig. 5; see Fig. S4 in the supplemental material).

The *rpoD* amplicon method identified more unique species than the cultivation method (Fig. 5), and species belonging to particular groups (i.e., the *P. lutea* group)

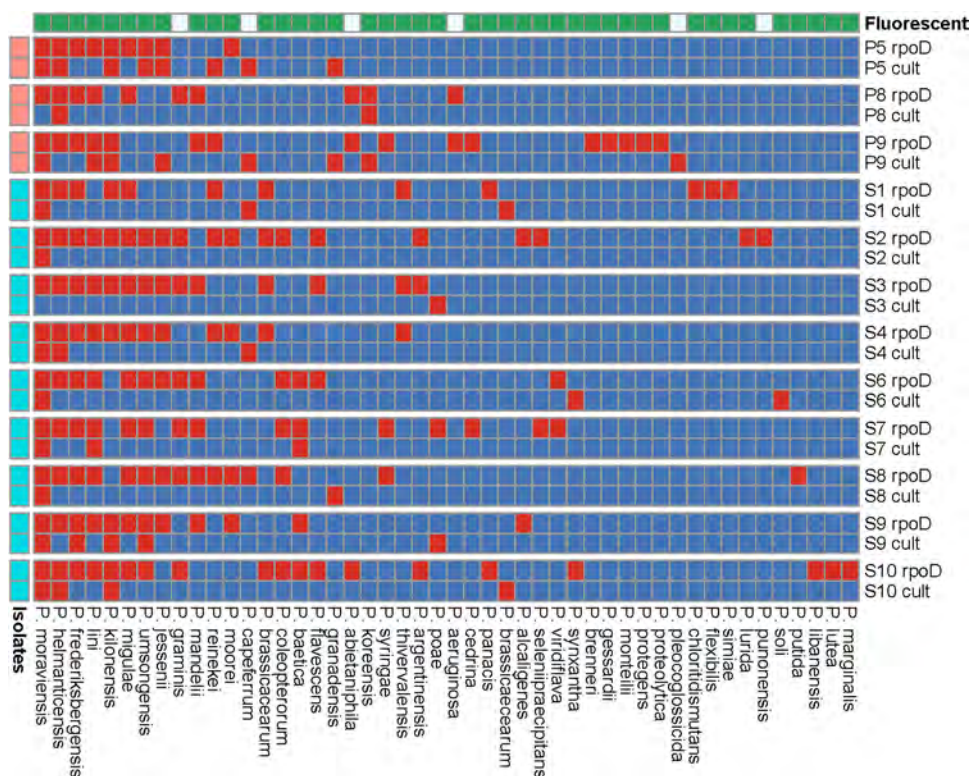


**FIG 5** Heat map of the presence (red) and absence (blue) of *Pseudomonas* species identified across sites by the *rpoD* amplicon method and the cultivation approach for each of the sampled sites. Thirty isolates were sampled from each of the sites P5, P8, and P9 and 10 from the sites S1 to S10 (leftmost color annotation). Fluorescent species are highlighted by green in the upper color annotation. The row labels “rpoD” and “cult” denote analysis by *rpoD* sequencing and culture, respectively.

and subgroups (i.e., the *P. mandelii* and *P. gessardii* subgroups of *P. fluorescens*) were almost exclusively identified by the amplicon method but not by the cultivation-based method. The same pattern emerged in the lesser-studied sites, S1 to S10, where *rpoD* profiling identified between 12 and 19 species compared to the cultivation approach, which found between 0 and 5.

## DISCUSSION

Global food demand is growing, and since petrochemical-based industrial farming is unlikely to be sustainable for future generations, there is an urgent need for novel and sustainable biocontrol agents. Species of the *Pseudomonas* genus are promising as plant biocontrol agents and since beneficial traits are typically linked to particular species, we developed a high-throughput method for metataxonomic assignment of these species in natural microbiomes. The method correctly identified all species of a *Pseudomonas* mock community. In soil samples, *rpoD* amplicon sequencing allowed a much higher degree of *Pseudomonas* species differentiation than both traditional 16S rRNA V3-V4 sequencing and culturing. The *rpoD* profiling enables quick identification and prioritization of soils with specific *Pseudomonas* communities for further analysis and culturing.

A total of 14 primer pairs targeting the genus *Pseudomonas* (26–31) were examined using *in silico* PCR. The primer pair PsEG30F and PsEG790R (21) outperformed all other pairs, and in further analysis of the *rpoD* genes from 465 *Pseudomonas* species, two alternative forward primers were identified. However, the PsEG30F and PsEG790R primers had superior performance and were ultimately selected for further testing. Multiple studies (20, 21, 26, 32, 33) have shown that the *rpoD* gene is a good candidate for identification at the species and strain levels for the genus of *Pseudomonas*, especially compared to the 16S rRNA gene (20). The second-best candidate was identified as the *gap* primers of Sarkar and Guttman (28). However, these primers also amplified non-*Pseudomonas* species *in vitro* (data not shown) and were therefore not further considered. The PsEG30F and PsEG790R amplicons were adapted to an Illumina system, which unfortunately has too short of a read length to overlap, necessitating a new bioinformatic pipeline drawing inspiration from annotation of transcriptome sequencing (RNA-seq) data, as well as a database based on the genomes from Hesse et al. (15).

When testing the method on a known mixture of pseudomonads, *P. libanensis* and *P. putida* were underestimated. Through *in silico* investigation, *P. libanensis* was poorly targeted by the primers, implying poor amplification efficiency (data not shown). The *rpoD* genes of *P. putida* KT2440 (in the mixture), *P. putida* NBRC14164 (in the database), and *P. montellii* DSM14164 (in the database) were compared in a phylogenetic tree (see Fig. S5 in the supplemental material), and although the three species are extremely closely related, KT2440 and DSM14164 are nearly identical and likely to overlap in the investigation. In the future, the *rpoD* database could be expanded to contain more strains for each species to give a wider coverage for such fringe cases. Such an addition could also lead to a strain-level differentiation in future studies. Alternatively, this occurrence could also indicate that *P. putida* and *P. montellii* generally are very closely related and difficult to separate. According to Hesse et al. (15), the two species are also extremely closely related based on the protein phylogeny of 100 gene orthologues.

The V3-V4 amplicon data for the *in vitro* DNA sample predominantly identified one species in the sample—*P. extremorientalis* or *P. fluorescens*—both of which belong to the subgroup *P. fluorescens* (15). This was also seen in the study by Mulet et al. (20), where species of the *Pseudomonas* genus at most had 2% dissimilarity in the 16S rRNA gene, and hence this gene does not allow a species-level resolution.

The *rpoD* amplicon methodology was used to profile the *Pseudomonas* population in soil samples. The relative abundances across replicates were very similar, yet some variation was observed, which could be caused by spatial differences within the soil sampled (34). Replicate variance was associated with low *Pseudomonas* load, as a negative correlation ( $r = -0.455$ ) was observed between the multivariate variance of the replicates (e.g., the beta dispersion) and the observed *Pseudomonas* CFU/g soil. To our

knowledge the closest non-16S rRNA gene-based amplicon study of *Pseudomonas* is by Sánchez et al. (22), where an *rpoD* amplicon methodology was used to identify *Pseudomonas* species in a water sample. However, a direct comparison is difficult, since Sánchez et al. (22) analyzed a single river sample with no replicates and used 454 sequencing and a blastn similarity search followed by OTU clustering rather than Illumina sequencing and bowtie mapping as in our study. The use of the 454 system, discontinued in 2016, results in longer (300 to 600 bp) single-end reads, thus avoiding the issues with nonoverlapping reads, although they are also too short to cover the entire amplicon. Use of single-end reads allows for analytically simpler OTU-based pipelines, but discards the phylogenetically important paired-end information of our approach, and hence has lower sensitivity. Sánchez et al. (22) assigned 10.8% (716 sequences) of the *rpoD* gene sequences to one of 26 species in their database. Using the genomes of Hesse et al. (15), the database now includes 166 *Pseudomonas* species, three of which are subspecies. Many of the *rpoD* reads were not mapped to our *Pseudomonas* database, which is likely due to the high stringency in our alignment approach and artifacts stemming from the low-template PCR: e.g., when *Pseudomonas* is in low abundance compared to other bacteria. Optimization of the PCR protocol may alleviate this.

The microbial composition as determined by V3-V4 16S rRNA amplicon sequencing was highly similar across biological replicates, with small differences between the sample sites. The three wheat-associated sites (S3, S7, and S9) clustered together, but had less overlap than a cluster with sites S3, S6, and S9, which all had different vegetation. Microbial communities in agricultural soils are influenced by physiochemical properties of the soil, the growth condition of the crops, the individual plant genotype, and/or the evolution of the microbial communities over a multitude of seasons, and the present study did not have access to such metadata that potentially could explain differences. The major outlier of the sites was the P8 site, mainly due to the high content of *Acidobacteria* (group 1), suggested to correlate with Cu and Mn concentrations (35), coinciding with a high relative abundance of *P. frederiksbergensis*.

The resolution at the species level was compared between the *rpoD* and the V3-V4 amplicon sequencing methods. The *Pseudomonas* species resolution based on the latter was lower than that found by the *rpoD* amplicon sequencing, which was consistent with the control experiment using 16 known species of pseudomonads. This is most likely a combination of the low dissimilarity in the 16S rRNA gene, the annotation method, and the database. It is important to note the usefulness of V3-V4 rRNA gene amplicon sequencing as a tool to determine the overall composition of the prokaryotic community. Of note, we observed different microbial communities across the different soils, even in soils having the same plant host. The *rpoD* amplicon methodology did not achieve a community-level resolution and is therefore best used in combination with standard 16S profiling to achieve full profiling of soil.

The *rpoD* profiling was compared to cultivation of *Pseudomonas* species from three soil samples and provided the same groups or subgroups; however, the *rpoD* amplicon sequencing method was able to identify more unique species than were found by cultivation. In particular, species belonging to the *P. lutea* group and the *P. mandelii* and *P. gesardii* subgroups of *P. fluorescens* were captured by the *rpoD* amplicon method but not by cultivation. The nutrient content of the isolation medium can influence the recovery of the *Pseudomonas* diversity from environmental samples (19). King's B agar medium (36) is a nutrient-rich medium for *Pseudomonas* isolation, and while this is an effective and commonly used cultivation method, it is possible that a larger number of *Pseudomonas* species could have been cultivated using a wider range of cultivation media. Overall, the *rpoD* amplicon methods can be used to find soil rich in *Pseudomonas* species and identify samples rich in potential beneficial or useful pseudomonads.

A few species were exclusively found by the culture-independent approach, and some of these are promising as bioinoculants for plant protection (Fig. 5). For example, strains of *Pseudomonas frederiksbergensis* (from the *P. mandelii* subgroup), which were

found in all *rpoD* profiles, but only once by cultivation (in sample S9), are effective bioinoculants for enhancing cold stress tolerance in plants (37). In addition, *Pseudomonas abietaniphila* (from the *P. lutea* group), which was found in three *rpoD* profiles (P8, P9, and S10) but not in any cultivations, can suppress plant diseases caused by *Botrytis cinerea* by degradation of oxalate produced by the fungi (38). Also, we have recently shown that the genes for biosynthesis of the antifungal compound thioquinolobactin are rarely found, but are tightly linked to biocontrol strains within the *P. gessardii* subgroup of *P. fluorescens* (39). Here, we find such species in P9 only with the cultivation-independent method.

With the *rpoD* amplicon approach, it is possible to profile and prioritize samples for intensive cultivation of strains that produce specific bioactive metabolites for biocontrol or exhibit other plant beneficial traits.

**Conclusion.** In this study, an *rpoD* gene amplicon-based technique to differentiate species within the genus *Pseudomonas* was developed. The method can differentiate individual species far beyond what traditional 16S rRNA gene amplicon sequencing can and is proposed as a new standard for high-throughput profiling of *Pseudomonas* in environmental microbial communities.

## MATERIALS AND METHODS

**In silico investigations of *Pseudomonas* species.** A *Pseudomonas* genome collection consisting of the 165 genomes from Hesse et al. (15) as well as 465 complete genome sequences of *Pseudomonas* was downloaded from NCBI (downloaded 18 February 2019). Using an *in silico* PCR algorithm (*in\_silico\_PCR*; [https://github.com/egonozer/in\\_silico\\_pcr](https://github.com/egonozer/in_silico_pcr)) (one mismatch, one deletion/insertion), 14 primer sets targeting nine different genes from previous studies (Table 1) were evaluated based on (i) the proportion of *Pseudomonas* genomes amplified, (ii) how well the amplicons followed their given phylogenetic classification, and (iii) the proportion of non-*Pseudomonas* genomes amplified (see Table S1 in the supplemental material). The *in silico* PCR products were aligned with MUSCLE v3.8.1551 (40), and a phylogenetic tree was generated with FastTree v2.1.10 (41) from the alignment. For phylogenetic evaluation, the output tree was qualitatively compared to the whole-genome-based tree of Hesse et al. (15). A custom database was built by using the PsEG30F/PsEG790R primers on the *rpoD* genes of the type strains included in the study by Hesse et al. (15). An issue encountered in the *in silico* analysis was the poor annotations of uploaded genomes, where we found multiple instances of incorrectly annotated genomes, which we corrected by selecting the *rpoD* genes of outliers and reidentifying them according to the type strain genomes of Hesse et al. (15).

***Pseudomonas* strains.** Sixteen different *Pseudomonas* species were used in the *in vitro* testing of the *rpoD* amplicon (Table 2). Seven were type culture collection strains, and nine were isolates obtained from ongoing projects in our laboratory. They were identified to the species level by Sanger sequencing of the *rpoD* gene as described above. The strains were grown in 10 ml Luria-Bertani (LB) broth (Lennox; Carl Roth GmbH & Co. KG, Karlsruhe, Germany) overnight at 30°C with aeration (shaking, 200 rpm).

**Soil samples.** Bulk soil samples were collected from 13 sites in mid-August 2019 close to harvest season. The samples were collected by scooping root-associated soil into a sterile Falcon tube. The sites were distributed across Zealand, Denmark, and included different types of vegetation and produce; 10 samples of field soil were collected, including corn (S1), fallow (grass [S2]), wheat (S3, S7, and S9), rye (S4), barley (S5), rapeseed (S6), grass seed (S8), and Lucerne (S10). In addition, three samples of pristine grassland were collected, including short (P5 and P9) and tall (P8) grass. The soil samples were stored at 5°C for a maximum of 2 weeks prior to analyses.

**Isolation of *Pseudomonas* from soil samples.** Soil was sieved (4.75- by 4.75-mm grid) and mixed with 0.9% NaCl in a ratio of 1 g to 9 ml and 10-fold serially diluted. Dilutions were plated on 1/4-diluted King's B<sup>+++</sup> agar plates (Sigma-Aldrich) supplemented with 13 mg/liter chloramphenicol, 40 mg/liter ampicillin, and 100 mg/liter cycloheximide (25). The plates were incubated at 30°C for 5 days. The plates were examined under UV light after 2 and 5 days to reveal fluorescent colonies. LB agar plates were streaked with up to 30 colonies from the P5, P8, and P9 sites as well as 10 from the S1 to S10 sites and incubated at 30°C for 2 days. The colonies were selected based on fluorescence and distinct colony morphology.

**DNA extraction from pure cultured *Pseudomonas* and soil samples.** For identification of *Pseudomonas* isolated from soil, DNA from each bacterial colony was extracted by boiling in demineralized H<sub>2</sub>O (dH<sub>2</sub>O) at 99°C for 15 min. For soil samples and selected *Pseudomonas* strains, genomic DNA (gDNA) was extracted with a DNAeasy Powersoil kit (Qiagen, Hilden, Germany) according to the manufacturer's instructions. The extractions of gDNA from soil were done in five biological replicates for each site. As a negative control, 250  $\mu$ l sterile dH<sub>2</sub>O was extracted for gDNA using the same methodology. The gDNA was stored at -20°C. The DNA extraction of soil was done at the latest 2 days after cultivation of soil *Pseudomonas*.

**Identification of *Pseudomonas* isolates from soil samples.** *Pseudomonas* species isolated from soil were identified by full-length sequencing of the *rpoD* gene. The 25- $\mu$ l PCR mixture contained 10.6  $\mu$ l Sigma Water, 12.5  $\mu$ l 2 $\times$  TEMPase, 0.8  $\mu$ l forward primer (10  $\mu$ M PsEG30F [5'-ATYGAAATCGCCAARCG-3']), 0.8  $\mu$ l

reverse primer (10  $\mu$ M PsEG790R [5'-CGGTTGATKTCCTGA-3']), and 0.3  $\mu$ l template DNA. The PCR program was (i) 1 cycle of 95°C for 15 min, (ii) 30 cycles of 95°C for 30 s, 51°C for 30 s, and 72°C for 30 s, and (iii) 1 cycle of 72°C for 5 min (21). PCR products were sequenced at Macrogen Europe (Amsterdam, The Netherlands). The *rpoD* sequences were classified using blastn against the custom-built *rpoD* gene database.

**Defined *in vitro* DNA mixture for *Pseudomonas* profiling.** As a positive control, a defined *Pseudomonas* DNA mixture was made as an equimolar mixture of individual extractions of the strains in Table 2, as measured by Nanodrop (Denovix DS-11; Saveen & Werner AB, Linhansvågen, Sweden). The equimolar mixture was based on DNA concentrations.

**Amplicon preparation, purification, and sequencing.** Amplicons were prepared by amplifying DNA using barcoded primers (see Table S2 in the supplemental material). The five biological replicates of each soil site, five technical replicates of the *in vitro* DNA mixture (positive control), and the negative control all were amplified using both the *rpoD*-specific primers and primers targeting the V3-V4 region of the 16S rRNA gene. Each sample used identical barcodes across both primer sets (Table S2) and Illumina adaptors for the two setups. For the amplification of *rpoD* genes, a 25- $\mu$ l PCR mixture containing 10.15  $\mu$ l Sigma Water, 12.5  $\mu$ l 2 $\times$  TEMPase, 0.8  $\mu$ l forward primer (10  $\mu$ M barcoded PsEG30), 0.8  $\mu$ l reverse primer (10  $\mu$ M barcoded PsEG790), 0.25  $\mu$ l MgCl<sub>2</sub> (25 mM), and 0.5  $\mu$ l template DNA was used. The PCR program was as follows: (i) 15 min at 95°C, (ii) 40 cycles of 30 s at 95°C, 30 s at 51°C, and 30 s at 72°C, and (iii) 5 min at 72°C. The amplicons were stored at -20°C until purification.

For the amplification of V3-V4 regions, a 25- $\mu$ l PCR mixture containing 10.6  $\mu$ l Sigma Water, 12.5  $\mu$ l 2 $\times$  TEMPase, 0.8  $\mu$ l forward primer (10  $\mu$ M barcoded 341F [5'-CCTACGGGNGGCWGCAG-3']), 0.8  $\mu$ l reverse primer (10  $\mu$ M barcoded 805R [5'-GACTACHVGGGTATCTAATCC-3']), and 0.3  $\mu$ l template DNA was used (42). The PCR program was as follows: (i) 15 min at 95°C, (ii) 30 cycles of 30 s at 95°C, 30 s at 60°C, and 30 s at 72°C, and (iii) 5 min at 72°C. The amplicons were stored at -20°C until purification.

The amplicons were purified using an Agencourt AMPure XP kit (Beckman Coulter, Brea, CA, USA) following the manufacturer's instructions. The products were eluted in Tris (10 mM, pH 8.5) buffer. After purification, the PCR products were pooled in equimolar concentrations.

The amplicon pools were delivered to the Cfb NGS Lab (Novo Nordisk Foundation Center for Biosustainability, DTU, Kongens Lyngby, Denmark) for sequencing on an Illumina MiSeq 300PE platform (MiSeq reagent kit v3; PE300).

**Enumeration of soil bacteria.** The number of cells in each soil site was quantified using quantitative PCR (qPCR). The qPCR targeted the V3 region of the 16S rRNA gene using the primers 338F and 518R (43). A 20- $\mu$ l PCR mixture containing 5.2  $\mu$ l Sigma Water, 10  $\mu$ l Luna Universal qPCR master mix (New England Biolabs, Inc., Bionordika Denmark A/S, Denmark), 1.4  $\mu$ l of each primer (10  $\mu$ M), and 2  $\mu$ l template DNA was used. The accompanying instructions for the qPCR program were followed. A standard curve relating cycle thresholds ( $C_T$ ) to CFU/g soil was prepared by combining CFU/g versus  $C_T$  for *Bacillus subtilis* ATCC 6051 and *Pseudomonas moorei* DSM 12647 ( $R^2 = 0.86$ ,  $E = 174.5\%$ ). ATCC 6051 and DSM 12647 were incubated overnight in 5 ml LB broth at 30°C with aeration. At an optical density at 600 nm ( $OD_{600}$ ) of approximately 1 (circa 24 h of growth), DNA was extracted from the cultures and further diluted. The standard curves were prepared in biological duplicates.

**Processing the V3-V4 and *rpoD* amplicons.** The V3-V4 amplicons were cleaned, merged, quality filtered, and chimera checked before quality-aware clustering at 99% similarity and mapping against the RDP-II SSU database (v11.5) (46) using the BION-meta software (Danish Genome Institute, Aarhus, Denmark). For the *rpoD* amplicons (PsEG30F and PsEG790R), the BION-meta software (Danish Genome Institute, Aarhus, Denmark) was used to demultiplex the amplicons. The fastp function (44) was used for quality filtering. Since the paired reads do not overlap, clustering was avoided, and instead, each read pair was aligned to the custom database of *rpoD* genes using bowtie2 (23). The resulting SAM-file was then filtered for only concordant pairs mapped with a quality of >10 using samtools (45). Data for both sets of amplicons were normalized to 100,000 reads for each sample before further analysis. Centrifuge was used for profiling of non-*Pseudomonas* reads using the *p+h+v* database (24).

**Statistics.** The amplicon sequencing data for both *rpoD* and V3-V4 were analyzed by non-metric multidimensional scaling (NMDS) to compare the diversities between the replicates and sample sites. To determine the multivariable variation within groups, the beta dispersion was calculated using R v3.6.2 package vegan with default settings and tested using a Mann-Whitney U test. Multiple distances were evaluated for robustness, and the Bray-Curtis distance was chosen since this distance metric had the best trade-off in terms of separation of sites and stress of the NMDS.

**Data availability.** The raw amplicon sequencing data from the Illumina sequencing are available at the Sequencing Read Archive (SRA) as BioProject PRJNA613913. Code for both *in silico* primer analysis and the bioinformatic classification pipeline is available at <https://github.com/mikaells/PseudomonasRPOD>.

## SUPPLEMENTAL MATERIAL

Supplemental material is available online only.

**FIG S1**, PDF file, 0.1 MB.

**FIG S2**, PDF file, 1.2 MB.

**FIG S3**, PDF file, 0.2 MB.

**FIG S4**, PDF file, 0.3 MB.

**FIG S5**, PDF file, 0.04 MB.

**TABLE S1**, DOCX file, 0.01 MB.

**TABLE S2**, DOCX file, 0.01 MB.

**TABLE S3**, DOCX file, 0.01 MB.

## ACKNOWLEDGMENTS

We thank local farmers and governmental agencies, who provided sites for soil collection, Heiko T. Kiesevalter for assistance with sampling and providing *Bacillus subtilis* ATCC 6051, and the laboratory technicians Jette Melchiorson, Sophia Rasmussen, and Susanne Koefoed for support.

This study was carried out as part of the Center of Excellence for Microbial Secondary Metabolites funded by The Danish National Research Foundation (DNRF137).

## REFERENCES

- Spiers AJ, Buckling A, Rainey PB. 2000. The causes of *Pseudomonas* diversity. *Microbiology* 146:2345–2350. <https://doi.org/10.1099/00221287-146-10-2345>.
- Lloyd-Jones G, Laurie AD, Tizzard AC. 2005. Quantification of the *Pseudomonas* population in New Zealand soils by fluorogenic PCR assay and culturing techniques. *J Microbiol Methods* 60:217–224. <https://doi.org/10.1016/j.mimet.2004.09.011>.
- Selezska K, Kazmierczak M, Müsken M, Garbe J, Schobert M, Häussler S, Wiehlmann L, Rohde C, Sikorski J. 2012. *Pseudomonas aeruginosa* population structure revisited under environmental focus: impact of water quality and phage pressure. *Environ Microbiol* 14:1952–1967. <https://doi.org/10.1111/j.1462-2920.2012.02719.x>.
- Monteil CL, Lafolie F, Laurent J, Clement JC, Simler R, Travi Y, Morris CE. 2014. Soil water flow is a source of the plant pathogen *Pseudomonas syringae* in subalpine headwaters. *Environ Microbiol* 16:2038–2052. <https://doi.org/10.1111/1462-2920.12296>.
- Keel C, Schneider U, Maurhofer M, Voisard C, Laville J, Burger U, Wirthner P, Haas D, Defago G. 1992. Suppression of root diseases by *Pseudomonas fluorescens* CHA0: importance of the bacterial secondary metabolite 2,4-diacetylphloroglucinol. *Mol Plant Microbe Interact* 5:4–13. <https://doi.org/10.1094/MPMI-5-004>.
- Milus EA, Rothrock CS. 1997. Efficacy of bacterial seed treatments for controlling *Pythium* root rot of winter wheat. *Plant Dis* 81:180–184. <https://doi.org/10.1094/PDIS.1997.81.2.180>.
- Niu GL, Zhang JJ, Zhao S, Liu H, Boon N, Zhou NY. 2009. Bioaugmentation of a 4-chloronitrobenzene contaminated soil with *Pseudomonas putida* ZWL73. *Environ Pollut* 157:763–771. <https://doi.org/10.1016/j.envpol.2008.11.024>.
- Khan H, Parmar N, Kahlon RS. 2016. *Pseudomonas*-plant interactions. I. Plant growth promotion and defense-mediated mechanisms, p 419–468. In Kahlon RS (ed), *Pseudomonas: molecular and applied biology*, 1st ed. Springer International Publishing, Cham, Switzerland.
- Matthijs S, Tehrani KA, Laus G, Jackson RW, Cooper RM, Cornelis P. 2007. Thioquinolobactin, a *Pseudomonas* siderophore with antifungal and anti-*Pythium* activity. *Environ Microbiol* 9:425–434. <https://doi.org/10.1111/j.1462-2920.2006.01154.x>.
- Lanteigne C, Gadkar VJ, Wallon T, Novinscak A, Filion M. 2012. Production of DAPG and HCN by *Pseudomonas* sp. LBUM300 contributes to the biological control of bacterial canker of tomato. *Phytopathology* 102:967–973. <https://doi.org/10.1094/PHYTO-11-11-0312>.
- Mousa WK, Raizada MN. 2016. Natural disease control in cereal grains, p 257–263. In Wrigley C, Corke H, Seetharaman K, Faubion J (ed), *Encyclopedia of food grains*, 2nd ed. Oxford Academic Press, Oxford, United Kingdom.
- Wang C, Wang D, Zhou Q. 2004. Colonization and persistence of a plant growth-promoting bacterium *Pseudomonas fluorescens* strain CS85, on roots of cotton seedlings. *Can J Microbiol* 50:475–481. <https://doi.org/10.1139/w04-040>.
- Gopalakrishnan S, Srinivas V, Prakash B, Sathya A, Vijayabharathi R. 2015. Plant growth-promoting traits of *Pseudomonas geniculata* isolated from chickpea nodules. *3 Biotech* 5:653–661. <https://doi.org/10.1007/s13205-014-0263-4>.
- Oteino N, Lally RD, Kiwanuka S, Lloyd A, Ryan D, Germaine KJ, Dowling DN. 2015. Plant growth promotion induced by phosphate solubilizing endophytic *Pseudomonas* isolates. *Front Microbiol* 6:745. <https://doi.org/10.3389/fmicb.2015.00745>.
- Hesse C, Schulz F, Bull CT, Shaffer BT, Yan Q, Shapiro N, Hassan KA, Varghese N, Elbourne LDH, Paulsen IT, Kyrpides N, Woyke T, Loper JE. 2018. Genome-based evolutionary history of *Pseudomonas* spp. *Environ Microbiol* 20:2142–2159. <https://doi.org/10.1111/1462-2920.14130>.
- Stefanato FL, Trippel C, Uszkoreit S, Ferrafiat L, Grenga L, Dickens R, Kelly N, Kingdon AD, Ambrosetti L, Findlay KC, Cheema J, Trick M, Chandra G, Tomalin G, Malone JG, Truman AW. 2019. Pan-genome analysis identifies intersecting roles for *Pseudomonas* specialized metabolites in potato pathogen inhibition. *bioRxiv* 783258. <https://www.biorxiv.org/content/10.1101/783258v1>.
- Mendes R, Kruijt M, De Bruijn I, Dekkers E, Van Der Voort M, Schneider JHM, Piceno YM, DeSantis TZ, Andersen GL, Bakker PAHM, Raaijmakers JM. 2011. Deciphering the rhizosphere microbiome for disease-suppressive bacteria. *Science* 332:1097–1100. <https://doi.org/10.1126/science.1203980>.
- Mehrabi Z, McMillan VE, Clark IM, Canning G, Hammond-Kosack KE, Preston G, Hirsch PR, Mauchline TH. 2016. *Pseudomonas* spp. diversity is negatively associated with suppression of the wheat take-all pathogen. *Sci Rep* 6:29905. <https://doi.org/10.1038/srep29905>.
- Aagot N, Nybroe O, Nielsen P, Johnsen K. 2001. An altered *Pseudomonas* diversity is recovered from soil by using nutrient-poor *Pseudomonas*-selective soil extract media. *Appl Environ Microbiol* 67:5233–5239. <https://doi.org/10.1128/AEM.67.11.5233-5239.2001>.
- Mulet M, Gomila M, Lemaitre B, Lalucat J, García-Valdés E. 2012. Taxonomic characterisation of *Pseudomonas* strain L48 and formal proposal of *Pseudomonas entomophila* sp. nov. *Syst Appl Microbiol* 35:145–149. <https://doi.org/10.1016/j.syapm.2011.12.003>.
- Mulet M, Bennisar A, Lalucat J, Garcí E, García-Valdés E. 2009. An rpoD-based PCR procedure for the identification of *Pseudomonas* species and for their detection in environmental samples. *Mol Cell Probes* 23:140–147. <https://doi.org/10.1016/j.mcp.2009.02.001>.
- Sánchez D, Matthijs S, Gomila M, Tricot C, Mulet M, García-Valdés E, Lalucat J. 2014. rpoD gene pyrosequencing for the assessment of *Pseudomonas* diversity in a water sample from the Woluwe River. *Appl Environ Microbiol* 80:4738–4744. <https://doi.org/10.1128/AEM.00412-14>.
- Langmead B, Salzberg SL. 2012. Fast gapped-read alignment with Bowtie 2. *Nat Methods* 9:357–359. <https://doi.org/10.1038/nmeth.1923>.
- Kim D, Song L, Breitwieser FP, Salzberg SL. 2016. Centrifuge: rapid and sensitive classification of metagenomic sequences. *Genome Res* 26:1721–1729. <https://doi.org/10.1101/gr.210641.116>.
- Landa BB, De Werd HAE, McSpadden Gardener BB, Weller DM. 2002. Comparison of three methods for monitoring populations of different genotypes of 2,4-diacetylphloroglucinol-producing *Pseudomonas fluorescens* in the rhizosphere. *Phytopathology* 92:129–137. <https://doi.org/10.1094/PHYTO.2002.92.2.129>.
- Lu S, Tian Q, Zhao W, Hu B. 2017. Evaluation of the potential of five house-keeping genes for identification of quarantine *Pseudomonas syringae*. *J Phytopathol* 165:73–81. <https://doi.org/10.1111/jph.12538>.
- Hilario E, Buckley TR, Young JM. 2004. Improved resolution on the phylogenetic relationships among *Pseudomonas* by the combined analysis of atpD, carA, recA and 16S rDNA. *Antonie Van Leeuwenhoek* 86:51–64. <https://doi.org/10.1023/B:ANTO.0000024910.57117.16>.
- Sarkar SF, Guttman DS. 2004. Evolution of the core genome of *Pseudomonas syringae*, a highly clonal, endemic plant pathogen. *Appl Environ Microbiol* 70:1999–2012. <https://doi.org/10.1128/AEM.70.4.1999-2012.2004>.
- Santos SR, Ochman H. 2004. Identification and phylogenetic sorting of bacterial lineages with universally conserved genes and proteins. *Environ Microbiol* 6:754–759. <https://doi.org/10.1111/j.1462-2920.2004.00617.x>.

30. Yamamoto S, Kasai H, Arnold DL, Jackson RW, Vivian A, Harayama S. 2000. Phylogeny of the genus *Pseudomonas*: intrageneric structure reconstructed from the nucleotide sequences of *gyrB* and *rpoD* genes. *Microbiology* 146:2385–2394. <https://doi.org/10.1099/00221287-146-10-2385>.
31. Ait Tayeb L, Ageron E, Grimont F, Grimont PAD. 2005. Molecular phylogeny of the genus *Pseudomonas* based on *rpoB* sequences and application for the identification of isolates. *Res Microbiol* 156:763–773. <https://doi.org/10.1016/j.resmic.2005.02.009>.
32. Yamamoto S, Harayama S. 1998. Phylogenetic relationships of *Pseudomonas putida* strains deduced from the nucleotide sequences of *gyrB*, *rpoD* and 16S rRNA genes. *Int J Syst Bacteriol* 48:813–819. <https://doi.org/10.1099/00207713-48-3-813>.
33. Mulet M, Lalucat J, García-Valdés E. 2010. DNA sequence-based analysis of the *Pseudomonas* species. *Environ Microbiol* 12:1513–1530. <https://doi.org/10.1111/j.1462-2920.2010.02181.x>.
34. Ettema CH, Wardle DA. 2002. Spatial soil ecology. *Trends Ecol Evol* 17:177–183. [https://doi.org/10.1016/S0169-5347\(02\)02496-5](https://doi.org/10.1016/S0169-5347(02)02496-5).
35. Chaves MG, Silva GG, Rossetto R, Edwards RA, Tsai SM, Navarrete AA. 2019. Acidobacteria subgroups and their metabolic potential for carbon degradation in sugarcane soil amended with vinasse and nitrogen fertilizers. *Front Microbiol* 10:1680. <https://doi.org/10.3389/fmicb.2019.01680>.
36. King EO, Ward MK, Raney DE. 1954. Two simple media for the demonstration of pyocyanin and fluorescin. *J Lab Clin Med* 44:301–307.
37. Chatterjee P, Samaddar S, Anandham R, Kang Y, Kim K, Selvakumar G, Sa T. 2017. Beneficial soil bacterium *Pseudomonas frederiksbergensis* Os261 augments salt tolerance and promotes red pepper plant growth. *Front Plant Sci* 8:705. <https://doi.org/10.3389/fpls.2017.00705>.
38. Lee Y, Choi O, Kang B, Bae J, Kim S, Kim J. 2020. Grey mould control by oxalate degradation using non-antifungal *Pseudomonas abietaniphila* strain ODB36. *Sci Rep* 10:1605. <https://doi.org/10.1038/s41598-020-58609-z>.
39. Sazinas P, Hansen ML, Aune MI, Fischer MH, Jelsbak L. 2019. A rare thioquinolobactin siderophore present in a bioactive *Pseudomonas* sp. DTU12.1. *Genome Biol Evol* 11:3529–3533. <https://doi.org/10.1093/gbe/evz267>.
40. Edgar RC. 2004. MUSCLE: multiple sequence alignment with high accuracy and high throughput. *Nucleic Acids Res* 32:1792–1797. <https://doi.org/10.1093/nar/gkh340>.
41. Price MN, Dehal PS, Arkin AP. 2010. FastTree 2—approximately maximum-likelihood trees for large alignments. *PLoS One* 5:e9490. <https://doi.org/10.1371/journal.pone.0009490>.
42. Klindworth A, Pruesse E, Schweer T, Peplies J, Quast C, Horn M, Glöckner FO. 2013. Evaluation of general 16S ribosomal RNA gene PCR primers for classical and next-generation sequencing-based diversity studies. *Nucleic Acids Res* 41:e1. <https://doi.org/10.1093/nar/gks808>.
43. Einen J, Thorseth IH, Øvreås L. 2008. Enumeration of Archaea and Bacteria in seafloor basalt using real-time quantitative PCR and fluorescence microscopy. *FEMS Microbiol Lett* 282:182–187. <https://doi.org/10.1111/j.1574-6968.2008.01119.x>.
44. Chen S, Zhou Y, Chen Y, Gu J. 2018. Fastp: an ultra-fast all-in-one FASTQ preprocessor. *Bioinformatics* 34:i884–i890. <https://doi.org/10.1093/bioinformatics/bty560>.
45. Li H, Handsaker B, Wysoker A, Fennell T, Ruan J, Homer N, Marth G, Abecasis G, Durbin R, 1000 Genome Project Data Processing Subgroup. 2009. The Sequence Alignment/Map format and SAMtools. *Bioinformatics* 25:2078–2079. <https://doi.org/10.1093/bioinformatics/btp352>.
46. Cole JR, Chai B, Farris RJ, Wang Q, Kulam SA, McGarrell DM, Garrity GM, Tiedje JM. 2005. The Ribosomal Database Project (RDP-II): sequences and tools for high-throughput rRNA analysis. *Nucleic Acids Res* 33:294–296. <https://doi.org/10.1093/nar/gki038>.

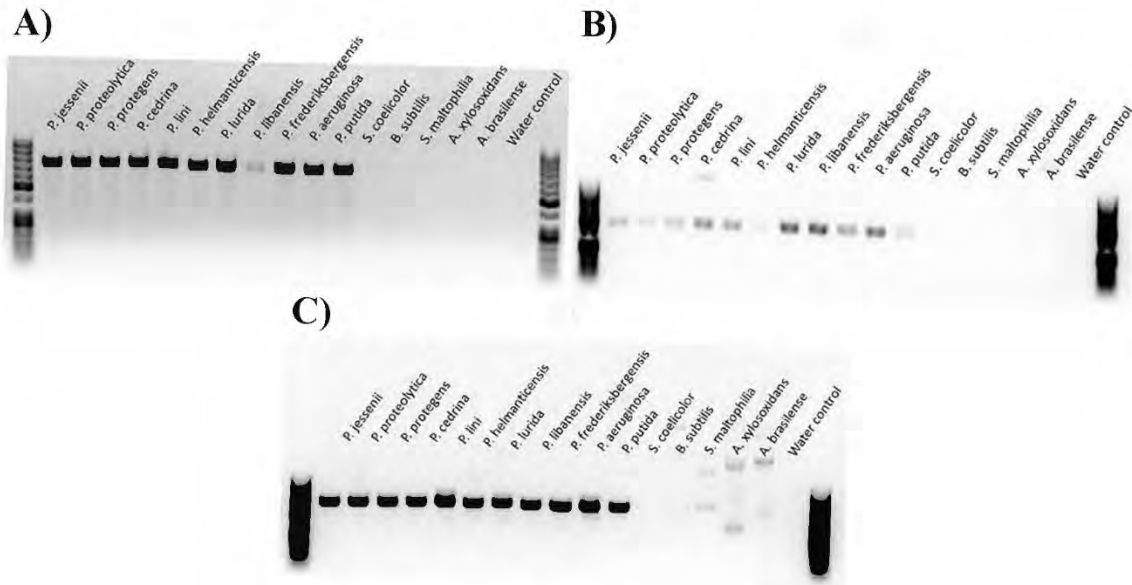


**Figure S1:** Gel electrophoresis of PCR products generated from members of the synthetic community using A) PsEG30F / PsEG790R, B) PsEG30F / PsJL490R, and C) PsEG30F / PsJL628R. Contrast have been enhanced. Ladders are 50 bp GeneRuler (ThermoFisher Scientific, Vilnius, Lithuania).

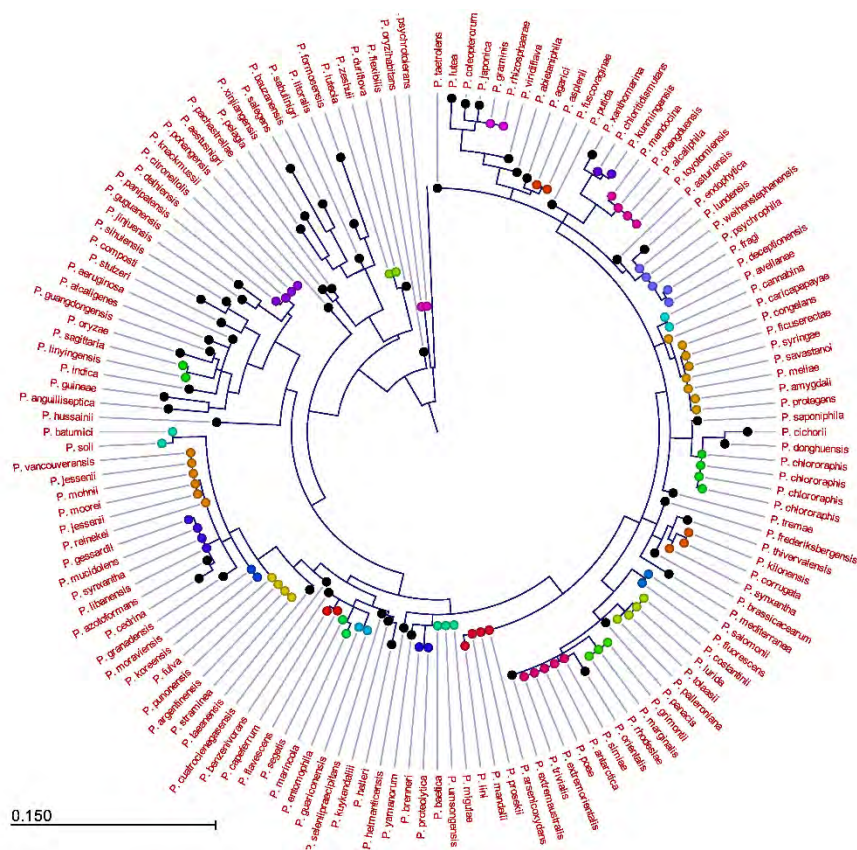


**Figure S2.** Phylogenetic tree of the *in silico* PCR amplicons generated from the 16S rRNA gene using V3V4 primers. The PCR products were clustered at 97% similarity and aligned with MUSCLE v3.8.1551 (39) and a phylogenetic tree was generated with FastTree v2.1.10 (40) from the alignment. Tips are coloured as clades generated by TreeCluster with similar colors denoting highly similar or identical amplicons.

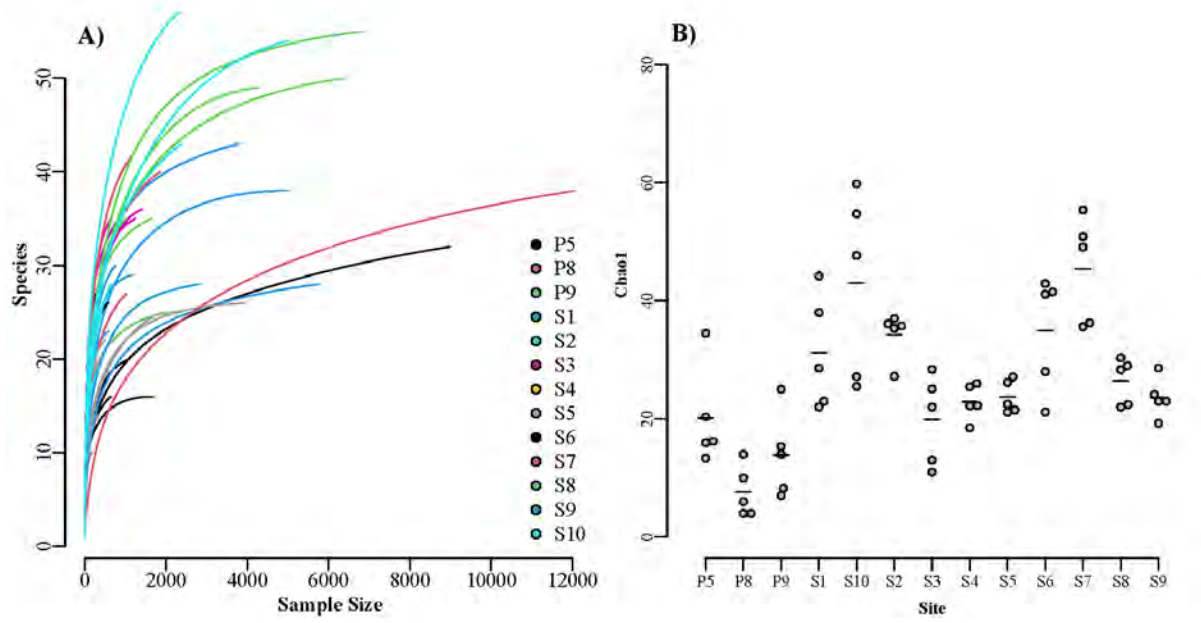


**Figure S3:** Alpha diversity of the *Pseudomonas* population as described using the *rpoD*-methodology. A) rarefaction curves and B) Chao1 diversity.

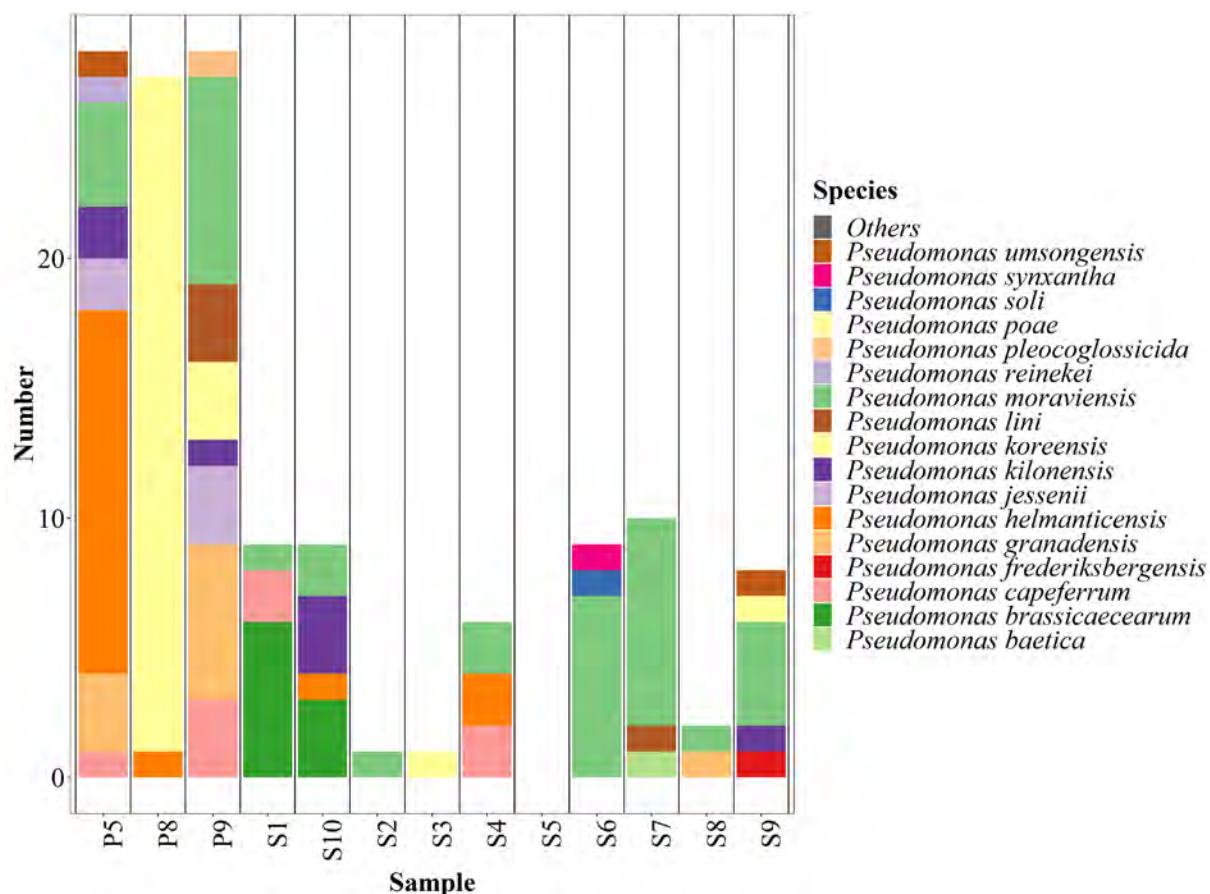


**Figure S4.** Number and identity of *Pseudomonas* species isolated by cultivation from the 13 soil sample sites.

*rpoD* similarities between the custom database and KT2440

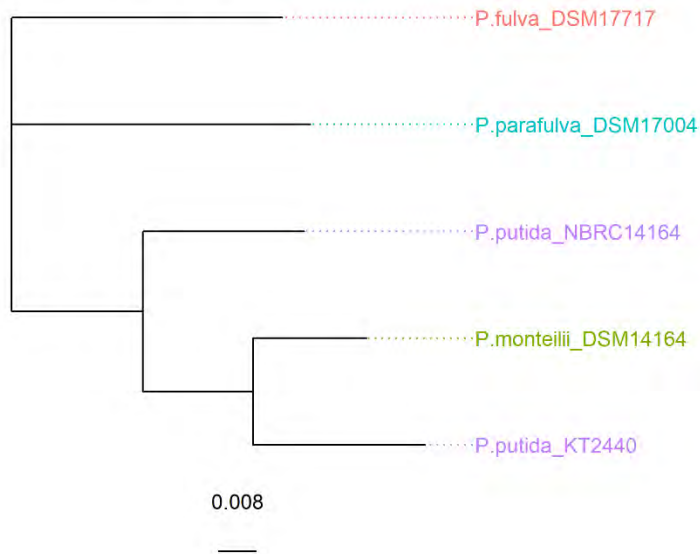


**Figure S5.** Phylogenetic tree of the *in silico* PCR amplicons generated from the *rpoD* gene of *P. putida* KT2440 and four closely related species. The PCR products were aligned with MUSCLE v3.8.1551 (39) and a phylogenetic tree was calculated with FastTree v2.1.10 (40) from the alignment.

**Table S1:** Genomes of non-*Pseudomonas* used to test *Pseudomonas* gene primer specificity profiling.

Phyla/Division	Species	Strain	RefSeq accession
Actinobacteria	<i>Mycobacterium tuberculosis</i>	HN-506	GCF_002357975.1
Actinobacteria	<i>Streptomyces coelicolor</i>	A3(2)	GCF_000203835.1
Actinobacteria	<i>Bifidobacterium bifidum</i>	S6	GCF_003390735.1
Firmicutes	<i>Bacillus subtilis</i>	3610	GCF_002055965.1
Firmicutes	<i>Clostridium acetobutylicum</i>	ATCC 824	GCF_000008765.1
Firmicutes	<i>Staphylococcus aureus</i>	NCTC 8325	GCF_000013425.1
Sphingobacteria	<i>Sphingobacterium</i> sp.	21	GCF_000192845.1
Sphingobacteria	<i>Sphingobacterium</i> sp.	B29	GCF_001952815.1
Alphaproteobacteria	<i>Azospirillum brasilense</i>	Az39	GCF_000632475.1
Alphaproteobacteria	<i>Agrobacterium tumefaciens</i>	S33	GCF_001551895.1
Alphaproteobacteria	<i>Agrobacterium tumefaciens</i>	Ach5	GCF_000971565.1
Betaproteobacteria	<i>Achromobacter xylosoxidans</i>	MN001	GCF_001051055.1
Betaproteobacteria	<i>Bordetella pertussis</i>	Tohama I	GCF_000195715.1
Betaproteobacteria	<i>Azospira oryzae</i>	PS	GCF_000236665.1
Gammaproteobacteria	<i>Stenotrophomonas maltophilia</i>	K279a	GCF_000072485.1
Gammaproteobacteria	<i>Pectobacterium carotovorum</i>	14A	GCF_003932035.1
Gammaproteobacteria	<i>Salmonella enterica</i>	SL1344	GCF_000210855.2
Gammaproteobacteria	<i>Xanthomonas axonopodis</i>	LMG26789	GCF_003698225.1
Ascomycota	<i>Botrytis cinerea</i>	B05.10	GCF_000143535.2
Ascomycota	<i>Aspergillus niger</i>	CBS 513.88	GCF_000002855.3
Ascomycota	<i>Fusarium oxysporum</i>	4287	GCF_000149955.1
Ascomycota	<i>Penicillium expansum</i>	MD-8	GCF_000769745.1
Ascomycota	<i>Saccharomyces cerevisiae</i>	S288C	GCF_000146045.2
Nematoda	<i>Caenorhabditis elegans</i>	Bristol N2	GCF_000002985.6

**Table S2:** List of barcodes tagged on primers for Illuminia sequencing of amplicons of the *Pseudomonas rpoD* gene.

<b>Number</b>	<b>Barcode</b>
1	TTTTAATC
2	ATAATTAG
3	ACCAAATT
4	CTTATCAA
5	TGATCATT
6	AGAATCTA
7	TCAAGAAA
8	ATCGAAAT
9	ACATTTAC
10	TAGAAAAC
11	TTATCACC
12	AATAGGGT
13	ATTGCTGA
14	TGAGTTCT
15	GGCTATTT
16	CAAGAGAT
17	GGAATACA
18	AAGGCAAT
19	ACAAAACG
20	TTGAGTGA
21	GCTTCTGA
22	GGCAAGAT
23	GTGCTTTC
24	ACACACTG
25	CGATTCTG
26	GCAGAGTT
27	CGTCCTAT
28	GCTTGGTT
29	ACAGGCTT
30	TGACGCTT

**Table S3.** *In silico* PCR amplification of 165 genomes derived from Hesse et al. (15), 465 complete *Pseudomonas* genomes derived from NCBI and 24 non-*Pseudomonas* genomes using 14 different primer pairs.

Primer pair	Number of <i>in silico</i> PCR products (%)		
	Hesse et al <sup>15</sup> . <i>Pseudomonas</i>	NCBI complete <i>Pseudomonas</i>	Non- <i>Pseudomonas</i>
16S-341F / 16S-805R	146/166 (87.95)	465/465 (100.00)	18/24 (75.00)
16sF-LYP-3 / 16sR-LYP-3	0/166 (0.00)	0/465 (0.00)	0/24 (0.00)
16S-rRNA-F / 16S-rRNA-R	132/166 (79.52)	465/465 (100.00)	0/24 (0.00)
atpD-F / atpD-F	66/166 (39.76)	286/465 (61.51)	4/24 (16.67)
carA-F / carA-R	70/166 (42.17)	291/465 (62.58)	4/24 (16.67)
gapA-Fps / gapA-Rps	90/166 (54.22)	369/465 (79.35)	0/24 (0.00)
glt-F / glt-R	14/166 (8.43)	40/465 (8.60)	0/24 (0.00)
gyrBBAUP2 / APrU	0/166 (0.00)	1/465 (0.22)	0/24 (0.00)
UP-1E / APrU	166/166 (100.00)	465/465 (100.00)	6/24 (25.00)
recA-F / recA-R 409	109/166 (65.66)	416/465 (89.46)	2/24 (8.33)
LAPS / LAPS27	118/166 (71.08)	426/465 (91.61)	0/24 (0.00)
PsEG30F / PsJL490R	148/166 (89.16)	455/465 (97.85)	0/24 (0.00)
PsEG30F / PsJL628R	139/166 (83.73)	456/465 (98.06)	0/24 (0.00)
PsEG30F / PsEG790R	160/166 (96.39)	460/465 (98.92)	0/24 (0.00)

# Paper 2

---

A Whole-Cell Biosensor for Detection of 2,4-Diacetylphloroglucinol (DAPG)-Producing Bacteria from Grassland Soil

Hansen M.L., He Z., Wibowo M., and Jelsbak L.

*Applied and Environmental Microbiology*, 2021, 87(3), e01400-20



# A Whole-Cell Biosensor for Detection of 2,4-Diacetylphloroglucinol (DAPG)-Producing Bacteria from Grassland Soil

Morten Lindqvist Hansen,<sup>a</sup> Zhiming He,<sup>a</sup> Mario Wibowo,<sup>a</sup>  Lars Jelsbak<sup>a</sup>

<sup>a</sup>Department of Biotechnology and Biomedicine, Technical University of Denmark, Lyngby, Denmark

**ABSTRACT** Fluorescent *Pseudomonas* spp. producing the antibiotic 2,4-diacetylphloroglucinol (DAPG) are ecologically important in the rhizosphere, as they can control phytopathogens and contribute to disease suppression. DAPG can also trigger a systemic resistance response in plants and stimulate root exudation and branching as well as induce plant-beneficial activities in other rhizobacteria. While studies of DAPG-producing *Pseudomonas* have predominantly focused on rhizosphere niches, the ecological role of DAPG as well as the distribution and dynamics of DAPG-producing bacteria remains less well understood for other environments, such as bulk soil and grassland, where the level of DAPG producers are predicted to be low. In this study, we constructed a whole-cell biosensor for detection of DAPG and DAPG-producing bacteria from environmental samples. The constructed biosensor contains a *phlF* response module and either *lacZ* or *lux* genes as output modules assembled on a pSEVA plasmid backbone for easy transfer to different host species and to enable easy future genetic modifications. We show that the sensor is highly specific toward DAPG, with a sensitivity in the low nanomolar range (>20 nM). This sensitivity is comparable to the DAPG levels identified in rhizosphere samples by chemical analysis. The biosensor enables guided isolation of DAPG-producing *Pseudomonas*. Using the biosensor, we probed the same grassland soil sampling site to isolate genetically related DAPG-producing *Pseudomonas kilonensis* strains over a period of 12 months. Next, we used the biosensor to determine the frequency of DAPG-producing pseudomonads within three different grassland soil sites and showed that DAPG producers can constitute part of the *Pseudomonas* population in the range of 0.35 to 17% at these sites. Finally, we showed that the biosensor enables detection of DAPG produced by non-*Pseudomonas* species. Our study shows that a whole-cell biosensor for DAPG detection can facilitate isolation of bacteria that produce this important secondary metabolite and provide insight into the population dynamics of DAPG producers in natural grassland soil.

**IMPORTANCE** The interest in bacterial biocontrol agents as biosustainable alternatives to pesticides to increase crop yields has grown. To date, we have a broad knowledge of antimicrobial compounds, such as DAPG, produced by bacteria growing in the rhizosphere surrounding plant roots. However, compared to the rhizosphere niches, the ecological role of DAPG as well as the distribution and dynamics of DAPG-producing bacteria remains less well understood for other environments, such as bulk and grassland soil. Currently, we are restricted to chemical methods with detection limits and time-consuming PCR-based and probe hybridization approaches to detect DAPG and its respective producer. In this study, we developed a whole-cell biosensor, which can circumvent the labor-intensive screening process as well as increase the sensitivity at which DAPG can be detected. This enables quantification of relative amounts of DAPG producers, which, in turn, increases our understanding of the dynamics and ecology of these producers in natural soil environments.

**Citation** Hansen ML, He Z, Wibowo M, Jelsbak L. 2021. A whole-cell biosensor for detection of 2,4-diacetylphloroglucinol (DAPG)-producing bacteria from grassland soil. *Appl Environ Microbiol* 87:e01400-20. <https://doi.org/10.1128/AEM.01400-20>.

**Editor** Isaac Cann, University of Illinois at Urbana-Champaign

**Copyright** © 2021 American Society for Microbiology. All Rights Reserved.

Address correspondence to Lars Jelsbak, [lj@bio.dtu.dk](mailto:lj@bio.dtu.dk).

**Received** 23 June 2020

**Accepted** 16 November 2020

**Accepted manuscript posted online** 20 November 2020

**Published** 15 January 2021

**KEYWORDS** secondary metabolites, *Pseudomonas*, DAPG, synthetic biology, biocontrol, SEVA, antibiotic detection, biosensors, microbial ecology, secondary metabolite, soil microbiology

Secondary metabolites are well known for their potential as drugs in the medical industry. They were initially defined as dispensable compounds, nonvital to their respective producers. However, recent advances in genome mining and microbial ecology are beginning to shed light on the prevalence, role, and importance of these metabolites in natural environments. In soil ecology, species of fluorescent *Pseudomonas* isolated from naturally suppressive soils have received a great deal of attention due to their production of antimicrobial secondary metabolites, such as 2,4-diacetylphloroglucinol (DAPG). Suppression of wheat take-all disease caused by *Gaeumannomyces graminis* var. *tritici* was shown to be induced by years of crop monoculture and was associated with the root colonization of DAPG-producing fluorescent *Pseudomonas* (1). Moreover, production of DAPG was shown to be involved in disease control against the causative agent of tobacco black root rot, *Thielaviopsis basicola* (2). It has also been demonstrated that DAPG has antibacterial properties against the pathogen *Erwinia carotovora* subsp. *atroseptica* causing soft rot of potatoes (3).

The biosynthetic gene cluster related to DAPG production in *Pseudomonas* comprises eight genes, *phlACBDEFGH* (4, 5). Proteins encoded by the operon *phlACBD* are responsible for the synthesis of DAPG (4). The type III polyketide synthase PhID initially condenses three malonyl coenzyme A molecules into phloroglucinol (PG), which is further acetylated by the enzyme complex PhIACB into monoacetylphloroglucinol (MAPG) and DAPG (6). PhIE was identified as a putative membrane transporter with similarities to a known efflux pump in *Staphylococcus aureus* (4). The protein product of *phlG* has been described as a hydrolase that catalyzes the degradation of DAPG to MAPG, thus controlling the intracellular levels of DAPG (5, 7). Both *phlF* and *phlH* encode *tetR*-like repressors that inhibit transcription of *phlACBD* and *phlG*, respectively (5, 8). PhIF and PhIH bind to operator sites located in promoters upstream of the genes they regulate, thereby sterically blocking transcription. DAPG serves as the ligand for both repressors. Thus, in the presence of DAPG repression is relieved, leading to expression of *phlACBD* and *phlG*, which, in turn, leads to induced DAPG biosynthesis and posttranslational regulation (5, 8).

The complex of species belonging to the group *Pseudomonas fluorescens* has been well characterized over the past 3 decades, due to the potential of several species to act as biocontrol agents in agriculture. A recent study surveyed the phylogenetic relationship between 166 type strains of *Pseudomonas* (among which 66 belonged to the *P. fluorescens* group) based on amino acid sequences of 100 gene orthologues, which further proposed the existence of 10 subgroups within the *P. fluorescens* clade (9). However, despite the vast diversity among *P. fluorescens* group members, only a few species belonging to two subgroups, *Pseudomonas protegens* and *Pseudomonas corrugata*, are known to produce DAPG (1, 8). With the advances in genome mining and the increased availability of complete genomes, the biosynthetic gene cluster *phlACBDE* was recently identified in *Pseudomonas* species outside the *P. fluorescens* group, as well as in two genera of *Betaproteobacteria* (10). However, in these cases production of DAPG has not yet been demonstrated.

Identification and enumeration of DAPG-producing microorganisms have, to our knowledge, exclusively relied on DNA probe hybridization and PCR-based techniques. One of the most commonly employed techniques uses colony hybridization combined with a confirmatory PCR to verify the presence of *phlD* (11). A more recent method involves culture-independent real-time PCR to quantify populations of DAPG-producing *Pseudomonas* in the plant rhizosphere (12). A different approach is to quantify the amount of DAPG produced *in situ* by chemical analysis. Bonsall et al. demonstrated that an optimized extraction protocol enabled quantification of DAPG isolated directly from the plant rhizosphere (13). While these techniques have clear advantages, there

are several drawbacks that also exist. PCR-based methods are limited by DNA binding of specific primers, and measures have to be taken to address the quantity of diverse genotypes of DAPG producers. Chemical identification, on the other hand, is restricted by detection limits, which are directly correlated with the size of the bacterial population.

In recent years, the synthetic biology toolbox has expanded rapidly and the use of genetically engineered molecular circuits to sense molecules and conditions of interest has gained increased attention. These developments have given rise to whole-cell biosensors that utilize natural regulatory systems engineered to detect metabolites and small molecules (14, 15). Whole-cell biosensors rely on molecule recognition to either activate transcription or lift repression of a reporter gene and are thus often highly sensitive, with detection limits in the nano- to micromolar range (16–18). Furthermore, whole-cell biosensors are tunable by addition or alteration of genetic parts, which allows for higher sensitivity and increased specificity (15, 19). Lastly, biosensors may also be implemented as biological detectors for uncovering metabolic activities *in situ* (20, 21).

Studies of DAPG-producing *Pseudomonas* species have predominantly focused on rhizosphere niches, whereas the ecological role of DAPG as well as the distribution and dynamics of DAPG-producing bacteria is not well understood for other environments, such as bulk soil and grassland. In this study, we constructed a whole-cell biosensor as an alternative and efficient approach for detection of DAPG and directed isolation of DAPG-producing bacteria from environmental samples.

## RESULTS

### Construction of whole-cell DAPG biosensors with high sensitivity and specificity.

Two whole-cell biosensors were constructed to enable specific detection of DAPG and identification of DAPG-producing bacteria. The two sensors contain identical modules for DAPG sensing in combination with either the *lux* operon or the *lacZ* gene as a reporter (Fig. 1A). The biosensor plasmids were constructed as repressor-mediated modules in an *Escherichia coli* K-12  $\Delta$ *lacIZYA* host. In the absence of DAPG, the TetR-like repressor protein PhIF binds as a dimer to the *phlO* operator site (8) in the promoter upstream of the reporter gene. As bioavailable DAPG diffuses into the cytoplasm and binds to PhIF, the repression on the target  $P_{\text{phIF}}$  promoter is relieved. Two reporter modules were chosen. The *lux* operon was used as the output reporter to obtain a highly sensitive response measured in bioluminescence units. To enable agar plate screenings for investigating the distribution and dynamics of DAPG-producing bacteria in natural microbial communities, the *lacZ* gene was used as the second output reporter. To ensure stable inhibition of the  $P_{\text{phIF}}$  promoter under noninduced conditions, the *phlF* gene is constitutively expressed from the  $P_{\text{lacIQ}}$  promoter. Both genetic circuits were introduced into a pSEVA plasmid background (Fig. 1B) to allow for rapid and simple cloning, as well as efficient mobilization into distinct hosts by triparental mating.

To address the sensitivity and specificity of the whole-cell biosensors, microtiter bioassays were conducted. For characterization of the *lux* version (Fig. 1C), the *E. coli* host with pSEVA226-DAPG<sub>*lux*</sub> was grown in Luria-Bertani (LB) broth containing various concentrations of PG, MAPG, or DAPG with continuous measurements of luminescence and cell density. PG and MAPG are both precursors of DAPG and thus similar compounds, allowing determination of biosensor specificity toward DAPG. For each concentration of inducer, the average luminescence was normalized to cell density over a period of 35 min (8 data points, time [*t*] = 172 to 207 min). This corresponds to late exponential growth phase (see Fig. S1 in the supplemental material). The whole-cell biosensor exhibited excellent sensitivity toward DAPG, with a response to 20 nM being statistically significantly higher than the negative control without added DAPG (Student's *t* test, *P* = 0.01). The biosensor did not respond to the concentrations of PG tested, but a minor response to MAPG at >1.25  $\mu$ M was observed. For characterization of the *lacZ* version (Fig. 1D), the *E. coli* host with pSEVA225::DAPG<sub>*lacZ*</sub> was grown in LB

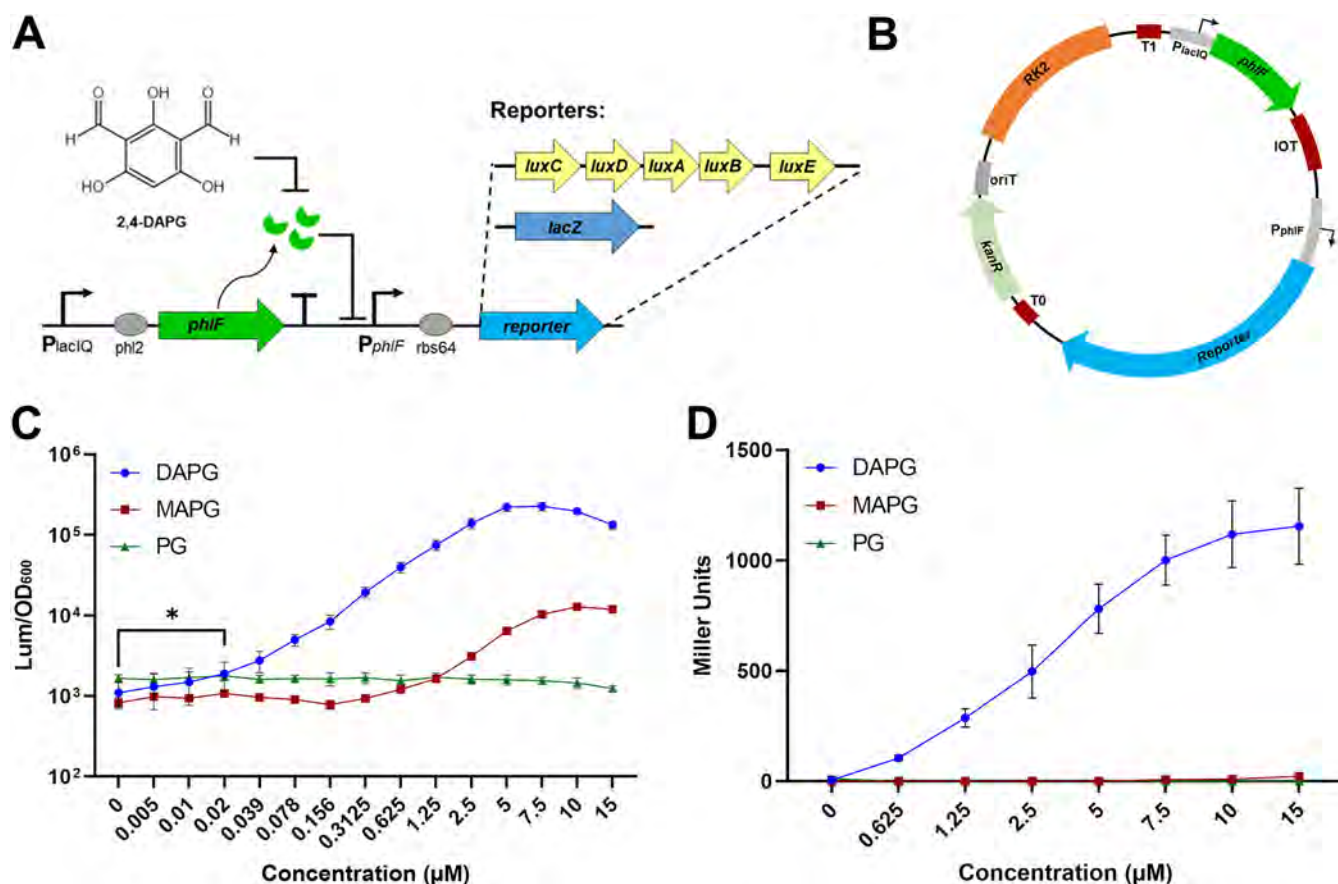


**FIG 1** Design of highly specific and sensitive whole-cell biosensors for DAPG detection. (A) Schematic illustration of the genetic circuit representing the DAPG biosensors with various reporter modules. (B) Map of the biosensor present on a pSEVA plasmid background with an RK2 replicon, origin of transfer (*oriT*), and a kanamycin resistance gene. Terminators (T0, T1, and IOT) are also indicated. (C) The response of the whole-cell biosensor harboring pSEVA226-DAPG<sub>lux</sub> to DAPG and similar molecules (PG and MAPG) measured in luminescence per OD<sub>600</sub>. (D) The response of the whole-cell biosensor harboring pSEVA225-DAPG<sub>lacZ</sub> to DAPG and similar molecules (PG and MAPG) measured in Miller units.

broth containing various concentrations of either PG, MAPG, or DAPG to allow for enzymatic expression. Subsequently, the biosensor response was determined in a  $\beta$ -galactosidase microtiter assay. Enzymatic activity of transcribed *lacZ* was estimated by continuously measuring the increase in *o*-nitrophenol concentration over time (Fig. S2). The output is displayed in Miller units [MU; determined by the equation  $MU = (5,000 \times OD_{420}/min)/OD_{600}$ , where  $OD_{420}$  is optical density at 420 nm]. Exposing the biosensor to 0.625  $\mu$ M DAPG yielded a statistically significantly higher response than for the negative control without added DAPG (Student's *t* test,  $P = 0.0032$ ).

**Detection of DAPG production from bacterial colonies during growth on agar surfaces.** After addressing the sensitivity and specificity of the biosensor, we proceeded to utilize it in the identification of DAPG-producing bacteria. We investigated the response of the whole-cell biosensor when coinoculated with known DAPG-producing bacteria commonly found in soil (Fig. 2). The biosensor harboring pSEVA225::DAPG<sub>lacZ</sub> was grown as a lawn on KBmalt agar (22) supplemented with 5-bromo-4-chloro-3-indolyl- $\beta$ -D-galactopyranoside (X-Gal). Inoculation of DAPG-producing cultures of *P. protegens* CHA0 and *P. protegens* DTU9.1 on these agar plates resulted in induction of the biosensor and production of clear blue halos surrounding the colonies after 24 h (Fig. 2A). We also constructed a  $\Delta$ *phlACBD* mutant strain of *P. protegens* DTU9.1 by allelic replacement, in which the DAPG biosynthesis genes were deleted (Materials and Methods). As expected, the mutant strain did not elicit a response from the biosensor (Fig. 2A) and did not produce DAPG detectable by liquid chromatography-mass spectrometry (LC-MS) analysis (Fig. 2B). We note that DAPG production in

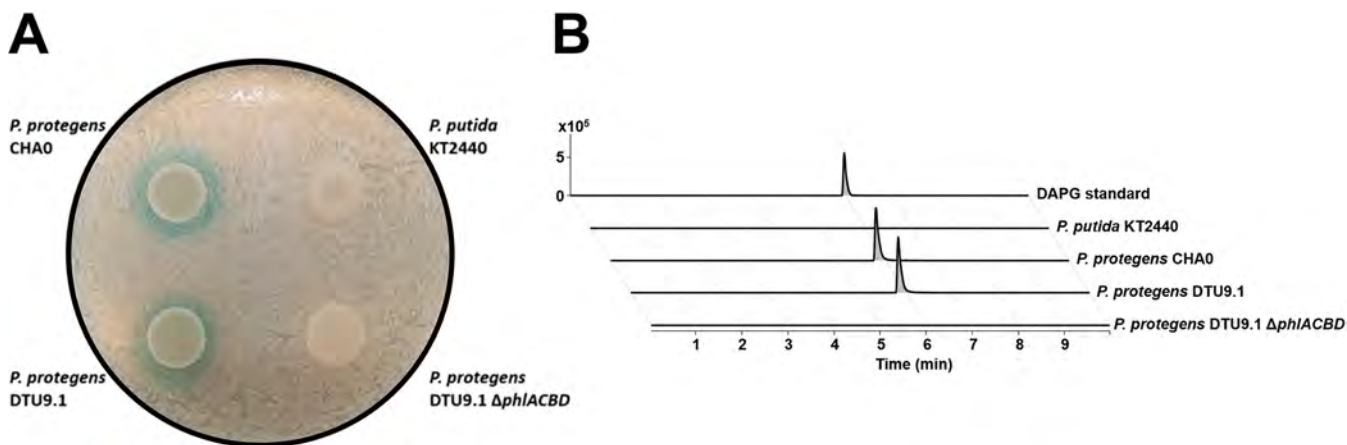


**FIG 2** Detection of DAPG produced by bacterial colonies grown on agar surfaces. (A) Four fluorescent *Pseudomonas* isolates were grown on a lawn of the biosensor with pSEVA225::DAPG<sub>lacZ</sub> on KBmalt medium supplemented with X-Gal. Wild-type *P. protegens* CHA0 and DTU9.1, known to produce DAPG, elicited a biosensor response after 24 h, whereas the negative controls, *P. putida* KT2440 and a  $\Delta$ phlACBD mutant of *P. protegens*, DTU9.1, did not. (B) Extracted ion chromatograms (EIC) for DAPG ( $m/z$  211.0601  $\pm$  5 ppm) of the four *Pseudomonas* extracts confirmed the production of DAPG after 24 h by *P. protegens* CHA0 and DTU9.1.

*Pseudomonas* species has been shown to be high under growth conditions including maltose, such as the conditions used in this study (8, 23). In concordance with these findings, we did not observe clear blue halos when LB agar was used (data not shown). We also tested *Pseudomonas putida* KT2440, which does not contain the DAPG biosynthetic gene cluster. Similar to the *P. protegens* DTU9.1  $\Delta$ phlACBD mutant, *P. putida* did not elicit a response in the biosensor after 24 h of growth. However, after prolonged incubation (>72 h) of *P. putida* KT2440, a slight blue coloring was detected surrounding the bacterial colony (Fig. S3).

Finally, we also explored if our setup can be used to identify DAPG production in species other than *Pseudomonas*. Recently, the genome of *Chromobacterium vaccinii* MWU328 was shown to contain genes with high similarity to the essential genes required for DAPG biosynthesis (*phlACBDE*) (10). We found that *C. vaccinii* MWU328 produced molecules that induced a response in the biosensor, resulting in a blue halo around the colony. A small amount of DAPG was subsequently confirmed by LC-MS (Fig. S4).

**Biosensor-guided identification of DAPG-producing *Pseudomonas*.** Next, we used our biosensor to guide the identification of DAPG-producing pseudomonads from environmental samples. To this end, we collected soil samples from the same grassland soil site (labeled P5) in both August 2018 and August 2019 and randomly isolated 30 fluorescent *Pseudomonas* strains at both time points. This site is located in Dyrehaven, which is a Danish natural reserve, thus representing a relatively unaffected, natural soil niche. Using the approach described above, all 60 isolates were screened on KBmalt agar plates supplemented with X-Gal and a lawn of the biosensor harboring pSEVA225::DAPG<sub>lacZ</sub>. A blue halo indicative of DAPG production was observed for one isolate from 2018 (isolate P5.21) and two isolates from 2019 (isolates P5.52 and P5.53) (Fig. 3A). Subsequent LC-MS analysis confirmed DAPG production in all three isolates (Fig. S5). For taxonomic identification of the 60 isolates, part of the housekeeping gene *rpoD* was sequenced for each isolate. The *rpoD* sequences were aligned to a database of 165 *Pseudomonas* type strains (9). Species identification of each isolate was determined based on the highest match to the type strains using nucleotide BLAST on the NCBI website. The diversity of cultivable fluorescent *Pseudomonas* remained similar, as species of *P. jessenii*, *P. koreensis*, and *P. corrugata* subgroups (as well as species of *P. putida*) were identified in the two samplings (Fig. 3B). However, isolates belonging to the *P. fluorescens* subgroup were found only in 2018.

The three DAPG-producing *Pseudomonas* isolates were identified as *P. kilonensis*. This species is part of the *P. corrugata* subgroup of fluorescent *Pseudomonas* (Fig. 3C,

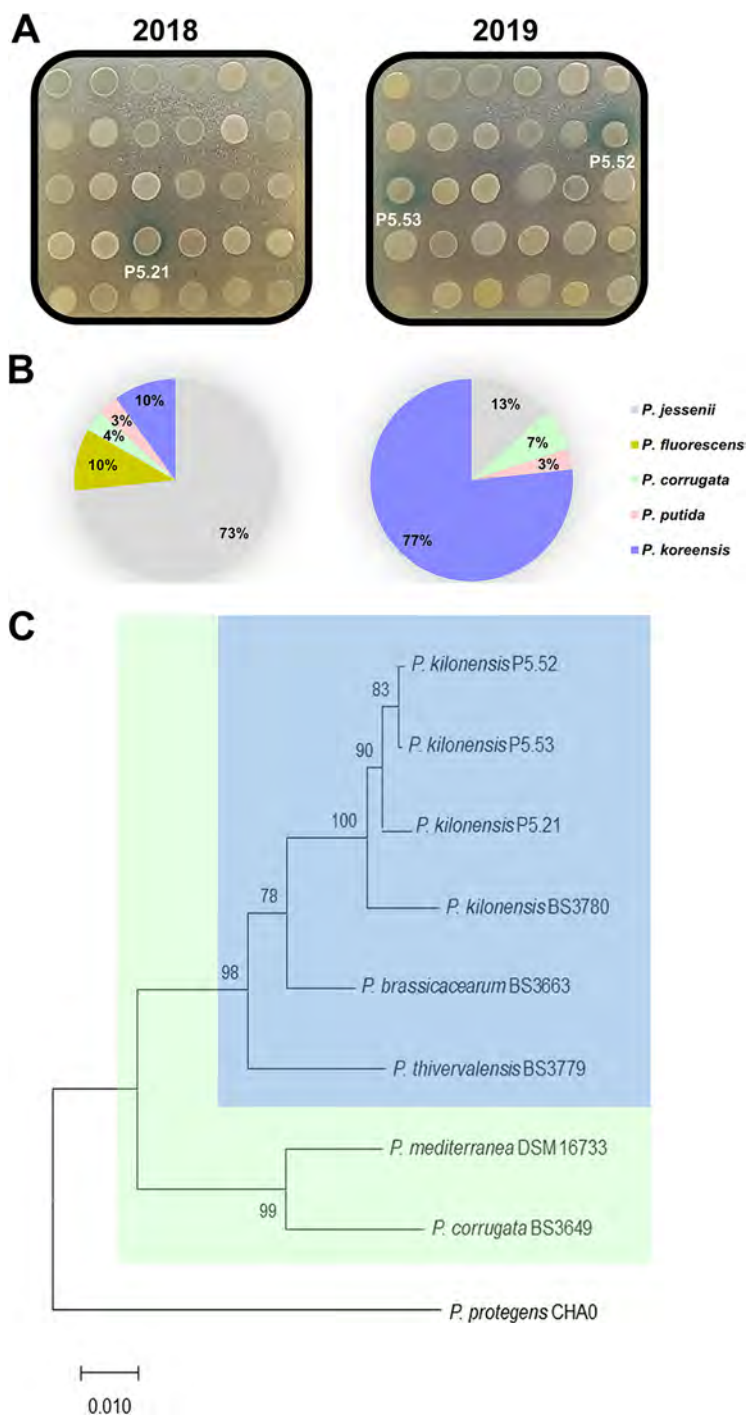


**FIG 3** Examination of fluorescent *Pseudomonas* from grassland soil for DAPG production. (A) Thirty fluorescent *Pseudomonas* isolates from grassland soil in 2018/2019 were grown on a lawn of the biosensor with pSEVA225::DAPG<sub>lacZ</sub> on KBmalt medium supplemented with X-Gal. The biosensor responded to one isolate from 2018 and two from 2019. (B) Part of the *rpoD* gene was sequenced and aligned to a database of 165 type strains of *Pseudomonas*. The three isolates eliciting a response

(Continued on next page)

**FIG 3** Legend (Continued)

from the biosensor were identified as *P. kilonensis*, which is part of the *P. corrugata* subgroup (9). (C) An *rpoD*-based neighbor-joining tree representing the phylogenetic relationship of the three *P. kilonensis* isolates to the *P. corrugata* subgroup. *P. protegens* CHA0 was included as an outlier. A bootstrap consensus tree (500 replicates) of the *rpoD* PCR products was constructed via the neighbor-joining method. The bootstrap percentage values are depicted next to each branching point. The *P. corrugata* subgroup is shown in a green area, whereas the species of this subgroup known to produce DAPG are in a blue box, along with the three soil isolates.

**TABLE 1** Frequencies of DAPG producers in natural soil microbiomes

Site	Total CFU/g of soil <sup>a</sup>	Blue halo		<i>phlD</i> PCR verified	
		Count (no./total)	% <sup>b</sup>	Count (no./total)	CFU/g of soil <sup>c</sup>
P5'	$1.7 \times 10^4$	6/288	2.08	1/6	60
P8	$5.7 \times 10^3$	5/288	1.74	1/5	20
P9	$6.9 \times 10^3$	49/288	17.01	49/49	$1.2 \times 10^3$

<sup>a</sup>Total CFU of bacteria cultivable on  $\frac{1}{4}$  KB<sup>+++</sup> medium, which is predominantly *Pseudomonas*.

<sup>b</sup>Proportion of isolates displaying a blue halo in relation to the 288 colonies tested.

<sup>c</sup>CFU per gram of soil of potential DAPG producers was calculated using the ratio of PCR-confirmed isolates compared to the total number of tested isolates times CFU per gram of soil of cultivable *Pseudomonas*.

green area). Members of this subgroup are known to harbor the biosynthetic gene cluster required for DAPG production (10). To determine the phylogenetic relationship of the three *P. kilonensis* isolates compared to the *P. corrugata* subgroup, we constructed an *rpoD*-based bootstrap consensus tree (500 replicates) with the neighbor-joining method (Fig. 3C). As expected, the three *P. kilonensis* isolates cluster together with the members of the *P. corrugata* subgroup known to produce DAPG (marked with a blue box). Taken together, these results show that genetically highly related DAPG-producing *Pseudomonas* organisms can be isolated from the same grassland soil site over a 12-month period.

#### Measuring the frequency of DAPG-producing pseudomonads in grassland soils.

To further explore the populations and frequencies of DAPG-producing pseudomonads in grassland soils, we sampled soil from three additional grassland sites (an area close to P5 labeled P5', P8, and P9) (see Materials and Methods). In total, we isolated 288 *Pseudomonas* strains as libraries in 96-well microplates from each of the three sites ( $n=864$ ). The three libraries were then screened for potential DAPG producers by replica plating them onto KBmalt agar supplemented with X-Gal and a lawn of the whole-cell biosensor harboring pSEVA225::DAPG<sub>lacZ</sub>. Simultaneously, the libraries were screened on separate plates for production of natural  $\beta$ -galactosidases, and isolates displaying a response were discarded from further analyses. Note that in this experimental setup (using replica plating), the development of blue halos around DAPG-producing colonies took longer than when larger aliquots of cultures were spotted onto the agar plates. After 48 h of incubation, the biosensor elicited a response to six isolates from P5', five isolates from P8, and 49 isolates from P9 (Table 1). Subsequently, we analyzed the colonies displaying a blue halo for the presence of *phlD*, as well as their taxonomy by sequencing part of *rpoD* and aligning it to the database of *Pseudomonas* type strains (9). For P5' and P8, one isolate from each site was confirmed to encode the polyketide synthase responsible for DAPG biosynthesis (Table 1), and both isolates were identified as *P. protegens* (Fig. 4). For P9, the 49 isolates with a surrounding blue halo were confirmed to have *phlD*, where 38 of those isolates belonged to *P. kilonensis* and the remaining 11 were identified as *P. protegens* (Fig. 4). The false positives from P5' and P8 were subsequently analyzed with LC-MS (see Materials and Methods) to confirm the absence of DAPG production. DAPG was not detected in any of the nine isolates.

## DISCUSSION

In this study, we constructed a highly sensitive whole-cell biosensor for detection

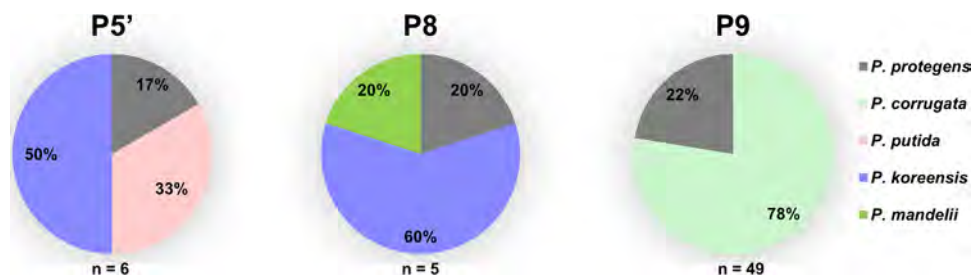


**FIG 4** Taxonomic identification of isolates with a surrounding blue halo in the high-throughput screening assay. For each isolate, part of the *rpoD* gene was sequenced and aligned to a database of 165 type strains of *Pseudomonas*. For both P5' and P8, one isolate was identified as *P. protegens*, whereas the remaining isolates belonged to either the *P. putida* group or the *P. koreensis* and *P. mandelii* subgroups of *P. fluorescens*, according to Hesse et al. (9). For P9, the *rpoD* gene of 49 isolates displaying a blue halo was sequenced. Only species of *P. kilonensis* and *P. protegens* were identified.

and guided isolation of DAPG-producing microorganisms. Utilization of genetic circuits to detect and report on the presence of small molecules is associated with advantages and disadvantages. Two apparent caveats associated with the *in vitro* agar-based biosensor-guided identification used in this study are that it is viable only for cultivable organisms and it requires conditions that allow cocultivation of the isolate of interest with the biosensor. One advantage of the biosensor is that it is not restricted to a narrow range of genotypes of DAPG producers, which is a limiting factor of PCR-based approaches. Additionally, with a detection limit of  $>20$  nM *in vitro* (Fig. 1C), the biosensor may have potential for use *in situ* to identify DAPG production in specific soil niches and thus serve as a promising alternative to chemical identification of DAPG, where the detection limit is in the low micromolar range (13).

We show that the biosensor is specific toward detection of DAPG. The biosensor did not respond to PG and elicited a minor response toward MAPG. This minor response was absent from its *lacZ* counterpart, which further demonstrates the sensitivity of the *lux* variant. We realize that we have used only two molecules (PG and MAPG) to represent natural DAPG analogues in our specificity assessment. It remains a possibility that other molecules can elicit a biosensor response. In a study by Yan et al. on the PhIH transcriptional regulator, it was demonstrated that multiple molecules with structural similarities to DAPG could bind to PhIH and induce a response, albeit significantly lower than the response induced by DAPG (5). Likewise, it was found that MAPG induced a minor response in the same study (5).

In order to demonstrate the biosensor response to bioavailable DAPG on agar surfaces, we inoculated DAPG producers and nonproducers on top of the whole-cell biosensor on agar plates. As expected, a blue halo was observed around the DAPG producers. Additionally, a blue coloring was absent around the nonproducers after 24 h. These findings also correlated with the LC-MS analysis. However, a slight blue halo was observed surrounding *P. putida* after prolonged incubation ( $>72$  h), suggesting that one or more compounds are secreted by this strain during late stationary phase which interact with PhIF, thus relieving repression of the reporter gene.

Subsequently, the biosensor was utilized for guided identification of DAPG-producing fluorescent *Pseudomonas*. The isolates were selected on  $\frac{1}{4}$  KB<sup>+++</sup> medium (see Materials and Methods), which has been shown to be optimal for isolation of fluorescent *Pseudomonas*, including DAPG producers (24). We screened 30 pseudomonads randomly isolated from the P5 site in both 2018 and 2019. DAPG producers were detected in both samplings based on a clear blue halo surrounding their colonies and were identified as *P. kilonensis* species, which are known to produce DAPG (10). Part of the *rpoD* gene was sequenced for all isolates and aligned to a database of *Pseudomonas* type strains (9), which revealed a remarkably similar diversity over a 12-month period (i.e., the same *Pseudomonas* subgroups were sampled at both time points). However,

despite the low sampling depth, the species abundance appeared to shift from *P. jessenii* to *P. koreensis*. From an ecological point of view, it is of interest that the DAPG producers seem to persist over time in relatively similar quantities.

Lastly, we sought to optimize the screening assay to a high-throughput 96-well microplate format. We isolated 288 *Pseudomonas* species from each of three soil sites (P5', P8, and P9). The sites are located in a Danish natural reserve (Dyrehaven); thus, we argued that they represent pristine grassland soil niches. It is worth noting that bulk soil is an extremely harsh environment with low nutrient availability, which might explain the small amount of CFU per gram of *Pseudomonas* compared to rhizosphere environments (11–13). We identified 6 and 5 isolates with blue halos around their colonies in P5' and P8, respectively. Yet only one isolate from each site was confirmed to encode the polyketide synthase responsible for DAPG production. Picard et al. isolated 156 *Pseudomonas* strains from bulk soil, but no DAPG producers were identified, although DAPG producers were isolated at a later stage from roots of maize plants grown in the same soil (25). It was speculated that DAPG-producing *Pseudomonas* organisms are present in bulk soil in quantities of  $<2.6 \times 10^2$  CFU g<sup>-1</sup>, which is comparable to the findings obtained in our study of grassland soil at P5' ( $6 \times 10^1$  g<sup>-1</sup>) and P8 ( $2 \times 10^1$  g<sup>-1</sup>) (Table 1). In P9, on the other hand, 17% of the isolates displayed a blue halo around their colonies, and the presence of *phlD* was confirmed for all isolates. However, during the course of our study, it became apparent that a deer-feeding site was located near the sampling site, with wheat being the main feed. This could potentially explain the high frequency of DAPG producers in P9, as DAPG-producing *Pseudomonas* bacteria, which are known to be associated with the roots of wheat (1), might have translocated into the soil surrounding the feeding site due to animal activities.

The false-positive isolates from the high-throughput screening (i.e., isolates that resulted in a biosensor response without the presence of DAPG biosynthesis genes) could potentially produce compounds similar to those made by *P. putida* (as described above), which interfere with PhIF. The *phIF* gene in the biosensor was cloned from *P. protegens* CHA0 (26), where it naturally functions as a transcriptional repressor of *phlACBD* (8). The false positives identified in our screen may secrete yet-unknown secondary metabolites that interact with the PhIF repressor, thus inducing biosynthesis of DAPG. This finding highlights the possibility for microbe-microbe interactions *in situ* leading to induced DAPG production by adjacent nonproducers. Interestingly, we found two isolates belonging to the *P. putida* group in the high-throughput screening, which may indicate that certain species of this group produce molecules that can induce expression of DAPG. Surprisingly, we also identified isolates of *P. koreensis* and *P. mandelii* that elicit a response from the biosensor, which further enhances the potential of yet-unexplored microbe-microbe interactions that could be addressed in future studies.

In conclusion, this study demonstrates the use of an engineered whole-cell biosensor for guided identification of DAPG-producing microorganisms. This approach surpasses the limits of previous PCR-based and chemical identification methods, although future optimization to further increase sensitivity and reduce unexpected response to false positives might be required.

## MATERIALS AND METHODS

**Strains, media, and growth conditions.** Plasmid cloning and genetic circuit characterization were performed in *Escherichia coli* K-12  $\Delta$ laciZYA or *E. coli* CC118- $\lambda$ pir. Cells were cultured in Luria-Bertani (LB) broth (Lennox; Merck, St. Louis, MO) with appropriate antibiotics. The antibiotic concentrations used were 25  $\mu$ g ml<sup>-1</sup> for kanamycin, 10  $\mu$ g ml<sup>-1</sup> for chloramphenicol, and 8  $\mu$ g ml<sup>-1</sup> for tetracycline. The engineered whole-cell biosensor was cultured by inoculating a single colony in 5 ml of LB broth supplemented with kanamycin and incubating it overnight at 37°C with shaking (200 rpm). For characterization of the biosensor response to DAPG producers, control strains were routinely cultured by inoculating a single colony in 5 ml of LB broth and incubating it overnight at 30°C with shaking (200 rpm). Control strains included *Pseudomonas putida* KT2440, *Pseudomonas protegens* DTU9.1 (previously isolated by our group), *Pseudomonas protegens* DTU9.1  $\Delta$ phlACBD (see below), and *Chromobacterium vaccinii* MWU328.

**Plasmid circuit construction.** Plasmid construction and DNA manipulation were performed following standard molecular biology techniques. The strain *E. coli* K-12  $\Delta$ laciZYA was transformed with all plasmid constructs by chemical transformation. The plasmid pAJM847 (GenBank accession number

MH101727.1), comprising the  $P_{lacIQ}$  promoter, *phlF*, the induction operon terminator (IOT), and the  $P_{phlF}$  promoter, was a kind gift from Christopher Voigt (26). The genetic circuit from pAJM847 was reorganized into pSEVA225T (GenBank accession number [KC847299.1](#)) (27) to obtain the DAPG biosensor. To this end, the fragment containing the  $P_{lacIQ}$  promoter, *phlF*, and the induction operon terminator was PCR amplified with AvrII and EcoRI overhangs (PlacI\_AvrII\_fw, 5'-TAAGCACCTAGGCGTTTTGGTCCAATGG; Term847\_EcoRI\_rev, 5'-TGCTTAGAATTCAGCGAGGAAGCACC). The purified PCR product was digested with appropriate restriction enzymes and inserted in pSEVA225T to yield pSEVA225:: $P_{lacIQ}$ -*phlF*. Subsequently, the fragment containing the  $P_{phlF}$  promoter was PCR amplified with EcoRI and HindIII overhangs (PphIF\_EcoRI\_fw, 5'-TAAGCAGAATCCCGACGTACGGTGG; PphIF\_HindIII\_rev, 5'-TGCTTAAAGCTTTATTTCCCTCTTCTCTAG). Purified PCR product was restriction digested and inserted in pSEVA225:: $P_{lacIQ}$ -*phlF* to yield the *lacZ* version of the DAPG biosensor (pSEVA225::DAPG<sub>*lacZ*</sub>). The *lux* operon (*luxCDABE* from *Photobacterium luminescens*) was PCR amplified from pUC18-mini-TN7T-Gm-*lux* with HindIII and SpeI overhangs (Lux\_HindIII\_fw, 5'-GAATTCAAGCTTATGACTAAAAAATTCATTC; Lux\_SpeI\_rev, 5'-GAATTCAGTAGGATATCAACTATCAAAAC). The purified PCR product was restriction digested and inserted in pSEVA225::DAPG<sub>*lacZ*</sub> to yield the *lux* version (pSEVA226::DAPG<sub>*lux*</sub>).

**Deletion of *phlACBD* by allelic replacement.** To abolish DAPG production in *P. protegens* DTU9.1, the biosynthesis genes, *phlACBD*, were deleted by allelic replacement according to the method of Hmelo et al. (28). In short, DNA fragments directly upstream of *phlA* (Up\_F, 5'-ATCCCGTCTAGACAGAGATTCGCAGTAAAAAAG; Up\_R, 5'-GGCGGGACAGGCACAGGCAGTCACATTTCTTATTCCATTCTTTTC) and directly downstream of *phlD* (Down\_F, 5'-TGTGACTGCCTGTGCCTG; Down\_R, 5'-ATCCGGGAGCTCTGAAAGCCGCCAGCC) were PCR amplified. The fragments were joined by splicing-by-overlap extension PCR with XbaI and SacI overhangs using primers Up\_F and Down\_R. The purified PCR product was restriction digested and inserted into pNJ1 (29). The resulting plasmid was mobilized into *P. protegens* DTU9.1 via triparental mating with *E. coli* HB101 harboring the helper plasmid pRK600. Merodiploid transconjugants were initially selected on *Pseudomonas* isolation agar (PIA; Merck, St. Louis, MO) supplemented with 50  $\mu\text{g ml}^{-1}$  of tetracycline. A second selection was performed on NSLB agar (10 g liter<sup>-1</sup> of tryptone, 5 g liter<sup>-1</sup> of yeast extract, 15 g liter<sup>-1</sup> of Bacto agar) with 15% sucrose. Candidates for successful deletion were confirmed by PCR and verified by Sanger sequencing at Eurofins Genomics.

**Luminescence dose/response microplate assay.** Overnight cultures of the whole-cell biosensor harboring pSEVA226-DAPG<sub>*lux*</sub> were prepared in six biological replicates as described above. Ninety-six-well black, clear-bottom microplates (In Vitro, Denmark) were prepared with LB broth supplemented with kanamycin and various concentrations of PG, MAPG, or DAPG (0, 0.005, 0.01, 0.02, 0.039, 0.078, 0.156, 0.3125, 0.625, 1.25, 2.5, 5, 7.5, 10, and 15  $\mu\text{M}$ ). The overnight cultures were diluted to inoculate the microplates to an initial OD<sub>600</sub> of 0.01. The plates were sealed with a semipermeable membrane (Breathe-Easy; Merck, St. Louis, MO) and incubated in a Cytation 5 microplate reader for 5 h at 37°C with shaking (600 rpm), with continuous measurements of luminescence and absorbance at OD<sub>600</sub>. These data and any other microplate assay data were collected with Gen5 2.07 software and exported to Excel 2016 and GraphPad for data analysis.

**$\beta$ -Galactosidase dose/response microplate assay.** Overnight cultures of the whole-cell biosensor harboring pSEVA225-DAPG<sub>*lacZ*</sub> were prepared in triplicate as described above. Transparent 96-well microplates (TPP; Merck, St. Louis, MO) were prepared with LB broth supplemented with kanamycin and various concentrations of PG, MAPG, or DAPG (0, 0.625, 1.25, 2.5, 5, 7.5, 10, and 15  $\mu\text{M}$ ). The overnight cultures were diluted to inoculate the microplates to an initial OD<sub>600</sub> of 0.01. Cultures were grown for 3 h at 37°C with shaking (600 rpm), followed by measurement of the endpoint OD<sub>600</sub>. Subsequently, 20  $\mu\text{l}$  from each well was transferred to new transparent 96-well microplates and mixed with 80  $\mu\text{l}$  of permeabilization buffer (0.1 M Na<sub>2</sub>HPO<sub>4</sub>, 0.02 M KCl, 0.002 M MgSO<sub>4</sub>, 0.8 mg ml<sup>-1</sup> of hexadecyltrimethylammonium bromide, 0.4 mg ml<sup>-1</sup> of sodium deoxycholate, 5.4  $\mu\text{l ml}^{-1}$  of  $\beta$ -mercaptoethanol) (30). The plates were incubated at 30°C with shaking (600 rpm) for 30 min to facilitate cell lysis. Next, 28  $\mu\text{l}$  of lysed cell culture from each well was transferred to 96-well black microplates and mixed with 172  $\mu\text{l}$  of substrate solution (0.06 M Na<sub>2</sub>HPO<sub>4</sub>, 0.04 M NaH<sub>2</sub>PO<sub>4</sub>, 1 mg ml<sup>-1</sup> of *o*-nitrophenyl- $\beta$ -D-galactopyranoside, 2.7  $\mu\text{l ml}^{-1}$  of  $\beta$ -mercaptoethanol) (30). The plates were sealed with a semipermeable membrane (Breathe-Easy; Merck, St. Louis, MO) and incubated in a Cytation 5 microplate reader for 16 h at 37°C with shaking (600 rpm), with continuous measurements of OD<sub>420</sub>. Data were collected and analyzed as described above.

**Detecting DAPG from bacterial cultures grown on agar surfaces.** Overnight cultures of the whole-cell biosensor harboring pSEVA225-DAPG<sub>*lacZ*</sub> and the control strains *P. putida* KT2440, *P. protegens* DTU9.1, *P. protegens* DTU9.1  $\Delta$ *phlACBD*, and *C. vaccinii* MWU328 were prepared as described above. The biosensor was normalized to an OD<sub>600</sub> of 1.0 and spread on King's agar B supplemented with malt extract (KBmalt) (20 g liter<sup>-1</sup> of Proteose peptone no. 3, 1.5 g liter<sup>-1</sup> of K<sub>2</sub>HPO<sub>4</sub>, 1.5 g liter<sup>-1</sup> of MgSO<sub>4</sub>, 7.5 g liter<sup>-1</sup> of malt extract, 10 ml liter<sup>-1</sup> of glycerol, and 20 g liter<sup>-1</sup> of Bacto agar) supplemented with 25  $\mu\text{g ml}^{-1}$  of 5-bromo-4-chloro-3-indolyl- $\beta$ -D-galactopyranoside (*X-Gal*; Thermo Fisher Scientific). Overnight cultures of the control strains were normalized to an OD<sub>600</sub> of 1.0 and inoculated as 20- $\mu\text{l}$  spots on the agar plates containing the biosensor. Agar plates were incubated at 30°C for 24 to 96 h. Plates were inspected for blue halos surrounding the bacterial spots every 24 h.

**Detection of DAPG by LC-MS.** Overnight cultures of the control strains *P. putida* KT2440, *P. protegens* DTU9.1, *P. protegens* DTU9.1  $\Delta$ *phlACBD*, and *C. vaccinii* MWU328 were prepared as described above. The cultures were normalized to an OD<sub>600</sub> of 1.0, inoculated as 20- $\mu\text{l}$  spots on KBmalt and malt agar plates, and incubated at 30°C for 24 h. An agar plug (6-mm diameter) of the bacterial culture was transferred to a vial and extracted with 1 ml of isopropanol-ethyl acetate (1:3, vol/vol), containing 1% formic acid, under ultrasonication for 60 min. The extracts were then transferred to new vials, evaporated under N<sub>2</sub>, and redissolved in 200  $\mu\text{l}$  of methanol for further sonication over 15 min. After centrifugation at

13,400 rpm for 3 min, the supernatants were transferred to high-performance liquid chromatography (HPLC) vials and subjected to ultrahigh-performance liquid chromatography-high resolution electrospray ionization mass spectrometry (UHPLC-HRESIMS) analysis. UHPLC-HRESIMS was performed on an Agilent Infinity 1290 UHPLC system equipped with a diode array detector (DAD). UV-visible spectra were recorded from 190 to 640 nm. Liquid chromatography of 1  $\mu$ l of extract was carried out using an Agilent Poroshell 120 phenyl-hexyl column (2.1 by 150 mm, 1.9  $\mu$ m) at 60°C using acetonitrile and H<sub>2</sub>O, both containing 0.02 M formic acid, as mobile phases. Initially, a linear gradient of 10% acetonitrile/H<sub>2</sub>O to 100% acetonitrile over 10 min was employed, followed by an isocratic wash of 100% acetonitrile for 2 min. The gradient was returned to 10% acetonitrile/H<sub>2</sub>O in 0.1 min and, finally, an isocratic condition of 10% acetonitrile/H<sub>2</sub>O for 1.9 min, all at a flow rate of 0.35 ml min<sup>-1</sup>. Mass spectrometry detection was performed in positive ionization on an Agilent 6545 quadrupole time of flight (QTOF) MS equipped with an Agilent dual-jet stream electrospray ion source with a drying gas temperature of 250°C, drying gas flow of 8 liters min<sup>-1</sup>, sheath gas temperature of 300°C, and sheath gas flow of 12 liters min<sup>-1</sup>. The capillary voltage was set to 4,000 V and nozzle voltage to 500 V. Mass spectrometry data analysis and processing were performed using Agilent MassHunter Qualitative Analysis B.07.00.

**Isolation of fluorescent *Pseudomonas* from grassland soil.** Three sites of undisturbed grassland were chosen (P5, 55°78'88"N, 12°55'83"E; P8, 55°79'52"N, 12°58'06"E; and P9, 55°79'12"N, 12°57'51"E). Soil was collected approximately 10 centimeters below the grass surface. Five grams of soil was suspended in 30 ml of sterile water and shaken vigorously for 1 min on a Vortex mixer. In order to isolate fluorescent *Pseudomonas*, the samples were serially diluted and plated onto ¼ KB<sup>+++</sup> (7.5 g liter<sup>-1</sup> of King's agar B, 10 ml liter<sup>-1</sup> of glycerol, 7.5 g liter<sup>-1</sup> of Bacto agar) supplemented with 100  $\mu$ g ml<sup>-1</sup> of cycloheximide, 13  $\mu$ g ml<sup>-1</sup> of chloramphenicol, and 40  $\mu$ g ml<sup>-1</sup> of ampicillin, as previously described (24). Agar plates were incubated at 30°C for 48 h. Fluorescent colonies were identified under UV light and restreaked on LB agar plates. Species identification of the soil isolates was performed by PCR, amplifying part of the *rpoD* gene with primers (PsEG30F, 5'-ATYGAATCGCCAARCG; PsEG790R, 5'-CGGTGATKCTCTGA) (31). PCR products were purified, sequenced, and aligned to a database of 166 known type strains of *Pseudomonas* (9).

**Biosensor-guided identification of DAPG producers from grassland soil.** Thirty fluorescent *Pseudomonas* isolates were randomly selected from sample site P5 both in 2018 and in 2019 as described above. Isolates were cultured overnight in LB broth at 30°C with shaking (200 rpm). An overnight culture of the biosensor harboring pSEVA225-DAPG<sub>lacZ</sub> was normalized to an OD<sub>600</sub> of 1.0 and spread onto KBmalt plates supplemented with 25  $\mu$ g ml<sup>-1</sup> of X-Gal. Overnight cultures of the *Pseudomonas* isolates were inoculated onto the agar plates as 20- $\mu$ l spots. Plates were incubated at 30°C for 24 to 48 h. Plates were inspected for blue halos surrounding the bacterial spots every 24 h. The DAPG-producing isolates were identified by PCR-based species identification, as described above. The phylogenetic relationship between the DAPG-producing isolates was determined by analyzing a phylogenetic tree with representatives of each *P. fluorescens* subgroup (9). In short, the PCR-amplified parts of the *rpoD* genes were Sanger sequenced and aligned using the MUSCLE algorithm, followed by construction of a bootstrap consensus tree (500 replicates) by the neighbor-joining method in MEGA X (32).

**High-throughput screening for DAPG producers in grassland soil.** In 2019, 288 fluorescent *Pseudomonas* isolates were randomly selected from three sample sites (P5', 55°78'78"N, 12°56'07"E; P8 and P9, see coordinates above). Fluorescent colonies were streaked on LB agar OmniTray (Nunc; Nalge Nunc International, Rochester, NY) and incubated for 24 h at 30°C. Isolates were cultured in transparent 96-well microplates in terrific broth (TB; 12 g liter<sup>-1</sup> of tryptone, 24 g liter<sup>-1</sup> of yeast extract, 0.17 M KH<sub>2</sub>PO<sub>4</sub>, 0.72 M K<sub>2</sub>HPO<sub>4</sub>, and 5 ml liter<sup>-1</sup> of glycerol). An overnight culture of the biosensor harboring pSEVA225-DAPG<sub>lacZ</sub> was normalized to an OD<sub>600</sub> of 0.5 and spread onto KBmalt OmniTrays supplemented with 50  $\mu$ g ml<sup>-1</sup> of X-Gal. The *Pseudomonas* isolates were inoculated on the OmniTrays with sterile replicators. The OmniTrays were incubated at 30°C for 48 h and inspected for blue halos surrounding the *Pseudomonas* colonies. Candidate isolates exhibiting a blue halo were screened by PCR for the presence of *phlD* with primers (B2BF, 5'-ACCCACCGCAGCATCGTTTATGAGC; BPR4, 5'-CCGCCGGTATGGAAGATGAAAAAGTC) (33). Moreover, *rpoD* was amplified from candidate colonies for species identification with primers PsEG30F and PsEG790R.

**Data availability.** All data are included here and in the supplemental material. Plasmid constructs and bacterial strains, including *Pseudomonas* isolates, will be made available by the corresponding author upon request.

## SUPPLEMENTAL MATERIAL

Supplemental material is available online only.

**SUPPLEMENTAL FILE 1**, PDF file, 1.3 MB.

## ACKNOWLEDGMENTS

We thank Victor de Lorenzo for providing the pSEVA plasmid used as vector background for the biosensor. We also thank Christopher Voigt for providing plasmid pAJM847. Moreover, we thank Pavelas Sazinas for advice on phylogenetic analysis, as well as Susanne Koefoed for technical assistance. We thank the members of the Centre for Microbial Secondary Metabolites (CeMiSt) for discussions.

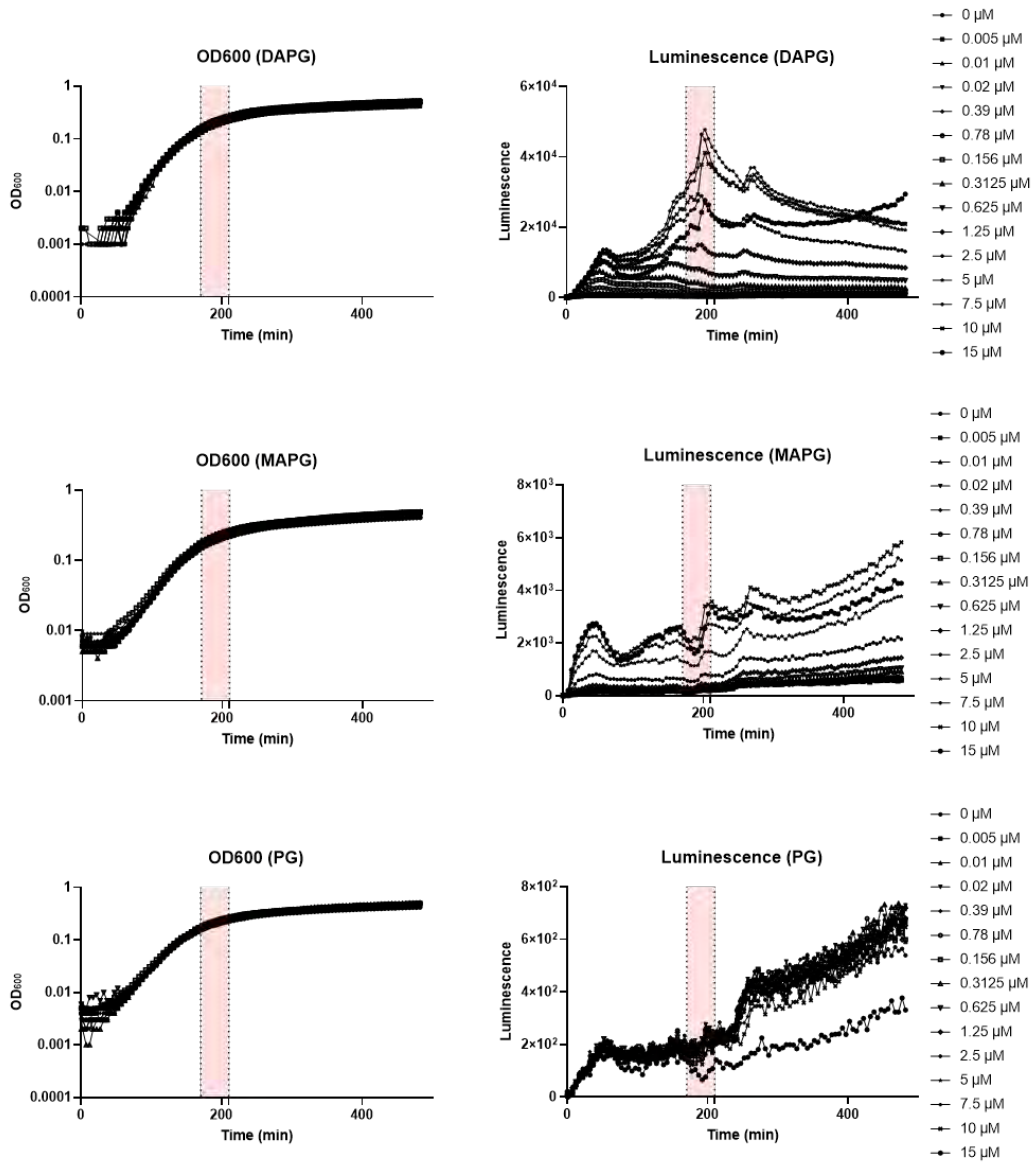
This study was funded by the Danish National Research Foundation (DNRF137) for the Centre for Microbial Secondary Metabolites.

## REFERENCES

- Raaijmakers JM, Weller DM. 1998. Natural plant protection by 2,4-diacetylphloroglucinol-producing *Pseudomonas* spp. in take-all decline soils. *Mol Plant Microbe Interact* 11:144–152. <https://doi.org/10.1094/MPMI.1998.11.2.144>.
- Ramette A, Moënne-Loccoz Y, Défago G. 2003. Prevalence of fluorescent pseudomonads producing antifungal phloroglucinols and/or hydrogen cyanide in soils naturally suppressive or conducive to tobacco black root rot. *FEMS Microbiol Ecol* 44:35–43. <https://doi.org/10.1111/j.1574-6941.2003.tb00108.x>.
- Cronin D, Moënne-Loccoz Y, Fenton A, Dunne C, Dowling DN, O'Gara F. 1997. Ecological interaction of a biocontrol *Pseudomonas fluorescens* strain producing 2,4-diacetylphloroglucinol with the soft rot potato pathogen *Erwinia carotovora* subsp. *atroseptica*. *FEMS Microbiol Ecol* 23:95–106. <https://doi.org/10.1111/j.1574-6941.1997.tb00394.x>.
- Bangera MG, Thomashow LS. 1999. Identification and characterization of a gene cluster for synthesis of the polyketide antibiotic 2,4-diacetylphloroglucinol from *Pseudomonas fluorescens* Q2-87. *J Bacteriol* 181:3155–3163. <https://doi.org/10.1128/JB.181.10.3155-3163.1999>.
- Yan X, Yang R, Zhao R-X, Han J-T, Jia W-J, Li D-Y, Wang Y, Zhang N, Wu Y, Zhang L-Q, He Y-X. 2017. Transcriptional regulator PhIH modulates 2,4-diacetylphloroglucinol biosynthesis in response to the biosynthetic intermediate and end product. *Appl Environ Microbiol* 83:e01419-17. <https://doi.org/10.1128/AEM.01419-17>.
- Yang F, Cao Y. 2012. Biosynthesis of phloroglucinol compounds in microorganisms—review. *Appl Microbiol Biotechnol* 93:487–495. <https://doi.org/10.1007/s00253-011-3712-6>.
- Bottiglieri M, Keel C. 2006. Characterization of PhIG, a hydrolase that specifically degrades the antifungal compound 2,4-diacetylphloroglucinol in the biocontrol agent *Pseudomonas fluorescens* CHA0. *Appl Environ Microbiol* 72:418–427. <https://doi.org/10.1128/AEM.72.1.418-427.2006>.
- Abbas A, Morrissey JP, Marquez PC, Sheehan MM, Delany IR, O'Gara F. 2002. Characterization of interactions between the transcriptional repressor PhIF and its binding site at the pHA promoter in *Pseudomonas fluorescens* F113. *J Bacteriol* 184:3008–3016. <https://doi.org/10.1128/jb.184.11.3008-3016.2002>.
- Hesse C, Schulz F, Bull CT, Shaffer BT, Yan Q, Shapiro N, Hassan KA, Varghese N, Elbourne LDH, Paulsen IT, Kyripides N, Woyke T, Loper JE. 2018. Genome-based evolutionary history of *Pseudomonas* spp. *Environ Microbiol* 20:2142–2159. <https://doi.org/10.1111/1462-2920.14130>.
- Almario J, Bruto M, Vacheron J, Prigent-Combaret C, Moënne-Loccoz Y, Muller D. 2017. Distribution of 2,4-diacetylphloroglucinol biosynthetic genes among the *Pseudomonas* spp. reveals unexpected polyphyletism. *Front Microbiol* 8:1218. <https://doi.org/10.3389/fmicb.2017.01218>.
- Raaijmakers JM, Weller DM, Thomashow LS. 1997. Frequency of antibiotic-producing *Pseudomonas* spp. in natural environments. *Appl Environ Microbiol* 63:881–887. <https://doi.org/10.1128/AEM.63.3.881-887.1997>.
- Mavrodi OV, Mavrodi DV, Thomashow LS, Weller DM. 2007. Quantification of 2,4-diacetylphloroglucinol-producing *Pseudomonas fluorescens* strains in the plant rhizosphere by real-time PCR. *Appl Environ Microbiol* 73:5531–5538. <https://doi.org/10.1128/AEM.00925-07>.
- Bonsall RF, Weller DM, Thomashow LS. 1997. Quantification of 2,4-diacetylphloroglucinol produced by fluorescent *Pseudomonas* spp. in vitro and in the rhizosphere of wheat. *Appl Environ Microbiol* 63:951–955. <https://doi.org/10.1128/AEM.63.3.951-955.1997>.
- Renella G, Giagnoni L. 2016. Light dazzles from the black box: whole-cell biosensors are ready to inform on fundamental soil biological processes. *Chem Biol Technol Agric* 3:8. <https://doi.org/10.1186/s40538-016-0059-3>.
- Wan X, Ho TYH, Wang B. 2019. Engineering prokaryote synthetic biology biosensors, p 1–37. *In* Thousand G (ed), *Handbook of cell biosensors*. Springer International Publishing, Cham, Switzerland.
- Kim HJ, Lim JW, Jeong H, Lee S-J, Lee D-W, Kim T, Lee SJ. 2016. Development of a highly specific and sensitive cadmium and lead microbial biosensor using synthetic CadC-T7 genetic circuitry. *Biosens Bioelectron* 79:701–708. <https://doi.org/10.1016/j.bios.2015.12.101>.
- Wang B, Barahona M, Buck M. 2015. Amplification of small molecule-inducible gene expression via tuning of intracellular receptor densities. *Nucleic Acids Res* 43:1955–1964. <https://doi.org/10.1093/nar/gku1388>.
- Hooshangi S, Thiberge S, Weiss R. 2005. Ultrasensitivity and noise propagation in a synthetic transcriptional cascade. *Proc Natl Acad Sci U S A* 102:3581–3586. <https://doi.org/10.1073/pnas.0408507102>.
- Wang B, Barahona M, Buck M. 2014. Engineering modular and tunable genetic amplifiers for scaling transcriptional signals in cascaded gene networks. *Nucleic Acids Res* 42:9484–9492. <https://doi.org/10.1093/nar/gku593>.
- Burmølle M, Hansen LH, Sørensen SJ. 2005. Use of a whole-cell biosensor and flow cytometry to detect AHL production by an indigenous soil community during decomposition of litter. *Microb Ecol* 50:221–229. <https://doi.org/10.1007/s00248-004-0113-8>.
- Mimee M, Nadeau P, Hayward A, Carim S, Flanagan S, Jerger L, Collins J, McDonnell S, Swartwout R, Citorik RJ, Bulović V, Langer R, Traverso G, Chandrakasan AP, Lu TK. 2018. An ingestible bacterial-electronic system to monitor gastrointestinal health. *Science* 360:915–918. <https://doi.org/10.1126/science.aas9315>.
- Baehler E, Bottiglieri M, Péchy-Tarr M, Maurhofer M, Keel C. 2005. Use of green fluorescent protein-based reporters to monitor balanced production of antifungal compounds in the biocontrol agent *Pseudomonas fluorescens* CHA0. *J Appl Microbiol* 99:24–38. <https://doi.org/10.1111/j.1365-2672.2005.02597.x>.
- Maurhofer M, Keel C, Haas D, Défago G. 1994. Pyoluteorin production by *Pseudomonas fluorescens* strain CHA0 is involved in the suppression of *Pythium* damping-off of cress but not of cucumber. *Eur J Plant Pathol* 100:221–232. <https://doi.org/10.1007/BF01876237>.
- Landa BB, De Werd HAE, McSpadden Gardener BB, Weller DM. 2002. Comparison of three methods for monitoring populations of different genotypes of 2,4-diacetylphloroglucinol-producing *Pseudomonas fluorescens* in the rhizosphere. *Phytopathology* 92:129–137. <https://doi.org/10.1094/PHYTO.2002.92.2.129>.
- Picard C, Di Cello F, Ventura M, Fani R, Guckert A. 2000. Frequency and biodiversity of 2,4-diacetylphloroglucinol-producing bacteria isolated from the maize rhizosphere at different stages of plant growth. *Appl Environ Microbiol* 66:948–955. <https://doi.org/10.1128/aem.66.3.948-955.2000>.
- Meyer AJ, Segall-Shapiro TH, Glassey E, Zhang J, Voigt CA. 2019. *Escherichia coli* “Marionette” strains with 12 highly optimized small-molecule sensors. *Nat Chem Biol* 15:196–204. <https://doi.org/10.1038/s41589-018-0168-3>.
- Silva-Rocha R, Martínez-García E, Calles B, Chavarría M, Arce-Rodríguez A, de las Heras A, Páez-Espino AD, Durante-Rodríguez G, Kim J, Nikel PI, Platero R, de Lorenzo V. 2013. The Standard European Vector Architecture (SEVA): a coherent platform for the analysis and deployment of complex prokaryotic phenotypes. *Nucleic Acids Res* 41:D666–D675. <https://doi.org/10.1093/nar/gks1119>.
- Hmelo LR, Borlee BR, Almlblad H, Love ME, Randall TE, Tseng BS, Lin C, Irie Y, Storek KM, Yang JJ, Siehnell RJ, Howell PL, Singh PK, Tolker-Nielsen T, Parsek MR, Schweizer HP, Harrison JJ. 2015. Precision-engineering the *Pseudomonas aeruginosa* genome with two-step allelic exchange. *Nat Protoc* 10:1820–1841. <https://doi.org/10.1038/nprot.2015.115>.
- Yang L, Hengzhuang W, Wu H, Damkiaer S, Jochumsen N, Song Z, Givskov M, Høiby N, Molin S. 2012. Polysaccharides serve as scaffold of biofilms formed by mucoid *Pseudomonas aeruginosa*. *FEMS Immunol Med Microbiol* 65:366–376. <https://doi.org/10.1111/j.1574-695X.2012.00936.x>.
- Zhang X, Bremer H. 1995. Control of the *Escherichia coli* rrrB P1 promoter strength by ppGpp. *J Biol Chem* 270:11181–11189. <https://doi.org/10.1074/jbc.270.19.11181>.
- Mulet M, Bannasar A, Lalucat J, García-Valdés E. 2009. An *rpoD*-based PCR procedure for the identification of *Pseudomonas* species and for their detection in environmental samples. *Mol Cell Probes* 23:140–147. <https://doi.org/10.1016/j.mcp.2009.02.001>.
- Kumar S, Nei M, Dudley J, Tamura K. 2008. MEGA: a biologist-centric software for evolutionary analysis of DNA and protein sequences. *Brief Bioinform* 9:299–306. <https://doi.org/10.1093/bib/bbn017>.
- McSpadden Gardener BB, Mavrodi DV, Thomashow LS, Weller DM. 2001. A rapid polymerase chain reaction-based assay characterizing rhizosphere populations of 2,4-diacetylphloroglucinol-producing bacteria. *Phytopathology* 91:44–54. <https://doi.org/10.1094/PHYTO.2001.91.1.44>.

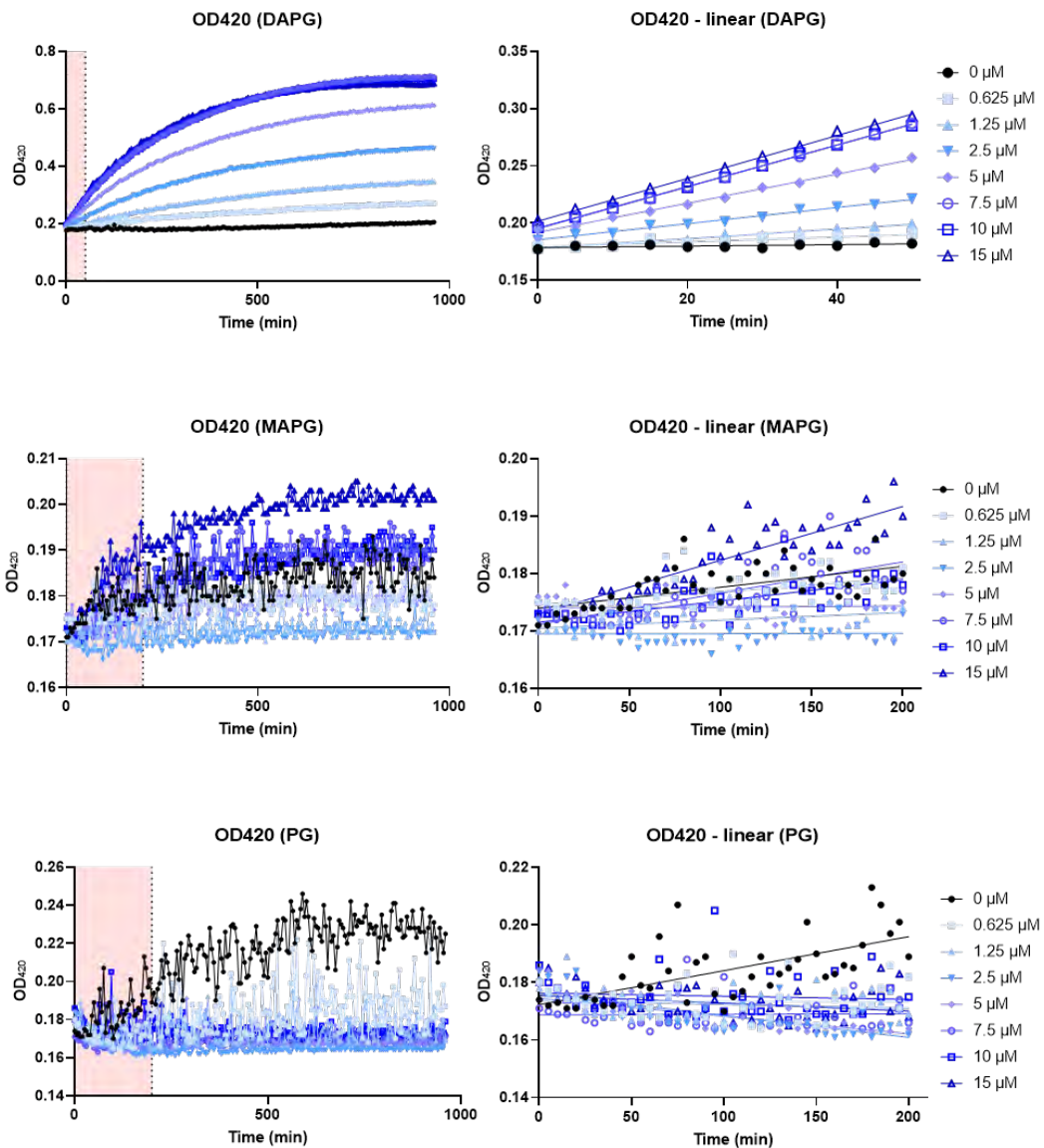
## SUPPLEMENTARY

**S1** Growth curves ( $OD_{600}$ ) and Luminescence curves for the whole-cell biosensor harbouring pSEVA225-DAPG<sub>lux</sub> grown in media supplemented with DAPG, MAPG and PG.



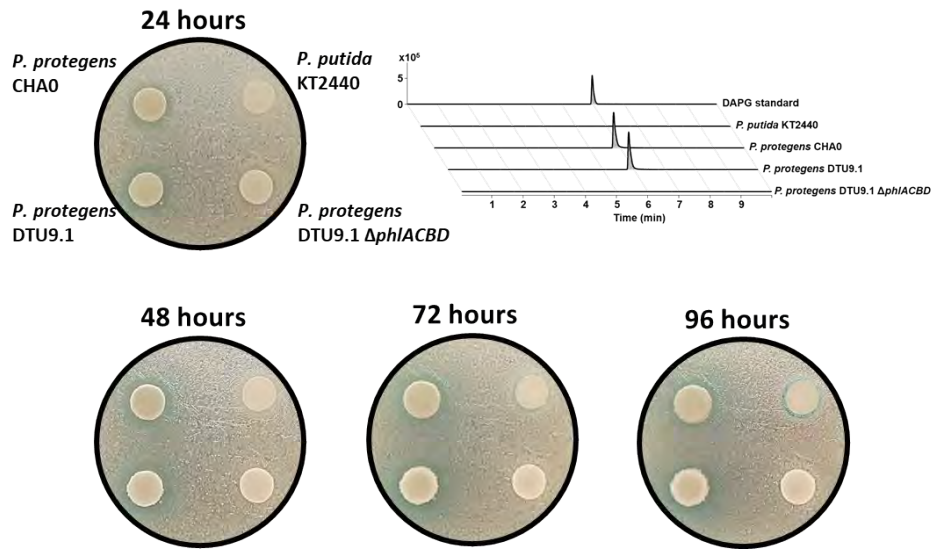
The whole-cell biosensor was grown in LB media supplemented with either PG, MAPG or DAPG at varying concentrations. Optical density at  $OD_{600}$  and luminescence was measured continuously over 5 hours. The light pink field indicates the area of data used to calculate an average value of luminescence normalized to  $OD_{600}$  ( $t = 172-207$  min). This corresponds to late exponential growth phase.

**S2** Graphs showing  $\beta$ -galactosidase activity measured as OD<sub>420</sub> for the whole-cell biosensor harbouring pSEVA225-DAPG<sub>lacZ</sub> grown in media supplemented with DAPG, MAPG and PG.



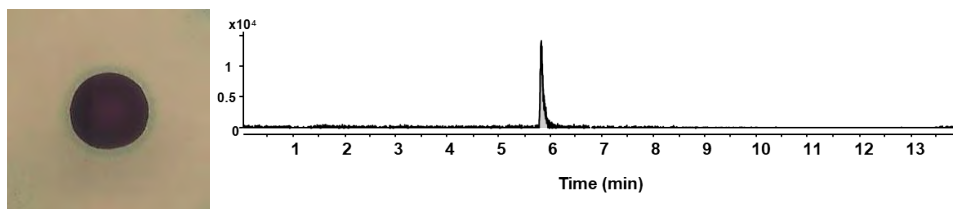
The whole-cell biosensor was grown in LB media supplemented with either PG, MAPG or DAPG at varying concentrations followed by measurement of  $\beta$ -galactosidase activity. Optical density at OD<sub>420</sub> was measured continuously over 16 hours. The light pink field indicates the phase of linear increase enzymatic activity, as shown on the graphs on the right. Linear regressions were used to estimate the OD<sub>420</sub>/min and calculate the biosensor response to varying concentrations of substrate in terms of Miller Units.

### S3 Picture series of DAPG-producing bacteria and controls growing on KBmalt agar surfaces



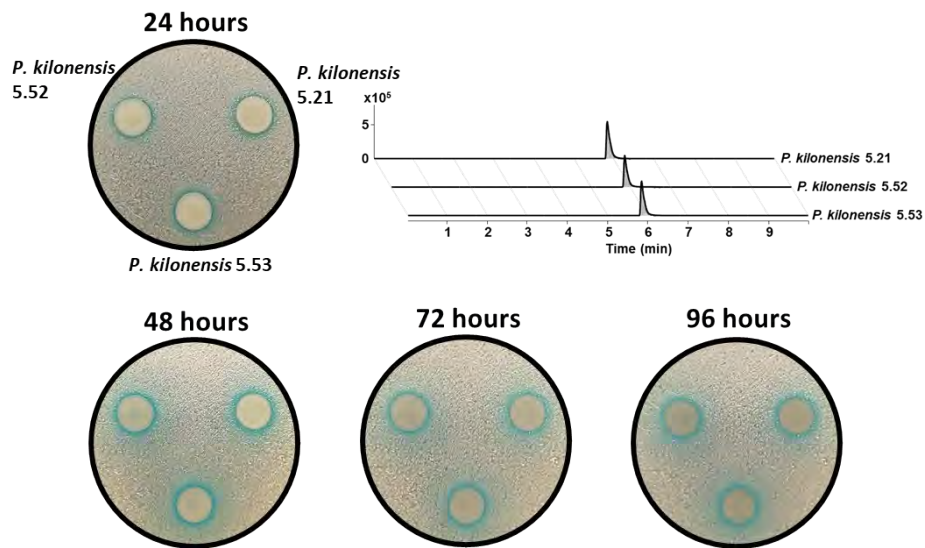
Four strains of *Pseudomonas* were grown on KBmalt agar supplemented with X-gal and a lawn of the whole-cell biosensor harbouring pSEVA225-DAPG<sub>lacZ</sub>. The two DAPG-producing strains, *P. protegens* CHA0 and DTU9.1 exhibited a response after 24-48 hours seen as a blue halo surrounding the colony. Two controls were included, *P. putida* KT2440 and a  $\Delta$ phlACBD mutant of *P. protegens* DTU9.1 incapable of synthesizing DAPG. No DAPG was detected from these controls by LCMS, but a slight blue colouring around *P. putida* was observed >72 hours.

### S4 Production of DAPG in *Chromobacterium vaccinii* MWU328.



DAPG production was confirmed for *C. vaccinii* MWU328 by growth on KBmalt agar supplemented with X-gal and a lawn of the whole-cell biosensor harbouring pSEVA225-DAPG<sub>lacZ</sub>. Moreover, DAPG was detected by LCMS.

**S5** Picture series of DAPG-producing soil isolates from P5, along with corresponding LCMS profiles.



The three isolates from P5, which were identified as *P. kilonensis*, were grown on KBmalt agar supplemented with X-gal and a lawn of the whole-cell biosensor harbouring pSEVA225-DAPG<sub>lacZ</sub>. A clear blue halo indicates the production of DAPG, which was further confirmed by LCMS.

# Paper 3

---

Communication is key: Sequential interspecies interactions affect production of antimicrobial secondary metabolites in *Pseudomonas protegens* DTU9.1

Hansen M.L., Wibowo M., Jarmusch S.A., Larsen T.O., and Jelsbak L.

*Submitted*

1 **Communication is key: Sequential interspecies interactions affect production**  
2 **of antimicrobial secondary metabolites in *Pseudomonas protegens* DTU9.1**

3 Morten Lindqvist Hansen, Mario Wibowo, Scott A. Jarmusch, Thomas Ostenfeld Larsen, and Lars  
4 Jelsbak<sup>#</sup>.

5

6 Department of Biotechnology and Biomedicine, Technical University of Denmark, Søtofts Plads bldg.  
7 221, DK-2800 Kgs Lyngby, Denmark

8

9 <sup>#</sup>corresponding author:

10 Lars Jelsbak (lj@bio.dtu.dk)

11

12 **ORCID**

13 MLH: 0000-0003-3927-2751

14 MW: 0000-0002-5739-0949

15 SAJ: 0000-0002-1021-1608

16 LJ: 0000-0002-5759-9769

17

18

19

20 **Running title:** Sequential interspecies interactions control secondary metabolism in *P. protegens*

21

22 **Keywords:** DAPG, pyoluteorin, cocultivation, interspecies interactions, Signaling, Mixed-species  
23 biofilm, biocontrol

## 24 **Abstract**

25 Soil- and rhizosphere microbiomes play important roles in suppression of plant pathogens through  
26 production of antagonistic secondary metabolites, yet mechanisms that determine the strength of  
27 pathogen control are not well understood. Many *Pseudomonas* species are associated with soil- and  
28 rhizosphere microbiomes, and their ability to suppress pathogens is well documented. Here, we  
29 investigate how interactions within the *Pseudomonas* genus affect their production of antimicrobial  
30 metabolites. From a biosensor-based screen, we identify *P. capeferrum* species as capable of  
31 modulating secondary metabolite production in *P. protegens*. We show that *P. capeferrum* alters  
32 production of pyoluteorin and 2,4-Diacetylphloroglucinol (DAPG) in *P. protegens* via two distinct and  
33 sequential mechanisms that depends on spatial proximity of the two species. Specifically, *P.*  
34 *capeferrum* secretes a diffusible signal that induce pyoluteorin production up to 100-fold in  
35 neighboring *P. protegens* colonies. In contrast, the interaction results in reduced DAPG production,  
36 but only within mixed-species colonies. Importantly, we found that increased pyoluteorin production  
37 and cell lysis of *P. capeferrum* is required for inhibition of DAPG production, suggesting that  
38 pyoluteorin-facilitated antibiosis of *P. protegens* on *P. capeferrum* leads to release of cell-associated  
39 metabolites and subsequent inhibition of DAPG production in *P. protegens*. As the interaction  
40 modulates *in vitro* bioactivity of the species, genus-specific interactions may assist in improving  
41 efficacy of biocontrol strains and consortia.

## 42 **Importance**

43 Microbial inoculants utilized as biocontrol agents to combat and control plant pathogenic  
44 microorganisms, such as *P. protegens*, have gained increasing attention as sustainable alternatives to  
45 chemical pesticides over the past decades. However, the *in situ* efficacy of these biocontrol inoculants  
46 is often severely reduced or absent compared to the observed *in vitro* efficacy. The effect of biocontrol  
47 agents is usually linked to their ability to produce antimicrobial secondary metabolites with activity  
48 against specific pathogenic microorganisms. Investigating the effects of microbial interactions from  
49 natural soil *Pseudomonas* on the production of antimicrobial secondary metabolites by the biocontrol  
50 inoculant will further our understanding of the natural biosynthesis of these metabolites and aid in  
51 bridging the anticipated and actual efficacy of biocontrol agents.

52

## 53 **Acknowledgements**

54 We thank professor Victor de Lorenzo for providing the SEVA plasmids used in this study. Additionally,  
55 we thank Mikael Lenz Strube for aiding with statistical data analysis, as well as Mikkel Anbo and  
56 members of the Centre for Microbial Secondary Metabolites (CeMiSt) for general scientific  
57 discussions.

58

## 59 **Funding**

60 This study was carried out as part of the Center of Excellence for Microbial Secondary Metabolites  
61 funded by The Danish National Research Foundation (DNRF137).

## 62 Introduction

63 Soil- and rhizosphere-associated microbiomes play critical roles in plant development and health, for  
64 example by production of antimicrobial metabolites that suppress plant diseases by antagonizing  
65 growth of phytopathogens (1–3). Understanding the processes that either potentiate or reduce this  
66 antagonism is essential for predicting the role and function of bacterial communities in controlling  
67 plant–pathogen interactions, and for enabling biological control applications in agriculture. Several  
68 studies have shown that antagonistic activity towards plant pathogens is related to bacterial diversity  
69 in ways that are not well understood (4–8). For example, using defined consortia of *Pseudomonas*  
70 species it has been shown that increasing genotypic richness (*i.e.* increasing number of genotypically  
71 similar consortia members) correlate with increased disease suppressiveness and antagonistic activity  
72 towards phytopathogens (5, 7). In contrast, another study has demonstrated that an increasing  
73 richness of distantly related *Pseudomonas* spp. is correlated with reduced pathogen inhibition (8).  
74 These and other examples suggest that genus-specific interactions among *Pseudomonas* species can  
75 affect the strengths of their antagonistic activities and highlights the importance in understanding the  
76 underlying microbial interaction processes.

77 *Pseudomonas* spp. are a group of soil bacteria that play key roles in plant growth promotion and  
78 control of crop pathogens due to production of various antimicrobial metabolites (2, 4). Among the  
79 fluorescent pseudomonads, *Pseudomonas protegens* has been studied intensively due to its potential  
80 as biocontrol agent and its array of antimicrobial secondary metabolites, including 2,4-  
81 diacetylphloroglucinol (DAPG), pyoluteorin, pyrrolnitrin, orfamide A and pyoverdine (9, 10). This  
82 bacterium has been shown to exhibit antimicrobial activity against pathogenic bacteria, fungi and  
83 oomycetes (11–13). At the mechanistic level, the biosynthesis and regulation of these metabolites has  
84 been well characterized in *P. protegens*, including that of DAPG and pyoluteorin. For the biosynthesis  
85 of DAPG, three molecules of malonyl-CoA are initially converted to phloroglucinol (PG) by the  
86 polyketide synthase, PhID. PG is subsequently acetylated by the PhIACB enzyme complex once to

87 mono-acetylphloroglucinol (MAPG) and twice to DAPG (14, 15). The biosynthetic operon, *phlACBDE*,  
88 is under transcriptional control by the PhIF repressor. Additionally, Bottiglieri et al. found that a gene  
89 located upstream, *phlG*, encodes the PhIG enzyme, which degrades intracellular DAPG to MAPG (16).  
90 The transcription of *phlG* is under control of the PhIH repressor (17). The biosynthesis of pyoluteorin  
91 starts with L-proline, which is converted to a dichloro-pyrrole by a three-step enzymatic process by  
92 PltF, PltE and PltA. Pyoluteorin is formed by the addition of a resorcinol ring to the dichloro-pyrrole  
93 moiety catalyzed by the enzyme complex, PltBCG (18, 19). Transcription of the biosynthetic operon,  
94 *pltLABCDEFG*, is activated by PltR. Recently, Yan et al. reported that the biosynthesis of DAPG and  
95 pyoluteorin is connected in *P. protegens* Pf-5, where the halogenase, PltM, converts the precursor,  
96 PG, from the DAPG pathway to PG-Cl and PG-Cl<sub>2</sub> (10). These molecules bind to the PltR activator, which  
97 in turn activates transcription of the pyoluteorin biosynthetic gene cluster.

98 The regulation of DAPG and pyoluteorin biosynthesis has been studied extensively in strains of *P.*  
99 *protegens*. It was demonstrated that these antimicrobial metabolites function in intra- and  
100 intercellular signaling circuits, as both molecules induced their own biosynthesis (20–22). Auto-  
101 induction of DAPG was demonstrated *in situ* on wheat roots, as expression from the *PphIA* promoter  
102 was induced in two distinct *Pseudomonas* spp. by co-inoculation with a DAPG-producing strain (22).  
103 Similarly, Brodhagen et al. reported that pyoluteorin functioned in positive autoregulation in *P.*  
104 *protegens* Pf-5 by inducing transcription of its respective biosynthetic gene cluster during growth on  
105 cucumber seedlings (21). Recently, it was further reported that the intermediate PG in the  
106 biosynthesis of DAPG contributes to the regulation of production of both DAPG and pyoluteorin in a  
107 concentration-dependent manner (23, 24). Additionally, production of both metabolites requires  
108 activation from the global regulatory system, Gac/Rsm (25). Overall, previous work in the field has  
109 illuminated the complex regulatory intra- and intercellular mechanisms involved in fine-tuning the  
110 production of DAPG and pyoluteorin in strains of *P. protegens*. Additionally, Dubuis et al.  
111 demonstrated that interspecies interactions between distantly related *Pseudomonas* spp. stimulated  
112 antimicrobial activity of *P. protegens* CHA0 against *Bacillus subtilis* presumably via Gac/Rsm-induced

113 production of DAPG (26). However, the effects of microbial interactions and their underlying  
114 molecular mechanisms affecting the biosynthesis of DAPG and pyoluteorin has remained less  
115 characterized.

116 In this study we investigate the effects of interspecies interactions between the soil isolate, *P.*  
117 *capeferrum* F8, and a potential biocontrol agent, *P. protegens* DTU9.1, on the production of the two  
118 antimicrobial metabolites, DAPG and pyoluteorin. Our results show that cocultivation of the two  
119 bacteria in a biofilm on agar surfaces inhibits the production of DAPG, while significantly inducing the  
120 biosynthesis of pyoluteorin in *P. protegens*. We reveal that the two regulatory mechanisms occur from  
121 two independent signals – a cell-associated signal and an extracellular metabolite from *P. capeferrum*  
122 F8. Moreover, we demonstrate that the cocultivation of the two *Pseudomonas* species enhances the  
123 antimicrobial efficiency against two known bacterial phytopathogens. Lastly, we show that the  
124 antibiosis of *P. protegens* DTU9.1 on *P. capeferrum* F8 due to pyoluteorin production leads to cell lysis  
125 of F8 and release of an unknown metabolite inhibiting DAPG production. Our work sheds light on  
126 interspecies interactions between soil *Pseudomonas* that affect the biosynthesis of antimicrobial  
127 secondary metabolites. This further emphasizes the necessity of studying microbial interactions to  
128 broaden our current understanding of the natural role and biosynthesis of secondary metabolites,  
129 while bridging the anticipated *in vitro* and actual *in situ* efficacy of biocontrol agents.

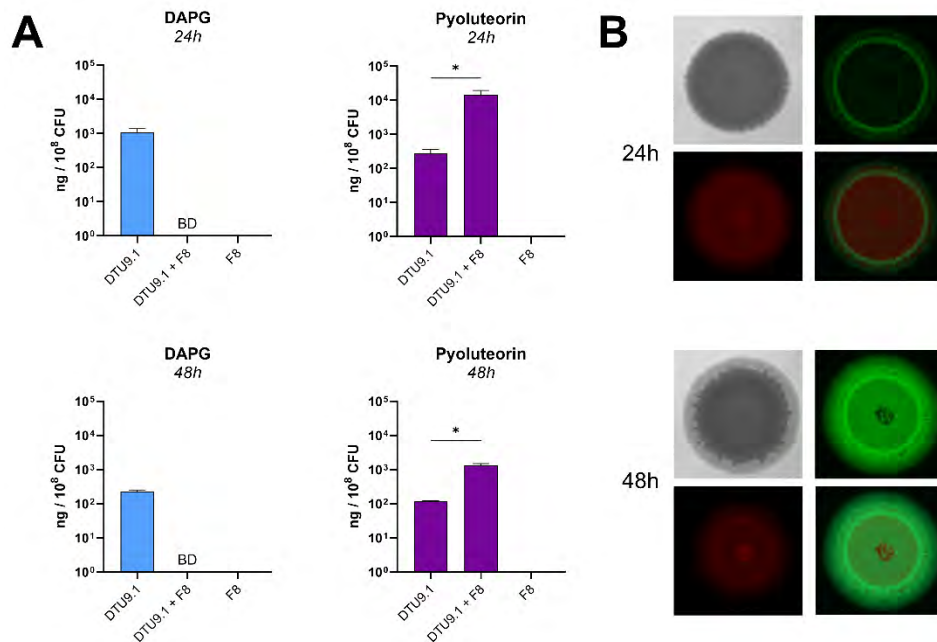
## 130 Results

### 131 *P. protegens* alters its secondary metabolism in coculture with a *P. capeferrum* soil isolate

132 In a previous screen for DAPG-producing *Pseudomonas* species from grassland soil samples, we  
133 identified a small fraction of isolates (9/864) unable to produce DAPG themselves, due to lack of the  
134 *phlACBDE* biosynthetic gene cluster (verified by PCR targeting *phlD* and chemical analysis). Yet the  
135 nine isolates were capable of eliciting a response in an engineered DAPG-responsive, PhIF-based  
136 whole-cell biosensor (27). We hypothesized that these isolates had the potential to modulate DAPG  
137 production in *Pseudomonas* species known to produce DAPG (such as *P. protegens*) and to affect  
138 secondary metabolite production through unknown cell-cell interactions. Indeed, preliminary  
139 cocultivation experiments between the nine isolates and a DAPG producer, *P. protegens* DTU9.1,  
140 suggested that two isolates could affect DAPG production. Based on their *rpoD* sequences, these two  
141 isolates are *P. capeferrum* spp. and we selected one of them, *P. capeferrum* F8, for further studies of  
142 its ability to modulate secondary metabolite production in *P. protegens* DTU9.1.

143 To investigate further if *P. capeferrum* F8 could interfere with the secondary metabolism in *P.*  
144 *protegens* DTU9.1, the isolate was cocultivated in a mixed-species colony on a KBmalt agar surface.  
145 Quantitative analysis of DAPG and pyoluteorin was carried out using liquid chromatography-high  
146 resolution mass spectrometry (LC-HRMS) on agar plugs covering the entire microbial colony. The  
147 concentrations of DAPG and pyoluteorin were normalized to colony forming units (CFU) of the  
148 producing bacterium (Figure 1A). As shown in Figure 1A, production of DAPG was inhibited below the  
149 limit of detection (LOD) in coculture with *P. capeferrum* F8. Contrarily, the soil isolate significantly  
150 induced a 10-100 fold increase in pyoluteorin production in *P. protegens* DTU9.1 after 24 hours ( $P =$   
151  $4.8 \cdot 10^{-2}$ ) and 48 hours ( $P = 7.8 \cdot 10^{-3}$ ). To examine the coculture dynamics, *P. capeferrum* F8 and *P.*  
152 *protegens* DTU9.1 were tagged with the Tn7 transposon from pBG42-*mKate* and pBG42-*gfp*,  
153 respectively. After 24 hours of growth, *P. capeferrum* F8 constituted most of the bacterial colony  
154 (Figure 1B). On the second day of incubation, the ratio of the two bacteria had shifted towards a

155 dominating presence of *P. protegens* DTU9.1. However, despite this shift in bacterial dominance in  
 156 the coculture, DAPG production remained below the LOD (Figure 1A).



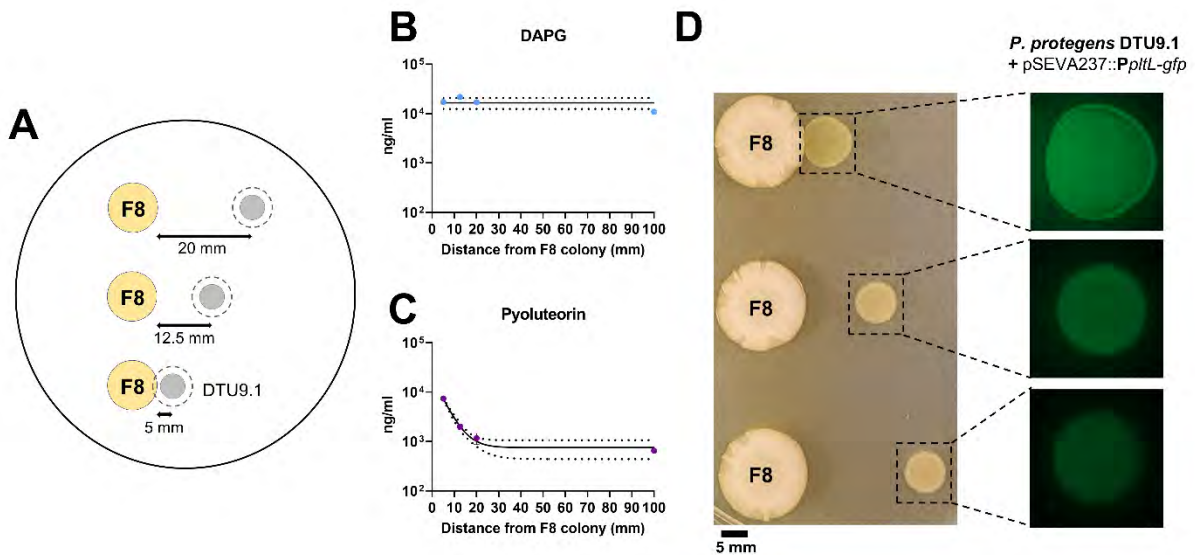
158 Figure 1 | *P. protegens* alters its secondary metabolism in coculture with *P. caepferrum* F8 on solid surface.  
 159 **A)** Concentration of DAPG and pyoluteorin after 24 and 48 hours of growth on KBmalt agar normalized to  
 160 10<sup>8</sup> CFU of *P. protegens* DTU9.1. BD = Below detection (\* equals  $P < 0.05$ ). **B)** Coculture dynamics of *P.*  
 161 *caepferrum* F8 (red – *mKate*) and *P. protegens* DTU9.1 (green – *gfp*) on KBmalt. Top left: Bright-field image.  
 162 Top right: *gfp* channel. Bottom left: *mKate* channel. Bottom right: Both channels. Fluorescence images  
 163 were obtained with 500 ms exposure time.

164

165 ***P. caepferrum* F8 affects metabolite production in *P. protegens* with two independent**  
 166 **signals**

167 Based on the coculture interaction results above, we attempted to attribute the altered secondary  
 168 metabolism in *P. protegens* DTU9.1 to secretion of a metabolite or signal from *P. caepferrum* using a  
 169 distance assay on KBmalt agar. First, *P. caepferrum* F8 was grown for 48 hours in bacterial colonies  
 170 (Figure 2A), followed by inoculating *P. protegens* DTU9.1 at a distance of 5, 12.5 and 20 mm from the  
 171 edge of the F8 colony. Agar plugs were extracted as indicated on Figure 2A after an additional 24 hours  
 172 of incubation. The concentrations of DAPG and pyoluteorin on Figure 2B and 2C show that DAPG  
 173 production is unaffected by diffusible signals from *P. caepferrum* F8, whereas pyoluteorin production

174 is induced in a distance-dependent manner. *P. protegens* DTU9.1 was grown under axenic conditions  
 175 as a control. To fit an overall non-linear regression model to the data, the control was assigned a 100  
 176 mm distance equivalent of the diameter of an entire petri dish. The fitted models are depicted as black  
 177 lines in Figure 2B and 2C with the 95% confidence intervals shown as dotted lines. The induction of  
 178 pyoluteorin as a function of distance is well described by a one phase decay function ( $R^2 = 0.9966$ )  
 179 having a decay rate of  $-0.2162$  ( $P = 8.1 \cdot 10^{-5}$ ). Closer inspection of the individual data points revealed  
 180 that pyoluteorin production in the two closest colonies (5 and 12.5 mm) was induced significantly  
 181 compared to the control as evidenced by ANOVA followed by Dunnett's test ( $P = 2.1 \cdot 10^{-5}$  and  $P = 3.2$   
 182  $\cdot 10^{-3}$ , respectively), whilst the 20 mm colony was not significantly induced.



184 Figure 2 | *P. capeferrum* F8 interferes with DAPG and pyoluteorin biosynthesis with two independent  
 185 molecular mechanisms. **A)** Schematic drawing of the distance assay setup. Dashed lines around *P.*  
 186 *protegens* DTU9.1 colonies indicate the size of the agar plug from which metabolites were extracted for  
 187 LCMS. **B)** and **C)** Concentration of DAPG and pyoluteorin from two independent experiments measured  
 188 with HR-LCMS. The control represents *P. protegens* DTU9.1 grown in isolation on KBmalt agar (set to  
 189 100mm distance to fit the model). Dotted lines represent the 95% confidence intervals of the  
 190 mathematical model. **D)** Distance assay with *P. protegens* DTU9.1 harboring pSEVA237::PpItL-gfp showing  
 191 that increased pyoluteorin production was due to induced transcription of the pyoluteorin biosynthetic  
 192 gene cluster in a distance-dependent manner. Fluorescence images were obtained with 500 ms exposure  
 193 time.

194

195 In Figure 2D, the secreted signal from *P. capeferrum* F8 induces the transcription of the pyoluteorin  
 196 biosynthetic gene cluster from the PpItL promoter, and this effect is decreased with increasing

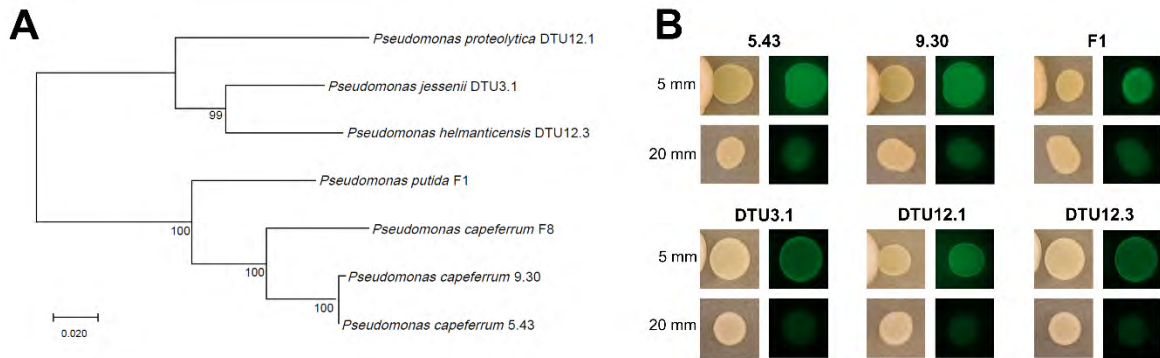
197 distance between the bacterial colonies. Additionally, exposing *P. protegens* DTU9.1 to the  
198 supernatant from a stationary phase culture of *P. capeferrum* F8 induced pyoluteorin production 10-  
199 fold ( $P = 2.9 \cdot 10^{-3}$ ). This indicates that *P. capeferrum* F8 secretes a signal during planktonic and biofilm  
200 growth, which induces transcription of the pyoluteorin biosynthetic gene cluster in *P. protegens*  
201 DTU9.1. In contrast, inhibition of DAPG production may require direct cell-to-cell contact between *P.*  
202 *protegens* DTU9.1 and *P. capeferrum* F8 as achieved within the mixed-species colonies (Figure 1).  
203 Overall, these findings suggests that DAPG inhibition and induction of pyoluteorin biosynthesis are  
204 affected by two independent molecular mechanisms.

205

### 206 **Distance-dependent induction of pyoluteorin biosynthesis is observed among distantly** 207 **related *Pseudomonas* species**

208 To explore the breadth of distance-dependent signaling from related species, we tested six additional  
209 isolates of *Pseudomonas* for their ability to induce pyoluteorin biosynthesis in *P. protegens* DTU9.1.  
210 We selected isolates from various *Pseudomonas* subgroups to view the larger context of the  
211 interaction within the *Pseudomonas* genera and test whether the distance related signal was specific  
212 to strains of *P. capeferrum*. Two species, *P. capeferrum* 5.43 and 9.30, were isolated from pristine soil  
213 environments at two different sampling sites in Dyrehaven independently from *P. capeferrum* F8. The  
214 three strains of *P. capeferrum*, as well as *P. putida* F1 represented isolates from the *P. putida* group.  
215 To investigate if the signaling extended beyond the *P. putida* group, the three soil isolates, *P. jessenii*  
216 DTU3.1, *P. proteolytica* DTU12.1, and *P. helmanticensis* DTU12.3 were included. They belong to three  
217 different subgroups in the *P. fluorescens* group: *P. jessenii*, *P. gessardii*, and *P. koreensis*, respectively.  
218 To compare the diversity of the tested strains, a phylogenetic tree was constructed based on  
219 sequencing of the *rpoD* gene. The bootstrap consensus tree (500 replicates) was generated with  
220 MEGA-X using the neighbor-joining method (Figure 3A). The four isolates belonging to the *P. putida*  
221 group (bottom branch in Figure 3A) expectedly cluster separately from the three remaining isolates.

222 However, as shown in Figure 3B, all tested isolates secreted a signal capable of inducing transcription  
 223 from the *PpItL* promoter in *P. protegens* DTU9.1 harboring pSEVA237::*PpItL* in a distance-dependent  
 224 manner. This indicates that the secreted signal is broadly distributed among distantly related species  
 225 of *Pseudomonas*.



227 Figure 3 | Distantly related species of the *Pseudomonas* induce pyoluteorin biosynthesis in *P. protegens*  
 228 DTU9.1. **A**) An *rpoD*-based neighbor-joining tree representing the phylogenetic relationship of the tested  
 229 isolates. The bootstrap consensus tree (500 replicates) was constructed with the neighbor-joining method.  
 230 The bootstrap percentage values are displayed next to each branching point. **B**) Distance assay with *P.*  
 231 *protegens* DTU9.1 harboring pSEVA237::*PpItL-gfp*. Fluorescence images were obtained with 500 ms  
 232 exposure time.

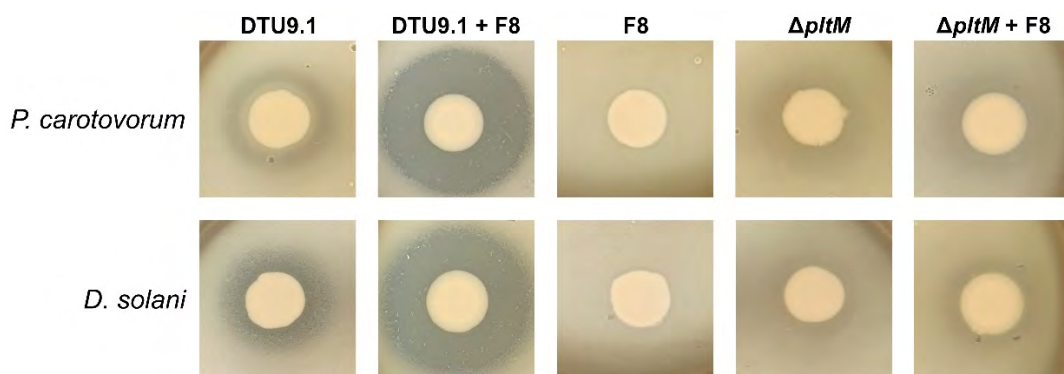
233

234

235 **The antimicrobial activity of *P. protegens* DTU9.1 against bacterial phytopathogens is**  
 236 **increased in coculture with *P. capeferrum* F8**

237 It has previously been shown that utilizing a diverse consortium of *Pseudomonas* species as biocontrol  
 238 inoculum can increase disease suppressiveness (7). The elevated pyoluteorin production in cocultures  
 239 between *P. protegens* DTU9.1 and *P. capeferrum* F8 suggest that such cocultures would exhibit  
 240 increased the suppression of growth of pyoluteorin-sensitive microorganisms compared to  
 241 monoculture. To test this, *Pseudomonas* species were cultivated in mono- and coculture colonies on  
 242 KBmalt agar for 48 hours to allow for metabolite production prior to chloroform-mediated cell  
 243 inactivation to avoid undesirable swarming. Subsequently, the plates were covered with a soft agar  
 244 layer inoculated with two known phytopathogenic bacteria, *Pectobacterium carotovorum* and *Dickeya*

245 *solani*. Inhibition was evaluated based on the size and turbidity of the clearing zone arising after an  
246 additional 24-48 hours of incubation. As shown in Figure 4, cocultivation leads to a substantial increase  
247 in antimicrobial effectiveness against both plant pathogens compared to both monocultures of  
248 *Pseudomonas*. To examine if the induced production of pyoluteorin was the cause of increased  
249 bioactivity, the *pltM* gene was knocked out in *P. protegens* DTU9.1 resulting in absence of pyoluteorin  
250 biosynthesis (10). As shown in Figure 4, bioactivity against both plant pathogens was lost in the  $\Delta pltM$   
251 mutant in mono- and coculture with *P. caepferrum* F8.



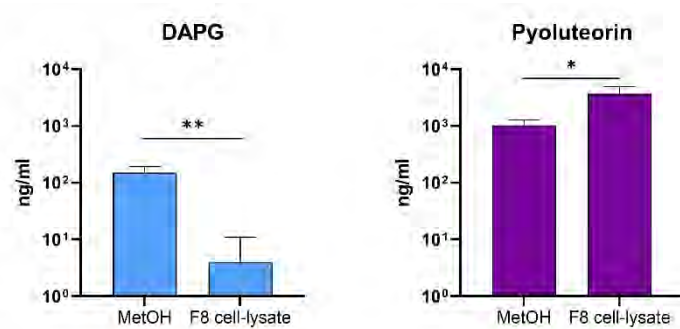
253 Figure 4 | The antimicrobial effectiveness of *P. protegens* DTU9.1 against bacterial phytopathogens increases  
254 in coculture with *P. caepferrum* F8. The antimicrobial activity of *P. protegens* DTU9.1 towards two bacterial  
255 phytopathogens, *P. carotovorum* and *D. solani*, was enhanced in coculture with *P. caepferrum* F8. The  
256  $\Delta pltM$  mutant of *P. protegens* DTU9.1 was unable to produce pyoluteorin. Pictures are representative of  
257 three biological replicates with similar results.

258

### 259 Cell-associated metabolite(s) of *P. caepferrum* F8 inhibits DAPG production in *P. protegens*

260 To elucidate the origin of the signal capable of inhibiting DAPG production in *P. protegens*, we  
261 examined the effect of cell-associated metabolites from *P. caepferrum* F8 on the secondary  
262 metabolism of *P. protegens*. A culture of *P. caepferrum* F8 was incubated in liquid KBmalt broth for 24  
263 hours followed by lysis of the cell pellet to release the cell-associated metabolites, followed by  
264 extraction using ethyl acetate to yield a crude extract. Finally, *P. protegens* DTU9.1 was cultivated in  
265 three independent biological replicates in KBmalt supplemented with methanol as control or crude  
266 lysate extract. The supernatants were collected after 24 hours and analyzed for the presence of DAPG

267 and pyoluteorin with LC-HRMS (Figure 5). The crude cell-lysate extract significantly inhibited DAPG  
 268 production 38-fold ( $P = 3.3 \cdot 10^{-3}$ ), where the DAPG concentration in two out of the three replicates  
 269 was below the LOD. The production of pyoluteorin was induced 4-fold ( $P = 2.2 \cdot 10^{-2}$ ). This suggests  
 270 that cell lysis of *P. capeferrum* F8 leads to release of cell-associated metabolites inhibiting the  
 271 production of DAPG. The minor induction of pyoluteorin biosynthesis is most likely due to small  
 272 amounts of extracellular signaling molecules associated with *P. capeferrum* F8 cells during washing  
 273 pre-lysis or that the inducing molecule is present intracellularly in low concentrations.



275 Figure 5 | Cell-associated metabolites of *P. capeferrum* F8 inhibits DAPG production in *P. protegens*.  
 276 Concentration of DAPG and pyoluteorin from three independent biological replicates of *P. protegens*  
 277 DTU9.1 cultured in KBmalt supplemented with methanol as control or crude cell-lysate extract.  
 278 Significance levels were calculated with the Student's *t*-test (\*\* equals  $P < 0.005$ , \* equals  $P < 0.05$ ).

279

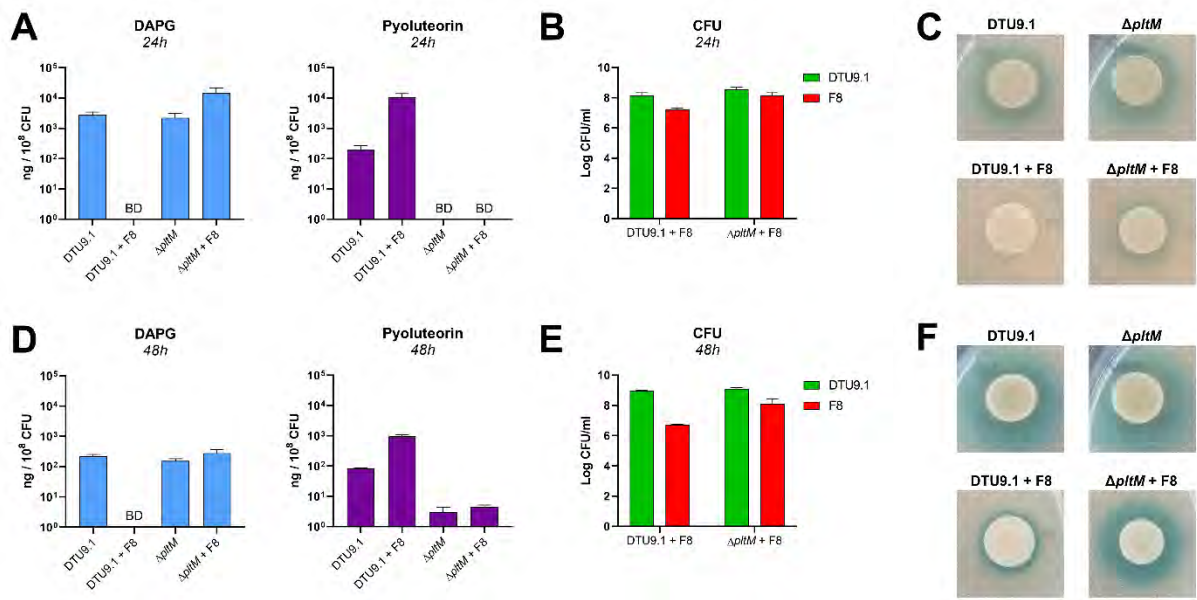
## 280 The antibiosis of *P. protegens* on *P. capeferrum* F8 leads to inhibition of DAPG production

281 Based on these results, we hypothesized that antibiosis of *P. protegens* DTU9.1 on *P. capeferrum* F8  
 282 in mixed-species cocultures could facilitate the release of cell-associated metabolites from *P.*  
 283 *capeferrum* leading to inhibition of DAPG production. We further hypothesized that the antimicrobial  
 284 metabolite, pyoluteorin, was responsible for the antibiosis. To test this hypothesis, we cultivated *P.*  
 285 *protegens* DTU9.1 WT and the  $\Delta pltM$  mutant in mono- and coculture colonies with *P. capeferrum* F8  
 286 on a KBmalt agar surface. The  $\Delta pltM$  deletion mutant of *P. protegens* DTU9.1 was incapable of  
 287 converting phloroglucinol (PG) to PG-Cl and PG-Cl<sub>2</sub> (10), which in turn rendered the bacterium unable  
 288 to initiate transcription of the pyoluteorin biosynthetic gene cluster. Cocultivation of *P. capeferrum* F8

289 and the  $\Delta pltM$  deletion mutant of *P. protegens* DTU9.1 restored production of DAPG to levels  
290 comparable to monocultures of *P. protegens* DTU9.1 WT and  $\Delta pltM$  mutant (Figure 6A and 6D),  
291 demonstrating that pyoluteorin production is required for the observed suppression of DAPG  
292 production. Interestingly, induction of pyoluteorin production in *P. protegens* DTU9.1 caused by  
293 cocultivation with *P. capeferrum* F8 was absent in the coculture with  $\Delta pltM$ . PltM converts PG to PG-  
294 Cl and PG-Cl<sub>2</sub>, which in turn binds to the PltR activator, thus activating transcription of the pyoluteorin  
295 biosynthetic gene cluster (10). The absence of pyoluteorin production in the coculture of the  $\Delta pltM$   
296 mutant and *P. capeferrum* F8 suggests that induced production of pyoluteorin by the signaling  
297 molecule from *P. capeferrum* F8 requires transcriptional initiation caused by halogenation of PG to  
298 PG-Cl and PG-Cl<sub>2</sub> (by PltM) (Figure 6A and 6D).

299 Cell counts of the bacteria residing in the mixed colonies further revealed that the absence of  
300 pyoluteorin in the  $\Delta pltM$  mutant improved the ability of the two *Pseudomonas* to co-exist (Figure 6B  
301 and 6E). The abundance of *P. capeferrum* F8 after 24 hours was increased 10-fold in coculture with  
302 the  $\Delta pltM$  mutant compared to wildtype *P. protegens* DTU9.1. This difference was further enlarged to  
303 30-fold after 48 hours, which suggests a much reduced antibiosis of *P. protegens* DTU9.1 on *P.*  
304 *capeferrum* F8 in the absence of pyoluteorin (Figure 6B and 6E). Importantly, this finding indicates that  
305 the cell-associated, DAPG-inhibiting signal from *P. capeferrum* F8 is located intracellularly requiring  
306 cell lysis for its release. Additionally, the absence of pyoluteorin production in the  $\Delta pltM$  mutant did  
307 not affect the ability of *P. protegens* DTU9.1 to dominate the mixed species coculture. Lastly,  
308 restoration of DAPG production in the cocultivation of *P. capeferrum* F8 and the  $\Delta pltM$  deletion  
309 mutant of *P. protegens* DTU9.1 was visualized utilizing the whole-cell DAPG biosensor harboring  
310 pSEVA225::DAPG<sub>lacZ</sub> (Figure 6C and 6F). Monocultures of *P. protegens* DTU9.1 WT and  $\Delta pltM$  mutant  
311 yielded a strong response as evidenced by a clear blue halo surrounding the colony of *Pseudomonas*.  
312 Cocultivation of *P. capeferrum* F8 and the  $\Delta pltM$  deletion mutant generated a similar response after  
313 48 hours of incubation but only a slight induction was observed after 24 hours. This suggests that the  
314 biosensor response had an unexpected delay, since the LC-HRMS data showed restoration of DAPG

315 production after 24 hours (Figure 6A). Taken together, these findings suggest that pyoluteorin  
 316 facilitates lysis of *P. caepiferrum* F8 leading to the release of one or more metabolites capable of  
 317 inhibiting DAPG production in *P. protegens* DTU9.1.



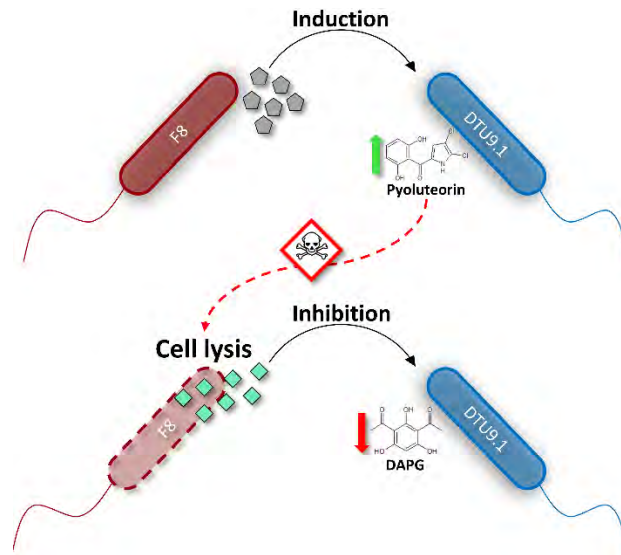
319 Figure 6 | Deletion of *pltM* restores DAPG production in coculture between *P. protegens* DTU9.1 and *P.*  
 320 *caepiferrum* F8. **A,D**) Concentration of DAPG and pyoluteorin normalized to CFU of *P. protegens* DTU9.1 and  
 321  $\Delta$ *pltM* mutant in mono- and coculture with *P. caepiferrum* F8 after 24 hours (**A**) and 48 hours (**D**). BD =  
 322 Below detection limit. **B,E**) Abundance of *P. protegens* DTU9.1 or  $\Delta$ *pltM* mutant and *P. caepiferrum* F8 in  
 323 mixed colonies on KBmalt agar after 24 hours (**B**) and 48 hours (**E**). Values represent means of two  
 324 independent experiments. **C,F**) *P. protegens* DTU9.1 and  $\Delta$ *pltM* mutant in mono- and coculture with *P.*  
 325 *caepiferrum* F8 in bacterial colonies on top of a lawn of the biosensor harboring pSEVA225::DAPG<sub>lacZ</sub> on  
 326 KBmalt + Xgal65 agar after 24 hours (**C**) and 48 hours (**F**).

## 327 Discussion

328 The biosynthesis of secondary metabolites has been extensively studied in strains of *P. protegens*,  
329 which has led to the characterization of complex intra- and intercellular regulatory mechanisms  
330 governing the fine-tuned production of specific metabolites (20–22, 24). However, bacteria most often  
331 reside in microbial communities in which communication mediated through chemical signaling adds  
332 another layer of regulatory complexity. Additionally, previous studies have demonstrated conflicting  
333 results correlating *Pseudomonas* spp. richness and the effects on ecologically relevant mechanisms  
334 mediated by secondary metabolites (e.g. antimicrobial activity and plant protection) (5–8). This  
335 supports the potential for uncharacterized, genus-specific interactions affecting secondary  
336 metabolism in *Pseudomonas* spp.. Here we report on the effects of interspecies interactions between  
337 two fluorescent *Pseudomonas* on the production of DAPG and pyoluteorin in *P. protegens* DTU9.1.  
338 Our work sheds light on interspecies interactions between soil *Pseudomonas* that affect the  
339 biosynthesis of antimicrobial secondary metabolites. This further emphasizes the necessity of studying  
340 microbial interactions to broaden our current understanding of the natural role and biosynthesis of  
341 secondary metabolites, while bridging the anticipated *in vitro* and actual *in situ* efficacy of biocontrol  
342 agents.

343 In this study, the cocultivation of *P. capeferrum* F8 and a potential biocontrol agent, *P. protegens*  
344 DTU9.1, led to induced expression of the pyoluteorin biosynthetic gene cluster, while production of  
345 DAPG was inhibited (below LOD). We propose the sequential signaling model (Figure 7) in which *P.*  
346 *protegens* initially responds to an extracellular, diffusible signal from *P. capeferrum* by inducing the  
347 biosynthesis of the antibacterial metabolite, pyoluteorin. The increased local concentration of  
348 pyoluteorin exceeds tolerable levels for *P. capeferrum*, leading to cell disruption. As a result of lysis  
349 within the *P. capeferrum* population, an intracellular signal (from *P. capeferrum*) is released, which  
350 subsequently inhibits production of DAPG in *P. protegens* DTU9.1. We speculate that the inhibition of  
351 DAPG production could be related to a yet uncharacterized ecological function, as the absence of

352 DAPG has no apparent benefit to either organism in this dual species interaction. Previously, it was  
353 reported that *P. aeruginosa* releases an intracellular signal upon cell lysis, which in turn induces the  
354 biosynthesis of antibacterial metabolites in neighboring kin cells (28). In the present study, however,  
355 we describe a dynamic, sequential interaction between two unrelated species of *Pseudomonas*  
356 affecting the biosynthesis of multiple secondary metabolites.



358 Figure 7 | Schematic overview of the altered secondary metabolism in *P. protegens* DTU9.1 in response to  
359 cocultivation with *P. caepiferrum* F8. *P. caepiferrum* F8 secretes a metabolite (grey pentagons), which  
360 induces biosynthesis of pyoluteorin in *P. protegens* DTU9.1. The increased concentration of pyoluteorin is  
361 toxic towards *P. caepiferrum* F8 leading to cell lysis and release of an intracellular metabolite (cyan  
362 diamonds), which in turn inhibits production of DAPG in *P. protegens*.

363

364 Bacterial communication mediated via chemical signaling is a concept that has been extensively  
365 studied. An explanation for the distance-dependent induction of pyoluteorin observed in this study  
366 could be related to an interaction arising from bacterial competition sensing (29–31). Such  
367 interactions often involve secretion of toxic metabolites proposed to have hormetic properties (*e.g.*  
368 stimulatory at subinhibitory concentrations and antagonistic at intolerable concentrations) (32). At  
369 subinhibitory concentrations the toxic metabolites may act as cues of nearby microbial danger,  
370 inducing responses in the sensing bacterium, such as modifications to its own secondary metabolome  
371 (31–34). As demonstrated recently, competitive interactions are commonly observed in interspecies  
372 interactions among closely related species, likely owing to similar nutrient preferences (35). Dubuis et

373 al. showed a Gac/Rsm-mediated induction of antimicrobial activity in *P. protegens* CHA0 resulting from  
374 interspecies interactions (26). In this study we have shown that *P. protegens* DTU9.1 induces  
375 biosynthesis of pyoluteorin in response to a secreted signal from *P. capeferrum* F8 (Figure 2), as well  
376 as related species of the *P. putida* group and distantly related *Pseudomonas* species (Figure 3). This  
377 could suggest that *P. protegens* DTU9.1 responds to a more general bacterial cue, indicating the  
378 presence of a competing species. For instance, Korgaonkar et al. demonstrated that *P. aeruginosa*  
379 induces production of phenazine in response to *N*-acetylglucosamine (GlcNAc) and peptidoglycan,  
380 which are common elements shed from bacterial cell walls into the surroundings during cell growth  
381 (36). However, preliminary results of exposing *P. protegens* DTU9.1 to purified GlcNAc did not show  
382 an induction of pyoluteorin biosynthesis. Thus, further investigations are necessary to identify the  
383 secreted metabolite from *P. capeferrum* F8 capable of inducing pyoluteorin production in *P.*  
384 *protegens*.

385 The biosynthesis of DAPG in *Pseudomonas* is under tight intra- and intercellular regulation and studies  
386 have shown that metabolites from interacting microbes can affect its production (20, 37). Schnider-  
387 Keel et al. showed that salicylate, a molecule with structural similarities to DAPG, could also inhibit  
388 biosynthesis of DAPG (20). Interestingly, Li et al. found that *P. putida* RW10S1 produced promysalin,  
389 which is a salicylate-containing antibiotic selectively targeting other *Pseudomonas* species (38). Since  
390 species of *P. putida* are closely related to *P. capeferrum* (39), we speculated if our soil isolate, *P.*  
391 *capeferrum* F8, possessed the genes required for salicylate and promysalin production. However, a  
392 tBLASTn analysis revealed the absence of this biosynthetic gene cluster. As displayed in Figure 5, the  
393 signal inhibiting DAPG production in *P. protegens* DTU9.1 could be either intracellular or membrane-  
394 associated in *P. capeferrum* F8. However, as shown in Figure 6B and 6E, the abundance of the signaling  
395 bacterium (*P. capeferrum* F8) was stably maintained at approximately  $10^8$  CFU/ml in the coculture  
396 with the  $\Delta$ *pltM* mutant compared to coculture with WT *P. protegens* DTU9.1, where the abundance  
397 of F8 declined 10-30 fold over the course of 48 hours. Nevertheless, biosynthesis of DAPG was restored  
398 to monoculture levels when the  $\Delta$ *pltM* mutant was cultured with *P. capeferrum* F8, thus indicating

399 that cell lysis of *P. capeferrum* F8 caused by the elevated pyoluteorin concentration in coculture with  
400 WT *P. protegens* DTU9.1 is necessary for the release of an intracellular signal and inhibition of DAPG  
401 production. Therefore, further analyses are needed to identify the intracellular chemical signal from  
402 *P. capeferrum* F8 capable of inhibiting DAPG production. Overall, our work and previous studies  
403 underline the importance of investigating microbial interactions to further elucidate the role of  
404 secondary metabolites in natural communities.

405 In the recent decades, employing specific species of isolated bacteria as microbial biocontrol agents  
406 has gained increased attention for the suppression of phytopathogenic fungi and bacteria as a  
407 sustainable alternative to potentially harmful pesticides. The effectiveness of such biocontrol  
408 inoculants relies in part on antimicrobial activity against plant pathogens, which can typically be  
409 attributed to the production of antimicrobial secondary metabolites. However, despite the  
410 improvements in *in vitro* screening for novel candidate biocontrol microbes, less than 1% end up as  
411 commercial products (40). The lack of efficacy *in situ* may in part be due to yet uncharacterized  
412 interactions between members of the natural soil microbiome and the introduced biocontrol agent.  
413 The bacterium, *P. protegens*, has been studied for decades for its biocontrol properties (2), and we  
414 show here that chemical interactions with another *Pseudomonas* species commonly found in soil and  
415 rhizosphere microbiomes (41) can radically alter its production of antimicrobial secondary metabolites  
416 (Figure 1) and its activity towards bacterial phytopathogens (Figure 4). We speculate that such  
417 phenotype-altering chemical interactions play an important role in determining the efficiency of  
418 biocontrol. Indeed, there are several recent demonstrations of improved plant growth promoting  
419 properties, as well as the overall bioactivity against plant-pathogenic microorganisms, by use of mixed  
420 species inoculants. For example, Niu et al. demonstrated that a synthetic microbial community  
421 consisting of seven species greatly reduced the severity of blight disease on maize seedling caused by  
422 the phytopathogen, *Fusarium verticillioides* (42). Additionally, Zhuang et al. reported that a synthetic  
423 consortium consisting of six *Pseudomonas* spp. significantly affected plant growth promotion of radish  
424 seedlings (43). Our results support that co-inoculation of two *Pseudomonas* strains; *P. protegens*

425 DTU9.1 and *P. capeferrum* F8, augments the *in vitro* bioactivity against two known phytopathogens,  
426 *P. carotovorum* and *D. solani* (Figure 4). Even though we also demonstrate a secondary microbial  
427 interaction leading to the inhibition of DAPG production, we suggest that natural conditions such as  
428 soils and plant roots might facilitate a flux in community members resulting in a distance-dependent  
429 induction of pyoluteorin of those in closer proximity and production of DAPG from those further apart.  
430 This study therefore represents a defined mode of action for bacterial consortia applied as biocontrol  
431 inoculum in a natural setting and provides a stepping-stone into the much-needed mode of action  
432 studies in closer-to-field studies. An improved understanding of the underlying signalling events  
433 affecting microbial secondary metabolism may enable designs of signal-optimized microbial  
434 biocontrol consortia that potentiates production of relevant secondary metabolites to show improved  
435 efficiency in plant protection compared to single-species biocontrol.

## 436 **Methods**

### 437 **Microorganisms and cultivation**

438 Bacteria were routinely cultured in Luria-Bertani broth (LB, Merck) with appropriate antibiotics. *E. coli*  
439 was cultured by inoculating a single colony in 5 ml LB broth and incubating overnight at 37° C with  
440 shaking (200 rpm). *Pseudomonas* were cultured by inoculating a single colony in 5 ml LB broth and  
441 incubating overnight at 30° C with shaking (200 rpm). Plasmid cloning was performed in *Escherichia*  
442 *coli* CC118- $\lambda$ pir. Microorganisms used in this study are summarized in the Supplementary Table 1.  
443 Primers used for cloning and verification are found in the Supplementary Table 2.

### 444 **Tagging *Pseudomonas* with fluorescent transposons for visualization of coculture dynamics**

445 To visualize the development of bacterial cocultivation on solid agar surfaces, *P. protegens* DTU9.1  
446 and *P. capeferrum* F8 were chromosomally tagged with Tn7 transposons carrying a constitutively  
447 expressed *gfp* or *mKate* gene, respectively. The plasmid, pBG42-*gfp*, was a kind gift from Victor de  
448 Lorenzo (44). The *mKate*-version was cloned by replacing *gfp* with a PCR-amplified *mKate* gene from  
449 phymKate (45) with BciI/HindIII overhangs. The cloned plasmid, pBG42-*mKate*, was verified by Sanger  
450 sequencing at Eurofins Genomics.

451 The plasmids were mobilized into *Pseudomonas* by quad-parental mating and the Tn7 transposon was  
452 subsequently integrated chromosomally downstream of *glmS* in a transposase-dependent manner.  
453 For the quad-parental mating the optical density at OD<sub>600</sub> was normalized to 1.0 for *E. coli* HB101  
454 harboring pRK600, *E. coli* CC118  $\lambda$ pir harboring pTNS2, *E. coli* CC118  $\lambda$ pir harboring pBG42-*gfp*/*mKate*  
455 and the recipient *Pseudomonas*. Then, the bacterial suspensions were mixed in a 1:1:1:1 ratio,  
456 concentrated 50 times and finally spotted on an LB agar plate incubated at 30°C O/N. Transconjugants  
457 were selected on *Pseudomonas* Isolation Agar (PIA, Merck) supplemented with 50  $\mu$ g ml<sup>-1</sup> gentamycin  
458 and confirmed to be expressing *gfp* or *mKate* constitutively by examination under a fluorescence  
459 microscope.

460 **Cocultivation of *P. protegens* DTU9.1 and *P. capeferrum* F8 on solid surface**

461 For bacterial cocultivations, 1 ml samples of *Pseudomonas* O/N cultures were washed twice in 0.9%  
462 NaCl by centrifuging at 10,000 rpm for 1 minute, followed by discarding the supernatant and  
463 resuspending the pellet in fresh liquid. Subsequently, the optical density at OD<sub>600</sub> was normalized to  
464 1.0. For cocultivations on agar surfaces, the bacterial suspensions of *P. protegens* DTU9.1 and *P.*  
465 *capeferrum* F8 were mixed in a 1:1 ratio, followed by spotting on KBmalt agar (20 g l<sup>-1</sup> Proteose  
466 peptone No. 3, 1.5 g l<sup>-1</sup> K<sub>2</sub>HPO<sub>4</sub>, 1.5 g l<sup>-1</sup> MgSO<sub>4</sub>, 7.5 g l<sup>-1</sup> malt extract, 10 ml l<sup>-1</sup> glycerol and 20 g l<sup>-1</sup>  
467 Bacto agar).

468 **Distance assay**

469 A distance assay was carried out to determine if *P. capeferrum* F8 produced a single molecule affecting  
470 both DAPG and pyoluteorin production in *P. protegens* DTU9.1. Initially, *P. capeferrum* F8 was  
471 normalized to OD<sub>600</sub> = 1.0 and spotted in 20 µl on KBmalt agar plates. The plates were incubated at  
472 30°C for 48 hours. Then, a culture of *P. protegens* DTU9.1 was normalized to OD<sub>600</sub> = 1.0 and spotted  
473 in 5 µl with varying distance to the edge of the *P. capeferrum* F8 colony (5, 12.5 and 20 mm). As a  
474 control, *P. protegens* DTU9.1 was spotted in isolation on a separate plate. The plates were incubated  
475 at 30°C for 24 hours, followed by agar plug extraction for LC-MS. The decay of pyoluteorin production  
476 as a function of distance to the edge of the *P. capeferrum* F8 colony was modelled with a one phase  
477 decay function in GraphPad Prism v8.3.0, where Y<sub>0</sub> represents the intercept and K represents the  
478 decay rate.

479 
$$Y = (Y_0 - Plateau) \cdot e^{-K \cdot X} + Plateau$$

480 Induction of pyoluteorin production in a distance-dependent manner was further analyzed for related  
481 species of the *P. putida* group. The phylogenetic relationship between the six tested isolates and the  
482 17 type strains of the *P. putida* group (39) was determined by analyzing a phylogenetic tree. Part of  
483 the *rpoD* genes amplified with primers, PsEG30F and PsEG790R (see Supplementary Table 2), were

484 Sanger sequenced and aligned using the MUSCLE algorithm, followed by construction of a bootstrap  
485 consensus tree (500 replicates) by the neighbor-joining method in MEGA X (46).

#### 486 **Construction of pSEVA237::Pp*ltL* reporter fusions**

487 To investigate the effect of the secreted signal from *P. capeferrum* F8 on the transcription of the  
488 pyoluteorin biosynthetic gene cluster, a P*p*ltL** reporter fusion was constructed in pSEVA237<sub>RBS30</sub> with  
489 a strong ribosomal binding site (RBS30). The promoter region was PCR-amplified with BamHI/HindIII  
490 overhangs and ligated with pSEVA237<sub>RBS30</sub>. The cloned reporter fusion was verified by Sanger  
491 sequencing at Eurofins Genomics.

492 The plasmid was subsequently mobilized into *P. protegens* DTU9.1 by tri-parental mating. Initially, the  
493 optical density at OD<sub>600</sub> was normalized to 1.0 for *E. coli* HB101 harboring pRK600, *E. coli* CC118  $\lambda$ *pir*  
494 harboring pSEVA237::P*p*ltL** and the recipient *Pseudomonas*. Then, the bacterial suspensions were  
495 mixed in a 1:1:1 ratio, concentrated 50 times and finally spotted on an LB agar plate incubated at 30°C  
496 O/N. A transconjugant was selected on PIA supplemented with 50  $\mu$ g ml<sup>-1</sup> kanamycin and confirmed  
497 to be expressing *gfp* by examination under a fluorescence microscope.

#### 498 **Cell-lysate assay**

499 To investigate the effect of cell-associated metabolites from *P. capeferrum* F8 on the metabolite  
500 production in *P. protegens* DTU9.1 a cell-lysate assay was performed. Firstly, the cell-lysate was  
501 prepared by lysis of cell pellet from 4 ml O/N culture of *P. capeferrum* F8 with NEB gDNA Tissue Lysis  
502 Buffer (New England Biolabs) and lysozyme from chicken egg-white (Sigma-Aldrich). Cell-associated  
503 metabolites were extracted with ethyl:acetate (EtOAc) extraction and resuspended in methanol  
504 (MetOH) to a concentration of 1 mg/ml. Then, *P. protegens* DTU9.1 was inoculated to an initial OD<sub>600</sub>  
505 = 0.001 in 10 ml KBmalt broth supplemented with 50  $\mu$ l MetOH (control) or 50  $\mu$ l cell-lysate extract.  
506 Tubes were incubated at 30° C with shaking (200 rpm) for 24 hours, followed by sterile filtration of the  
507 supernatant. Levels of DAPG and pyoluteorin were analyzed with HR-LCMS.

## 508 **Deletion of *pltM* in *P. protegens* DTU9.1**

509 To obtain a strain of *P. protegens* DTU9.1 incapable of synthesizing pyoluteorin, *pltM* was deleted by  
510 allelic replacement according to Hmelo et al. (47). In short, DNA fragments directly upstream and  
511 directly downstream of the gene of interest were PCR amplified. The fragments were joined by  
512 splicing-by-overlap extension PCR with XbaI/SacI overhangs. The purified PCR product was restriction-  
513 digested and inserted in pNJ1 (48). The resulting plasmid, pNJ1-*pltM*-del, was mobilized into *P.*  
514 *protegens* DTU9.1 via triparental mating with *E. coli* HB101 harboring the helper plasmid pRK600.  
515 Merodiploid transconjugants were initially selected on PIA supplemented with 50 µg ml<sup>-1</sup> tetracycline.  
516 A second selection was performed on NSLB agar (10 g l<sup>-1</sup> tryptone, 5 g l<sup>-1</sup> yeast extract, 15 g l<sup>-1</sup> Bacto  
517 agar) with 15% v/v sucrose. Candidates for successful deletion were confirmed by PCR and verified by  
518 Sanger sequencing at Eurofins Genomics.

## 519 **Detection of DAPG with a whole-cell biosensor**

520 For biosensor-guided detection of DAPG production, 1 ml O/N culture of *E. coli* CC118  $\lambda$ *pir* harboring  
521 pSEVA225::DAPG<sub>lacZ</sub> was washed twice in 0.9% NaCl and its optical density at OD<sub>600</sub> set to 0.5. Then,  
522 100 µl of the biosensor suspension was spread on KBmalt plates supplemented with 65 µg ml<sup>-1</sup> 5-  
523 bromo-4-chloro-3-indolyl-β-D-galactopyranoside (Xgal, Thermo Fisher Scientific). *Pseudomonas*  
524 mono- and cocultures normalized to OD<sub>600</sub> = 1.0 were spotted on top as 20 µl colonies. All agar plates  
525 were incubated at 30°C.

## 526 **Detection of secondary metabolites with HR-LCMS**

527 To extract secondary metabolites of mono- and cocultivated *Pseudomonas*, an agar plug covering the  
528 bacterial colony (6 mm diameter) was transferred to a vial and extracted with 1 ml of isopropanol:ethyl  
529 acetate (1:3, v/v), containing 1% formic acid, under ultrasonication for 60 min. Extracts were  
530 subsequently evaporated under N<sub>2</sub> and re-dissolved in 200 µl of methanol for further sonication for  
531 15 min. Lastly, the samples were centrifuged at 13400 rpm for 3 minutes and supernatants transferred

532 to HPLC vials and subjected to ultra high-performance liquid chromatography-high resolution  
533 electrospray ionization mass spectrometry (UHPLC-HRESIMS) analysis.

534 HR-LCMS was performed on an Agilent Infinity 1290 UHPLC system. Liquid chromatography of 1  $\mu$ L or  
535 5  $\mu$ L extract was performed using an Agilent Poroshell 120 phenyl-C<sub>6</sub>column (2.1  $\times$  150 mm, 1.9  $\mu$ m)  
536 at 60 °C using CH<sub>3</sub>CN and H<sub>2</sub>O, both containing 20 mM FA. Initially, a linear gradient of 10% CH<sub>3</sub>CN/H<sub>2</sub>O  
537 to 100% CH<sub>3</sub>CN over 10 min was employed, followed by isocratic elution of 100% CH<sub>3</sub>CN for 2 min.  
538 Then, the gradient was returned to 10% CH<sub>3</sub>CN/H<sub>2</sub>O in 0.1 min and finally isocratic condition of 10%  
539 CH<sub>3</sub>CN/H<sub>2</sub>O for 1.9 min, all at a flow rate of 0.35 min ml<sup>-1</sup>. HRMS data was recorded in positive  
540 ionization on an Agilent 6545 QTOF MS equipped with an Agilent Dual Jet Stream electrospray ion  
541 (ESI) source with a drying gas temperature of 250 °C, drying gas flow of 8 min l<sup>-1</sup>, sheath gas  
542 temperature of 300 °C and sheath gas flow of 12 min l<sup>-1</sup>. Capillary voltage was 4000 V and nozzle  
543 voltage was set to 500 V. HRMS data was processed and analyzed using Agilent MassHunter  
544 Qualitative Analysis B.07.00. HPLC grade solvents (VWR Chemicals) were used for extractions while  
545 LCMS grade solvents (VWR Chemicals) were used for LCMS.

## 546 References

- 547 1. R. L. Berendsen, C. M. J. Pieterse, P. A. H. M. Bakker, The rhizosphere microbiome and plant  
548 health. *Trends Plant Sci.* **17**, 478–486 (2012).
- 549 2. D. Haas, G. Défago, Biological control of soil-borne pathogens by fluorescent pseudomonads.  
550 *Nat. Rev. Microbiol.* **3**, 307–319 (2005).
- 551 3. J. M. Whipps, Microbial interactions and biocontrol in the rhizosphere. *J. Exp. Bot.* **52**, 487–511  
552 (2001).
- 553 4. R. Mendes, *et al.*, Deciphering the rhizosphere microbiome for disease-suppressive bacteria.  
554 *Science* **332**, 1097–1100 (2011).
- 555 5. A. Jousset, *et al.*, Biodiversity and species identity shape the antifungal activity of bacterial  
556 communities. *Ecology* **95**, 1184–1190 (2014).
- 557 6. J. Becker, N. Eisenhauer, S. Scheu, A. Jousset, Increasing antagonistic interactions cause  
558 bacterial communities to collapse at high diversity. *Ecol. Lett.* **15**, 468–474 (2012).
- 559 7. J. Hu, *et al.*, Probiotic diversity enhances rhizosphere microbiome function and plant disease  
560 suppression. *MBio* **7**, e01790-16 (2016).
- 561 8. Z. Mehrabi, *et al.*, *Pseudomonas* spp. diversity is negatively associated with suppression of the  
562 wheat take-all pathogen. *Sci. Rep.* **6**, 1–10 (2016).
- 563 9. Z. Ma, *et al.*, Biosynthesis, chemical structure, and structure-activity relationship of orfamide  
564 lipopeptides produced by *Pseudomonas* protegens and related species. *Front. Microbiol.* **7**, 1–  
565 16 (2016).
- 566 10. Q. Yan, B. Philmus, J. H. Chang, J. E. Loper, Novel mechanism of metabolic co-regulation  
567 coordinates the biosynthesis of secondary metabolites in *Pseudomonas* protegens. *Elife* **6**,  
568 e22835 (2017).
- 569 11. A. Ramette, Y. Moëne-Loccoz, G. Défago, Prevalence of fluorescent pseudomonads producing  
570 antifungal phloroglucinols and/or hydrogen cyanide in soils naturally suppressive or conducive  
571 to tobacco black root rot. *FEMS Microbiol. Ecol.* **44**, 35–43 (2003).
- 572 12. J. M. Raaijmakers, D. M. Weller, Natural Plant Protection by 2,4-Diacetylphloroglucinol-  
573 Producing *Pseudomonas* spp. in Take-All Decline Soils. *Mol. Plant-Microbe Interact.* **11**, 144–  
574 152 (1998).
- 575 13. K. Murata, M. Suenaga, K. Kai, Genome Mining Discovery of Protegenins A–D, Bacterial  
576 Polyynes Involved in the Antioomycete and Biocontrol Activities of *Pseudomonas* protegens .  
577 *ACS Chem. Biol.* (2021) <https://doi.org/10.1021/acscchembio.1c00276> (July 1, 2021).
- 578 14. J. Achkar, M. Xian, H. Zhao, J. W. Frost, Biosynthesis of Phloroglucinol. *J. Am. Chem. Soc.* **127**,  
579 5332–5333 (2005).
- 580 15. M. G. Bangera, L. S. Thomashow, Identification and Characterization of a Gene Cluster for  
581 Synthesis of the Polyketide Antibiotic 2,4-Diacetylphloroglucinol from *Pseudomonas*  
582 *fluorescens* Q2-87. *J. Bacteriol.* **181**, 3155–3163 (1999).
- 583 16. M. Bottiglieri, C. Keel, Characterization of PhlG, a hydrolase that specifically degrades the  
584 antifungal compound 2,4-diacetylphloroglucinol in the biocontrol agent *Pseudomonas*  
585 *fluorescens* CHA0. *Appl. Environ. Microbiol.* **72**, 418–27 (2006).

- 586 17. X. Yan, *et al.*, Transcriptional Regulator PhlH Modulates 2,4-Diacetylphloroglucinol Biosynthesis  
587 in Response to the Biosynthetic Intermediate and End Product. *Appl. Environ. Microbiol.* **83**,  
588 e01419-17 (2017).
- 589 18. P. C. Dorrestein, E. Yeh, S. Garneau-Tsodikova, N. L. Kelleher, C. T. Walsh, Dichlorination of a  
590 pyrrolyl-S-carrier protein by FADH<sub>2</sub>- dependent halogenase PltA during pyoluteorin  
591 biosynthesis. *Proc. Natl. Acad. Sci.* **102**, 13843–13848 (2005).
- 592 19. M. G. Thomas, M. D. Burkart, C. T. Walsh, Conversion of L-proline to pyrrolyl-2-carboxyl-S-PCP  
593 during undecylprodigiosin and pyoluteorin biosynthesis. *Chem. Biol.* **9**, 171–184 (2002).
- 594 20. U. Schnider-Keel, *et al.*, Autoinduction of 2,4-diacetylphloroglucinol biosynthesis in the  
595 biocontrol agent *Pseudomonas fluorescens* CHA0 and repression by the bacterial metabolites  
596 salicylate and pyoluteorin. *J. Bacteriol.* **182**, 1215–1225 (2000).
- 597 21. M. Brodhagen, M. D. Henkels, J. E. Loper, Positive Autoregulation and Signaling Properties of  
598 Pyoluteorin, an Antibiotic Produced by the Biological Control Organism *Pseudomonas*  
599 *fluorescens* Pf-5. *Appl. Environ. Microbiol.* **70**, 1758–1766 (2004).
- 600 22. M. Maurhofer, E. Baehler, R. Notz, V. Martinez, C. Keel, Cross Talk between 2,4-  
601 Diacetylphloroglucinol-Producing Biocontrol *Pseudomonads* on Wheat Roots. *Appl. Environ.*  
602 *Microbiol.* **70**, 1990–1998 (2004).
- 603 23. J. C. Clifford, *et al.*, Phloroglucinol functions as an intracellular and intercellular chemical  
604 messenger influencing gene expression in *Pseudomonas protegens*. *Environ. Microbiol.* **18**,  
605 3296–3308 (2016).
- 606 24. T. A. Kidarsa, N. C. Goebel, T. M. Zabriskie, J. E. Loper, Phloroglucinol mediates cross-talk  
607 between the pyoluteorin and 2,4-diacetylphloroglucinol biosynthetic pathways in  
608 *Pseudomonas fluorescens* Pf-5. *Mol. Microbiol.* **81**, 395–414 (2011).
- 609 25. K. A. Hassan, *et al.*, Inactivation of the GacA response regulator in *Pseudomonas fluorescens*  
610 Pf-5 has far-reaching transcriptomic consequences. *Environ. Microbiol.* **12**, 899–915 (2010).
- 611 26. C. Dubuis, D. Haas, Cross-species GacA-controlled induction of antibiosis in pseudomonads.  
612 *Appl. Environ. Microbiol.* **73**, 650–654 (2007).
- 613 27. M. L. Hansen, Z. He, M. Wibowo, L. Jelsbak, A Whole-Cell Biosensor for Detection of 2,4-  
614 Diacetylphloroglucinol (DAPG)-Producing Bacteria from Grassland Soil. *Appl. Environ.*  
615 *Microbiol.* **87**, e01400–e01420 (2021).
- 616 28. M. Le Roux, *et al.*, Kin cell lysis is a danger signal that activates antibacterial pathways of  
617 *pseudomonas aeruginosa*. *Elife* **2015**, 1–65 (2015).
- 618 29. D. M. Cornforth, K. R. Foster, Competition sensing: the social side of bacterial stress responses.  
619 *Nat. Rev. Microbiol.* **11**, 285–293 (2013).
- 620 30. M. LeRoux, S. B. Peterson, J. D. Mougous, Bacterial danger sensing. *J. Mol. Biol.* **427**, 3744–  
621 3753 (2015).
- 622 31. S. Westhoff, G. P. van Wezel, D. E. Rozen, Distance-dependent danger responses in bacteria.  
623 *Curr. Opin. Microbiol.* **36**, 95–101 (2017).
- 624 32. J. Davies, G. B. Spiegelman, G. Yim, The world of subinhibitory antibiotic concentrations. *Curr.*  
625 *Opin. Microbiol.* **9**, 445–453 (2006).
- 626 33. P. Garbeva, M. W. Silby, J. M. Raaijmakers, S. B. Levy, W. De Boer, Transcriptional and  
627 antagonistic responses of *Pseudomonas fluorescens* Pf0-1 to phylogenetically different

- 628 bacterial competitors. *ISME J.* **5**, 973–985 (2011).
- 629 34. M. I. Abrudan, *et al.*, Socially mediated induction and suppression of antibiosis during bacterial  
630 coexistence. *Proc. Natl. Acad. Sci.* **112**, 11054–11059 (2015).
- 631 35. J. Kehe, *et al.*, Positive interactions are common among culturable bacteria. *Sci. Adv.* **7**, 1–10  
632 (2021).
- 633 36. A. K. Korgaonkar, M. Whiteley, *Pseudomonas aeruginosa* enhances production of an  
634 antimicrobial in response to N-acetylglucosamine and peptidoglycan. *J. Bacteriol.* **193**, 909–  
635 917 (2011).
- 636 37. B. K. Duffy, G. Défago, Zinc Improves Biocontrol of Fusarium Crown and Root Rot of Tomato by  
637 *Pseudomonas fluorescens* and Represses the Production of Pathogen Metabolites Inhibitory to  
638 Bacterial Antibiotic Biosynthesis. *Phytopathology* **87**, 1250–1257 (1997).
- 639 38. W. Li, *et al.*, Promysalin, a Salicylate-Containing *Pseudomonas putida* Antibiotic, Promotes  
640 Surface Colonization and Selectively Targets Other *Pseudomonas*. *Chem. Biol.* **18**, 1320–1330  
641 (2011).
- 642 39. C. Hesse, *et al.*, Genome-based evolutionary history of *Pseudomonas* spp. *Environ. Microbiol.*  
643 **20**, 2142–2159 (2018).
- 644 40. J. J. Parnell, *et al.*, From the lab to the farm: An industrial perspective of plant beneficial  
645 microorganisms. *Front. Plant Sci.* **7**, 1110 (2016).
- 646 41. R. L. Berendsen, *et al.*, Unearthing the genomes of plant-beneficial *Pseudomonas* model strains  
647 WCS358, WCS374 and WCS417. *BMC Genomics* **16**, 1–23 (2015).
- 648 42. B. Niu, J. N. Paulson, X. Zheng, R. Kolter, Simplified and representative bacterial community of  
649 maize roots. *Proc. Natl. Acad. Sci.* **114**, E2450–E2459 (2017).
- 650 43. L. Zhuang, *et al.*, Synthetic community with six *Pseudomonas* strains screened from garlic  
651 rhizosphere microbiome promotes plant growth. *Microb. Biotechnol.* **14**, 488–502 (2021).
- 652 44. S. Zobel, *et al.*, Tn7-Based Device for Calibrated Heterologous Gene Expression in *Pseudomonas*  
653 *putida*. *ACS Synth. Biol.* **4**, 1341–1351 (2015).
- 654 45. J. Van Gestel, F. J. Weissing, O. P. Kuipers, A. ´ Kos, T. Kovács, Density of founder cells affects  
655 spatial pattern formation and cooperation in *Bacillus subtilis* biofilms. *ISME J.* **8**, 2069–2079  
656 (2014).
- 657 46. S. Kumar, M. Nei, J. Dudley, K. Tamura, MEGA: A biologist-centric software for evolutionary  
658 analysis of DNA and protein sequences. *Brief. Bioinform.* **9**, 299–306 (2008).
- 659 47. L. R. Hmelo, *et al.*, Precision-engineering the *Pseudomonas aeruginosa* genome with two-step  
660 allelic exchange. *Nat. Protoc.* **10**, 1820–1841 (2015).
- 661 48. L. Yang, *et al.*, Polysaccharides serve as scaffold of biofilms formed by mucoid *Pseudomonas*  
662 *aeruginosa*. *FEMS Immunol. Med. Microbiol.* **65**, 366–376 (2012).
- 663 49. D. T. Gibson, J. R. Koch, R. E. Kallio, Oxidative degradation of aromatic hydrocarbons by  
664 microorganisms. I. Enzymic formation of catechol from benzene. *Biochemistry* **7**, 2653–2662  
665 (2002).
- 666 50. P. Sazinas, M. L. Hansen, M. I. Aune, M. H. Fischer, L. Jelsbak, A Rare Thioquinolobactin  
667 Siderophore Present in a Bioactive *Pseudomonas* sp. DTU12.1. *Genome Biol. Evol.* **11**, 3529–  
668 3533 (2019).

- 669 51. P. Sazinas, *et al.*, Complete Genome Sequence of a Bioactive *Pseudomonas* sp. Strain, DTU12.3,  
670 Isolated from Soil in Denmark. *Microbiol. Resour. Announc.* **8** (2019).
- 671 52. M. Herrero, V. De Lorenzo, K. N. Timmis, Transposon vectors containing non-antibiotic  
672 resistance selection markers for cloning and stable chromosomal insertion of foreign genes in  
673 gram-negative bacteria. *J. Bacteriol.* **172**, 6557–6567 (1990).
- 674 53. H. W. Boyer, D. Roulland-dussoix, A complementation analysis of the restriction and  
675 modification of DNA in *Escherichia coli*. *J. Mol. Biol.* **41**, 459–472 (1969).
- 676 54. B. Kessler, V. de Lorenzo, K. N. Timmis, A general system to integrate *lacZ* fusions into the  
677 chromosomes of gram-negative eubacteria: regulation of the Pm promoter of the TOL plasmid  
678 studied with all controlling elements in monocopy. *MGG Mol. Gen. Genet.* **233**, 293–301  
679 (1992).
- 680 55. K. H. Choi, *et al.*, A Tn7-based broad-range bacterial cloning and expression system. *Nat.*  
681 *Methods* **2**, 443–448 (2005).
- 682

684 Supplementary Table 1

Strains and plasmids	Genotype	Source
<b>Strains</b>		
<i>P. protegens</i> DTU9.1	Wild-type	In-house collection
<i>P. capeferrum</i> F8	Wild-type soil isolate	(27)
<i>P. capeferrum</i> 5.43	Wild-type soil isolate	(27)
<i>P. capeferrum</i> 9.30	Wild-type soil isolate	(27)
<i>P. putida</i> F1	Wild-type	(49)
<i>P. jessenii</i> DTU3.1	Wild-type soil isolate	In-house collection
<i>P. proteolytica</i> DTU12.1	Wild-type soil isolate	(50)
<i>P. helmanticensis</i> DTU12.3	Wild-type soil isolate	(51)
<i>E. coli</i> CC118	$\Delta(\text{ara-leu}), \text{araD}, \Delta\text{lacX74}, \text{galE}, \text{galk}, \text{phoA20}, \text{thi-1}, \text{rpsE}, \text{rpoB}, \text{argE}(\text{Am}), \text{recA1}(\lambda\text{pir})$	(52)
<i>E. coli</i> HB101	F <sup>-</sup> , <i>araC14</i> , <i>leuB6</i> (Am), $\Delta(\text{gpt-proA})62$ , <i>lacY1</i> , <i>glnX44</i> (AS), <i>galK2</i> (Oc), $\lambda^{-}$ , <i>recA13</i> , <i>rpsL20</i> , <i>xylA5</i> , <i>mlt</i> <sup>-1</sup> , <i>thiE1</i> , [ <i>hdsS20</i> ]	(53)
<i>P. protegens</i> DTU9.1	$\Delta\text{pltM}$	This study
<i>P. protegens</i> DTU9.1	Chromosomally integrated Tn7 element of pBG42- <i>gfp</i>	This study
<i>P. capeferrum</i> F8	Chromosomally integrated Tn7 element of pBG42- <i>mKate</i>	This study
<b>Plasmids</b>		
pRK600	Helper plasmid for plasmid conjugation	(54)
pTNS2	Helper plasmid carrying the transposase	(55)
pSEVA231		SEVA database
pSEVA237 <sub>RBS30</sub>	pSEVA231 with a promoterless <i>gfpmut3</i> gene and a strong RBS30	This study
pSEVA237::P <i>pltL</i>	pSEVA237 <sub>RBS30</sub> with the P <i>pltL</i> promoter	This study
pBG42- <i>gfp</i>	Tn7 element with the strong p14g promoter upstream of <i>msfgfp</i>	(44)
pBG42- <i>mKate</i>	Tn7 element with the strong p14g promoter upstream of <i>mKate</i>	This study
pSEVA225::DAPG <sub>lacZ</sub>		(27)
pNJ1		(48)
pNJ1- <i>pltM</i> -del	pNJ1 with the homology regions required for <i>pltM</i> deletion by allelic replacement	This study

Name	Sequence <sup>a,b</sup>	Note
<b>pBG42-<i>mKate</i> cloning</b>		
mKate_BclI_fw	5'- <u>tatattgatca</u> TGTCAGAACTTATCAAGGA AAATATG	Amplification of <i>mKate</i>
mKate_HindIII_rev	5'- <u>aagctt</u> TTAACGGTGTCCCAATTTAC	Amplification of <i>mKate</i>
pBG42_HindIII_fw	5'- <u>tatataagctt</u> GAAAACCTGGCGACTAG	Amplification of pBG42 backbone
pBG42_BclI_rev	5'- <u>atcgatgatca</u> TTAGAAAACCTCCTTAG	Amplification of pBG42 backbone
pTn7_rep-seq_fw	5'- CCGAACAGGCTTATGTCAAG	Verification of pBG42- <i>mKate</i>
<b>pSEVA237 reporter cloning</b>		
gfpmut3_BamHI_RBS30_Xbal	5'- <u>tatatggatc</u> caaagaggagaa <u>ctaga</u> ATGCGT AAAGGAGAAGAAC	Amplification of <i>gfp</i> with strong RBS30
gfpmut3_HindIII_rev	5'- <u>aagctt</u> TTATTTGTATAGTTCATCCATGCC	Amplification of <i>gfp</i> with strong RBS30
PS1	5'- AGGGCGGCGGATTGTCC	Verification of pSEVA237 variants
pltL-pro_SacI_fw	5'- <u>tatatagctc</u> TCCTAAATCCTTTTAG AATTTTAG	Amplification of <i>PplTL</i>
pltL-pro_BamHI_rev	5'- <u>actgaggatcc</u> AGACGTACGCTCCTG	Amplification of <i>PplTL</i>
<b><i>pltM</i> deletion</b>		
Up_F <sub><i>pltM</i></sub>	5'- <u>atccccgtctaga</u> CACGATATTGCGCCACGAAG	Amplification of homology region upstream of <i>pltM</i>
Up-R <sub><i>pltM</i></sub>	5'- <b>cagcgtttccagagc</b> <u>gaccacctt</u> CGCCGA AAACCACAACACTTC	Amplification of homology region upstream of <i>pltM</i>
Down_F <sub><i>pltM</i></sub>	5'- AAGGTGGTCGCTCTGGAAAG	Amplification of homology region downstream of <i>pltM</i>
Down_R <sub><i>pltM</i></sub>	5'- <u>atccggagctc</u> CATCGACCCTAGGCGTTTCTC	Amplification of homology region downstream of <i>pltM</i>
<i>pltM</i> -del_fw	5'- TTGGGTAGCTCATCCTTGCG	Verification of <i>pltM</i> deletion
<i>pltM</i> -del_rev	5'- GCGCAGAATCAATAGCCTCG	Verification of <i>pltM</i> deletion
<b><i>rpoD</i> sequencing</b>		
PsEG30F	5'- ATYGAAATCGCCAARCG	Amplification of part of the <i>rpoD</i> gene
PsEG790R	5'- CGGTTGATKCCTTGA	Amplification of part of the <i>rpoD</i> gene

687

688 a. CAPITAL letters represent the priming part

689 b. Underlined characters represent restriction sites attached as primer overhang690 c. **Bold** characters represent the first 25 nucleotides downstream of the region targeted for

691 deletion to achieve successful overlap-extension PCR attached as primer overhang

# Paper 4

---

Counter-acting *Pseudomonas* invasion: Community-level resistance towards *Pseudomonas*-produced secondary metabolites

Hansen M.L., Dènes Z., Wibowo M., Jarmusch S.A., Andersen A.J.C., Strube M.L., and Jelsbak L.

*In preparation*

1 **Counter-acting *Pseudomonas* invasion: Community-level resistance**  
2 **towards *Pseudomonas*-produced secondary metabolites**

3 Morten L. Hansen, Zsófia Dènes, Mario Wibowo, Scott A. Jarmusch, Aaron J. C. Andersen, Mikael L.  
4 Strube and Lars Jelsbak<sup>#</sup>.

5 Department of Biotechnology and Biomedicine, Technical University of Denmark, Søtofts Plads bldg. 221, DK-2800 Kgs  
6 Lyngby, Denmark

7

8 <sup>#</sup>corresponding author:

9 Lars Jelsbak (lj@bio.dtu.dk)

10

11 **ORCID**

12 MLH: 0000-0003-3927-2751

13 ZD: 0000-0003-0087-1052

14 MW: 0000-0002-5739-0949

15 SAJ: 0000-0002-1021-1608

16 AJCA: 0000-0002-3876-7480

17 MLS: 0000-0003-0905-5705

18 LJ: 0000-0002-5759-9769

19

20 **Running title:** Community-level resistance towards *Pseudomonas*-produced secondary metabolites

21

22 **Keywords:** DAPG, pyoluteorin, orfamide A, SynCom, microbial interactions, *Pseudomonas* invasion,  
23 secondary metabolites.

## 24 **Abstract**

25 The model biocontrol species, *Pseudomonas protegens*, produces multiple antimicrobial compounds  
26 that are toxic to a range of different soil microorganisms, including plant pathogens. The role of  
27 antagonistic secondary metabolites in suppression of soil-borne phytopathogens has been clearly  
28 documented, whereas their contribution to the ability of *P. protegens* to invade natural soil and  
29 rhizosphere microbiomes remains less clear. Here, we use a four-species synthetic community  
30 cultivated *in vitro* in an artificial soil to determine the effects of antibiotic production in relation to *P.*  
31 *protegens* community invasion. Secondly, we use the system to identify community traits that affect  
32 the secondary metabolism of *P. protegens*. We show that *P. protegens* readily invades and alters the  
33 community composition, and that invasion into the community led to altered production of key  
34 antimicrobial metabolites (DAPG, pyoluteorin and orfamide A) in *P. protegens*. Surprisingly, mutants  
35 unable to produce these antibiotics invade the community as efficiently as wildtype producers do, and  
36 wildtype and non-producers cause similar perturbations in the composition of the synthetic  
37 community. The absence of a clear antibiotic-mediated impact on the otherwise antibiotic-sensitive  
38 microbes of the community was not a result of low, non-toxic levels of antibiotics. Specifically, we find  
39 that antibiotics pyoluteorin and orfamide A can reach levels that are toxic to individual community  
40 members, suggesting the existence of community-level resistance mechanisms towards the toxic  
41 metabolites. For the cyclic lipopeptide, orfamide A, we identify the underlying resistance mechanism  
42 by which the Gram-positive *Rhodococcus globerulus* D757 enzymatically inactivates the antibiotic.  
43 Furthermore, we observe degradation of the inactivated orfamide A, which could indicate a novel  
44 community-level catabolism of an antimicrobial secondary metabolite. The ability of *P. protegens* to  
45 invade the community despite these resistance mechanisms is best explained by nutrient competition  
46 and the faster growth rate of the invader. Altogether, the demonstration that the synthetic  
47 community have mechanisms for constraining or dampening invasion by means of detoxifying  
48 antibiotics may provide a mechanistic explanation to inconsistencies in biocontrol effectiveness *in situ*.

## 49 **Acknowledgements**

50 We thank Carlos N. Lozano-Andrade and Ákos T. Kovács for providing the strains comprising the  
51 synthetic microbial community, as well as introducing the use of the hydrogel bead system. Likewise,  
52 we thank the members of the Center for Microbial Secondary Metabolites (CeMiSt) for general  
53 scientific discussions.

54

## 55 **Funding**

56 This study was carried out as part of the Center of Excellence for Microbial Secondary Metabolites  
57 funded by The Danish National Research Foundation (DNRF137).

## 58 Introduction

59 Natural niches such as soil and rhizosphere surrounding plant roots are inhabited by complex and  
60 diverse, yet stable microbial communities (1–6). Despite the vast diversity of indigenous soil  
61 microorganisms, the presence of bacteria belonging to key phyla have been linked to the  
62 suppressiveness of certain soils towards diseases caused by phytopathogens. One of these phyla is the  
63 Proteobacteria and more specifically members of the Pseudomonadaceae family (7). Pioneering  
64 studies demonstrated that transplantation of disease-suppressive soil containing fluorescent  
65 *Pseudomonas* into a field comprised of soil conducive to phytopathogenic invasion successfully  
66 rendered the soil suppressive to subsequent pathogen outbreaks (8, 9). These findings, among others,  
67 have encouraged extensive research into the concept of biocontrol and utilization of beneficial  
68 microbes, such as *Pseudomonas protegens*, in the control of pathogenic microorganisms via  
69 production of antimicrobial secondary metabolites (10, 11). However, the contribution of these  
70 secondary metabolites to the ability of the *Pseudomonas* biocontrol agent to invade natural soil and  
71 rhizosphere microbiomes remains less clear. Likewise, knowledge is currently limited on the effect of  
72 microbial interactions occurring between the invading biocontrol agent and the indigenous  
73 microorganisms on the production of antimicrobial secondary metabolites, and thus the efficacy of  
74 the biocontrol agent. One approach to address these topics is to incorporate synthetic microbial  
75 communities of naturally co-occurring microorganisms as a representative *in vitro* model to  
76 investigate the effects of *Pseudomonas* invasion.

77 In a broad sense, microbiologists have employed two contrasting methods to investigate the  
78 ecological complexity of natural environments (12). The reductionists strive to control as many  
79 experimental factors as possible by defining simplistic and predictable ecosystems consisting of one  
80 or few species to allow for detailed hypothesis testing, while sacrificing true ecological context (12,  
81 13). In contrast, holistic approaches apply meta-omics (14) and *in situ* detection methods (7, 15) to  
82 deduce microbiome functions and diversity, while seeking to preserve the genotypic, environmental,

83 and functional complexity of natural environments (13). An intermediate method to bridge the gap  
84 between these two approaches and overcome the challenges in analyzing the features of communities  
85 is to establish a simpler, synthetic microbial community (SynCom) under controlled laboratory  
86 conditions (16, 17). SynComs represent a useful tool for investigating the outcomes of multiple biotic  
87 interactions that would not be achievable by a single microbe, while reducing the complexity of the  
88 inherently diverse natural microbial community (12, 18). Niu et al. utilized a seven-membered  
89 bacterial SynCom to identify a keystone species dictating the development of community composition  
90 (17). Another study incorporated a bacterial SynCom comprised of representatives of the seven most  
91 abundant phyla in the phyllosphere to elucidate the effects of plant genotypes on microbiota  
92 composition (19). Thus, the engineering of SynComs has greatly enhanced our ability to investigate  
93 the effects of genotypic complexity within microbial communities. Simultaneously, advances in  
94 laboratory systems, such as the development of artificial soils (20), provide a novel and useful option  
95 for studying the effects of environmental complexity and spatial distribution (13). Artificial hydrogel-  
96 based soil was recently utilized to demonstrate microbial interactions in a soil-like environment (21).  
97 Thus, combining the use of an artificial soil system and a defined microbial SynCom represents a  
98 compelling approach to investigate microbial interactions, while maintaining genotypic and  
99 environmental complexity.

100 Fluorescent *Pseudomonas* are renowned for their antibiotic production (10, 11), role in disease-  
101 suppressiveness (8, 9), and plant growth promotion (22, 23). Several studies have shown the  
102 biocontrol effects of different fluorescent *Pseudomonas* towards important phytopathogenic  
103 microorganisms, such as *Gaeumannomyces graminis* var. *tritici* (24), *Rhizoctonia solani* (25), and  
104 *Pythium ultimum* (26). Particularly, the species *P. protegens* has been studied extensively for its vast  
105 repertoire of antimicrobial secondary metabolites, including 2,4-diacetylphloroglucinol (DAPG) (24),  
106 pyoluteorin (26), orfamide A (27), pyrrolnitrin (28), and pyoverdine (29). Research has clearly  
107 demonstrated the effect of antimicrobial secondary metabolites and inhibition of targeted  
108 phytopathogenic microorganisms. However, knowledge remains limited on the contribution and

109 impacts of these *Pseudomonas*-produced metabolites in the ability of the bacteria to invade  
110 indigenous soil and rhizosphere microbiomes. Previous studies have indicated that inoculation with  
111 various species of fluorescent *Pseudomonas* had only temporary, spatially limited, and transient  
112 effects on the natural rhizosphere microbiomes utilizing both culture-dependent (30, 31) and culture-  
113 independent (32, 33) approaches. Contrarily, the integration of fluorescent *Pseudomonas* has also  
114 been shown to cause significant perturbations within indigenous microbiomes (34, 35). As alluded to  
115 by Castro-Sowinski et al., the impact of *Pseudomonas* invasion depends on the indigenous  
116 microorganisms and the potential microbial interactions occurring between them (36). Thus, there is  
117 a clear need to systematically investigate the interactions between indigenous microorganisms and  
118 the invading *Pseudomonas* affecting the success of invasion, microbial community composition and  
119 secondary metabolism of the invader.

120 In this study we chose the hydrogel-based bead system (20) as *in vitro* model system, as it has been  
121 shown to mimic soil characteristics allowing for spatial distribution of microbes, as well as surface  
122 colonization. We utilized the system to explore the contribution of the secondary metabolites, DAPG,  
123 pyoluteorin, and orfamide A, to the ability of *P. protegens* DTU9.1 to invade a four-membered SynCom  
124 (37) within a soil-like environment. We showed that *P. protegens* readily invaded and altered the  
125 community composition. Surprisingly, mutants of *P. protegens* DTU9.1 unable to produce the  
126 antimicrobial metabolites invaded the community as efficiently as the wildtype strain did, and  
127 wildtype and non-producers caused similar perturbations in the composition of the synthetic  
128 community. Additionally, we investigated the effect of cultivating *P. protegens* DTU9.1 alongside the  
129 SynCom on the production and the fate of *Pseudomonas*-produced secondary metabolites. We  
130 observed an induced production of DAPG and pyoluteorin when *P. protegens* DTU9.1 was cocultivated  
131 with the SynCom. Interestingly, we discovered that the Gram-positive *Rhodococcus globerulus* D757  
132 was able to reduce the level of orfamide A below the minimal inhibitory concentration by hydrolyzing  
133 the ester-bond of the macrocyclic ring, thus linearizing and inactivating the cyclic lipopeptide. This  
134 study emphasizes the vast and complex microbial interactions potentially occurring *in situ* among

135 indigenous soil bacteria affecting the secondary metabolism of invading biocontrol agents, such as *P.*  
136 *protegens*.

137

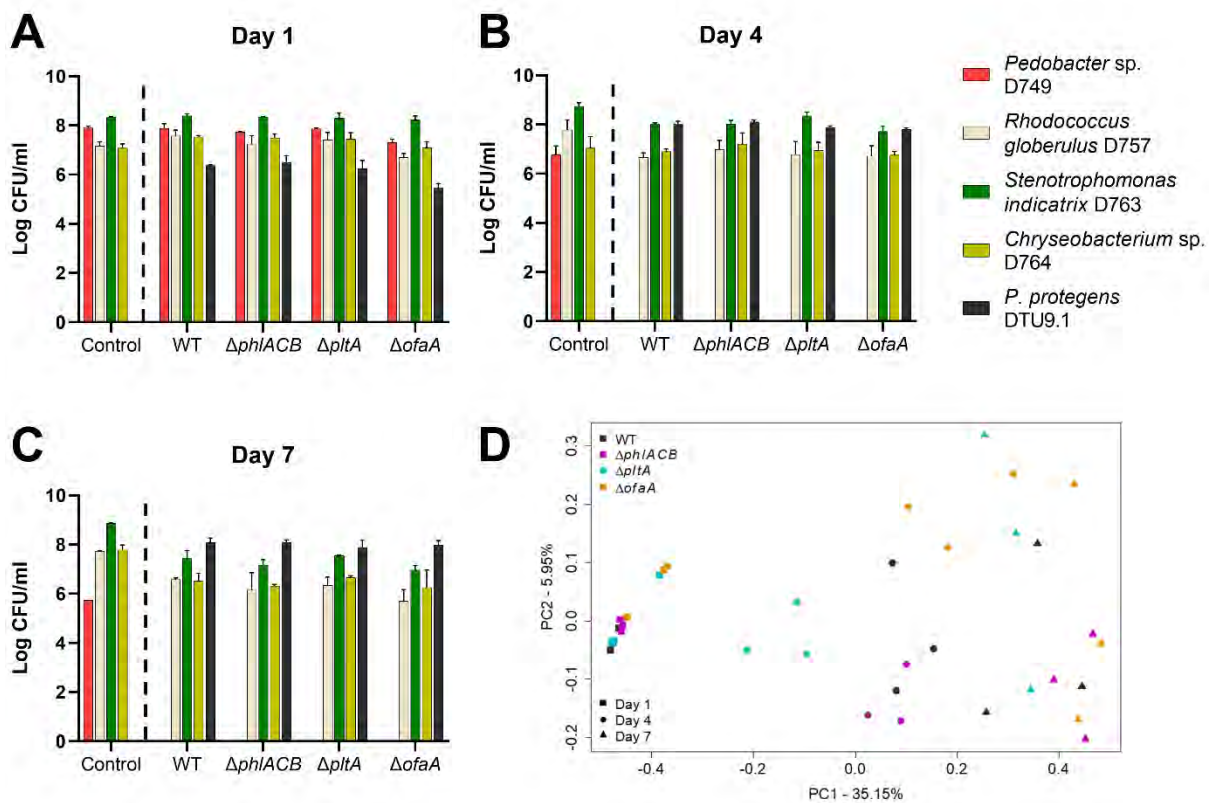
## 138 **Results**

### 139 ***P. protegens* DTU9.1 invades a four-membered synthetic microbial community in a soil-like** 140 **environment**

141 To explore the microbial interactions and their effects on community composition over time, a porous  
142 hydrogel bead system was chosen as cultivation system (20), as it has been shown to mimic soil  
143 characteristics (20, 21). Initially, it was determined if *P. protegens* DTU9.1 could colonize and maintain  
144 itself in the artificial soil-like environment when cultivated axenically (Figure S1A). After four days of  
145 cultivation, the system reached a plateau of approximately  $1 \cdot 10^8$  CFU/ml, which was maintained at  
146 the seventh and final day of the experiment. Furthermore, knock-out mutants incapable of producing  
147 DAPG ( $\Delta phlACB$ ), pyoluteorin ( $\Delta pltA$ ), or orfamide A ( $\Delta ofaA$ ) were constructed and tested for their  
148 cultivation ability within the hydrogel bead system. The secondary metabolites played an insignificant  
149 role in the ability of *P. protegens* DTU9.1 to colonize the soil-like environment axenically (Figure S1A).  
150 Additionally, it was verified that *P. protegens* DTU9.1 produced detectable amounts of DAPG,  
151 pyoluteorin, and orfamide A after seven days of cultivation in the bead system using HR-LCMS (Figure  
152 S1B). However, using our experimental setup, we were unable to detect other biologically relevant  
153 secondary metabolites known to be produced by *P. protegens*, such as pyrrolnitrin, pyoverdine and  
154 hydrogen cyanide.

155 Next, we investigated the effect of the three metabolites DAPG, pyoluteorin, and orfamide A on the  
156 ability of *P. protegens* DTU9.1 to invade a soil-like environment inhabited by a SynCom of four soil  
157 bacteria (*Pedobacter* sp. D749, *Rhodococcus globerulus* D757, *Stenotrophomonas indicatrix* sp. D763,  
158 and *Chryseobacterium* sp. D764). After 24 hours of cultivation, presence of all SynCom members was

159 observed (Figure 1A), while *P. protegens* DTU9.1 had very low abundance likely owing to the low  
 160 concentration of *Pseudomonas* in the initial inoculum compared to the SynCom members. However,  
 161 on the fourth day and onwards, *Pedobacter* sp. D749 was no longer detectable in the systems  
 162 inoculated with the variants of *P. protegens* DTU9.1 (Figure 1B and 1C). On the other hand, the control  
 163 system without *Pseudomonas* allowed the survival of *Pedobacter* throughout the experiment, albeit  
 164 with cell counts close to the detection limit at the seventh day sampling (Figure 1C). Moreover, on the  
 165 fourth day, *P. protegens* DTU9.1 had reached cell numbers ( $\approx 1 \cdot 10^8$  CFU/ml), which were maintained  
 166 throughout the experiment comparable to axenic cultivation. On the seventh day of incubation *P.*  
 167 *protegens* DTU9.1 constituted the majority of the bacterial biomass regardless of variant (Figure 1C).



168

169 Figure 1 | *P. protegens* DTU9.1 invades a four-membered synthetic microbial community in a soil-like  
 170 environment. Abundance was determined as colony forming units in the hydrogel bead system of each  
 171 SynCom member and the introduced *P. protegens* DTU9.1 variant; WT,  $\Delta phiACB$ ,  $\Delta pltA$  and  $\Delta ofaA$  on Day  
 172 1 (A), Day 4 (B) and Day 7 (C). The dotted line indicates the separation of data (right) used for the Principal  
 173 Coordinate Analysis. Data was derived from three biological replicates. D) A Principal Coordinate Analysis  
 174 (PCoA) was performed on CFU data of the systems inoculated with variants of *P. protegens* DTU9.1 to  
 175 compare the effects of sampling time (symbols) and the variant of *P. protegens* DTU9.1 on the  
 176 bacterial composition in a soil-like environment.

177 The overall effect of DAPG, pyoluteorin and orfamide A on community composition over time was  
178 evaluated with a Principal Coordinate Analysis (PCoA) using Bray-Curtis distances (Figure 1D). The  
179 analysis was performed on of non-logarithmic transformed CFU data of the bacterial abundance in the  
180 systems inoculated with variants of *P. protegens* DTU9.1 (WT,  $\Delta phlACB$ ,  $\Delta pltA$ , and  $\Delta ofaA$ ) to allow  
181 visualization of more subtle changes. The analysis suggested that the major factor affecting abundance  
182 was the sampling time, as three separate clusters representing the three sampling times appeared  
183 across the first principal component, which explained most of the variance in the data (35.15%). An  
184 overall PERMANOVA using sampling time, genotypic variant of invading *P. protegens* DTU9.1, and their  
185 interaction as fixed effects further confirmed the significance of sampling time on the community  
186 composition ( $P = 9.99 \cdot 10^{-5}$ ,  $R^2 = 0.75$ ). Measuring the growth rates of each SynCom member and the  
187 four variants of *P. protegens* DTU9.1 in liquid broth revealed that *Pseudomonas* grew significantly  
188 faster than each SynCom member (Figure S2), whereas *Pedobacter* sp. D749 had the slowest growth  
189 rate. This could explain the observed significant effect of sampling time on community composition,  
190 which was dominated by *P. protegens* DTU9.1 on the seventh day regardless of variant. However, from  
191 the overall PERMANOVA analysis the genotypic variant of *P. protegens* DTU9.1 also appeared to have  
192 a minor, but significant effect on the bacterial composition ( $P = 0.029$ ), whereas the interaction  
193 between sampling time and genotypic variant was not significant ( $P = 0.063$ ). The significant effect of  
194 genotypic variant on the community composition was further investigated by individual day-wise  
195 PERMANOVA analyses, revealing that the *Pseudomonas*-produced secondary metabolites primarily  
196 affected the microbial composition in the early and middle stages of community establishment (Day  
197 1:  $P = 0.035$ ,  $R^2 = 0.52$ ; Day 4:  $P = 5.00 \cdot 10^{-4}$ ,  $R^2 = 0.71$ ; Day 7: n.s.,  $R^2 = 0.36$ ). As indicated by the PCoA  
198 (Figure 1D), the bacterial composition in the systems with the  $\Delta pltA$  and  $\Delta ofaA$  mutants differed  
199 noticeably on Day 4 compared to the systems inoculated with *P. protegens* DTU9.1 WT and the  
200  $\Delta phlACB$  mutant. This could suggest that the metabolites, pyoluteorin and orfamide A, play an  
201 important role during early and middle stages of community assembly as *P. protegens* establishes a  
202 suitable growth niche.

203 Based on this finding we evaluated the tolerance of each SynCom member towards pyoluteorin and  
 204 orfamide A by estimating the minimal inhibitory concentration (MIC) during liquid cultivation. As  
 205 summarized in Table 1, three members (*Pedobacter* sp. D749, *R. globerulus* D757 and  
 206 *Chryseobacterium* sp. D764) were equally susceptible to pyoluteorin with an MIC = 8 µg/ml, while the  
 207 MIC of pyoluteorin towards *S. indicatrix* D763 was 16 µg/ml. Orfamide A, on the other hand, only  
 208 exhibited antimicrobial activity against the Gram-positive *R. globerulus* D757 with an MIC = 8 µg/ml.  
 209 The three other SynCom members survived cultivation in the highest tested concentration of orfamide  
 210 A. We were thus unable to accurately estimate the MIC, though it appeared larger than 64 µg/ml  
 211 (Table 1). Additionally, we tested the susceptibility of each SynCom member towards DAPG,  
 212 pyoluteorin, and orfamide A utilizing an *in vitro* inhibition assay on agar surfaces (Figure S3). The  
 213 antibiotic activity of pyoluteorin towards all members was confirmed, whereas antibiosis of *R.*  
 214 *globerulus* D757 caused by orfamide A was not observed in this experimental setup.

215 Table 1 | Minimal inhibitory concentrations of pyoluteorin and orfamide A against the four SynCom members

	Minimal Inhibitory Concentration (µg ml <sup>-1</sup> )	
	Pyoluteorin	Orfamide A
<i>Pedobacter</i> sp. D749	8	> 64
<i>R. globerulus</i> D757	8	8
<i>S. indicatrix</i> D763	16	> 64
<i>Chryseobacterium</i> sp. D764	8	> 64

216

217

218 **The secondary metabolome of *P. protegens* DTU9.1 is altered during cocultivation with a**  
 219 **four-membered SynCom**

220 Motivated by the results of the MIC assays, we calculated the concentrations of DAPG, pyoluteorin,  
 221 and orfamide A, with HR-LCMS after seven days of axenic cultivation of *P. protegens* DTU9.1 within  
 222 the hydrogel bead system (Table 2). The levels of pyoluteorin were below the MIC towards all four  
 223 SynCom members at 5.85 ± 0.56 µg/ml. On the other hand, the concentration of orfamide A during

224 axenic cultivation of *P. protegens* DTU9.1 exceeded the levels necessary to inhibit the growth of *R.*  
 225 *globerulus* D757. Next, we investigated if cultivation within a soil-like environment alongside a semi-  
 226 synthetic microbial community affected the production of DAPG, pyoluteorin, and orfamide A.  
 227 Secondary metabolites were extracted from the bead system inoculated with *P. protegens* DTU9.1 WT  
 228 and SynCom on the seventh and final day of the experiment and analyzed with HR-LCMS (Table 2).  
 229 The production of DAPG and pyoluteorin was induced when *P. protegens* was cultivated with the  
 230 SynCom, whereas only the concentration of DAPG was significantly increased ( $P = 0.0087$ ). This could  
 231 suggest that *P. protegens* senses ecological competition from the SynCom members, which in turn  
 232 leads to induced production of antimicrobial secondary metabolites as a mode of counter-attack (38).  
 233 Interestingly, the concentration of orfamide A was significantly reduced when *P. protegens* was  
 234 cultivated with the SynCom compared to axenic growth ( $P = 0.0002$ ). Thus, it could indicate that one  
 235 or multiple SynCom members either inhibit production of orfamide A or secrete enzymes capable of  
 236 inactivating orfamide A.

237 Table 2 | Concentration of secondary metabolites from *P. protegens* DTU9.1 after 7 days of growth in a soil-like  
 238 environment

	Log CFU/ml <sup>a</sup>	Secondary metabolite (µg/ml)		
	<i>Pseudomonas</i>	DAPG	Pyoluteorin	Orfamide A
<b><i>P. protegens</i> DTU9.1</b>	8.07 ± 0.11	3.96 ± 0.82	5.85 ± 0.56	25.58 ± 2.11
<b><i>P. protegens</i> DTU9.1 + SynCom</b>	8.08 ± 0.15 <sup>b</sup>	9.16 ± 1.30	10.12 ± 2.19	3.87 ± 0.75
<b>Statistical significance<sup>c</sup></b>	n.s.	$P = 0.0087$	$P = 0.0556$	$P = 0.0002$

239

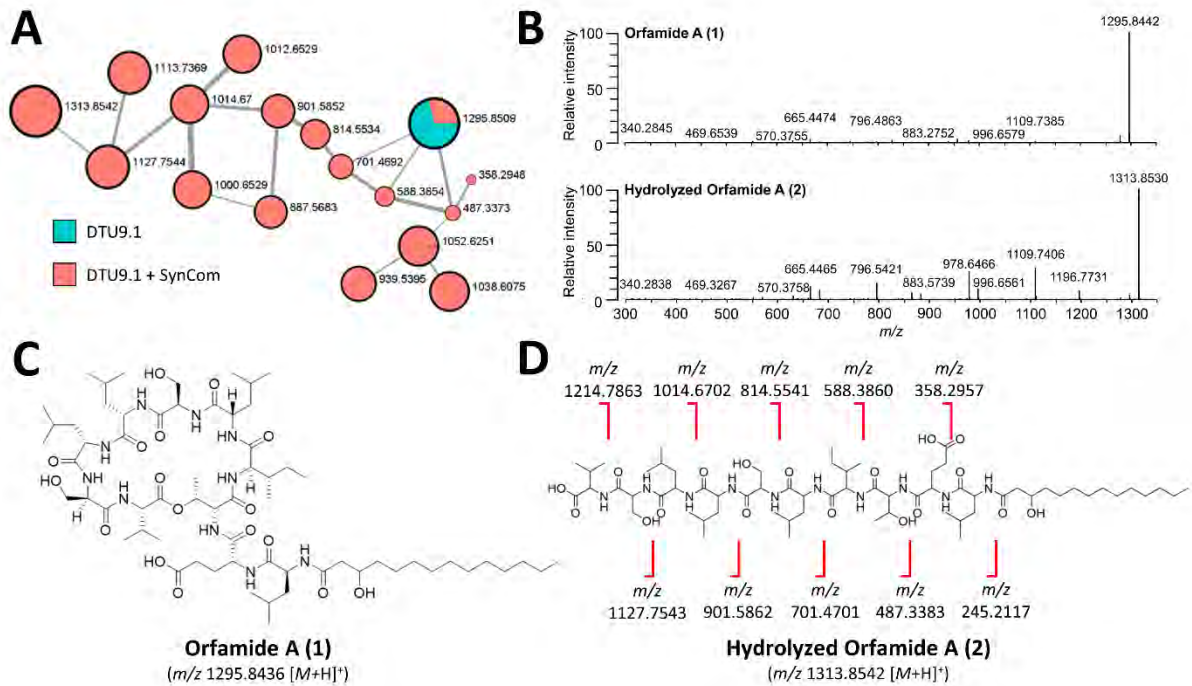
240 <sup>a</sup> CFU/ml of *P. protegens* DTU9.1 either grown alone or with the SynCom for seven days in the bead system.

241 <sup>b</sup> *P. protegens* DTU9.1 constituted approximately 75% of the total bacterial abundance in the microbial  
 242 community.

243 <sup>c</sup> Significance of the difference in secondary metabolite concentration was analyzed by Student's *t*-test.

244 **Orfamide A is degraded during coculture of *P. protegens* DTU9.1 and SynCom in a soil-like**  
245 **environment**

246 To further investigate the fate of orfamide A (**1**) during coculture of *P. protegens* DTU9.1 and the  
247 SynCom, the MS data from the HR-LCMS analyses of metabolites was subjected to Global Natural  
248 Product Social (GNPS) molecular network analysis (39) to identify potential chemical relationships  
249 between metabolites across the three systems (Figure S4). This revealed a separate molecular family  
250 displaying the presence of orfamide A ( $m/z$  1295.85) during both axenic cultivation of *P. protegens*  
251 DTU9.1 and cocultivation with the SynCom (Figure 2A). Interestingly, the molecular family also  
252 contained metabolites with related fragmentation patterns to orfamide A that only appeared during  
253 cocultivation of *P. protegens* DTU9.1 and the SynCom. One feature,  $m/z$ -value of 1313.8542,  
254 corresponded to the mass of orfamide A with the addition of 18 Da (Figure 2A). This could indicate  
255 either hydrolysis of an amide bond or hydrolysis of the ester bond connecting the macrocyclic ring of  
256 orfamide A. From the fragmentation analysis it was determined that hydrolysis of the ester bond  
257 occurred (Figure 2B). Hydrolysis of the ester bond resulted in the linearized congener of orfamide A  
258 (**2**) when *P. protegens* DTU9.1 was cultivated alongside the SynCom in the bead system (Figure 2D).  
259 Furthermore, potential degradation products of orfamide A were also present in the same molecular  
260 family (Figure 2A). Initially, degradation was verified by analyzing the extracted ion chromatograms  
261 (EICs) for each of the degradation products, confirming their presence in the extract and not the  
262 possibility of in-source fragmentation (Figure S5). Subsequently, fragmentation patterns were further  
263 analyzed, confirming degradation products emanating from the hydrolyzed ester bond (Figure S6). A  
264 similar phenomenon was observed for orfamide B through the presence of degradation products ( $m/z$   
265 1113.7369,  $m/z$  1000.65, and  $m/z$  887.5683 in Figure 2A). The remaining degradation products of  
266 orfamide B were present in concentrations too low for the cut-off used for the GNPS analysis, but  
267 were observed in the raw data (data not shown). Taken together, these results could indicate that  
268 one or multiple SynCom members are able to hydrolyze orfamide A (and orfamide B) from *P.*  
269 *protegens* DTU9.1 and degrade the linearized lipopeptide.



270

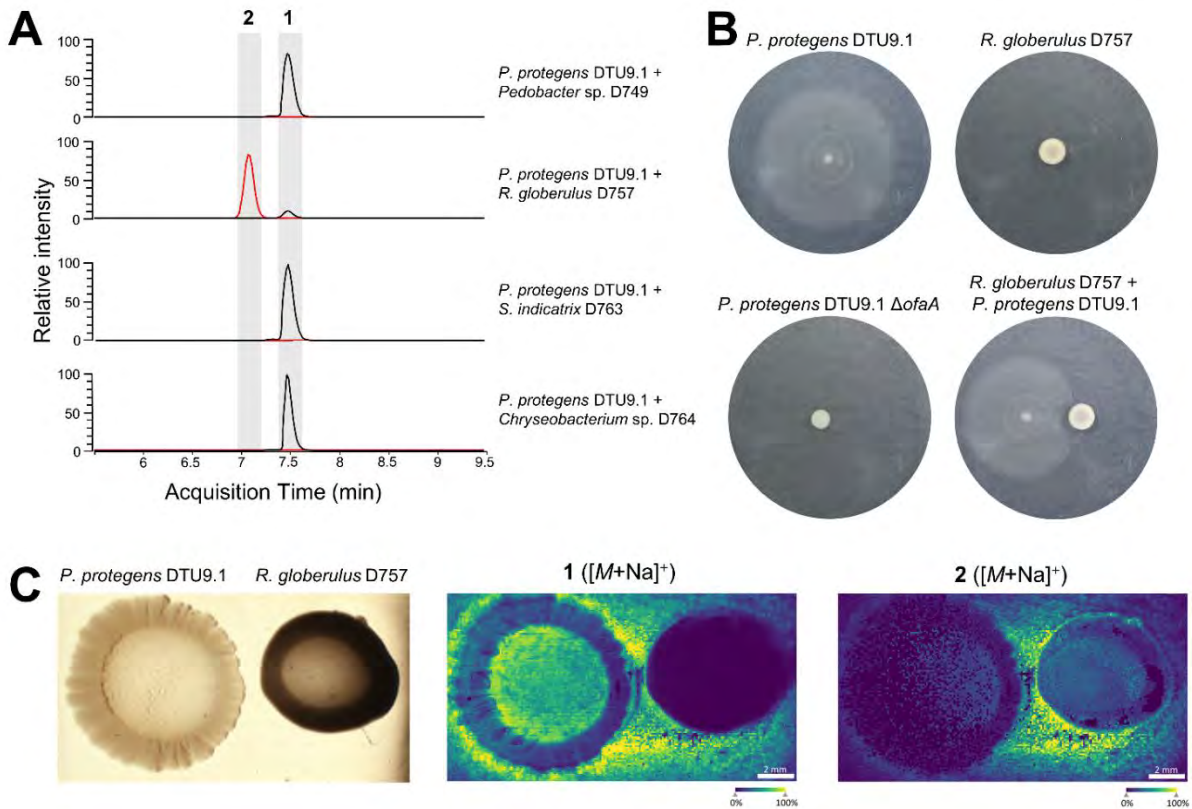
271 Figure 2 | Orfamide A is degraded during coculture of *P. protegens* DTU9.1 and SynCom in a soil-like  
 272 environment. **A**) Molecular family of metabolites related to orfamide A derived from the molecular  
 273 network (GNPS). Values next to nodes represent  $m/z$ -values and node size is scaled to metabolite mass.  
 274 Colors inside nodes represent relative abundance in the system with axenically grown *P. protegens* DTU9.1  
 275 (Cyan) or the coculture between *P. protegens* DTU9.1 and the SynCom (Red). Edges between nodes  
 276 represent molecular similarity based on cosine scores. **B**) Observed fragmentation patterns of **1** and **2**  
 277 revealed by tandem mass spectrometry (MS/MS). **C**) Structure of orfamide A (**1**). **D**) Structure of hydrolyzed  
 278 orfamide A (**2**) and the calculated masses of each degradation product.

279

280 ***R. globerulus* D757 linearizes orfamide A as a resistance mechanism and prevents**  
 281 ***Pseudomonas* swarming**

282 In order to explore the degradation of orfamide A, we turned to dual-species interactions on agar  
 283 surfaces to investigate if a single community member was responsible for linearization by hydrolysis  
 284 and degradation. First, *P. protegens* DTU9.1 was cocultivated with each of the four SynCom members  
 285 individually in mixed species colonies on 0.1x TSA. MS data of the metabolites extracted from an agar  
 286 plug covering the entire bacterial colony revealed that the Gram-positive *R. globerulus* D757 was able  
 287 to hydrolyze the ester bond of **1** yielding the linearized product, **2** (Figure 5A). Additionally, we  
 288 monitored the interaction between *P. protegens* DTU9.1 and *R. globerulus* D757 by MALDI Mass

289 Spectrometry Imaging (MALDI-IMS) to validate that the linearization of orfamide A indeed occurs  
 290 extracellularly in the interface between the two bacteria. The two species were cultivated for 4 days  
 291 on 0.1x TSA plate prior to matrix application and imaging. As displayed in Figure 5C, orfamide A (**1**)  
 292 was secreted evenly around the *P. protegens* DTU9.1 colony, while the linearized product (**2**) was  
 293 observed only in the interface between the two bacteria.



294

295 Figure 3 | *Rhodococcus* linearizes Orfamide A as a defensive anti-swarming mechanism. **A)** Extracted ion  
 296 chromatograms (EIC) for **1** (black,  $m/z$  1295.8436  $\pm$  5 ppm) and **2** (red,  $m/z$  1313.8542  $\pm$  5 ppm) detected  
 297 in agar plugs from co-cultures of *P. protegens* DTU9.1 and the respective SynCom member on 0.1x TSA  
 298 plates. **B)** Swarming assay of *P. protegens* DTU9.1 and *R. globerulus* D757 on soft 0.1x TSA plates. **C)** MALDI  
 299 imaging of colonies of *P. protegens* DTU9.1 and *R. globerulus* D757 showing hydrolysis of Orfamide A after  
 300 4 days of incubation.

301

302 Lastly, we investigated the impact of linearizing orfamide A on the swarming motility of *P. protegens*  
 303 DTU9.1. Initially, *R. globerulus* D757 was cultivated for 24 hours on soft 0.1x TSA prior to adding *P.*  
 304 *protegens* DTU9.1 to allow for production and secretion of esterases capable of hydrolyzing the ester  
 305 bond of orfamide A. Subsequently, *P. protegens* DTU9.1 was added at a distance of 15mm to the edge

306 of the *Rhodococcus* colony and plates incubated for another 48 hours. As observed in Figure 5B,  
307 orfamide A is essential to the swarming motility of *P. protegens* DTU9.1, since the  $\Delta ofaA$  mutant had  
308 completely lost the ability to swarm. Interestingly, a clearing zone appeared in the interface between  
309 *Rhodococcus* and *Pseudomonas*, suggesting that linearization of orfamide A is sufficient to inhibit the  
310 swarming motility (Figure 5B). This could further indicate that *R. globerulus* D757 hydrolyses orfamide  
311 A as a defensive mechanism to inhibit the invasive spread of *P. protegens* DTU9.1. Finally, we also note  
312 that neither of the degradation products observed in Figure 2A could be detected in either of the dual-  
313 species interactions. Thus, degradation of orfamide A might be a sequential event following hydrolysis  
314 involving one or more of the remaining three SynCom members.

## 315 Discussion

316 In this study we utilized a four-membered bacterial SynCom cultivated in an artificial hydrogel soil  
317 environment to evaluate the contribution of secondary metabolites from a *P. protegens* strain on the  
318 ability of the *Pseudomonas* to invade and establish within the simplified microcosm. This experimental  
319 approach has several appealing advantages, including simple monitoring of community perturbations  
320 and extraction of secondary metabolites for chemical analysis. Similarly, Bodenhausen et al.  
321 demonstrated the use of a defined synthetic community approach to investigate the effect of plant  
322 genotypes on community composition (19). Although the genotypic complexity of our four-membered  
323 SynCom is far from a representation of the natural soil microbial diversity (1, 6), the simplified system  
324 applied in this study has allowed for the systematic analysis of community-level interactions affecting  
325 secondary metabolism in *P. protegens* DTU9.1. We demonstrated that *P. protegens* readily invaded  
326 and altered the community composition. Unexpectedly, mutants unable to produce these antibiotics  
327 invaded the community as efficiently as wildtype producers did and caused similar perturbations in  
328 the composition of the synthetic community (Figure 1). The absence of a clear antibiotic-mediated  
329 impact on the otherwise antibiotic-sensitive SynCom members (Table 1 and Figure S3) was not a result  
330 of low, non-toxic levels of antibiotics (Table 2). Similarly, previous studies reported the lack of advert  
331 effects on indigenous microorganisms *in situ* upon introduction of the biocontrol strain, *P. protegens*  
332 CHA0, despite large fractions of subsequently isolated rhizobacteria displaying sensitivity towards  
333 antimicrobial metabolites produced by the biocontrol strain *in vitro* (41, 42). This could suggest that  
334 sensitive bacteria either colonize distinct niches separated from the antibiotic-producing biocontrol  
335 strain *in situ* or that naturally co-occurring microorganisms sustain toxic levels of antimicrobial  
336 metabolites via community-level resistance mechanisms, such as multi-species biofilm formation (43)  
337 or enzymatic inactivation of antimicrobial metabolites (44).

338 Microbial interactions among co-existing microorganisms have been studied extensively over the past  
339 decade to identify and understand the diverse means by which these microbes communicate and

340 compete. Foster and Bell reported that interspecies competition among bacteria isolated from the  
341 same site was the far most dominant type of interaction (45). This could suggest that bacteria have  
342 evolved intricate sensing mechanisms to respond to danger cues secreted by competing organisms  
343 (38, 46). In our study we found that the invading *P. protegens* DTU9.1 significantly increased its  
344 production of the antimicrobial metabolites, DAPG and pyoluteorin, during cocultivation with the  
345 four-membered SynCom (Table 2). This could suggest that the biosynthesis of these metabolites is  
346 induced in *P. protegens* as a response to cues secreted by one or more competing members of the  
347 SynCom. However, as shown in Figure 1, the perturbations in community composition were affected  
348 mostly by the invasion of *Pseudomonas* and only slightly by the production of secondary metabolites.  
349 Simultaneously, the concentration of pyoluteorin exceeded the minimal inhibitory concentration  
350 towards *Pedobacter* sp. D749, *R. globerulus* D757, and *Chryseobacterium* sp. D764 on the seventh day  
351 of the experiment. Robleto et al. found that introduction of a trifolitoxin-producing *Rhizobium etli*  
352 strain into the rhizosphere of bean plants dramatically reduced the diversity of trifolitoxin-sensitive  
353 bacteria, while sparing the remaining microbiome (47). Thus, an extended incubation time of our  
354 hydrogel bead systems could reveal the effects of induced pyoluteorin production leading to a  
355 reduction or extinction of pyoluteorin-sensitive SynCom members.

356 Additionally, we observed a significant reduction in the concentration of the nonribosomal cyclic  
357 lipopeptide, orfamide A, during cocultivation of *P. protegens* DTU9.1 and the four-membered SynCom.  
358 Lipopeptides from fluorescent *Pseudomonas* are versatile metabolites most notably known for their  
359 antimicrobial properties and involvement in bacterial motility (48, 49). Particularly, Gram-positive  
360 bacteria have been associated with increased susceptibility towards lipopeptides, due to the lack of a  
361 protective cell wall (50). On the other hand, it has been reported that many Gram-positive  
362 Actinobacteria possess resistance mechanisms towards lipopeptides mediated by enzymatic  
363 inactivation (51, 52). In our study, secondary metabolites were extracted from the hydrogel bead  
364 systems and analyzed by HR-LCMS on the seventh and final day of the experiment. By incorporating  
365 Global Natural Products Social networking on the MS data, we identified a molecular family related to

366 orfamide A upon invasion of *P. protegens* DTU9.1 into the microbial SynCom (Figure 2A). The  $m/z$ -  
367 value of one molecule, **2** ( $m/z$  1313.8542), corresponded to the exact mass of orfamide A with the  
368 addition of a water molecule. This could suggest enzyme-catalyzed hydrolysis of one of seven amide  
369 linkages or hydrolysis of the thermodynamically more sensitive ester bond connecting the macrocyclic  
370 ring. Tandem mass-spectrometry confirmed the latter case (Figure 2B). By performing pairwise dual-  
371 species cocultivations between *P. protegens* DTU9.1 and each of the SynCom members on an agar  
372 surface, we subsequently identified the Gram-positive *R. globerulus* D757 as responsible for the  
373 hydrolysis of orfamide A (Figure 3). According to D'Costa et al., hydrolysis of the ester bond was the  
374 most common resistance mechanism by which Actinobacteria enzymatically inactivated cyclic  
375 lipopeptides (52). MALDI imaging further revealed the hydrolysis to be caused by a secreted enzyme  
376 (Figure 3C). This prompted us to search the genome of *R. globerulus* D757 for annotated extracellular  
377 esterases, as D'Costa et al. could demonstrate that ring-opening by hydrolysis was caused by a single  
378 esterase in *Streptomyces* sp. WAC4713 (52). Three candidate genes were identified in *R. globerulus*  
379 D757, while none of the other SynCom members possessed genes encoding extracellular esterases.  
380 Thus, a future study may involve either heterologous expression of these genes followed by protein  
381 purification or construction of knock-out mutants in *R. globerulus* D757 to identify the enzyme capable  
382 of hydrolyzing orfamide A.

383 While enzymatic inactivation of orfamide A is a resistance mechanism in *R. globerulus* D757, this  
384 biotransformation could also be a prerequisite for subsequent degradation by one or more of the  
385 other SynCom members (Figure 2A). Therefore, the linearization of orfamide A may alter its natural  
386 role. The biotransformation of *Pseudomonas*-produced cyclic lipopeptides has been reported recently  
387 (21, 53). Zhang et al. found that coculture between a *Pseudomonas* and a *Paenibacillus* strain led to  
388 the enzymatic modification of syringafactin, thus changing the chemical structure of the lipopeptide  
389 giving it amoebicidal properties (21). Likewise, Hermenau et al. demonstrated that Gram-positive  
390 *Mycetocola* strains could disarm the activity of the mushroom pathogen, *P. tolaasii*, by hydrolysis of  
391 the ester bonds in both *Pseudomonas*-produced cyclic lipopeptides, tolaasin I and pseudodesmin A,

392 thus preventing pathogenesis (53). In our study, we identified multiple degradation products of  
393 orfamide A (Figure 2A). The dual-species cocultures only revealed hydrolysis of orfamide A by *R.*  
394 *globerulus* D757, while none of the degradation products were observed (Figure 3A). This could  
395 suggest that the linearized product of orfamide A, **2**, represents a potential food-source to be  
396 catabolized by one or more of the remaining SynCom members. A pioneering study has previously  
397 demonstrated the ability of isolated soil bacteria to utilize penicillin as sole carbon source to support  
398 growth by enzymatically catabolizing the antibiotic (54). Here, we utilized a synthetic community  
399 approach to discover a novel potential community-level inactivation and degradation of an  
400 antimicrobial metabolite. Further investigation of the impact of orfamide A catabolism will be the  
401 subject for future studies.

402

## 403 **Conclusion**

404 In summary, by utilizing a synthetic community approach we found that antimicrobial secondary  
405 metabolites from a *P. protegens* strain contribute marginally to the ability of the *Pseudomonas* to  
406 invade and establish within a four-membered SynCom, despite the concentration of pyoluteorin and  
407 orfamide A reaching toxic levels. Secondly, we demonstrated that cocultivation of *P. protegens* DTU9.1  
408 and the SynCom significantly altered the production and presence of the *Pseudomonas*-produced  
409 metabolites. Most notably, we observed the enzymatic inactivation of orfamide A caused by the  
410 antibiotic-sensitive strain, *R. globerulus* D757. Interestingly, the hydrolysis-mediated linearization of  
411 orfamide A might serve as a prerequisite for subsequent degradation, thus representing a novel,  
412 community-level catabolism of an antimicrobial secondary metabolite. Altogether, our study  
413 emphasizes the value of synthetic community approaches to investigate the impact of secondary  
414 metabolites on indigenous microorganisms, as well as the effects of microbial interactions affecting  
415 the biosynthesis and fate of those secondary metabolites.

## 416 **Methods**

### 417 **Microorganisms and cultivation**

418 Plasmid cloning was performed in *Escherichia coli* CC118- $\lambda$ pir. Cells were cultured in Luria-Bertani (LB)  
419 broth (Lennox, Merck, St. Louis, MO, USA) with appropriate antibiotics. The antibiotic concentration  
420 used was 10  $\mu\text{g ml}^{-1}$  for chloramphenicol, and 8  $\mu\text{g ml}^{-1}$  and 50  $\mu\text{g ml}^{-1}$  for tetracycline for *E. coli* and  
421 *P. protegens*, respectively. *E. coli* CC118  $\lambda$ pir was cultured by inoculating a single colony in 5 ml LB  
422 broth and incubating overnight at 37° C with shaking (200 rpm). *P. protegens* DTU9.1 and members of  
423 the semi-synthetic community were cultured by inoculating a single colony in 5 ml LB broth and  
424 incubating overnight at 30° C with shaking (200 rpm). The community members include *Pedobacter*  
425 sp. D749 (Accession: CP079218), *R. globerulus* D757 (Accession: CP079698), *S. indicatrix* D763  
426 (Accession: CP079106), and *Chryseobacterium* sp. D764 (Accession: CP079219).

### 427 **Generation of secondary metabolite deficient mutants**

428 To generate mutants in *P. protegens* DTU9.1 incapable of synthesizing DAPG, pyoluteorin and  
429 orfamide A, genes required for biosynthesis were deleted by allelic replacement according to Hmelo  
430 et al. (55). Primers used for cloning and verification are summarized in Supplementary Table 1. In  
431 short, DNA fragments directly upstream and directly downstream of *the gene of interest* were PCR  
432 amplified. The fragments were joined by splicing-by-overlap extension PCR with XbaI and SacI  
433 overhangs. The purified PCR product was restriction-digested and inserted in pNJ1 (56). The resulting  
434 plasmid was mobilized into *P. protegens* DTU9.1 via triparental mating with *E. coli* HB101 harboring  
435 the helper plasmid pRK600. Merodiploid transconjugants were initially selected on *Pseudomonas*  
436 Isolation Agar (PIA, Merck) supplemented with 50  $\mu\text{g ml}^{-1}$  tetracycline. A second selection was  
437 performed on NSLB agar (10 g l<sup>-1</sup> tryptone, 5 g l<sup>-1</sup> yeast extract, 15 g l<sup>-1</sup> Bacto agar) with 15% v/v  
438 sucrose. Candidates for successful deletion were confirmed by PCR and verified by Sanger sequencing  
439 at Eurofins Genomics.

440

#### 441 **Inhibition assays**

442 The *in vitro* inhibitory effect of *P. protegens* DTU9.1 and the secondary metabolite deficient mutants  
443 was examined with agar plate inhibition assays. The members of the synthetic microbial community  
444 were the target bacteria. For the antibacterial inhibition assay, cultures of *P. protegens* DTU9.1 WT,  
445  $\Delta phlACB$ ,  $\Delta pltA$  and  $\Delta ofaA$  were grown O/N. The cultures were washed twice in 0.9% (w/v) NaCl at  
446 10,000 rpm for 1 minute followed by measuring the optical density at OD<sub>600</sub>. The optical density was  
447 set to 1.0 and 10 $\mu$ l bacterial suspension was spotted on 0.1x Tryptic Soy Agar (TSA, Sigma). The plates  
448 were incubated at RT for 24 hours to allow for secondary metabolite production. O/N cultures of the  
449 target bacteria were prepared in LB media. After 24 hours of incubation, the *Pseudomonas* on the 0.1x  
450 TSA plates were killed with chloroform vapors for 30 minutes, followed by evaporation of residual  
451 chloroform in a fume hood for another 30 minutes. The optical density at OD<sub>600</sub> of the target bacteria  
452 was set to 2.0 and 500 $\mu$ l was added to 6ml 0.1x Tryptic Soy Broth (TSB, Sigma) containing 0.3% agar  
453 pre-heated to 42°C. The soft agar was spread evenly on top of the 0.1x TSA plates with killed  
454 *Pseudomonas* and incubated at RT for 48 hours followed by examining the inhibition zones.

#### 455 **Integration of *P. protegens* DTU9.1 in a semi-synthetic microbial community**

456 The effect of introducing *P. protegens* DTU9.1 and the above-mentioned secondary metabolite-  
457 deficient mutants into a semi-synthetic bacterial community was investigated in an artificial soil  
458 medium composed of spherical hydrogel beads. The beads were prepared according to Ma et al. (20).  
459 In short, a polymer solution was prepared as a 4:1 mixture of 9.6 g l<sup>-1</sup> gellan gum (Phytigel™, Sigma)  
460 and 2.4 g l<sup>-1</sup> sodium alginate (Sigma) dissolved in distilled water. Spherical beads with a diameter of  
461 approximately 3-4 mm were formed by dropping polymer solution into a cross-linker solution  
462 containing 20 g l<sup>-1</sup> CaCl<sub>2</sub> with a 10 ml syringe. Then, the beads were soaked in 0.1x TSB (Sigma) for 1  
463 hour followed by sieving the beads to remove residual TSB medium. Finally, 20 ml beads were  
464 transferred to a 50 ml Falcon tubes. Cultures of the four community members and *P. protegens* WT  
465  $\Delta phlACB$ ,  $\Delta pltA$  and  $\Delta ofaA$  were grown O/N. The optical density at OD<sub>600</sub> of *Pedobacter* and  
466 *Rhodococcus* was set to 2.0, for *Stenotrophomonas* and *Chryseobacterium* it was set to 0.1 and for *P.*

467 *protegens* DTU9.1 and mutants it was set to 0.001. Bacterial inoculation suspensions were prepared  
468 by mixing equal volumes in a total volume of 2 ml. Lastly, the prepared beads were inoculated with  
469 the 2 ml bacterial suspension. Inoculated bead systems were incubated static at RT and samples  
470 collected after 1, 4 and 7 days. Sampling was performed by briefly shaking the bead systems followed  
471 by extracting approximately 1 ml beads into new 15 ml Falcon tubes. Extracted beads were  
472 subsequently diluted in 0.9% (w/v) NaCl according to their weight to normalize the amount of bacterial  
473 cells. The tubes were shaken on a vortex for 10 minutes at maximum speed to disrupt the hydrogel  
474 beads. After vortexing, dilutions were spread on 0.1x TSA plates and incubated at RT for 48 hours  
475 before counting CFU/ml. The remaining liquid (approx. 5 ml) of the processed samples were saved for  
476 chemical detection of secondary metabolites.

#### 477 **Detection of secondary metabolites with LC-MS**

478 To extract secondary metabolites in the hydrogel bead samples, 5 ml isopropanol:ethyl acetate (1:3,  
479 v/v), containing 1% formic acid was added to the samples followed by shaking the tubes briefly. The  
480 tubes were centrifuged for 3 minutes at 4650 x g. Extracts were then evaporated under N<sub>2</sub> O/N. The  
481 dried extracts were re-suspended in 200 µl methanol (MeOH) and centrifuged for 3 minutes at 4650  
482 x g. The supernatant was transferred to HPLC vials and subjected to ultra high-performance liquid  
483 chromatography-high resolution electrospray ionization mass spectrometry (UHPLC-HRESIMS)  
484 analysis.

485 HR-LCMS was performed on an Agilent Infinity 1290 UHPLC system. Liquid chromatography of 1 µl or  
486 5 µl extract was performed using an Agilent Poroshell 120 phenyl-C<sub>6</sub>column (2.1 × 150 mm, 1.9 µm) at  
487 60 °C using CH<sub>3</sub>CN and H<sub>2</sub>O, both containing 20 mM FA. Initially, a linear gradient of 10% CH<sub>3</sub>CN/H<sub>2</sub>O  
488 to 100% CH<sub>3</sub>CN over 10 min was employed, followed by isocratic elution of 100% CH<sub>3</sub>CN for 2 min.  
489 Then, the gradient was returned to 10% CH<sub>3</sub>CN/H<sub>2</sub>O in 0.1 min and finally isocratic condition of 10%  
490 CH<sub>3</sub>CN/H<sub>2</sub>O for 1.9 min, all at a flow rate of 0.35 min ml<sup>-1</sup>. HRMS data was recorded in positive  
491 ionization on an Agilent 6545 QTOF MS equipped with an Agilent Dual Jet Stream electrospray ion  
492 (ESI) source with a drying gas temperature of 250°C, drying gas flow of 8 min l<sup>-1</sup>, sheath gas

493 temperature of 300°C and sheath gas flow of 12 min l<sup>-1</sup>. Capillary voltage was 4000 V and nozzle  
494 voltage was set to 500 V. The HRMS data was processed and analyzed using Agilent MassHunter  
495 Qualitative Analysis B.07.00. HPLC grade solvents (VWR Chemicals) were used for extractions while  
496 LCMS grade solvents (VWR Chemicals) were used for LCMS.

#### 497 **GNPS molecular networking**

498 A molecular network was created using the Feature-Based Molecular Networking (57) workflow on  
499 GNPS (<https://gnps.ucsd.edu>, (39)). The workflow run can be found at this link:

500 <https://gnps.ucsd.edu/ProteoSAFe/status.jsp?task=1ad207802221433ca5431d22f2638d0e>. Raw

501 data was processed using MZmine2.53 (58). Data was filtered by removing all MS/MS fragment ions  
502 within +/- 17 Da of the precursor m/z. MS/MS spectra were window filtered by choosing only the top  
503 6 fragment ions in the +/- 50 Da window throughout the spectrum. Additional settings include:  
504 precursor ion mass tolerance was set to 0.05 Da, MS/MS fragment ion tolerance to 0.05 Da, and edges  
505 were filtered to have a cosine score above 0.7 and more than 10 matched peaks. The spectra in the  
506 network were then searched against GNPS spectral libraries (39, 59). The library spectra were filtered  
507 in the same manner as the input data. All matches kept between network spectra and library spectra  
508 were required to have a score above 0.7 and at least 6 matched peaks. The DEREPLICATOR was used  
509 to annotate MS/MS spectra (60). The molecular networks were visualized using Cytoscape 3.8.2 (61).

#### 510 **Swarming assay**

511 SynCom members were cultured O/N and cell pellets washed twice with 0.9% NaCl followed by  
512 adjusting OD<sub>600</sub> to 1.0. Bacterial suspensions (5 µl) were spotted on soft 0.1x TSA (0.6% agar) and  
513 incubated for 24 hours at RT. Simultaneously, *P. protegens* DTU9.1 was grown O/N. Cells were washed  
514 twice with 0.9% NaCl and OD<sub>600</sub> adjusted to 1.0. The bacterial suspension (5 µl) was spotted 15 mm  
515 from the edge of each SynCom member. Plates were incubated for another 48 hours at RT before  
516 pictures were taken.

## 517 **MALDI Sample preparation**

518 Bacterial strains were cultured on 10 ml 0.1x TSA plates at 22°C. After 4 days of incubation, the  
519 microbial colony and surrounding agar was sectioned and mounted on an IntelliSlides conductive tin  
520 oxide glass slide (Bruker). The sample was covered with matrix by spraying 1.75 ml of a matrix solution  
521 in a nitrogen atmosphere. The matrix solution was 2,5-dihydrobenzoic acid (DHB) of 20 mg ml<sup>-1</sup>  
522 concentration in ACN/MeOH/H<sub>2</sub>O (70:25:5, v/v/v) according to (62).

## 523 **MALDI Imaging Mass Spectrometry (IMS)**

524 Sample was dried in a desiccator overnight prior to IMS measurement. The sample was then subjected  
525 to timsTOF flex mass spectrometer (Bruker) for MALDI-IMS acquisition. Calibration was done using  
526 red phosphorus. The sample was run in positive MS scan mode with 100 µm raster width and a mass  
527 range of 100-2000 Da. Briefly, a photograph of the colonies was loaded onto Fleximaging software,  
528 three teach points were selected to align the background image with the sample slide, measurement  
529 regions were defined, and the automatic run mode was then employed. The settings in the  
530 timsControl were as follow: Laser: imaging 100 µm, Power Boost 3.0%, scan range 26 µm in the XY  
531 interval, and laser power 90%; Tune: Funnel 1 RF 300 Vpp, Funnel 2 RF 300 Vpp, Multipole RF 300 Vpp,  
532 isCID 0 eV, Deflection Delta 70 V, MALDI plate offset 100 V, quadrupole ion energy 5 eV, quadrupole  
533 los mass 100 *m/z*, collision energy 10 eV, focus pre TOF transfer time 75 µs, pre-pulse storage 8 µs.  
534 After data acquisition, the data was analyzed using SCiLS software.

## 535 **Statistics**

536 Multivariate analysis of community composition was performed using PERMANOVA on Bray-Curtis  
537 distances and the model formulation  $Y \sim \text{Time} + \text{Variant} + \text{Time}:\text{Variant}$ . Follow-up PERMANOVAs  
538 were performed on each time point with only Variant as the dependent variable. Univariate  
539 comparison of CFU counts and metabolite concentrations in SynCom versus axenic culture of *P.*  
540 *protegens* DTU9.1 was carried out using Student's *t*-tests assuming equal variance.

541 **References**

- 542 1. S. Bickel, D. Or, Soil bacterial diversity mediated by microscale aqueous-phase processes across  
543 biomes. *Nat. Commun.* **11**, 1–9 (2020).
- 544 2. M. Vos, A. B. Wolf, S. J. Jennings, G. A. Kowalchuk, Micro-scale determinants of bacterial  
545 diversity in soil. *FEMS Microbiol. Rev.* **37**, 936–954 (2013).
- 546 3. W. B. Whitman, D. C. Coleman, W. J. Wiebe, Prokaryotes: The unseen majority. *Proc. Natl.*  
547 *Acad. Sci.* **95**, 6578–6583 (1998).
- 548 4. E. E. Kuramae, *et al.*, Soil characteristics more strongly influence soil bacterial communities  
549 than land-use type. *FEMS Microbiol. Ecol.* **79**, 12–24 (2012).
- 550 5. C. Quince, T. P. Curtis, W. T. Sloan, The rational exploration of microbial diversity. *ISME J.* **2**,  
551 997–1006 (2008).
- 552 6. L. Roesch, *et al.*, Pyrosequencing enumerates and contrasts soil microbial diversity. *ISME J.* **1**,  
553 283–290 (2007).
- 554 7. R. Mendes, *et al.*, Deciphering the rhizosphere microbiome for disease-suppressive bacteria.  
555 *Science* **332**, 1097–1100 (2011).
- 556 8. F. Scher, R. Baker, Mechanism of Biological Control in a Fusarium-Suppressive Soil.  
557 *Phytopathology* **70**, 412–417 (1980).
- 558 9. E. Stutz, G. Défago, H. Kern, Naturally Occurring Fluorescent Pseudomonads Involved in  
559 Suppression of Black Root Rot of Tobacco. *Phytopathology* **76**, 181–185 (1986).
- 560 10. D. Haas, G. Défago, Biological control of soil-borne pathogens by fluorescent pseudomonads.  
561 *Nat. Rev. Microbiol.* **3**, 307–319 (2005).
- 562 11. J. M. Raaijmakers, M. Vlami, J. T. de Souza, Antibiotic production by bacterial biocontrol agents.  
563 *Antonie Van Leeuwenhoek* **81**, 537–547 (2002).
- 564 12. O. Marín, B. González, M. J. Poupin, From Microbial Dynamics to Functionality in the  
565 Rhizosphere: A Systematic Review of the Opportunities With Synthetic Microbial Communities.

- 566 *Front. Plant Sci.* **12**, 1–12 (2021).
- 567 13. R. Tecon, *et al.*, Bridging the Holistic-Reductionist Divide in Microbial Ecology. *mSystems* **4**, 1–  
568 5 (2019).
- 569 14. J. Raes, I. Letunic, T. Yamada, L. J. Jensen, P. Bork, Toward molecular trait-based ecology  
570 through integration of biogeochemical, geographical and metagenomic data. *Mol. Syst. Biol.* **7**,  
571 1–9 (2011).
- 572 15. J. G. Lauritsen, *et al.*, Identification and Differentiation of *Pseudomonas* Species in Field  
573 Samples Using an *rpoD* Amplicon Sequencing Methodology. *mSystems* **6**, 1–14 (2021).
- 574 16. G. T, S. OS, Synthetic microbial communities. *Curr. Opin. Microbiol.* **18**, 72–77 (2014).
- 575 17. B. Niu, J. N. Paulson, X. Zheng, R. Kolter, Simplified and representative bacterial community of  
576 maize roots. *Proc. Natl. Acad. Sci. U. S. A.* **114**, E2450–E2459 (2017).
- 577 18. R. S. C. de Souza, J. S. L. Armanhi, P. Arruda, From Microbiome to Traits: Designing Synthetic  
578 Microbial Communities for Improved Crop Resiliency. *Front. Plant Sci.* **11**, 1–7 (2020).
- 579 19. N. Bodenhausen, M. Bortfeld-Miller, M. Ackermann, J. A. Vorholt, A Synthetic Community  
580 Approach Reveals Plant Genotypes Affecting the Phyllosphere Microbiota. *PLOS Genet.* **10**,  
581 e1004283 (2014).
- 582 20. L. Ma, *et al.*, Hydrogel-based transparent soils for root phenotyping in vivo. *Proc. Natl. Acad.*  
583 *Sci. U. S. A.* **166**, 11063–11068 (2019).
- 584 21. S. Zhang, R. Mukherji, S. Chowdhury, L. Reimer, P. Stallforth, Lipopeptide-mediated bacterial  
585 interaction enables cooperative predator defense. *Proc. Natl. Acad. Sci. U. S. A.* **118**,  
586 e2013759118 (2021).
- 587 22. J. Hu, *et al.*, Probiotic diversity enhances rhizosphere microbiome function and plant disease  
588 suppression. *MBio* **7**, e01790-16 (2016).
- 589 23. L. Zhuang, *et al.*, Synthetic community with six *Pseudomonas* strains screened from garlic  
590 rhizosphere microbiome promotes plant growth. *Microb. Biotechnol.* **14**, 488–502 (2021).
- 591 24. C. Keel, *et al.*, Suppression of Root Diseases by *Pseudomonas fluorescens* CHA0: Importance of

- 592 the Bacterial Secondary Metabolite 2,4-Diacetylphloroglucinol. *Mol. Plant-Microbe Interact.* **5**,  
593 4–13 (1992).
- 594 25. C. R. Howell, R. D. Stipanovic, Control of *Rhizoctonia solani* on Cotton Seedlings with  
595 *Pseudomonas fluorescens* and With an Antibiotic Produced by the Bacterium. *Phytopathology*  
596 **69**, 480–482 (1979).
- 597 26. M. Maurhofer, C. Keel, D. Haas, G. Défago, Pyoluteorin production by *Pseudomonas*  
598 *fluorescens* strain CHA0 is involved in the suppression of *Pythium* damping-off of cress but not  
599 of cucumber. *Eur. J. Plant Pathol.* **100**, 221–232 (1994).
- 600 27. J. Y. Jang, *et al.*, Identification of orfamide A as an insecticidal metabolite produced by  
601 *Pseudomonas protegens* F6. *J. Agric. Food Chem.* **61**, 6786–6791 (2013).
- 602 28. J. M. Ligon, *et al.*, Natural products with antifungal activity from *Pseudomonas* biocontrol  
603 bacteria. *Pest Manag. Sci.* **56**, 688–695 (2000).
- 604 29. J. W. Kloepper, J. Leong, M. Teintze, M. N. Schroth, *Pseudomonas* siderophores: A mechanism  
605 explaining disease-suppressive soils. *Curr. Microbiol.* **4**, 317–320 (1980).
- 606 30. D. L. F, S. EJ, W. JM, F. JS, L. JM, Impact of Field Release of Genetically Modified *Pseudomonas*  
607 *fluorescens* on Indigenous Microbial Populations of Wheat. *Appl. Environ. Microbiol.* **61**, 3443–  
608 3453 (1995).
- 609 31. G. M, *et al.*, Impact of biocontrol *Pseudomonas fluorescens* CHA0 and a genetically modified  
610 derivative on the diversity of culturable fungi in the cucumber rhizosphere. *Appl. Environ.*  
611 *Microbiol.* **67**, 1851–1864 (2001).
- 612 32. R. Roquigny, *et al.*, Deciphering the Rhizosphere and Geocaulosphere Microbiomes of Potato  
613 Following Inoculation with the Biocontrol Agent *Pseudomonas fluorescens* Strain LBUM223.  
614 *Phytobiomes J.* **2**, 92–99 (2018).
- 615 33. K. Buddrus-Schiemann, M. Schmid, K. Schreiner, G. Welzl, A. Hartmann, Root Colonization by  
616 *Pseudomonas* sp. DSMZ 13134 and Impact on the Indigenous Rhizosphere Bacterial  
617 Community of Barley. *Microb. Ecol.* **60**, 381–393 (2010).

- 618 34. J. Kozdrój, J. T. Trevors, J. D. van Elsas, Influence of introduced potential biocontrol agents on  
619 maize seedling growth and bacterial community structure in the rhizosphere. *Soil Biol.*  
620 *Biochem.* **11**, 1775–1784 (2004).
- 621 35. J. A. Jiménez, A. Novinscak, M. Fillion, Inoculation With the Plant-Growth-Promoting  
622 Rhizobacterium *Pseudomonas fluorescens* LBUM677 Impacts the Rhizosphere Microbiome of  
623 Three Oilseed Crops. *Front. Microbiol.* **11**, 1–15 (2020).
- 624 36. S. Castro-Sowinski, Y. Herchkovitz, Y. Okon, E. Jurkevitch, Effects of inoculation with plant  
625 growth-promoting rhizobacteria on resident rhizosphere microorganisms. *FEMS Microbiol.*  
626 *Lett.* **276**, 1–11 (2007).
- 627 37. C. N. Lozano-Andrade, M. Wibowo, M. L. Strube, Á. T. Kovács, Synthetic community invasion  
628 depends on secondary metabolite production in *Bacillus subtilis*. *Manuscr. prep.* (2021).
- 629 38. D. M. Cornforth, K. R. Foster, Competition sensing: the social side of bacterial stress responses.  
630 *Nat. Rev. Microbiol.* **11**, 285–293 (2013).
- 631 39. M. Wang, *et al.*, Sharing and community curation of mass spectrometry data with Global  
632 Natural Products Social Molecular Networking. *Nat. Biotechnol.* **34**, 828–837 (2016).
- 633 40. C. N. Lozano-Andrade, M. L. Strube, Á. T. Kovács, Complete genome sequences of four soil-  
634 derived isolates for studying synthetic microbial community assembly. *Manuscr. prep.* (2021).
- 635 41. A. Natsch, C. Keel, N. Hebecker, E. Laasik, G. Défago, Impact of *Pseudomonas fluorescens* strain  
636 CHA0 and a derivative with improved biocontrol activity on the culturable resident bacterial  
637 community on cucumber roots. *FEMS Microbiol. Ecol.* **27**, 365–380 (1998).
- 638 42. J. E. Johansen, *et al.*, Impact of biocontrol strain *Pseudomonas fluorescens* CHA0 on  
639 rhizosphere bacteria isolated from barley (*Hordeum vulgare* L.) with special reference to  
640 Cytophaga-like bacteria. *J. Appl. Microbiol.* **93**, 1065–1074 (2002).
- 641 43. B. M, *et al.*, Enhanced biofilm formation and increased resistance to antimicrobial agents and  
642 bacterial invasion are caused by synergistic interactions in multispecies biofilms. *Appl. Environ.*  
643 *Microbiol.* **72**, 3916–3923 (2006).

- 644 44. J. Davies, Inactivation of Antibiotics and the Dissemination of Resistance Genes. *Science* **264**,  
645 375–382 (1994).
- 646 45. K. R. Foster, T. Bell, Competition, Not Cooperation, Dominates Interactions among Culturable  
647 Microbial Species. *Curr. Biol.* **22**, 1845–1850 (2012).
- 648 46. S. Westhoff, G. P. van Wezel, D. E. Rozen, Distance-dependent danger responses in bacteria.  
649 *Curr. Opin. Microbiol.* **36**, 95–101 (2017).
- 650 47. E. A. Robleto, J. Borneman, E. W. Triplett, Effects of bacterial antibiotic production on  
651 rhizosphere microbial communities from a culture-independent perspective. *Appl. Environ.*  
652 *Microbiol.* **64**, 5020–5022 (1998).
- 653 48. S. Götze, P. Stallforth, Structure, properties, and biological functions of nonribosomal  
654 lipopeptides from pseudomonads. *Nat. Prod. Rep.* **37**, 29–54 (2020).
- 655 49. J. M. Raaijmakers, I. De Bruijn, O. Nybroe, M. Ongena, Natural functions of lipopeptides from  
656 *Bacillus* and *Pseudomonas*: more than surfactants and antibiotics. *FEMS Microbiol. Rev.* **34**,  
657 1037–1062 (2010).
- 658 50. N. Geudens, J. C. Martins, Cyclic Lipodepsipeptides From *Pseudomonas* spp. – Biological Swiss-  
659 Army Knives. *Front. Microbiol.* **9**, 1–18 (2018).
- 660 51. V. M. D’Costa, K. M. McGrann, D. W. Hughes, G. D. Wright, Sampling the Antibiotic Resistome.  
661 *Science* **311**, 374–377 (2006).
- 662 52. V. M. D’Costa, *et al.*, Inactivation of the lipopeptide antibiotic daptomycin by hydrolytic  
663 mechanisms. *Antimicrob. Agents Chemother.* **56**, 757–764 (2012).
- 664 53. R. Hermenau, S. Kugel, A. J. Komor, C. Hertweck, Helper bacteria halt and disarm mushroom  
665 pathogens by linearizing structurally diverse cyclolipopeptides. *Proc. Natl. Acad. Sci. U. S. A.*  
666 **117**, 23802–23806 (2020).
- 667 54. T. S. Crofts, *et al.*, Shared strategies for  $\beta$ -lactam catabolism in the soil microbiome. *Nat. Chem.*  
668 *Biol.* **14**, 556–564 (2018).
- 669 55. L. R. Hmelo, *et al.*, Precision-engineering the *Pseudomonas aeruginosa* genome with two-step

- 670 allelic exchange. *Nat. Protoc.* **10**, 1820–1841 (2015).
- 671 56. L. Yang, *et al.*, Polysaccharides serve as scaffold of biofilms formed by mucoid *Pseudomonas*  
672 *aeruginosa*. *FEMS Immunol. Med. Microbiol.* **65**, 366–376 (2012).
- 673 57. L.-F. Nothias, *et al.*, Feature-based molecular networking in the GNPS analysis environment.  
674 *Nat. Methods* **17**, 905–908 (2020).
- 675 58. T. Pluskal, S. Castillo, A. Villar-Briones, M. Orešič, MZmine 2: Modular framework for  
676 processing, visualizing, and analyzing mass spectrometry-based molecular profile data. *BMC*  
677 *Bioinformatics* **11**, 1–11 (2010).
- 678 59. H. Horai, *et al.*, MassBank: a public repository for sharing mass spectral data for life sciences.  
679 *J. Mass Spectrom.* **45**, 703–714 (2010).
- 680 60. H. Mohimani, *et al.*, Dereplication of microbial metabolites through database search of mass  
681 spectra. *Nat. Commun.* **9**, 1–12 (2018).
- 682 61. P. Shannon, *et al.*, Cytoscape: A Software Environment for Integrated Models of Biomolecular  
683 Interaction Networks. *Genome Res.* **13**, 2498–2504 (2003).
- 684 62. W. L. Friesen, *et al.*, Two-Dimensional Graphene as a Matrix for MALDI Imaging Mass  
685 Spectrometry. *J. Am. Soc. Mass Spectrom.* **26**, 1963–1966 (2015).
- 686

687 **Supplementary**688 **Supplementary Table 1**

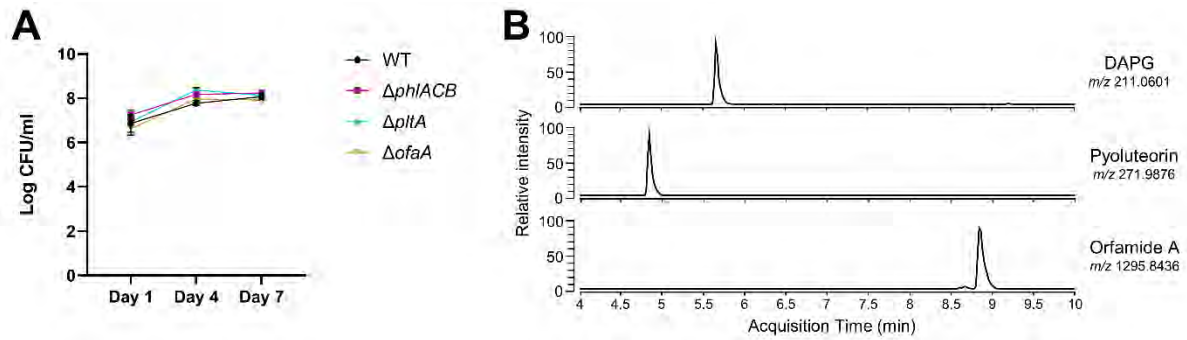
<b>Name</b>	<b>Sequence<sup>a,b,c</sup></b>	<b>Note</b>
<b><i>phiACB</i> deletion</b>		
Up_F <sub><i>phiA</i></sub>	5'- <u>atcccg</u> <u>tctaga</u> CAGAGATTTGCGAGTAAAAAG	Amplification of homology region upstream of <i>phiA</i>
Up-R <sub><i>phiA</i></sub>	5'- <b>catcgacgatttccgaagcgatcac</b> TTTCCTCTTGA TTCCATTCTTTTC	Amplification of homology region upstream of <i>phiA</i>
Down_F <sub><i>phiB</i></sub>	5'- GTGATCGCTTCGGAAATCG	Amplification of homology region downstream of <i>phiB</i>
Down_R <sub><i>phiB</i></sub>	5'- <u>atccgggagctc</u> ACAACGAGGAGAATTCCAG	Amplification of homology region downstream of <i>phiB</i>
<i>phiACB</i> -del_fw	5'- GTGCGAGTTCAATCATCTGG	Verification of <i>phiACB</i> deletion
<i>phiACB</i> -del_rev	5'- CTCTCGTAGTTGAGCCGTTTC	Verification of <i>phiACB</i> deletion
<b><i>pltA</i> deletion</b>		
Up_F <sub><i>pltA</i></sub>	5'- <u>atcccg</u> <u>tctaga</u> AGCGCCTTCATTCTAAATC	Amplification of homology region upstream of <i>pltA</i>
Up-R <sub><i>pltA</i></sub>	5'- <b>gatgcaaagtaatgcatcgaag</b> TGCCCACT CCCTGTTAGGC	Amplification of homology region upstream of <i>pltA</i>
Down_F <sub><i>pltA</i></sub>	5'- CTTCGATGCGCATTACTTTG	Amplification of homology region downstream of <i>pltA</i>
Down_R <sub><i>pltA</i></sub>	5'- <u>atccgggagctc</u> CTGTCCAGCGAAGAGAGTT	Amplification of homology region downstream of <i>pltA</i>
<i>pltA</i> -del_fw	5'- GTTCTTTGCATGTTGAGAAAGAGCAG	Verification of <i>pltA</i> deletion
<i>pltA</i> -del_rev	5'- GGAACGCTCCAGTCCACC	Verification of <i>pltA</i> deletion
<b><i>ofaA</i> deletion</b>		
Up_F <sub><i>ofaA</i></sub>	5'- <u>atcccg</u> <u>tctaga</u> CTGCGACAGGCTTTGAG AAAC	Amplification of homology region upstream of <i>ofaA</i>
Up-R <sub><i>ofaA</i></sub>	5'- <b>ccggcggggaaaagcacttgacgagcc</b> TTCA TGCGCGCCCC	Amplification of homology region upstream of <i>ofaA</i>
Down_F <sub><i>ofaA</i></sub>	5'- GGCCGCTGCAAGTGCTTTTC	Amplification of homology region downstream of <i>ofaA</i>
Down_R <sub><i>ofaA</i></sub>	5'- <u>atccgggagctc</u> CCAGATGTTGCGAA ACGGTAC	Amplification of homology region downstream of <i>ofaA</i>
<i>ofaA</i> -del_fw	5'- CGCATTGATCAGCCTCGTAC	Verification of <i>ofaA</i> deletion
<i>ofaA</i> -del_rev	5'- GTAGTTGAGCATGGCGCTGAAC	Verification of <i>ofaA</i> deletion

689

690 a. CAPITAL letters represent the priming part

691 b. Underlined characters represent restriction sites attached as primer overhang692 c. **Bold** characters represent the first 25 nucleotides downstream of the region targeted for

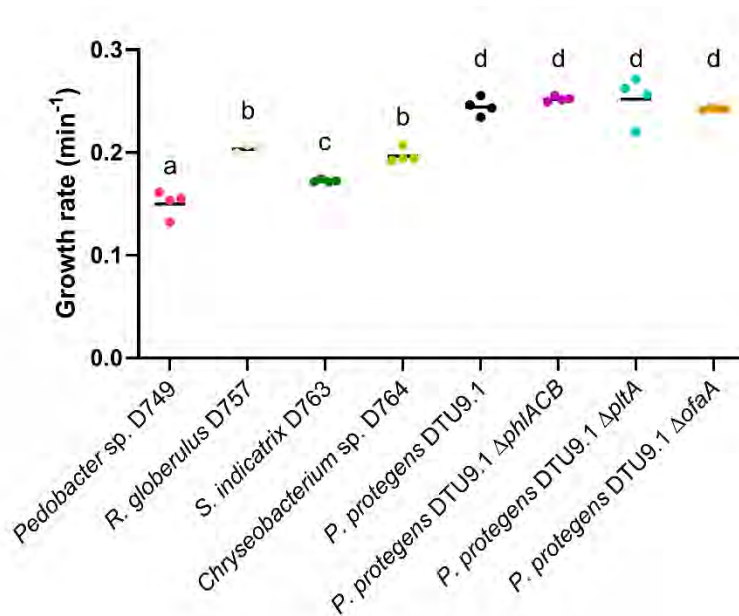
693 deletion to achieve successful overlap-extension PCR



694

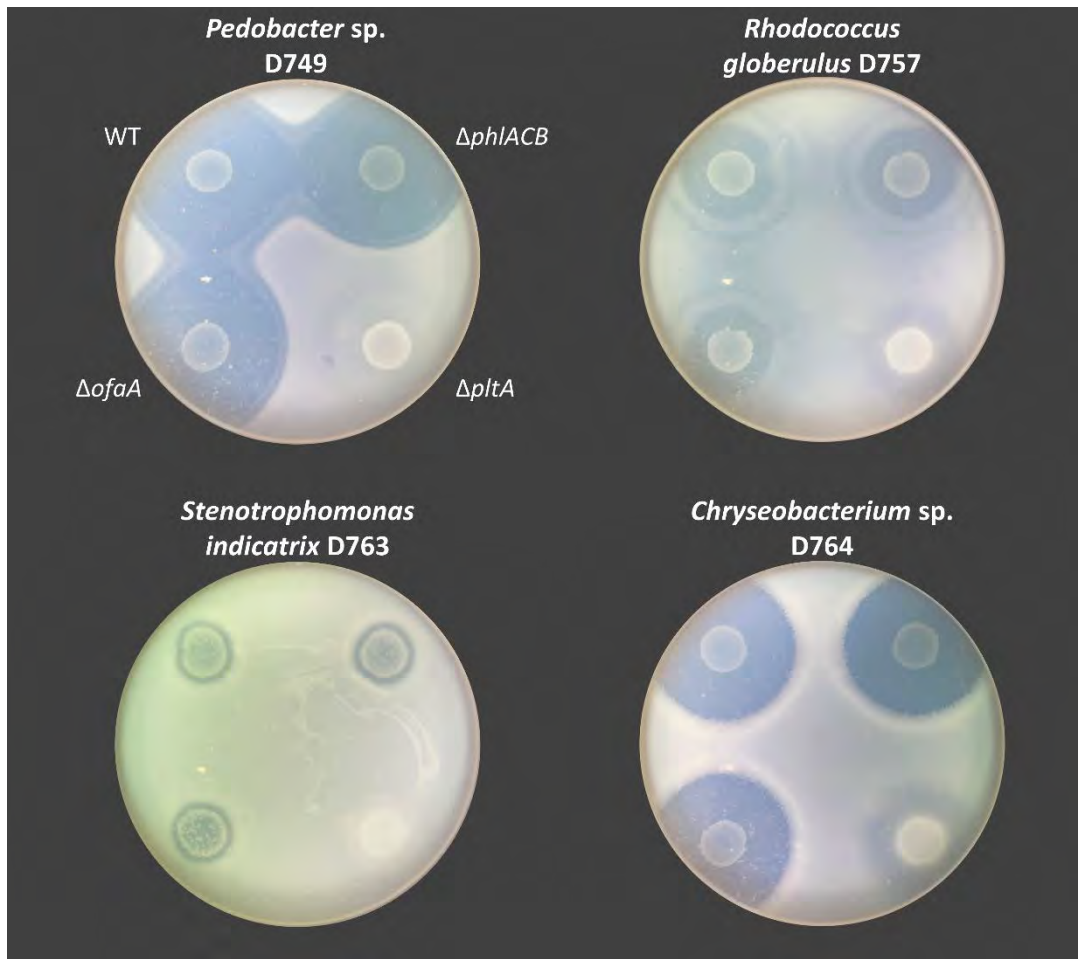
695 Figure S1 | *P. protegens* DTU9.1 thrives in a soil-like environment. **A)** Growth curves of *P. protegens* DTU9.1 WT,  
 696  $\Delta phlACB$ ,  $\Delta pltA$  and  $\Delta ofaA$  in the hydrogel bead system. Samples were collected after 1, 4 and 7 days from three  
 697 biological replicates. **B)** Extracted ion chromatograms (EIC) for DAPG ( $m/z$  211.0601  $\pm$  5 ppm), Pyoluteorin ( $m/z$   
 698 271.9876  $\pm$  5 ppm) and orfamide A ( $m/z$  1295.8436  $\pm$  5 ppm) confirm the production of these secondary  
 699 metabolites after 7 days of growth of *P. protegens* DTU9.1 WT in the hydrogel bead system.

700



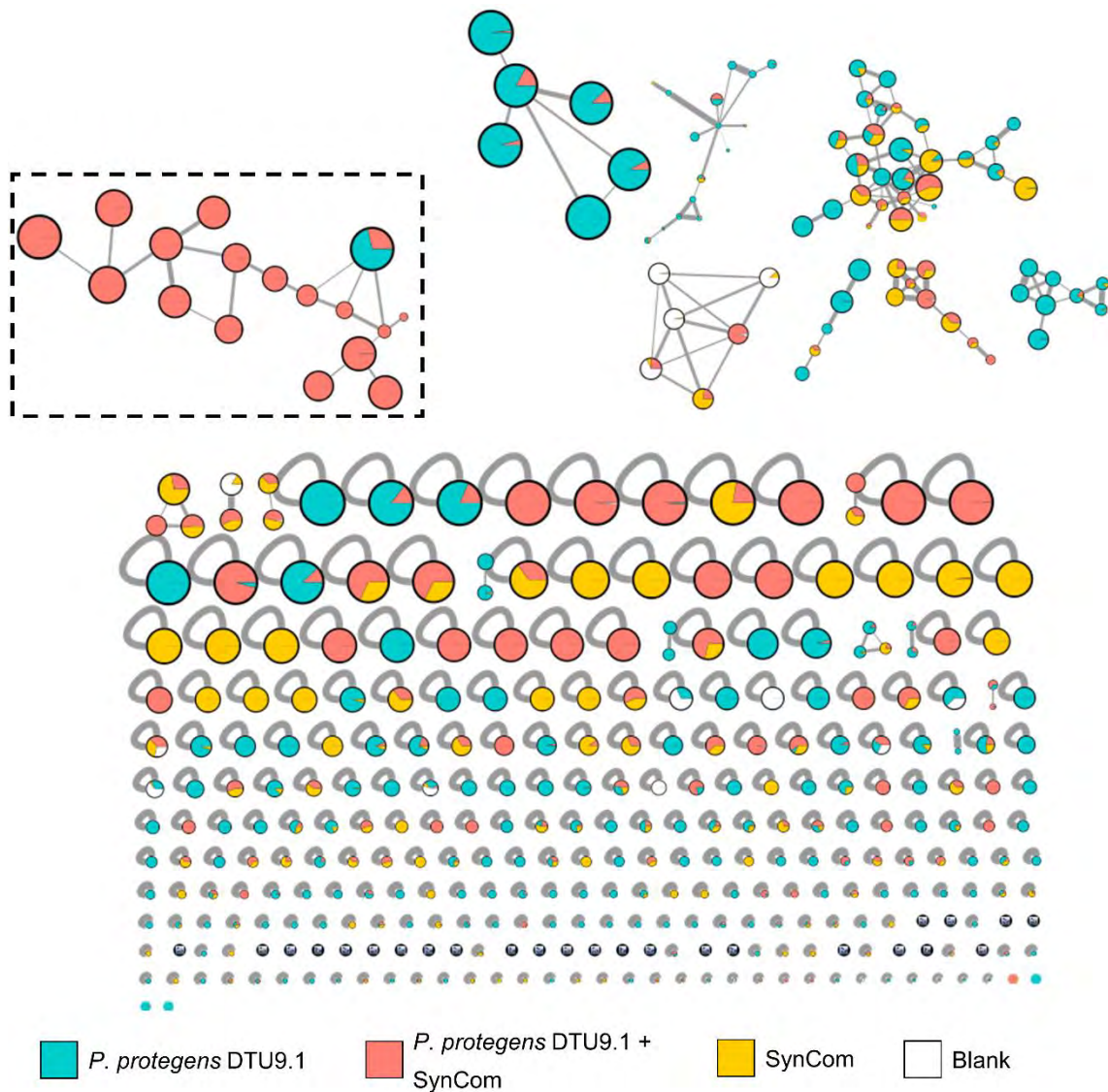
701

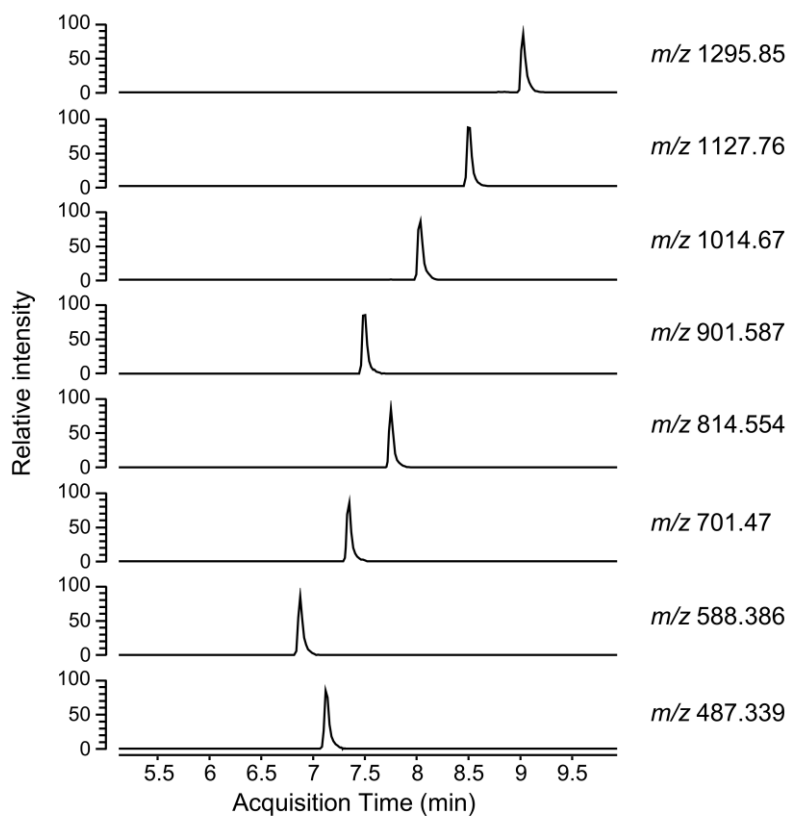
702 Figure S2 | *P. protegens* DTU9.1 grows significantly faster than the four SynCom members. Growth rates of  
 703 *Pedobacter* sp. D749, *R. globerulus* sp. D757, *S. indicatrix* D763, and *Chryseobacterium* sp. D764., as well as *P.*  
 704 *protegens* DTU9.1 WT,  $\Delta phlACB$ ,  $\Delta pltA$ , and  $\Delta ofaA$  in 0.1x TSB liquid broth. Data was derived from 4 biological  
 705 replicates. Letters above indicate treatments significantly different from one another, as determined by a Tukey-  
 706 test ( $P < 0.05$ ).



707

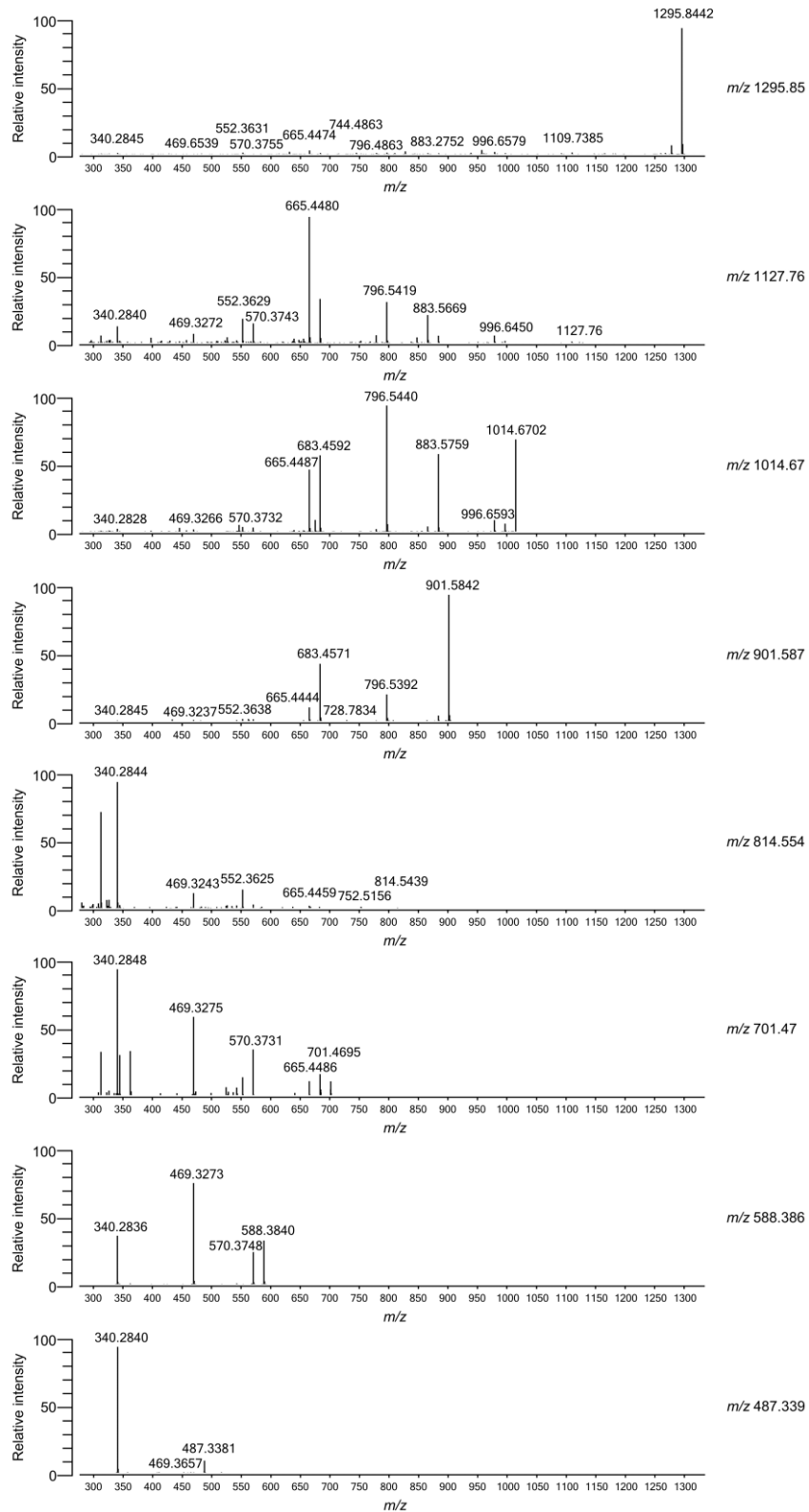
708 Figure S3 | **Pyoluteorin from *P. protegens* DTU9.1 is bactericidal towards all members of a synthetic microbial**  
709 **community.** Inhibition assay analyzing the *in vitro* bactericidal effect of DAPG, pyoluteorin and orfamide A on the  
710 four SynCom members: *Pedobacter* sp. D749, *R. globerulus* sp. D757, *S. indicatrix* D763, and *Chryseobacterium*  
711 sp. D764.





720

721 Figure S5 | **Extracted ion chromatograms confirmed the presence of degradation products.** Extracted ion  
 722 chromatograms (EIC) of orfamide A and the observed degradation products after 7 days of cocultivation between  
 723 *P. protegens* DTU9.1 and the SynCom in the hydrogel bead system. Each degradation product has a different  
 724 retention time, thus denying the possibility of them being products of in-source fragmentation.



725

726 Figure S6 | Tandem mass spectrometry revealed the relatedness of degradation products to orfamide A.  
 727 Observed fragmentation patterns of orfamide A ( $m/z$  1295.85) and the degradation products. Similarities  
 728 between the patterns confirmed the relatedness of each degradation product to orfamide A, representing the  
 729 loss of amino acids from the C-terminal end of the linearized lipopeptide.